Analysis of *Opuntia Ficus-Indica* Triggered Cellular Mechanisms in the Protection Against Cellular Stressors

Jeremy Pullicino

2023

Final report presented to the Faculty of Medicine and Surgery in part fulfilment of the requirements for the degree of Doctor in Philosophy at the University of Malta

Supervisor: Prof Thérèse Hunter BS Hons (NY) MS (NY) PhD (Cran UK)

&

Co-Supervisor: Prof Pierre Schembri Wismayer M.D., Ph.D.(Glas.)

Dedication

To my wife Rebecca, the compass that guides me through life's journey, your strength, grace, and boundless kindness have transformed my world into a sanctuary of warmth and understanding. Every step we take together is a testament to the remarkable bond we share, a bond that grows stronger with every passing day. Through life's challenges and triumphs, your unwavering support has been my anchor, and your love, the fuel that propels my dreams forward. Your laughter is my refuge, and your presence, my solace. In your embrace, I find home. This dedication is a humble tribute to the extraordinary woman you are—my confidante, my partner-in-crime, and my forever love. May our days be filled with laughter, our nights with dreams, and our journey with endless love.

Acknowledgments

I would like to extend my heartfelt gratitude to all those who have contributed to the completion of this thesis.

First and foremost, I am deeply thankful to my thesis supervisors, Prof Thérèse Hunter and Prof Pierre Schembri Wismayer, for their invaluable guidance, support and patience throughout the entire research process. Their expertise and insightful feedback have been instrumental in shaping the direction of this work. They went beyond the call of duty and never gave up on me even in the darkest of moments and for that fact I am eternally grateful and in their debt. A special thanks to Nutribiotech Services Limited, Malta and Dr Charles Saliba for providing the prickly pear extract and carrier.

My sincere appreciation goes to all my colleagues, whose hands-on assistance, collaboration and discussions have offered fresh perspectives and stimulating insights that have undoubtedly contributed to the depth and breadth of this study.

I extend my gratitude to my family and friends for their unwavering encouragement, understanding, and motivation. Their belief in my abilities has been a driving force behind the completion of this endeavour.

This journey would not have been possible without the collective efforts, support, and inspiration from these individuals. Their contributions have left an indelible mark on this thesis and have played a crucial role in my academic and personal growth.

With heartfelt appreciation,

Jeremy

The research work disclosed in this publication is partially funded by the Endeavour Scholarship Scheme (Malta). This Scholarship is part-financed by the European Union - European Social Fund (ESF) under Operational Programme II – Cohesion Policy 2014-2020, "Investing in human capital to create more opportunities and promote the well-being of society".

European Union- European Structural and Investment Funds
Operational Programme II – Cohesion Policy 2014-2020

Investing in human capital to create more opportunities and promote the well being of society

Scholarship part-financed by the European Union European Social Fund (ESF)

Co-financing rate: 80% EU Funds; 20% National Funds

Investing in your future

Abstract

The aim of the study was to analyse the ability, effectiveness, and mechanisms of action of the selected plant extract – prickly pear extract (PPE) – from the fruit of a local cultivar of *Opuntia ficus-indica* provided by and proprietary to Nutribiotech Services Limited, Malta, as a mode of protection against the cellular damage induced by cellular stressors on human dermal fibroblasts. Specifically, the cellular stressors used were heat stress, oxidative stress and UV irradiation, and these have the potential to exert deleterious effects on the cellular microarchitecture and physiology that may result in pathologies secondary to the effect of these injurious stimuli including but is not limited to, sunburn, cellular aging, and carcinogenesis. A cytoprotective effect was observed on exposure of human dermal fibroblasts to cytotoxic levels of heat stress (44°C for 1 h), menadione induced oxidative stress (25 μM, 12.5 μM and 6.25 μM), UVC (10 μJ/m^2) and UVA (5 J/cm^2) irradiation by varying degrees instigated by PPE (0.002 %, 0.004 %, 0.01 %, 0.02 %, 0.04 % and 0.08 %) treatment, reaching zenith at PPE (0.04 %) when considering the totality of the results of the Cell Titre Glo / Presto blue viability assay and scratch assay. Mechanistic elucidation was performed by means of transcriptome analysis using RNA sequencing focusing on the effect of PPE (0.04 %) treatment at alleviating the observed deleterious effect of heat stress (44°C for 1 h) and menadione induced oxidative stress (6.25 μM). The results indicate that the *Opuntia ficus-indica* extract used in this study provided protection against both heat and oxidative stress through the modulation of gene expression primarily related to cell cycle, incorrect/unfolded protein response (UPR), DNA repair and cytokine systems. In heat stress, a *TP53* independent downregulation of cell cycle through *GADD45G*, *GADD45A*, *MDM2* upregulation as well as an increase in cellular response to UPR showed by upregulation of *DNAJB9*, *HSPA5*, *HSPA1A*, *HSPA1B*. In oxidative stress, upregulated DNA repair and cell cycle pathways characterised by the upregulation of the genes *RAD51AP1*, *ESCO2*, *POLQ* and *GINS2* with the concomitant downregulation of pathways related to morphogenesis and differentiation as well as RNA and ribosome processing. The upregulation of *SESN2* is further evidence of the antioxidant effects of the PPE. Finally, the downregulation of inflammatory cytokine genes *CXCL3*, *CXCL8*, *IL33*, oxytocin receptor gene *OXTR*, *SOCS* cytokine signalling genes as well as the overall downregulation of the JAK-STAT pathway and the genes *IL6*, *JAK3* are also indicative of a protective effect conferred by the PPE against oxidative stress. These findings advance the frontiers of knowledge in plant-based dermatoprotection and possibly open an avenue for the prophylactic application of *Opuntia ficus-indica* extracts as a defence against the deleterious implications of a plethora of cellular stressors.

Keywords: human dermal fibroblasts, prickly pear extract, cellular stressors, cytoprotective effect, cell cycle, DNA repair, unfolded protein response and cytokine system.

Contents

List of Figures

List of Tables

List of Abbreviations

Abbreviation	Explanation
ABTS	2,20 -Azino-bis(3-ethylbenzothiazoline-6-sulfonic acid)
CAT	Catalase
cDNA	Complementary DNA
CPM	Counts per million
CUPRAC	Cupric reducing antioxidant capacity
DEGs	Differentially expressed genes
DMEM	Dulbecco`s Modified Eagle Medium
DMSO	Dimethyl sulfoxide
DPPH	2,2-Diphenyl-1-picrylhydrazyl
ECM	Extracellular matrix
ER	Endoplasmic reticulum
ETC	Electron transport chain
FBS	Foetal Bovine Serum
FDR	False discovery rate
FRAP	Ferric reducing antioxidant power
GAGE	Generally applicable gene-set enrichment
GSH	Reduced glutathione
HDFs	Human Dermal Fibroblasts
HEPA	High-efficiency particulate air
HS	Heat shock system
HSP	Heat shock protein
iDEP	Integrated differential expression and pathway analysis
IR	Infrared
KW	Kruskal-Wallis
LncRNA	Long non-coding RNA

MDA	Malonaldialdehyde
MED	Minimal erythemal dose
MPO	Myeloperoxidase
nHDFs	Human Neonatal Dermal Fibroblasts
PARP	ADP-ribose polymerase
PBS	Dulbecco`s Phosphate Buffered Saline
PCA	Principle component analysis
PDGF	Platelet-derived growth factor
PDI	Protein disulfide isomerase
PG	Propylene glycol
PP	Prickly pear
PPE	Prickly pear extract
PPEC	Prickly pear extract carrier
RNA-seq	RNA sequencing
RNS	Reactive nitrogen species
ROS	Reactive oxygen species
RQN	RNA quality number
RT-PCR	Real-time polymerase chain reaction
SAHF	Senescence-associated heterochromatin foci
SASP	Senescence-associated secretory phenotype
SM	Smooth muscle
SOD	Superoxide dismutase
SPF	Sun protective factor
SPSS	Statistical package for the social sciences
T2DM	Type 2 diabetes mellitus
TGF-β	Transforming growth factor β
TNF-α	Tissue necrosis factor-α
UPR	Unfolded protein response
UV	Ultraviolet
UVR	Ultraviolet radiation

Vis	Visible
WNT	Wingless-related integration site

Chapter 1 Introduction

1.1. The Prickly Pear cactus - *Opuntia ficus-indica*

The prickly pear cactus (*Opuntia ficus-indica*) as seen in Figure 1.1, often referred locally as 'bajtar tax-xewk' is a naturalized alien cactus species first introduced to the Maltese island in circa 1492 AD. Locally, in an agricultural perspective, the prickly pear (PP) is predominantly utilized on the margins of agricultural land to serve as a boundary and windbreaker for productive crops and is not exorbitantly harvested for horticultural utilization (Mifsud, 2010).

Figure 1.1: The Prickly Pear – *Opuntia ficus-indica*
The overall plant showing cladodes, fruit, flowers and seeds in its natural environment

Opuntia ficus-indica is a succulent dicotyledonous angiosperm forming part of the approximately 1500 members of the Cactaceae family, possessing the ability to thrive in both arid and semi-arid environments due to the ability to accumulate biomass even under conditions of drought (Butera et al., 2002; Ogburn & Edwards, 2010). The geographical distribution of the *Opuntia* species is vast presumably due its ability to regenerate under harsh conditions from most of compositional organs (Feugang et al., 2006). Thus, *Opuntia* species can be encountered frequently across temperate regions in the Mediterranean basin to the subtropics in Africa the Americas and Asia and even colder regions such as Canada (Feugang et al., 2006; Kaur et al., 2012). The prickly pear provides agricultural economic value and is used to produce a wide array of tea, jam, juice, oil and alcohol as well as for the consumption of its fruit and cladodes

which are considered to be health-promoting (Del Socorro Santos Díaz et al., 2017; El-Mostafa et al., 2014; Kaur & Dufour, 2012). Furthermore, in traditional medicine, *Opuntia ficus-indica* has been used for the management of chronic (obesity, diabetes, inflammatory and cardiovascular diseases) as well as acute conditions (burns, wounds, edema, and viral infection) (Del Socorro Santos Díaz et al., 2017; Saenz, 2000). However, studies into the mechanism of the positive effects of *Opuntia spp.* on human physiology remains underdeveloped and thus cactus product underutilized (Feugang et al., 2006). Therefore, this chapter will provide an overview of some of the major modern developments and scientific rational around the use of *Opuntia ficus-indica* in relation to human health, disease prevention, therapy, and overall wellbeing to satisfy the growing demand for nutraceuticals and the use of natural products for curative and/or preventive effects.

1.1.1. Major constituents

The *Opuntia spp* are laden with a variety of potentially bioactive nutritional compounds and appears to be an excellent source of study for both nutraceuticals and therapeutics. The exact quantities of these cactus compounds are variable with effect from environmental conditions, plant maturity, soil type, plant part and species all coming into consideration. The gambit of biological effects and potential therapeutic application for the bioactive compounds can be found thereafter (Del Socorro Santos Díaz et al., 2017; El-Mostafa et al., 2014).

1.1.2. Mineral Composition

Minerals are inorganic molecules, present ubiquitously throughout the length and breadth of the human biological system and through numerous means facilitate an innumerable amount of metabolic processes vital for the persistence of life. Any form of disturbance or deficiency in the natural mineral balance will result in a characteristic condition owning to the reflecting the function of the mineral within the biological system (Soetan et al., 2009). The mineral composition (Mg, Na, P, Zn, Cu, Fe, Ca, K, Mn) in various parts of *O. ficus-indica* are shown in Table 1.1 with noted predominance of potassium, phosphorus, calcium, sodium, and magnesium (El-Mostafa et al., 2014).

Table 1.1: The distribution of minerals in *Opuntia ficus-indica* - mg/100g tissue.

Main Component Identified	Pulp	Seeds	Cladode
Calcium	27.6	16.2	5.64 – 17.95
Magnesium	27.7	74.8	8.80
Sodium	0.8	67.6	0.3 – 0.4
Potassium	161	163	2.35 – 55.20
Iron	1.5	9.45	0.09
Phosphorus	-	152	0.15 – 2.59
Zinc	-	1.45	0.08
Copper	-	0.32	-
Manganese	-	Trace	0.19 – 0.29

The numerous different types of minerals that can be found in the various anatomical parts of *Opuntia ficus-indica* plant with values expressed as mg/100g of plant tissue. Adapted with permission from Nopal Cactus (*Opuntia ficus-indica*) as a Source of Bioactive Compounds for Nutrition, Health and Disease, by El-Mostafa et al., 2014, Molecules, 19(9), p. 14879-14901. Copyright 2014 by authors.

1.1.3. Vitamins

The major constituent vitamin contents of *Opuntia spp* (Table 1.2) include vitamin C, vitamin K, vitamin E (α-, β-, γ- and δ-tocopherol), however the exact concentration is dependent on the cultivar as well as the anatomical organ of origin. The vitamin content besides providing a valuable component to human health constitutes a major role in the antioxidant biological properties of *Opuntia spp* related products (Del Socorro Santos Díaz et al., 2017; Ramadan & Mörsel, 2003).

Table 1.2: The distribution of vitamins in *Opuntia ficus-indica* - mg/100g tissue.

	Pulp	Seeds	Skin	Cladode
Vitamin K1	53.2	52.5	109	-
Vitamin C	34 - 40	-	-	7 - 22
Vitamin B1	-	-	-	0.14
Vitamin B2	-	-	-	0.60
Vitamin B3	-	-	-	0.46
α-Tocopherol	84.9	56	1760	-
β-Tocopherol	12.6	12	222	-
γ-Tocopherol	7.9	33	174	-
σ-Tocopherol	422	5	26	-
Total vitamin E	527.4	106	2182	-

The numerous different types of vitamins that can be found in the various anatomical parts of *Opuntia ficus-indica* plant with values expressed as mg/100g of plant tissue. Adapted with permission from Nopal Cactus (*Opuntia ficus-indica*) as a Source of Bioactive Compounds for Nutrition, Health and Disease, by El-Mostafa et al., 2014, Molecules, 19(9), p. 14879-14901. Copyright 2014 by authors

1.1.4. Phytosterols

Phytosterols, also known as plant sterols are analogous to cholesterol in animal products and possess a similar structure to that of cholesterol with some modifications (Awad & Fink, 2000). Several phytosterols can be isolated from different parts of the *O. ficus-indica* fruit (Table 1.3) (El-Mostafa et al., 2014). However, the major documented sterol constituent, β-sitosterol has been intensively investigated with respect to its effect on human physiology. In fact it has been observed to offer protection against cardiovascular disease through the lowering of cholesterol absorption, antioxidant effect as well as the ability to inhibit the growth of a number of cancer cell lines namely LNCaP human prostate cancer, MDA-MB-231 human breast cancer, HT-29 human colon cancer (Awad & Fink, 2000; Ostlund, 2004; Ramadan & Mörsel, 2003).

Table 1.3: The distribution of phytosterols in *Opuntia ficus-indica* - g/kg tissue.

Main Component Identified	Pulp	Seed	Skin
Lanosterol	0.76	0.28	1.66
β-Sitosterol	11.2	6.75	21.1
Stigmasterol	0.73	0.30	2.12
Campesterol	8.74	1.66	8.76
Ergosterol	-	-	0.68

The numerous different types of phytosterols that can be found in the various anatomical parts of *Opuntia ficus-indica* plant with values expressed as g/kg of plant tissue. Adapted with permission from Nopal Cactus (*Opuntia ficus-indica*) as a Source of Bioactive Compounds for Nutrition, Health and Disease, by El-Mostafa et al., 2014, Molecules, 19(9), p. 14879-14901. Copyright 2014 by authors

1.1.5. Polyphenols

Polyphenols make up a large family of organic phytochemicals produced as a by-product of plant metabolism (Lecour & Lamont, 2011). Polyphenols are characterized by the inclusion of phenolic groups or structural components and can be broadly divided into 4 categories (flavonoids, phenolic acids, lignans and stilbenes) depending on the aggregated distribution of these components throughout polyphenol structure. Thus far in nature more than 8000 polyphenols have been identified and can be found in large quantities in fruits, vegetables, cereals, legumes tea and coffee (Ganesan & Xu, 2017). In plants the polyphenols serve as an important defence to negate the harmful effect of UV radiation, pathogens, extreme climactic conditions, and oxidative stress. The bioavailability of polyphenols is highly variable and often

these must be hydrolysed by intestinal enzyme or colonic microflora. Furthermore, the biological effects differ wildly between polyphenols which accumulate in concentration in tissues until enough concentration has been accumulated to exert a biological active effect. Though their short- and long-term health effects have not yet been fully characterized in humans, polyphenols are potent antioxidants and numerous studies have indicated diverse biological properties (Figure 1.2) and have indicated an inverse association between the risk of chronic disease and the consumption of polyphenol rich diet (Pandey & Rizvi, 2009). Current knowledge dictates that the protective effect observed is likely due to the 'biological scavenger theory' whereby polyphenolic compounds negate free radicals by the transformation into more stable chemical complex negating the possibility of further deleterious effects (Cory et al., 2018). All parts of the *Opuntia ficus-indica* are rich with a wide array of polyphenols (Table 1.4) however the exact contents vary depending on several factors including specific plant part, climate, age, soil specifications and environmental conditions (El-Mostafa et al., 2014).

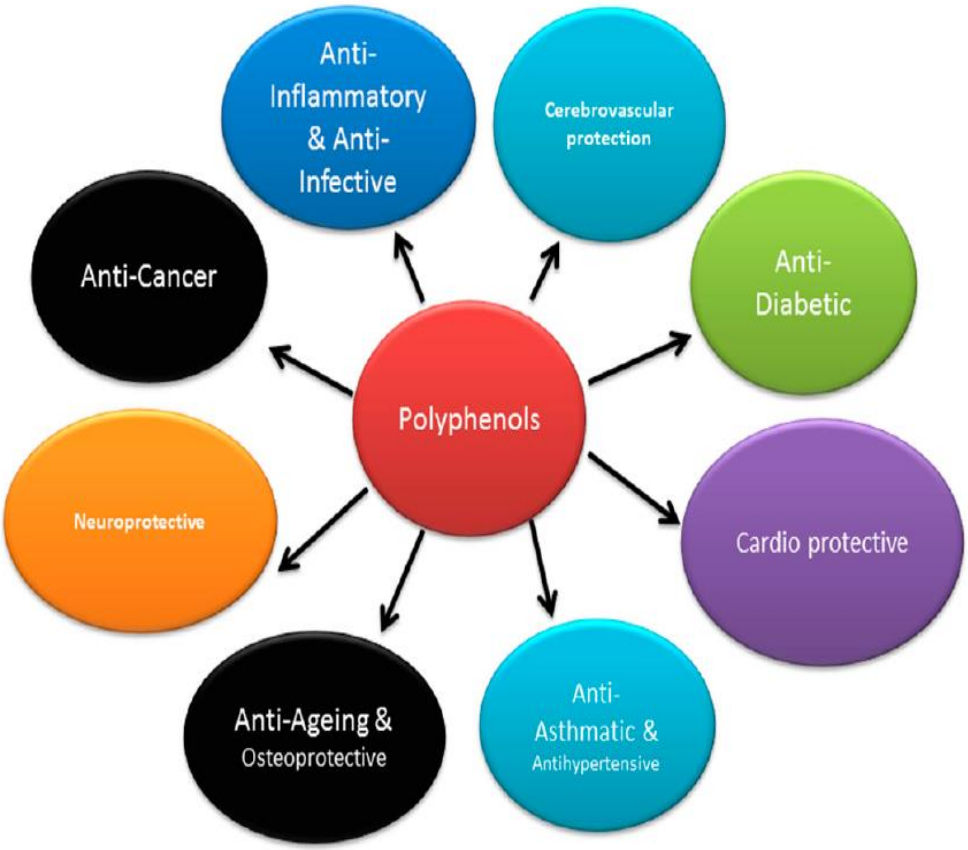

Figure 1.2: Application of polyphenols in humans.
The known biological and medical application polyphenols in humans. Adapted with permission from A Critical Review on Polyphenols and Health Benefits of Black Soybeans, by Ganesan & Xu, 2017, Nutrients, 9(5), p. 455. Copyright 2017 by authors.

Table 1.4: The distribution of polyphenols in *Opuntia ficus-indica* - mg/100g tissue.

Plant tissue	Main identified components	Content in mg/100g
Cladode	Gallic acid	0.64 – 2.37
	Coumaric acid	14.08 – 16.18
	3,4-dihydroxybenzoic	0.06 – 5.02
	4-hydroxybenzoic	0.5 – 4.72
	Ferulic acid	0.56 – 34.77
	Salicylic acid	0.58 – 3.54
	Isoquercetin	2.29 – 39.67
	Isorhamnetin-3-*O*-glucoside	4.59 – 32.21
	Nicotiflorin	2.89 – 146.5
	Rutin	2.36 – 26.17
	Narcissin	14.69 – 137.1
Pulp	Total phenolic acid	218.8
	Quercetin	9
	Isorhamnetin	4.94
	Kaempferol	0.78
	Luteolin	0.84
	isorhamnetin glycosides	50.6
	Kaempferol	2.7
Seed	Total phenolic acid	48 – 89
	Feruloyl-sucrose isomer 1	7.36 – 17.62
	Feruloyl-sucrose isomer 2	2.9 – 17.1
	Sinapoyl-diglucoside	12.6 – 23.4
	Total Flavonoids	1.5 – 2.6
	Total Tannins	4.1 – 6.6
Skin fruits	Total phenolic acid 45,700	45,700
	Total Flavonoid 6.95	6.95
	Kaempferol 0.22	0.22
	Quercetin 4.32	4.32
	Isorhamnetin	2.42 - 91

The numerous different types of polyphenols that can be found in the various anatomical parts of *Opuntia ficus-indica* plant with values expressed as mg/100g of plant tissue. Adapted with permission from Nopal Cactus (*Opuntia ficus-indica*) as a Source of Bioactive Compounds for Nutrition, Health and Disease, by El-Mostafa et al., 2014, Molecules, 19(9), p. 14879-14901. Copyright 2014 by authors.

1.1.6. Betalains

Betalains are a nitrogen containing water-soluble class of pigmented molecules of with approximately seventy-eight distinctive structures have been identified and characterized(Belhadj Slimen et al., 2017). The biosynthetic precursor of betalains is betalamic acid and the condensation with amino acids or their derivatives results in the formation of the yellow-orange betaxanthins while the condensation with *cyclo*-DOPA or its glucosyl derivatives results in the formation of red-violet betacyanins shown in Figure 1.3 (Strack et al., 2003). The occurrence of betalains in *Opuntia ficus-indica* contributes to the distinctive coloration of the flowers and fruit of this *Cactaceae* family member which in turn is dependent on the ratio of betacyanins to betaxanthins (Feugang et al., 2006). Betalains are highly effective

free radical scavenger with an antioxidant capacity 3-4 times that of ascorbic acid (Stintzing & Carle, 2007). Studied on animal and cell models have noted the ability of betanins to appear to prevent DNA damage together with anti-inflammatory, anti-proliferative, anti-microbial properties as well as the ability to induce antioxidant activity (e.g. glutathione peroxidase and heme oxygenase 1) (Rodriguez-Amaya, 2019).

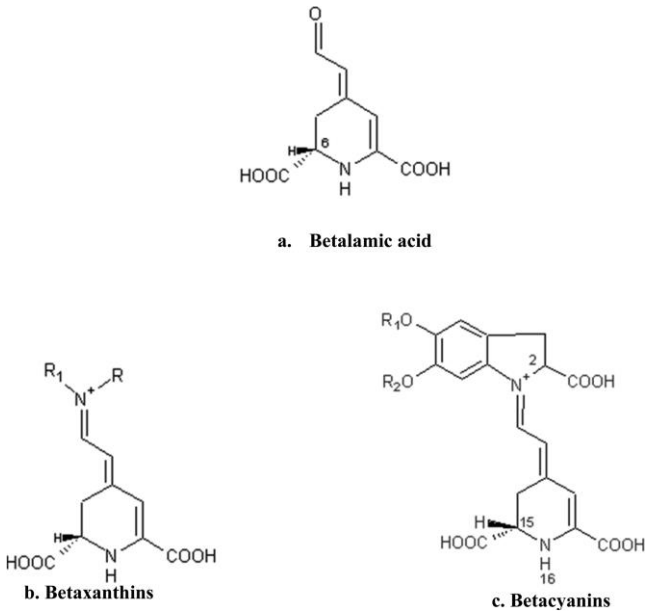

Figure 1.3: The structure of Betalains.
The structure of different types of betalains; betalamic acid (a), betaxanthins (b) and betacyanins (c). Adapted with permission from Chemical and Antioxidant Properties of Betalains, by Belhadj Slimen, I. et al., 2017, Agricultural and Food Chemistry, 65(4), p. 675-689. Copyright 2017 by American Chemical Society.

1.1.7. Biological and Medical Relevance of Cactus products

Opuntia ficus-indica extracts and compounds have been reported to have a diverse range of biological properties which have been elucidated through numerous experimental models. These biological indicators include but are not limited to antimicrobial activity, antiviral ability, anti-inflammatory effect, antioxidant effect, heat shock protein stimulation, as well as the protective properties with respect to the development of diabetes, obesity, cerebral ischemia, rheumatism, cardiovascular diseases, malignancy and alcoholism (Del Socorro Santos Díaz et al., 2017; Feugang et al., 2006; Kaur et al., 2012; Osuna-Martínez et al., 2014).

1.1.7.1. Antimicrobial activities

Water based extracts of *Opuntia ficus-indica* fruits (100 mg dry pulp in 50 ml water) have been observed to have anti-microbial effects against a wide range of bacterial species including *Staphylococcus aureus, Pseudomonas aeruginosa,* and *Enterococcus faecium* as well as an inhibitory effect against *Salmonella* spp. and *Escherichia coli* O157:H7 (Palmeri et al., 2018). Furthermore, extracts of *Opuntia ficus-indica* were seen to be of pharmacological interest due to the observed bactericidal effect, and thus potential at preventing major food-borne bacterial gastroenteritis caused by *Campylobacter jejuni* and *Campylobacter coli* and *Vibrio cholerae* (Castillo et al., 2011; Sánchez et al., 2010). Additionally, owing to the phytochemical constituent astragalin anti-COVID 19 utility of *Opuntia ficus-indica* is being investigated with promise (Iacopetta et al., 2022).

1.1.7.2. Anti-Inflammatory/Antioxidant Effect

The use of *Opuntia ficus-indica* products has been seen to have an anti-inflammatory effect or/and antioxidant effect in numerous studies both *in vitro* and *in vivo*. These effects are related as most antioxidants are also anti-atherogenic due to the ability to neutralize ROS (Camaré et al., 2017).

Opuntia ficus-indica fruit juice was shown to reduce gastric lesions in rat models partially attributed to the betanin components and facilitated through the attenuation of myeloperoxidase (MPO) activity and tissue necrosis factor-α (TNF-α) proinflammatory cytokine production, both of which are major influencers in inflammation induced tissue damage (Kim et al., 2012).

Studies by Bardaa et al., 2020 demonstrated that a methanolic extract of *Opuntia ficus-indica* flowers was seen to reduce the inflammatory histology and cytology as well as the increase of catalase (CAT), superoxide dismutase (SOD) and reduced glutathione (GSH) as well as malonaldialdehyde level (MDA) levels in Carrageenan-induced rat paw edema. This is all indicative of anti-inflammatory activity (Ammar et al., 2018). Similar *in vivo* findings were also observed using prickly pear oil on the same animal model (Bardaa et al., 2020).

A flavonoid-rich concentrate from *Opuntia ficus-indica* juice was shown to have an attenuating effect on induced inflammatory stress through a reduction in the expression of IL-8 and TNF-

α coupled with a reduction in oxidative stress (reduction in protein oxidation) on Caco-2 intestinal cells (Matias et al., 2014).

An ethanol extract of *Opuntia ficus-indica* suppressed carrageenan-induced rat paw edema as well as provided a potent anti-inflammatory protection against gastric lesions (Park et al., 1998). This anti gastric ulcer activity in rat models was also noted utilizing cladodes of *Opuntia ficus-indica* (Galati et al., 2001). Similar ethanol extracts were seen to have highly promising antioxidant properties with regards to superoxide and hydroxyl racial scavenging as well as protection against DNA breakages and protection of mouse splenocytes against glucose oxidase-mediated cellular cytotoxicity (Lee et al., 2002).

Opuntia ficus-indica fruit extract was observed to reduce the deleterious effects of ethanol on rat erythrocytes through the reduction of MDA, an increase in GSH and an increase in radical scavenging ability together with a general reduction in erythrocyte hemolysis when compared to untreated ethanol exposed erythrocytes (Alimi et al., 2012). Ethanol fed rats had their oxygen radical scavenging activity restored to normal levels on treatment with prickly pear juice with the restoration of GSH levels (Bensadón et al., 2010).

1.1.7.3. Alcohol Hangover

The use of *Opuntia ficus-indica* extracts have been reported to alleviate alcohol induced symptoms of hangover such as nausea and dry mouth in humans. This effect is likely correlated with reduction of the inflammation activation induced because of alcohol overindulgence caused by the by-products of alcohol metabolism and impurities present within the alcohol beverage (Wiese et al., 2004).

1.1.7.4. Anti-diabetic

Type 2 diabetes mellitus (T2DM) is a highly prevalent chronic metabolic condition characterized by hyperglycaemia secondary to relative insulin deficiency and resistance, resulting in long term complication relating in macro/microvasculature multi-organ damage (Olokoba et al., 2012). In traditional medicine *Opuntia spp* have long been associated with the treatment of hyperglycaemia resulting from T2DM and in fact numerous studies have now

demonstrated the anti-diabetic hypoglycaemic activity of *Opuntia spp* in diabetic rats as well as diabetic humans (Feugang et al., 2006). An overview of numerous human clinical studies shows a consistent reductive effect on serum glucose levels while all the while being inconsistent with respect to the effect on insulin levels by plant part specific *Opuntia spp* products, in particular cladode leaf or cladode leaf and fruit products. Although many modes of action have been proposed for this hypoglycaemic effect, such as; fibre content reducing rate of absorption, insulin like factors present in plant material or/and increase in glucose metabolism, the exact mechanism as yet remains elusive (Gouws et al., 2019).

1.1.7.5. Anti-Cancer

Opuntia ficus-indica extracts (fruit, cladodes, and roots) have been highlighted by numerous studies for anti-cancer properties on numerous neoplastic cell lines.

The ability of betanin isolated from *Opuntia ficus-indica* fruit to inhibit the growth of human chronic myeloid leukaemia cell line (K562) through the activation of the apoptotic intrinsic pathway mediated through the mitochondrial release of cytochrome C into the cytosol and ADP-ribose polymerase (PARP) cleavage (Sreekanth et al., 2007).

Intestinal epithelial cancer cells (Caco-2) were affected cytotoxically by *Opuntia ficus-indica* products through caspase cascade apoptosis described by Antunes-Ricard et al. 2014 or possibly the expression of the tumour suppressor protein p16INK4a, described by Naselli et al. 2014 (Antunes-Ricardo et al., 2014; Naselli et al., 2014).

The use of cactus extract from *Opuntia spp* that has led mitochondrial dependent apoptosis in ovarian cancer cell lines (SKOV3 and OVC420) secondary to a pro-oxidant effect which has led to the production of ROS (Feugang et al., 2010).

Numerous other carcinogenic cell lines were seen to be affected by *Opuntia spp* products, these include human colon cancer (HT-29 and SW-480), mammary (MCF-7), glioblastoma (U87MG), hepatic (HepG2) and cervical (HeLa) (Del Socorro Santos Díaz et al., 2017).

1.1.7.6. Heat Shock Proteins production

Heat shock protein production has been seen to be instigated by treatment with prickly pear cactus (*Opuntia ficus-indica*) extract with the potential to provide protection against various stressors and resultant deleterious consequences.

An *Opuntia ficus-indica* extract has been shown to reduce inflammation response in human clinical trials through the reduction of C-reactive protein levels following alcohol consumption (Wiese et al., 2004). Furthermore, in equine studies this same extract was seen to increase HSP72 levels when utilized prophylactically prior to intensive and excessive exercise(Martinod et al., 2007). Furthermore, in harmony to the above in aquatic studies relating to fish, elevated levels of HSPs were observed following pre-treatment with extract prior to introduction of stressor (e.g. Heat stress or toxic elements) in particular HSP70 and HSP90 (Roberts et al., 2010).

In congruence with previous work, work on the Common carp (*Cyprinus carpio*) that was pre-treated with a water-soluble form of *Opuntia ficus-indica* extract showed an increase in the levels of HSP70 during ammonia perturbation which correlated with increased stress tolerance and thus survival (Sung et al., 2012). This form of the extract has been seen to be an inducer of HSP production (HSP70) in invertebrates (*Artemia franciscana naupliiin*) both in presence and absence of subsequent stressors and thus could serve as an anti-stress agent (Baruah et al., 2012).

1.1.7.7. Ultraviolet Radiation

Limited information is available with respect to the effect of *Opuntia ficus-indica* extract against UV related damage, however some studies have indicated a potential alleviating effect. Although *Opuntia ficus-indica* extract was not seen to possess any significant sun protective factor (SPF) properties, extract pre-treatment prior to UVA exposure on human keratinocytes appeared to provide a clear protective effect against UV-induced cellular stress processes, including ROS production, GSH depletion and lipid peroxidation as well as a reduction of apoptosis as indicated by the lack of caspase-3 or caspase-7 cleavage (Petruk et al., 2017). Furthermore, opuntiol (6-hydroxymethyl-4-methoxy-2H-pyran-2-one, $C_7H_8O_4$) extracted from *Opuntia ficus-indica* was seen to prevent UVA-induced cytotoxicity in NIH-3T3 (Mouse embryo fibroblasts) cells preventing DNA single strand breaks and the loss of mitochondrial

transmembrane potential as well as the prevention of UVA mediated ROS generation, lipid peroxidation as well as the loss of enzymatic antioxidant activity (superoxide dismutase [SOD], catalase, and glutathione peroxidase (Ponniresan et al., 2020).

1.1.7.8. Thermoprotection

The mortality of sheep lymphocytes was shown to increase linearly as a function of intensity and duration of heat stress with a correlation H_2O_2 production. The use of *Opuntia ficus-indica* extract was observed to maintain viability of lymphocytes through the reduction of H_2O_2 and thus demonstrates the ability to reduce hyperthermia-induced oxidative stress with indications of betanin being the active agent (Belhadj Slimen et al., 2019).

1.2. Propylene Glycol

One of the main goals of pharmaceutical therapy is to develop a therapeutic agent that exhibits maximum bioavailability with minimal toxicity. This is challenging due to problems related to absorption, stability, distribution, and elimination. To get around these issues, a number of options are available including the modification of therapeutic molecules or developing new delivery systems for medications. (Kolate et al., 2014). Propylene glycol (PG) is a clear, viscous, practically odourless water soluble fluid ($C_3H_8O_2$) that is a di-functional alcohol with primary and a secondary hydroxyl groups (Martin & Murphy, 2000). PG is ubiquitous in modern living due to its commercially attractive properties as a solvent and humectant combined with a relatively low toxicity (McGowan et al., 2018; McMartin, 2014). The FDA and EMA has granted approval for the utilization of PG in pharmacological preparation and in fact it is a frequently applied co-solvent to increase the solubility and/or stability of numerous formulation such as paracetamol, phenobarbital and lorazepam (De Cock et al., 2013). However, it is also used as a solvent in a wider range of more widespread pharmaceutical preparations such as a solvent and coupling agent in shampoos, shaving creams, sunscreens and other similar formulations (Martin & Murphy, 2000). It is a well-known pharmaceutical excipient and as mentioned has a wide range of pharmacological uses and doses; humectant in topical preparations (15%), preservative in solution (15 – 30 %), co-solvent in aerosols (10 – 25 %), parenterals (10 – 60 %), oral solutions (10 – 25 %) and topical (5 – 80 %) (De Cock et al., 2013).

The pharmacokinetics of propylene glycol follows a predictable course where the absorption, distribution, metabolism and excretion have been extensively studied (McGowan et al., 2018). Entry of propylene glycol into a biological system is rapid and extensive through the oral, intravenous, intraperitoneal and aerosol route however, less so through the topical application unless applied to disrupted skin layers. Once internalized, PG exhibits low toxicity in both animals and humans, requiring very high doses to induce acute effects. In the context of clinical safety, the maximum daily dose considered to be safe regardless of duration and route of administration with exemption of not inhalation is as follows; Neonates (1 mg/kg), 1 month to 4 years (50 mg/kg) and 5 years and up (500 mg/kg). Clearance is achieved via the renal (45 %) and metabolic route (55 %). Transiting through the renal route PG is excreted unchanged or in conjunction with glucuronic acid in urine. The remainder of PG is metabolized into lactic acid and pyruvic acid; excessive clearance via this pathway results in the clinical representation of acute PG toxicity with can include central nervous system depression, hematologic toxicity,

cardiovascular dysfunction, renal toxicity, hyper osmolality and metabolic acidosis (McGowan et al., 2018; McMartin, 2014). However, studies have shown that PG exhibits exceptionally low toxicity and systemic toxicity is isolated to rare occurrences in extreme high doses through oral or intravenous acute route and even in these cases complete recovery is expected (Fowles et al., 2013).

A few studies have examined the effects of propylene glycol on cellular viability to understand its mechanism of toxicity. Cytotoxicity studies conducted on mouse fibroblasts have shown that PG is non-toxic showing no alteration in metabolic activity, mitochondrial activity or protein synthesis, however the concentrations tested were relatively low, only up to 100 µM (Song et al., 2012). E-liquid components that have been studied and PG (> 1 % v/v) was observed to inhibit cell proliferation by inducing apoptosis and enhancing DNA damage and cell cycle arrest in human small airway epithelial primary cells (Komura et al., 2022). PG was seen to have a toxic effect on human proximal tubule cells at a concentration of 50 mM (Morshed et al., 1998). The positive properties of PG should not be overshadowed by the negative effects discussed as systemic PG toxicity is considered uncommon and although evidence related to cytotoxicity is mixed, most studies suggest non-toxicity in cell culture at lower concentrations and as such PG is widely accepted for biomedical applications.

1.3. Skin

The skin is the largest organ in the human body and serves primarily as a biological bastion against the external environment and the army of insults that are thrown at the human body including; temperature fluctuations, trauma, pathogens, toxins and UV and is essential to the maintenance of homeostasis (Lopez-Ojeda et al., 2023). However the functions go far beyond the ability of the skin to act as a biological shield and the skin is a sensory and excitatory organ that has an endocrine function (sex steroids, melatonin and vitamin D) while also preventing the loss of essential body fluids, ensuring thermoregulation and contributing to immunological functions (Gilaberte et al., 2016). The skin is primarily composed of three layers the outer - epidermis, the middle - dermis and the inner – hypodermis which in consort with the resident cellular populations work in tandem to facilitate the physiology of the skin as seen in Figure 1.4 (Kolarsick et al., 2011).

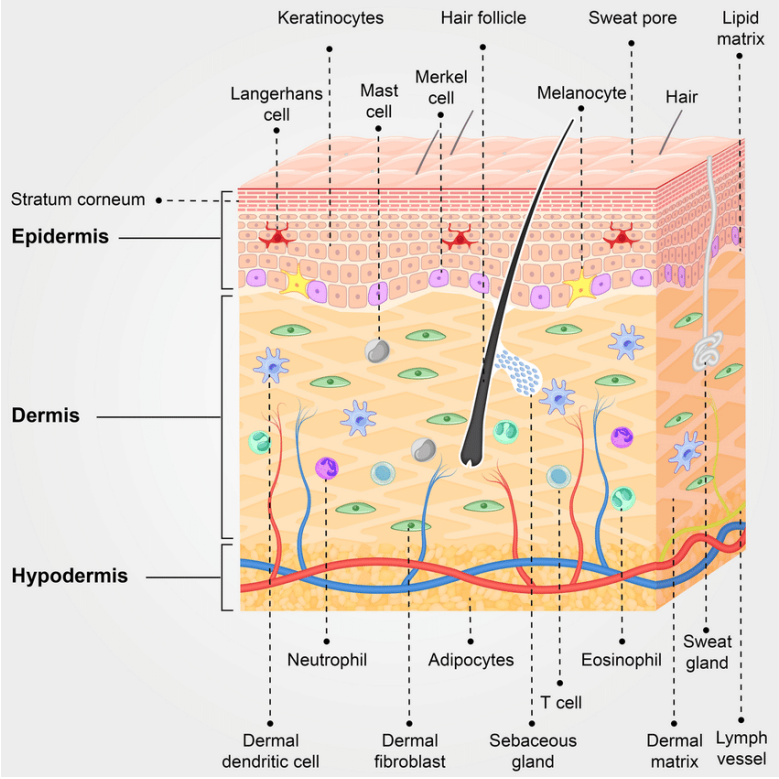

Figure 1.4: Schematic illustration of the skin and resident cell populations.
The skin is composed of the epidermis, dermis, and hypodermis and the various cell populations that reside in the extracellular matrix intertwined with blood and lymph vessels, hair follicles, sweat glands, sebaceous glands, and other appendages are placed within the dermis and hypodermis Adapted with permission from Non-coding RNAs in photoaging-related mechanisms: a new paradigm in skin health, by Soheilifar. et al., 2022, Journal of Biogerontology, 23, p. 289 - 306. Copyright 2022 by Springer Nature.

1.4. Fibroblasts

Fibroblasts are versatile mesenchymal cells found ubiquitously within the stroma of biological architecture and visually appear as elongated spindles with numerous cytoplasmic projections (Dick et al., 2023). Progress made in recent years has redefined the role of fibroblasts to far more than previously known (Figure 1.5). *In vitro* modelling can shed light to a broad spectrum of pathologies and emergent novel therapeutic possibilities. Fibroblasts have a considerable heterogeneity (as low as 20 % gene overlap) and tissue specific fibroblasts are specialized to generate the microarchitecture of the extracellular matrix (ECM) that best facilitates the development, repair and homeostasis of local organs. However with this in mind, fibroblasts across multiple tissues, such as heart, skeletal muscle, lungs and skin, do share common functions (Plikus et al., 2021). Fibroblasts are referred to canonically as cells that synthesize and maintain the ECM and in doing so provide the environment and communicative information to the surrounding cells through microarchitectural, biochemical and biomechanical signals regulated by mediators broadly described as cytokines, growth factors and metabolites. Fibroblasts are thus the major architects in matrisome construction and maintenance by depositing collagens, elastin, fibronectin, lamins and proteoglycans as well as ECM remodelling through the production of modifying enzymes such as matrix metalloproteinase and their inhibitors (Gomes et al., 2021). In the adult physiology, fibroblasts are relatively quiescent unless activated in response to stress that is often associated with tissue disorganization secondary to trauma. It is at this point that the importance of fibroblast plasticity becomes evident. This plasticity of fibroblasts refers to their ability to diverge from stem lineage model, in which undifferentiated cells produced differentiated cells along a linear inflexible path. This plasticity permits the normally quiescent fibroblasts to adapt to tissue damage to the surrounding microarchitecture and heavily facilitates wound healing. This plasticity permits post-mitotic mesenchymal fibroblast cells to renter cell cycle, function as progenitors and produce myofibroblasts which, on resolution of the instigating condition may either return to quiescent state or undergo apoptosis or senescence (Salminen, 2023). Myofibroblasts activation comes about as a result of several signalling pathways, including platelet-derived growth factor (PDGF) signalling, transforming growth factor β (TGF-β), Wingless-related integration site (WNT) and, to some extent, by inflammatory cytokines (TNF-α, IL-1 or IL-6) (Plikus et al., 2021).

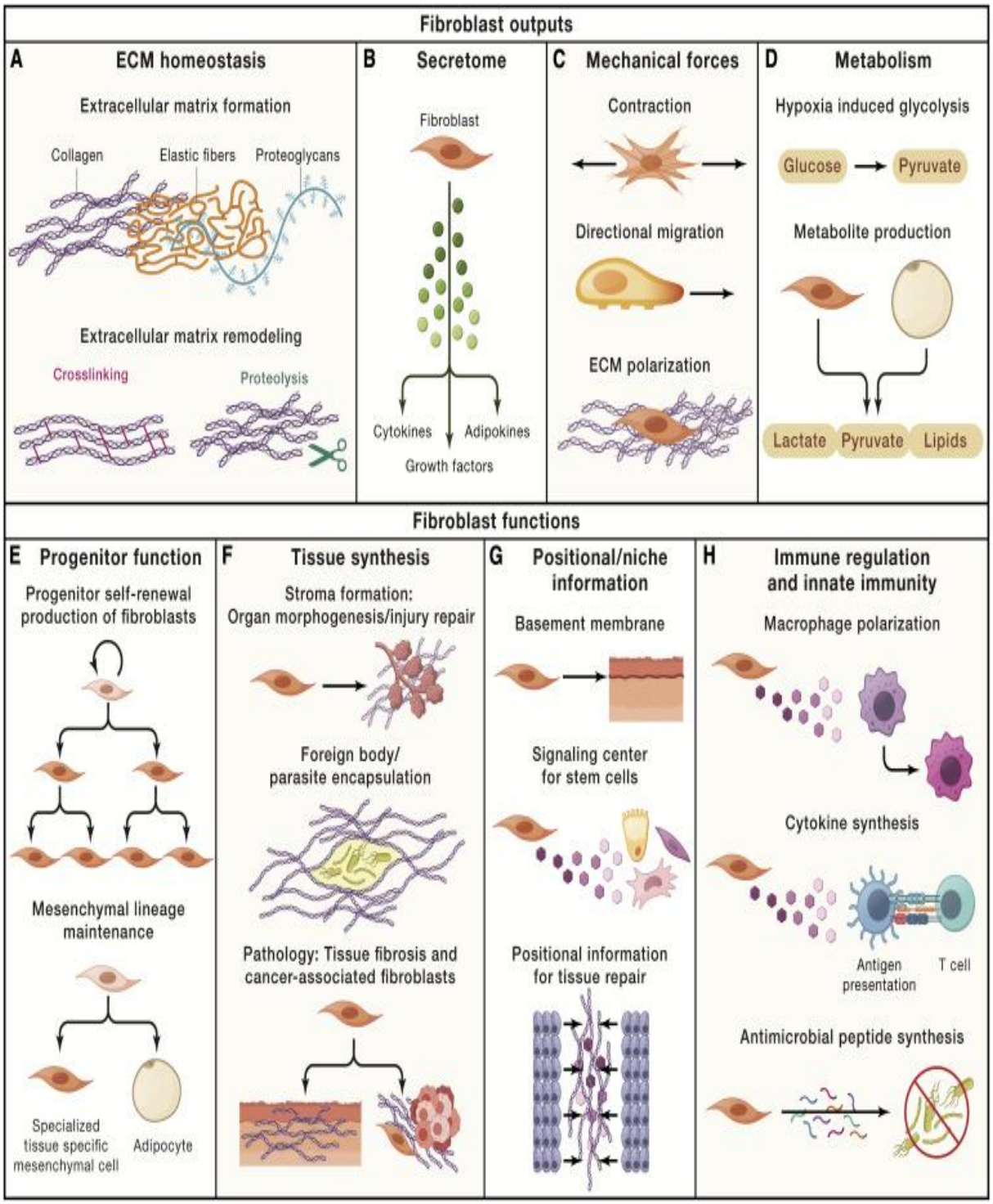

Figure 1.5: Summary of fibroblast output and functions.
The key outputs (A–D) of fibroblasts and their lineages includes extracellular matrix (ECM) homeostasis (A), secretion of signalling factors (B), mechanical force generation (C), and regulation of tissue metabolism (D). Fibroblasts (E–H) also function as progenitor cells for mesenchymal lineages (E), Tissue synthesis (F), provide intra-organ positional information and key signal contributors toward stem cells (G), as well as provide immune regulation (H) Adapted with permission from Fibroblasts: origins, definitions, and functions in health and disease, by Plikus. et al., 2022, Journal of Cell, 184(15), p. 3852 - 3872. Copyright 2022 by Elsevier.

These are activated fibroblasts that possess smooth muscle (SM) features such as the expression of α - SM actin and possession of intracellular gap junctions. These cells play a role in ECM synthesis and force generation which results in wound contraction secondary to ECM reorganization. Myofibroblasts morphologically present with a contractile apparatus of actin microfilaments and non-muscle myosin together know as stress fibres that terminate at the cell surface at an area known as the fibronexus. This specialized structure links the intracellular actin and extracellular fibronectin fibrils and provides mechano-transduction enabling the force generated by the myofibroblasts stress fibres to effect the ECM (Tomasek et al., 2002). Myofibroblasts also modulate resident immune cell functions and possess the ability to phagocytose dead cells (Plikus et al., 2021).

The utilization of primary fibroblasts rather than cancer cell lines for biological modelling has become fundamental in many avenues of studies particularly when focusing on cell cycle, apoptosis and DNA repair since they remain unaltered with respect to oncogene and tumour suppressor gene mutations which maintains intact cell cycle check points. This makes a fibroblast model a useful model for *in vitro* modelling for the effect of cellular stress in lieu of a biological organism due to cultivability and sensitivity to stressors. (Seluanov et al., 2010).

1.5. Earth and the electromagnetic spectrum

The Earth is constantly being immersed (Figure 1.6) in a continuous stream of electromagnetic solar radiation which can be divided into three major spectra based on wavelength (Narayanan et al., 2010). These are known as ultraviolet (UV) radiation (λ 280 – 400 nm), visible (Vis) light (λ 400 – 700 nm) and infrared (IR) radiation (λ 750 – 2800 nm) and make up 6 %, 52 % and 42 % respectively. The impact of solar radiation has been proven to have had an essential role in the evolution of life on this planet, however the sun`s radiant energy is a mixed blessing and excessive exposure is a major risk factor which has been proven to threaten health and well-being (Ichihashi et al., 2009; Polefka et al., 2012) The most clinically relevant of the terrestrial solar radiation is the ultraviolet region (200 – 400 nm) and can be split up into three components namely: UVA (320 - 400 nm), UVB (280 - 320 nm) and UVC (100 - 280 nm) and adequate photoprotection is required to circumvent the deleterious consequences of the aforementioned (Young, A. R. et al., 2017). Alternative forms of cosmic electromagnetic radiation do exist, such as radio waves (λ 1 cm – 100 km), microwaves (λ 1 mm – 1 cm) , x-rays (λ 0.1 – 10 nm) and gamma rays (λ >0.1 nm) however these are not considered to pose a health risk as the competent nature of the earth`s atmospheric barrier prevents these from reaching the surface which otherwise stunt or even eradicate life on the planet (Griessmeier et al., 2005; Zwinkels, 2015).

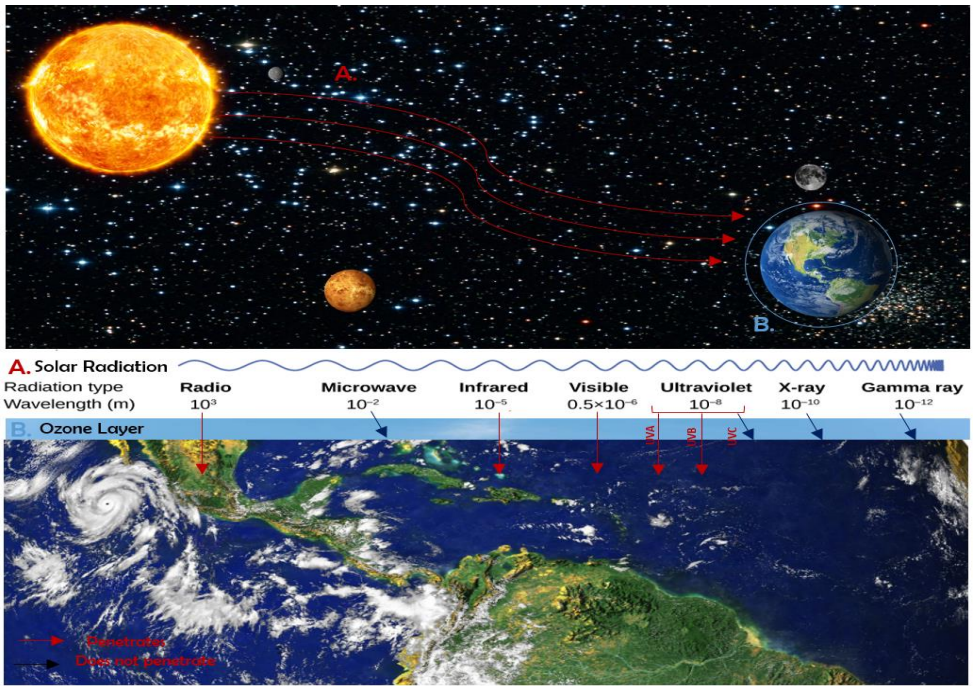

Figure 1.6: The complete electromagnetic spectrum

The complete electromagnetic spectrum being produced by the sun travelling in vacuum to earth, being filtered & attenuated by the atmosphere and finally bombarding the Earth`s surface. Adapted from (*The electromagnetic spectrum*)

1.6. Humanity and the sun - The drawbacks

Excessive solar exposure is a well-accepted risk factor for the development and aggravation of several pathologies (Queirós & Freitas, 2019). UVB accounts for approximately 5 % of the entire spectrum of terrestrial UV where its intensity peaks during the summer months between 10am and 5pm (Skotarczak et al., 2015). It is relatively high energy, and photons of UVB wavelength are absorbed directly by DNA (deoxyribonucleic acid) often causing aberrant alternations resulting in potentially mutagenic molecular lesions. Two of the most common mutagenic lesions include the formation of cyclobutane dimers between adjacent thymine or cytosine residues and the formation of pyrimidine (6-4) photoproducts among adjacent pyrimidine residues (Marrot & Meunier, 2008). In addition UVB leads to the formation of possibly the most recognisable UV related dermal insult, the formation of sunburn erythema, which is highly indicative of direct DNA damage, mediated through the induction of P53 and a plethora of inflammatory genes and pathways (Wondrak et al., 2006). In addition, UVB exposure can also be attributed to other adaptive responses such as keratinocyte proliferation (skin thickening) as well as melanogenesis (tanning) (Agar & Young, 2005; Brenner & Hearing, 2008).

UVA is minimally attenuated by stratospheric ozone and accounts for the majority of terrestrial UVR (95 %), where its intensity is independent of the time of the day or year. Although energetically weaker than UVB, UVA still has the potential to inflict critical cytotoxic damage to the skin (Gasparro, 2000; Park et al., 2009; Skotarczak et al., 2015). In a dissimilar, yet similarly detrimental manner UVA has an indirect photosensitization effect on key subcellular biomolecules, mediated by chromophores/photosensitizer such as flavins, porphyrins, tetracyclines, and in most circumstances in the presence of molecular oxygen (DeRosa & Crutchley, 2002). These chromophores absorb a photon of radiation. This leads to their excitation to a higher energy state which causes them to interact with adjacent molecules that undergo energy- or electron transfer resulting in the generation of reactive species capable of inducing oxidation. This leads to the initial formation of •R, $1O_2$, and •O and the subsequent formation of additional reactive species (H_2O_2, •OH, and •OOR) through secondary reactions (Cadet et al., 2009; DeRosa & Crutchley, 2002; Wondrak et al., 2006). Although not generally attributed to an overt cutaneous response (sunburn erythema), UVA is still considered a major causative agent towards the induction of photoaging, immunosuppression and photocarcinogenesis through the generation of reactive oxygen species that have a destructive effect on the structure of proteins and nucleic acids (Gasparro, 2000; Seite et al., 2010). The

most dangerous of all the UV radiation, UVC has the shortest wavelength thus the highest energy, however it is absorbed in a large part by the stratospheric ozone layer (Skotarczak et al., 2015).

There is irrefutable biological and epidemiologic data connecting skin malignancies to UV exposure where UV is the causative agent for approximately 90 % of non-melanoma skin cancer and 65 % of melanomas (Linos et al., 2009; Narayanan et al., 2010). Thus, UVR is the primary etiologic factor for carcinogenesis of the skin through direct and indirect genomic DNA damage and mutation. The major causative events to the observed pathological response to UVR is the direct molecular rearrangement of genomic DNA forming specific photoproducts and the generation of ROS that can damage DNA through indirect photosensitizing reactions (D'Orazio et al., 2013; Merwald et al., 2006). One of the most obvious effects of excessive exposure to UVR is the visualisation of UV induced inflammation, commonly known as a "sunburn". This event results in the formation of ROS within the skin cells. This generation of ROS exacerbates the situation with the cell, resulting in damaged macromolecules including DNA, protein, and membrane lipids. Furthermore, the acute inflammation induced by sunburn also triggers immunosuppression and reduces the effectiveness of the body's immune surveillance of cancer cells (D'Orazio et al., 2013). Cells respond to UV damage through the activation of DNA repair mechanisms as well as the alternative cytoprotective methods such as the increased production of HSPs (Gilchrest & Eller, 1999). This is vital as the alteration of DNA can ultimately lead to the development of skin cancer. However, the degree of success at preventing a deleterious outcome, is highly depending on the UV wavelength, exposure dosage, degree of DNA photodamage and cell type. The cells may enter apoptosis which is a crucial mechanism in eliminating cells with unrepaired or unrepairable DNA damage that thus prevents carcinogenesis. However, in certain situations this programmed cell death fails to occur resulting in the development of skin malignancies (Ziegler et al., 1994).

UVC is the most proficient at DNA damage coming in the form of pyrimidine dimers and 6-4 photoproducts in turn making it the most consequential with respect to carcinogenesis (Gentile et al., 2003). However, likely owing to the fact that UVC does not reach the earth's surface unlike UVA/UVB this wavelength of UVR remains poorly studied with respect to bio-analysis of toxicity, although artificial sources do exist from welding lights. bactericidal lamps and photocuring devices (Masuma et al., 2013)

1.7. Humanity and the sun - The benefits

Humanities evolution occurred in a sun-drenched environment, and although focus is often placed on the deleterious ramifications of the solar spectrum, that very spectral composition, its intensity and duration do have beneficial effects, which often go uncharacterised, and through the simple act of deprivation result in negative consequences (Holick, 2001). This foresight led to perceptive effect of 300 years of misery in the industrialised world as generation after generation of children were plagued by severe bone deformities, growth retardation and rickets (Hess, 1921; Holick, 2006)Although this crisis was conquered, there are to this day, still wide-ranging propitious effects on human health and causal morbidity and resultant mortality through solar deprivation, underestimating such effects would be at humanities peril (Autier & Gandini, 2007; Melamed et al., 2008). However, through understanding the effects of deprivation one can value the importance of sensible solar exposure and look beneath the surface to understand the health-promoting benefits. These are centred around the photoproduction of vitamin D_3 & photo-synchronisation of the circadian rhythm mediated by solar interaction with human physiology. Vitamin D`s existence predates the Cambrian explosion and is more than likely one of the most ancient hormones having been photosynthesised by organisms for more than 700 million years (Holick, 2003). This evolutionary engraining makes it understandable that most cells possess vitamin D receptors, where an estimated 200 – 2000 genes may be directly or indirectly controlled by the biologically active hormonal form of vitamin D, 1,25(OH)2D (Holick, 2011). This quietly affects the length and breadth of human physiology and can result in varied deleterious consequences if Vitamin D is deficient while conversely will be preventative to these same deleterious effect if the auspices of normality are maintained (Bikle, 2000). Vitamin D hypovitaminosis can mainly attributed to environmental & lifestyle factors that bring about a reduction in solar exposure to the skin. These factors include but are not limited to; sunscreen use (Matsuoka et al., 1987), skin pigmentation (Holick et al., 1981), season of year - latitude – time of day (Webb et al., 1988) and type of clothing worn (Matsuoka et al., 1992).

1.8. Photoprotection – A three-pronged approach

Modern photoprotection is a three-pronged approach relying heavily on the synergistic utilization of adequate sunscreen preparation, appropriate clothing and acceptable behaviour in response to exposure to sunlight. Thus, the proper application and reapplication of sunscreen protection is only part of a comprehensive photoprotection program. However, an ideal sun screening agent should be able to provide exhaustive protection against critical cytotoxic damage to the skin by impinging solar radiation, thus reducing the incidence of photosensitizing events and resultant consequences. However, in providing this coverage it should not lead to harmful consequences and therefore, should also be non-toxic, non-irritating and chemically inert. In addition, its photo-stable UV absorbing molecules should be formulated in a manner to resist removal when exposed to liquid medium (sweat or water) while maintaining their ability to allow for a uniform spread across the skin surface (Giacomoni et al., 2010; Latha et al., 2013). However, to substantially ensure adequate photoprotection to the level stated on the product a minimum of 2 mg/cm^3 of sunscreen is required, equivalent to 35 ml, which should be applied every second h to maintain Sun Protective Factor (SPF) value (Jeanmougin et al., 2014). Modern sunscreen works through the combination of both physical and chemical filters which together provide a competent comprehensive barrier to UV radiation.

Physical filters are large inorganic molecules of mineral origin, which operate on the principle of forming a barrier on the dermal surface which reflect and scatter the entire UV spectrum. Physical filters include inorganic compounds such as titanium dioxide and zinc oxide and block against a broad range of the solar spectrum (Skotarczak et al., 2015). Chemical filters are organic molecules that are in the vast majority aromatic molecules possessing a conjugated carboxyl group. Their super-structure allows for the absorption of high-energy UV radiation in the UVA and/or UVB band and the subsequent conversion to lower energy radiation, thus circumventing the deleterious consequence and limiting skin damage. Chemical filters can fall into one of three categories UVB blocking, UVA blocking or Broad Spectrum which block both UVA as well as UVB (Latha et al., 2013).

The most widely accepted procedure for the evaluation of sunscreen protection potential is based on its efficacy to prevent sunburn and is known as SPF (Skotarczak et al., 2015). SPF is based on the ratio of minimal erythemal dose (MED) of the protected skin when compared to the unprotected skin (Jeanmougin et al., 2014). The MED being defined as the lowest dose of

UV radiation that causes a minimally perceptible erythema reaction at 24 h after irradiation (Heckman et al., 2013). The SPF can also be expressed in the form of formula.

$$SPF = \frac{MED\ protected\ Skin}{MED\ unprodected\ skin}$$

Although sunscreens are known to be a less effective barrier to UV rays when compared to solar avoidance and physical barriers (clothing & shade), it is still the most widely used means of photoprotection. Several limitations exist that impair the photoprotective ability of sunscreens originating from poor compliance and inappropriate application (Hibler & Wang, 2016). One of the major issues currently with photoprotection is the gross under application of sunscreen on intentional exposure to the sun, with a distribution average of 0.5 mg/cm^2 when compared to the recommended 2 mg/cm^2 used to establish SPF rating (Jeanmougin et al., 2014). This blatant difference results in the actual SPF being only 20 – 50% of that desired (Young, 2000). Furthermore to be effective, sunscreens must be applied 30 minutes prior to exposure the sun and reapplied every 2 h while exposed (Hibler & Wang, 2016). In addition, a sparsely known fact is correlation between the reduction of SPF factor and wearing of clothes. This is perfectly exemplified by a study carried out by Beyer et al., 2010 where it was noted that the best option to maintain the highest degree of photoprotection offered by the selected sunscreen is to abstain from dressing after the application or to wait a minimum of 8 minutes before clothing to ensure the minimal loss of photoprotection (Beyer et al., 2010).

The use of suitable clothing is a frequently overlooked tool which if used correctly can be utilized to provide a simple yet highly effective broad protective barrier against solar radiation (Gies, 2007; Hoffmann et al., 2001). A barrier which unlike sunscreens does not suffer from the same pitfalls which often cause discrepancies in the degree of photoprotection, which makes the use of sunscreens rather temperamentally idiosyncratic. On the other hand the use of appropriate clothing is far less ambiguous in its degree of offered protection (Diffey, 2001).

Photoprotection can be achieved through the limitation of personal exposure to UVR (natural & synthetic sources) and although some considerations (geographic, cloud cover, terrain) are beyond one`s control an individual's behaviour will significantly affect personal exposure to UVR. Solar avoidance at times were UVR is at an increased strength, wearing UVR protective

clothing, seeking shade, and the use of sun-protective products are ways to achieve this (Murphy & Ralph, 2016). Thus a considerable reduction in UVR exposure can be achieved at additional cost and through purely behavioural means; namely the avoidance of the 3 h surrounding solar noon (were ~ 50 % of the UV happens) as well as the use of shade, natural or man-made which block a vast amount of UVR (Eide & Weinstock, 2006).

1.9. Oxidative stress – A cellular perspective

Oxygen homeostasis is a great paradox in which the very components essential for life could also be a threat its existence (Davies, 2000). Oxidative stress is a state in which the net cellular creation and retention of reactive oxygen species (ROS) within cytosol outweighs the intrinsic capability to nullify and remove these reactive species (Pizzino et al., 2017). This shift in the balance between oxidants and antioxidants results in the build-up of these ROS within cellular and tissular systems leading to a deleterious interaction of such species with a large amount of macromolecules which constitute these very systems (carbohydrates, lipids, protein and DNA). This could instigate or progress the pathophysiology of a number of ailments namely; cancer, ageing, diabetes, atherosclerosis and neurodegeneration (Birben et al., 2012; Kruk et al., 2019; Liguori et al., 2018).

1.9.1. Characteristics of Reactive Oxygen Species

ROS are composed of free radicals and other non-radical reactive derivatives that could lead to the formation of free radicals, also called oxidants. A free radical is defined as an atom or molecules that contains one or multiple unpaired electrons in its outer orbit, making such particles unstable, short-lived, and highly reactive. These are the characteristics that confer the ability of radicals to attack molecules through the assimilation of electrons resulting in acquired stability and given radicalization leading to a cascade redox reaction ultimately leading to biomolecular damage. The ROS free radicals include superoxide anion ($O_2^{\bullet -}$), hydroxyl radical ($OH^{\bullet}$), alkoxyl radical ($RO^{\bullet}$) and peroxyl radical ($ROO^{\bullet}$), while non-radicals include hydrogen peroxide (H_2O_2), singlet oxygen ($^1O_2$), Ozone (O_3), organic peroxide (ROOH), hypochlorous acid (HOCl) and hypobromous acid (HOBr) and are formed as a by-product of cellular metabolism through the partial reduction of oxygen. However, the three major ROS of significance are hydrogen peroxide, superoxide anion and hydroxyl radical (Bae et al., 2011; Pham-Huy et al., 2008; Phaniendra et al., 2015; Pizzino et al., 2017; Ray et al., 2012).

1.9.2. Generation of Reactive Oxygen Species

The generation of ROS can originate from several endogenous and exogenous sources (Figure 1.7). While endogenous sources encompass the internal machinery of the cell often because of normal cellular metabolism or processes, exogenous sources constitute the multiple environment sources which can trigger an induced oxidative response

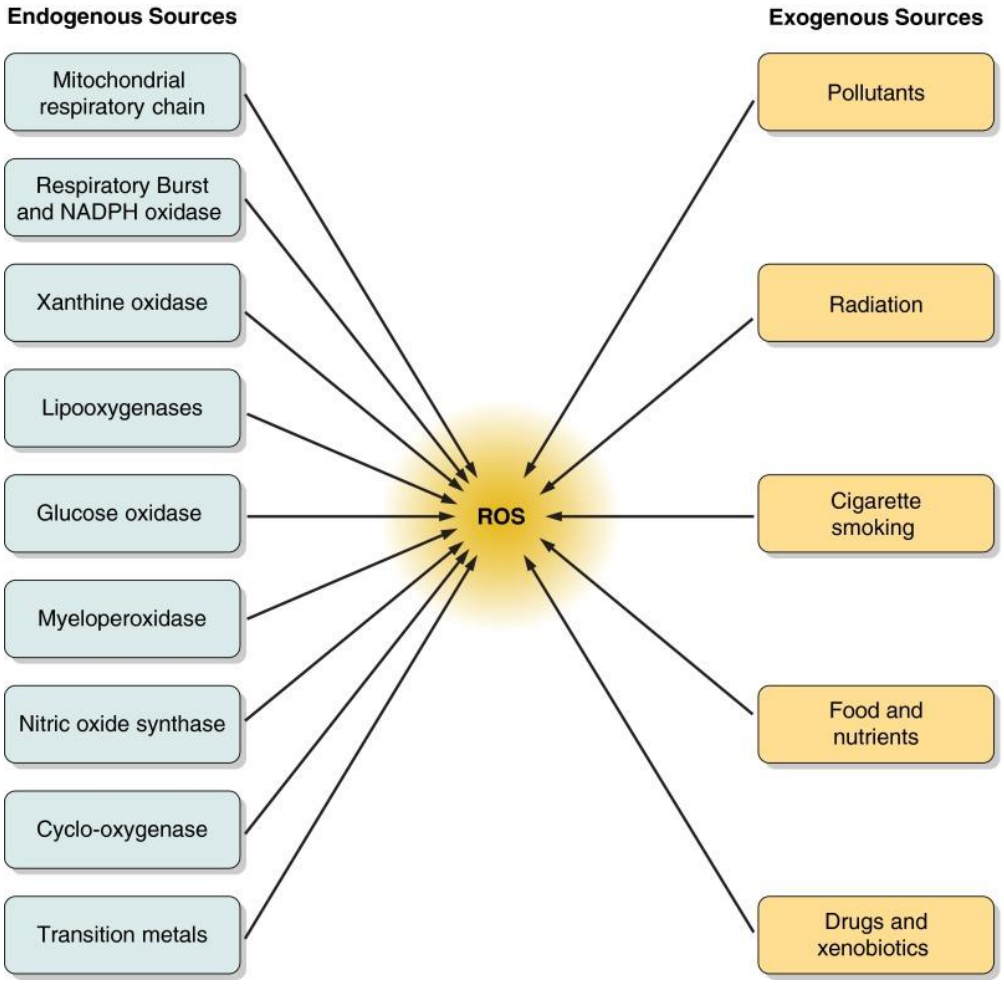

Figure 1.7: Examples of various sources of reactive oxygen species (ROS).
Reactive oxygen species originate from various sources both endogenously as well as exogenously and irrespective of their aetiology require nullification. Adapted with permission from Oxidative Stress: An Essential Factor in the Pathogenesis of Gastrointestinal Mucosal Diseases, by A. Bhattacharyya, R. Chattopadhyay, S. Mitra, et al, 2014, Physiological Reviews, 94(2), p. 334. Copyright 2014 by American Physiological Society.

1.9.3. Endogenous Sources of reactive oxygen species

Mitochondria are considered as the principle generators of the endogenous or intracellular ROS production in majority of cells during aerobic metabolism. As the power supply of the cell, mitochondria utilize oxygen (oxidative metabolism) during the synthesis of ATP by oxidative phosphorylation that is coupled to the electron transport chain (ETC) which is composed of complexes I – IV and cytochrome C found along the inner mitochondrial membrane and coenzyme Q (Kowaltowski et al., 2009). Normally electrons pass through the ETC until ultimately terminating in the reduction of oxygen into water. However, the transfer of electrons along the ETC does result in the incomplete oxygen reduction with the formation of superoxide anion, mainly at complex I and III of the ETC (Sharifi-Rad et al., 2020).

Peroxisomes are cytoplasmic organelles that contain enzymes (e.g., D-amino acid oxidase, acyl CoA oxidases, xanthine oxidase) that are involved in fatty acid oxidation, purine, glyoxylate and amino acid metabolism as well as being involved in H_2O_2 metabolism. However, as a direct consequence of these catalysing processes, ROS particularly superoxide anions and H_2O_2 are produced which despite high concentration of catalase within the peroxisome still leak outside and can cause oxidative stress related damage (Schrader & Fahimi, 2006).

Lysosomes are cytoplasmic organelles that utilize hydrolytic enzymes to degrade, amongst others, iron-rich macromolecules (proteins) and cellular components (mitochondria) resulting in the accumulation of intracellular iron (Boya, 2012). These iron molecules can react via the Fenton reaction with localized or translocated H_2O_2 resulting in the formation of OH• radicals. This can lead to membrane permeabilization and the release of the contents of lysosome which in part constitutes iron which translocated to various subcellular loci and on contact with H_2O_2 can lead to further OH• production and oxidative damage (Persson et al., 2005).

The endoplasmic reticulum (ER) is a dynamic organelle with various roles including protein synthesis/folding/transport, calcium storage, lipid metabolism and drug detoxification in specific cell types (Schwarz & Blower, 2016). The process of protein folding, primarily through the formation of intramolecular disulfide bonds is facilitated by protein disulfide

isomerase (PDI) and reticulum-resident protein (Ero1p) and results in induction of protein folding-induced oxidative stress protein (Chong et al., 2017). The process of xenobiotic detoxification within liver cells solubilizes the xenobiotic for easier excretion, however results in the production of ROS (H_2O_2) mainly through the monooxygenase reaction facilitated cytochromes P450 (Di Meo et al., 2016).

The plasma membrane possesses the ability to produce ROS mainly $O_2^{\bullet-}$ and H_2O_2 through membrane bound NADPH oxidases (NOX1 – NOX5) where different isoforms can be found in various cells (Suh et al., 1999). However, the most known of these ROS production targeted enzymes is found in phagocytic cells and is known as NOX2 which when activated generated large quantities of $O_2^{\bullet-}$ and H_2O_2 which are then used to target pathogenic intruders (external/internal) in a process known as a respiratory burst (Babior et al., 1973; Chanock et al., 1994).

1.9.4. Exogenous sources

Exogenous sources of ROS constitute the multiple environment sources, such as heat stress (Section 1.10) and non-ionizing radiation such as UV (Section 1.6), which can trigger an induced oxidative response. Some other examples are presented in Table 1.5.

Table 1.5: Exogenous sources of oxidative stress production.

Cigarette smoke	A significant generator of ROS where cigarette smoke can contain more than 10^{14} free radicals/puff as well as numerous oxidants and organic compounds which could result in secondary oxidative stress damage (Church & Pryor, 1985)**.**
Ozone exposure	Inhalation can overwhelm the antioxidant defences and can result in lipid peroxidation as the catalyst of oxygen reduction (Rivas-Arancibia et al., 2010).
Hyperoxia	This may result in the increased production of ROS secondary to increased oxygenation (Ottolenghi et al., 2020).
Ionizing radiation	Ionizing radiation (α, β, and γ rays and x-rays) in the presence of oxygen can all lead oxidative stress through the conversion of $OH^{\bullet}$, $O_2^{\bullet -}$ and organic radicals to H_2O_2 and ROOH which via Fenton reactions (Bhattacharyya et al., 2014).
Heavy Metals	Excessive levels of these ions (Fe, Cu, Cd, Hg, Ni, Pb and As) can lead to ROS through direct interaction with cellular molecules/radical producing system as well as metal catalysed Haber-Weiss/Fenton type mechanisms (Birben et al., 2012).
Foods	Nutritionally mediated oxidative stress is a mechanically diverse major risk factor resulting from a high carbohydrate and high animal-based diets as well as excessive fat consumption (Tan et al., 2018).
Chemotherapeutic Drugs	The primary toxic side effect of chemotherapeutic agents (e.g., anthracyclines, alkylating agents, and platinum coordination compounds) is the generation of ROS evident by reduced antioxidant levels and increased lipid peroxidation (Conklin, 2004).

1.9.5. Exogenous Antioxidants

Exogenous antioxidants (Table 1.6) are absorbed through proper nutrition and are vital in supplementing the endogenous antioxidant defences, in a unique yet equally important manner (Willcox et al., 2004).

Table 1.6: Exogenous sources of antioxidants

Vitamin A (Carotenoids)	Carotenoids exhibit broad antioxidant capabilities exemplified by the ability of beta-carotene to suppress lipid peroxidation and quench singlet oxygen (Bhattacharyya et al., 2014; Pham-Huy et al., 2008)
Vitamin C	Vitamin C must be absorbed nutritionally and is a principal antioxidant which reduces a wide array of ROS through electron donation (Bhattacharyya et al., 2014; Liguori et al., 2018).
Vitamin E	Vitamin E, particularly the biologically active α-tocopherol is an essential antioxidant that scavenges lipid peroxyl radicals thus protecting membranes from lipid peroxidation (Traber & Atkinson, 2007).
Minerals	The proper nutrition and absorption of 'antioxidant' minerals (Zn, Cu, Mn, Fe and Se) is vital for redox homeostasis as these are key components for antioxidant enzymes (e.g., Zn, Cu, Mn for SOD and Fe for catalase) (Di Meo et al., 2016).
Polyphenols	Polyphenols are known potent antioxidants and numerous studies have indicated diverse biological properties (Section 1.1.5) (Cory et al., 2018).

1.9.6. Endogenous Antioxidants

To counteract the effects of oxidants, the cell is equipped with a range of antioxidant defence mechanisms which can be broadly divided into enzymatic and non-enzymatic. The major cellular defensive line against ROS irrespective of the source are enzymatic and mainly comprise of catalase – Cat (dismutates H_2O_2 to H_2O and O_2), glutathione peroxidase - GPx (indirectly reduces H_2O_2 to H_2O), superoxide dismutase – SOD (dismutates $O_2^{\bullet-}$ to H_2O_2 and O_2) and heme-oxygenase (oxidative degeneration of heme) (Bhattacharyya et al., 2014; Birben et al., 2012; Chau, 2015). The second line of defence against ROS involves non-enzymatic endogenous antioxidants that are molecules characterised by the ability to inactivate these ROS and are represented by metal-binding proteins, transferring, ferritin, lactoferrin, albumin,

ceruloplasmin, metallothioneins, coenzyme Q10, glutathione, uric acid, melatonin, bilirubin and polyamine (Mirończuk-Chodakowska et al., 2018).

1.9.7. Macromolecular targets and consequences

When produced in excess, ROS creates a state known as oxidative stress which is a deleterious state that could greatly affect the major macromolecules of life (Figure 1.8) and can induce a variety of acute and chronic pathological processes such as;

Diabetes Mellitus which comprises of a group of chronic disorder resulting in hyperglycaemia due to defective secretion (type I) or resistance to the action of insulin (type II), are associated the development of an oxidative stress state (greater ROS & less antioxidants) and further pathology particularly related to micro/cardiovascular system if not correctly managed (Giacco & Brownlee, 2010).

Neurodegenerative diseases can be attributed to an innate susceptibility of the central nervous system to ROS due to the reduced levels of antioxidant enzymatic activity, elevated oxygen usage and high lipid content. A major complication of ROS on the central nervous system is lipid peroxidation leading to neuronal cell membrane malfunction and resultant potential damage. In fact, oxidative stress has been shown to be a major player in the pathophysiology of several neurodegenerative diseases such as Parkinson's, Alzheimer's, and Multiple sclerosis (Barnham et al., 2004).

Asthma is a common respiratory disorder characterized by chronic inflammation of the airways resulting in obstruction and reduced airflow. Numerous studies have now shown that a keystone in the pathophysiology of asthma is a net state of oxidative stress (greater ROS & less antioxidants) that results in tissue damage and thus inflammation (Cho & Moon, 2010).

Cataracts is a visual impairment characterized by increased eye lens opacity which possesses many risk factors (e.g., obesity, aging, smoking), however the oxidative stress have been shown to play a major role in the pathophysiology and both elevated levels of ROS and oxidation of DNA, lipids and proteins has been seen in cataract lenses compared to normal (Vinson, 2006).

Cardiovascular disease has a multifactorial pathophysiology with numerous risk factors. However, studies have now indicated that oxidative stress plays a part in the development of hypertension, congestive heart failure and atherosclerosis (Pham-Huy et al., 2008).

Cancer etiologically could result from or be exacerbated by ROS damage to the nuclear DNA which could result in oncogene activation and tumour suppressor gene inactivation which feeds the cycle and results in the creation of more ROS and further deleterious mutations (Phaniendra et al., 2015).

Rheumatoid arthritis is an autoimmune disease characterized by systemic inflammation in the joints resulting the pathogenesis of which centres around the generation of reactive oxygen species at the inflammation site with can lead to lipid peroxidation and the inhibition of the production of extracellular matrix (Jaswal et al., 2003).

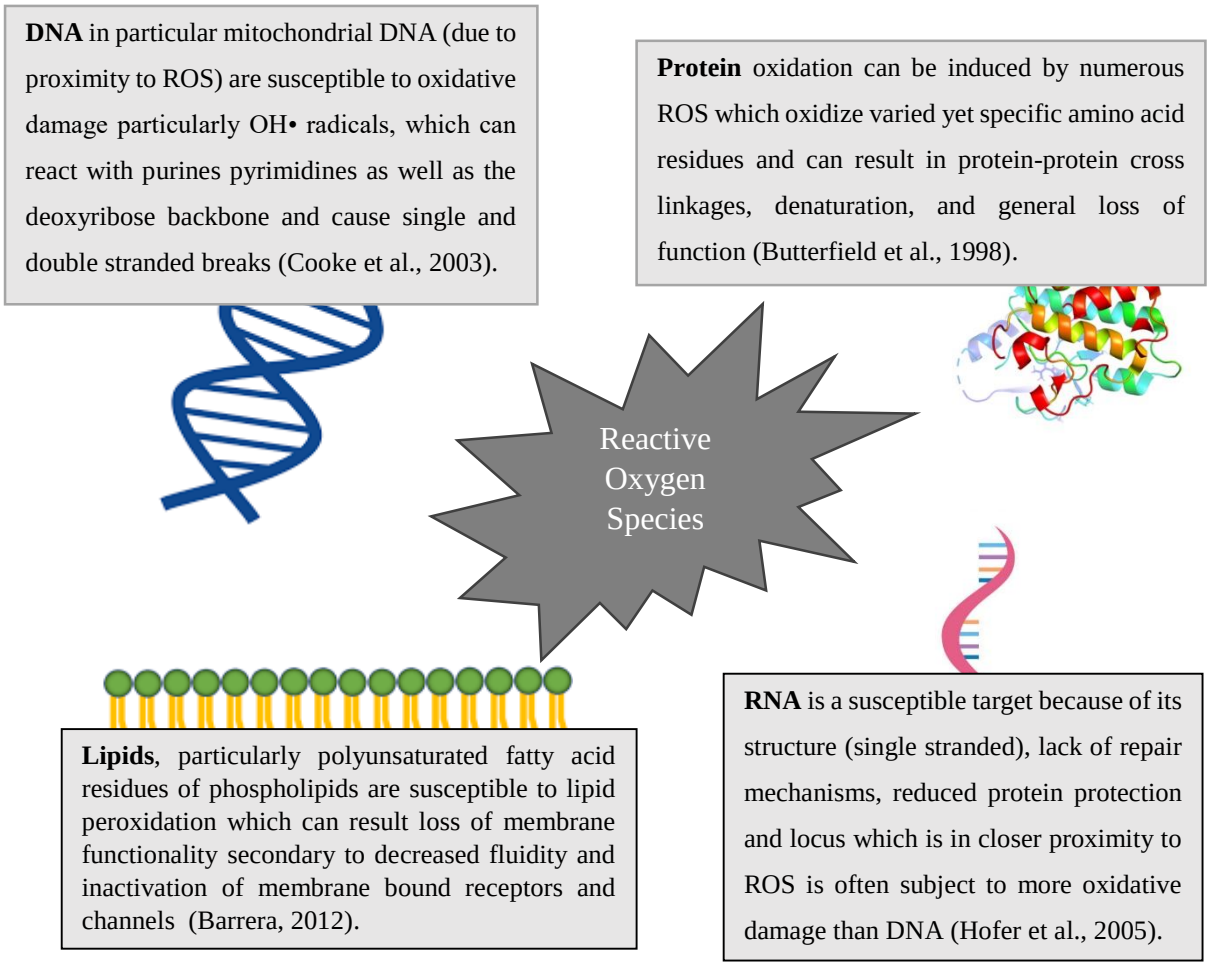

Figure 1.8: Major macromolecules affected by reactive oxygen species
When produced in excess, ROS creates a state known as oxidative stress which is a deleterious state that could greatly affect the major macromolecules of life is a varied of ways

1.9.8. Damage Alleviation

Fundamental for an organism's survival in an oxygen rich environment is the ability for damage alleviation and repair mechanisms for oxidized proteins, membrane lipids and DNA and number of strategies have been adapted by cellular biology to mitigate damage. Transient growth arrest is a cellular stress response intended to protect the mitotic cells from acute stress through induced growth arrest thus curtailing the prevalence of uncoiled and naked state DNA in diving cells which makes the Genome more susceptible to various forms for stress including oxidative stress and is known to be at least partially induced by gadd45, gadd153 and adapt15. Indirect repair mechanisms follow the same logical part regardless of the type of macromolecule that had been damaged. Firstly, the damaged macromolecules or section is recognized and excised, removed or degraded. This is then followed by the replacement of the entire macromolecule or the replacement of the damaged section (Davies, 2000).

1.9.9. Tools for the stimulation of oxidative stress

An important tool in the study of oxidative stress is Menadione, which is a quinone that is utilized as a model for studies of oxidative damage due to the mechanism to which a cytotoxic effect is instigated, through the generation of large quantities of ROS which can overwhelm the standard biological defences and lead to cellular injury and death (Castro et al., 2008; Chung et al., 1999).

1.10. A Cellular perspective to heat stress

Life has adapted to survive in a broad thermal range (0 – 113 °C) (Stetter, 2006). However, these adaptations to survival have hamstringed organisms into a narrow optimal growth temperature range, resulting in major stress if this range is even moderately exceeded (Richter et al., 2010). The effect of hyperthermia on cellular anatomy and physiology can be profound, to the extent of loss of viability, however this is dependent on the thermal dose (temperature + time) as well as the cell type (Roti Roti, 2008). On average heat shock becomes evident in eukaryotic cells when temperature is 3 - 8°C above normal which can result in hyperthermia-related damage to the cellular macromolecules (Welch & Suhan, 1985).

This small temperature increase within the hyperthermic range (40 - 47°C) has been observed to result in a disruption or malfunction of multiple cellular components namely, cytoskeleton, Golgi apparatus, nucleus, endoplasmic reticulum, and mitochondria as seen in Figure 1.9 (Roti Roti, 2008). One potential mechanism of cellular damage is through the disturbance of mitochondrial homeostasis, resulting in the overwhelming of the antioxidant defence mechanisms precipitating in heat-induced oxidative damage (Slimen et al., 2014). HS has been shown to lead to the inactivation of SOD activity as well as dramatically decreased glutathione (GSH) levels which together are required for complete detoxification of H_2O_2. This causes an accumulation of ROS, mitochondrial membrane depolarization which can result in heat-induced cytotoxicity (Katschinski et al., 2000). These ROS can then spread throughout the cell and lead to damage of various macromolecules affecting protein stability, making them more susceptible to HS related denaturation (Roti Roti, 2008). Hyperthermic heat stress results in extensive protein denaturation and resultant unspecific aggregation due to the exposure of normally buried hydrophobic residues that causes a massive imbalance in proteostasis, giving many of the phenotypic effects and counter effects evident in cellular hyperthermic heat stress (Lepock, 2005; Richter et al., 2010).

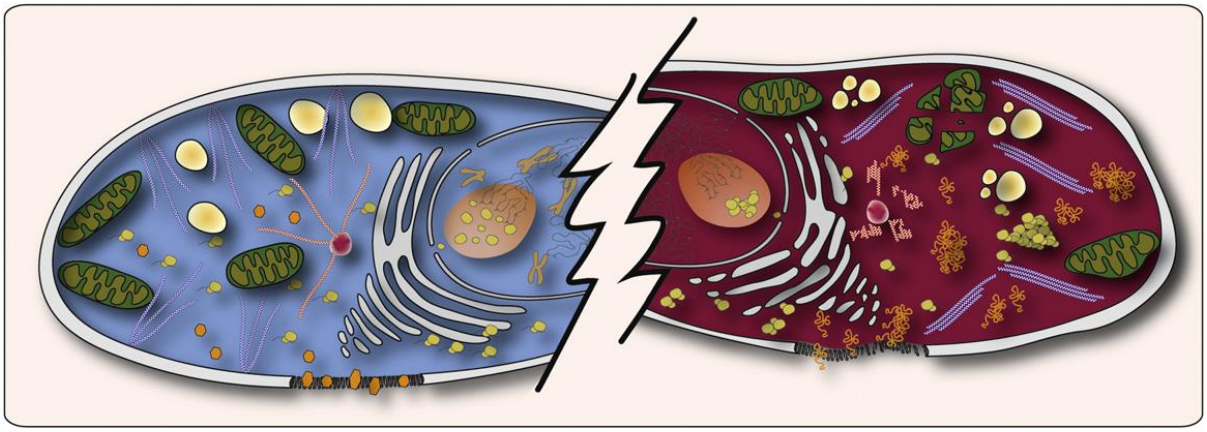

Figure 1.9: Effects of Heat Shock on the Organization of the Eukaryotic Cell
An unstressed eukaryotic cell (depicted on the left) compared to a cell experiencing heat stress (depicted on the right) both presenting distinct features. Heat stress induces alterations in the cytoskeleton, notably causing the transformation of actin filaments (depicted in blue) into stress fibres, along with the clustering of other filaments such as microtubules (depicted in red). Additionally, organelles like the Golgi apparatus and the endoplasmic reticulum (both depicted in white) undergo fragmentation and disintegration. The quantity and structural integrity of mitochondria (depicted in green) and lysosomes (displayed in a yellow-white gradient) decrease. Nucleoli, pivotal sites for ribosomal assembly (depicted in yellow), experience swelling, and prominent granular accumulations comprising ribosomal proteins become visible. These aggregations, known as stress granules (displayed in yellow), arise from the gathering of proteins and RNA in the cytosol, alongside protein aggregates (distinguished by their hexagonal and spaghetti-like structures, depicted in orange). Lastly, alterations in membrane morphology, the accumulation of membrane-associated proteins, and an augmentation in membrane fluidity are observed. Collectively, these effects culminate in the cessation of cellular growth and result in cell-cycle arrest, a characteristic indicated by the non-condensed chromosomes within the nucleus. Adapted with permission from The Heat Shock Response: Life on the Verge of Death, by K. Richter, M. Haslbeck, J. Buchner, 2010, Molecular Cell, 40(2), p. 253. Copyright 2010 by Elsevier.

The effect of loss of proteostasis is apparent throughout the cellular machinery however no more so than at the nucleus where aggregated proteins can critically accumulate in the nuclear matrix resulting in interference with transcription, replication, and DNA repair (Lepock, 2004).Formatting... The observed inhibition of DNA replication though the inhibition of replicons, elongation of replication fork and maturation of chromatin appears to be a regulated process that can be reversed upon cell cultivation under normal conditions and could be essential to genome integrity (Velichko et al., 2013). In fact, studies under HS on HDFs have shown G1/S phase arrest mediated by P53 which is translocated to the nucleus where it activates p23 which subsequently inhibits cyclin-CDK protein kinase complex (Nitta et al., 1997). However, this site-specific protein destabilization within the nucleus can cause further complications, most visible in S-phase cells through the creation of genomic instability and chromosomal aberrations not because of direct DNA damage but rather secondary to the

hyperthermic effects such as on the proteins involved in DNA replication/manipulation (Oei et al., 2015). This S-phase hypersensitivity on DNA replication is due to potential lethal lesions which could be repaired if the cell would be given the opportunity, through temporal distance to next DNA replication cycle not permitted during S-phase of the cell cycle rendering them as lethal devastations (VanderWaal et al., 2001). Together the totality of the effect of heat shock on the cell could lead cell cycle arrest, accumulation of aberrations which in turn could result in the loss of viability and trigger cell death. A significant portion of the phenotypic characteristics resultant of hyperthermia can be attributed to the aggregation of proteins and loss of proteostasis. Hence, it is logical to infer that the detrimental build-up of misfolded proteins acts as the signal to initiate protective responses. Intriguingly, this scenario proposes that the cell's reaction to heat is not driven by hyperthermia itself. Instead, it suggests that the heat shock response is prompted by the presence of unfolded proteins stemming from various stressors, such as oxidative stress, exposure to heavy metals, ethanol, or other harmful agents (Richter et al., 2010).

1.11. The protein problem

Proteins are the most versatile and functionally complex of the biological macromolecules and serve as the vehicle to which all genetic data is put into action. Eukaryotic mammalian cells are able to express a repertoire in excess of 100,000 individual protein specimens of varying lengths and complexities which fold to varying degrees into their native state which is required for the protein to achieve its biological function (Dobson et al., 1998).

However, since in the cytosol of a cell there are hundreds of ongoing macromolecular processes that involve proteins, these intra and inter protein interactions must be stringently controlled (Frydman, 2001). In fact, a defining dogma in protein biology is the ability of the cell to allow for native protein formation and the maintenance of the proteome integrity in the face of environmental stress (Hartl et al., 2011). This is vital concept as loss of protein homeostasis or proteostasis will lead to protein misfolding and aggregation which could progress to proteotoxicity and possibly the manifestation of related disease processes (Powers et al., 2009; Verghese et al., 2012). These include disorders such as type-2 diabetes, cystic fibrosis, dementia, cancer (melanoma), cardiovascular disease, Parkinson disease and Huntington's disease (Hartl et al., 2011; Young et al., 2004). However, to help confer a natural protection to cellular proteins and stave off the deleterious effects of environmental stresses, the cell produces molecular chaperones or heat shock proteins (Young et al., 2004).

1.12. Heat Shock Proteins

As the cell is exposed to external stresses that go beyond a moderate acceptable deviation from the norm, it can partake on one of two possible responses; apoptosis (programmed cell death) or a protective stress response (Feder & Hofmann, 1999). This protective cellular response was first observed by Ritossa (1962) where contrary to belief at the time, a transcriptional response could be stimulated in response to an environmental insult such as elevated temperature. This understanding led to the identification of heat shock proteins and the coining of the term Heat Shock Response. The terms 'Heat Shock Protein' and 'Heat Shock Response' are misnomers and are better described as stress protein and stress response due to the fact that all known stresses, if sufficiently intense can bring about this protective response through the up-regulation of one or more of these protective "Heat Shock Proteins" (Beere, 2004; Benjamin & McMillan, 1998; Feder & Hofmann, 1999).

Physiological stresses (Table 1.7) can result in an imbalanced intracellular environment where stress-induced conformational change and protein damage are abundant and can be evident on an organismal level through the development of symptomatic disease processes as well as the induction of a Heat Shock Protein (HSP) response through a common mechanism of transcriptional activation and preferential translation (Benjamin & McMillan, 1998). Although multiple intracellular pathways are involved in the restoration of cellular homeostasis and the prevention of the development of such disease processes, the most influential and well-described mechanism whose predominant function is the control of the stability of protein conformation, is the ubiquitous heat shock family of stress proteins (Díaz-Villanueva et al., 2015; Lindquist & Craig, 1988; Radons, 2016).

HSPs are molecular chaperones which are ubiquitously dispersed, cellular abundant, highly evolutionally conserved proteins that can account for 5-10 % of the total cellular protein content (Beere, 2004; Sarkar et al., 2011). They can be classified by size and include the HSP60 (58–65 kDa), HSP 70(68–75 kDa), HSP90 (82-90 KDa) and small HSPs (15 – 30 KDa) families. HSPs are intricately intertwined in vast array of proteome-maintenance functions, including *de novo* folding of proteins into their native conformation, refolding of denatured proteins, translocation of proteins macromolecules and facilitation of proteolytic degradation (Hartl et al., 2011; Sarkar et al., 2011). However, the precise function of each HSP and the mechanism of action involved in bringing their designated function to effect is family member specific.

Initially HSPs were only believed to be expressed during times of environmental stress as a mechanism brought into place by the cellular machinery to serve as a stabilizing force for proteasomic macromolecules insulted by a HSP stimulating external stress (Sarkar et al., 2011). However, it was later discovered that in addition to this 'stress response', several HSPs were also noted to be expressed in unstressed cells, with their expression only being upregulated in response to specific stimuli, including heat stress (Ellis, 1987; Feder & Hofmann, 1999; Latchman, 2001; Piano et al., 2004). The definition of such chaperones is a protein with the ability to reversibly interact with nearby proteins in order to stabilise or assist another protein to achieve its functionally active conformation without forming any part of its final structure (Hartl et al., 2011). Although heat shock proteins are synonymous with molecular chaperones, it is important to note that in fact not all heat shock proteins are chaperones (Gong et al., 2009).

Although historically, the focal point of research into HSPs has been the protective effect conferred to cells due the chaperone abilities of these proteins (Gething & Sambrook, 1992; Lindquist & Craig, 1988; Parsell & Lindquist, 1993). The function of HSPs has been shown to be far more expansive than once believed and now encompasses a broader avenue of action. These include an anti-apoptotic role (Beere, 2004), immunologic role (Javid et al., 2007) as well as cardiovascular role (Benjamin & McMillan, 1998; Latchman, 2001). Currently the upregulation of HSPs is of great therapeutic interest as a mechanism to confer cellular protection and thus provide a steadfast defence against a wide array of disease processes (Hartl et al., 2011).

Table 1.7: Environmental stressors that cause a heat shock response.

Psychological stress - (Sakharov et al., 2009) (Isosaki & Nakashima, 1998)	**Oxidative stress** - (Kalmar & Greensmith, 2009) (Ghosh et al., 2018)& (Tóth, Vígh, & Sántha, 2014)
Heat shock - (Ritossa, 1962)& (Satyal, Chen, Fox, Kramer, & Morimoto, 1998)**,** (Alagar Boopathy et al., 2022; Bouchama et al., 2017)	**Overload of the Endoplasmic reticulum** - (Henstridge, Whitham, & Febbraio, 2014)
Excessive Exercise - (Dimauro, Mercatelli, & Caporossi, 2016) & (Noble & Shen, 2012)	**Hypoglycaemia -** (Gobbel, Chan, & Chan, 1995) & (Bergstedt, Hu, & Wieloch, 1993), (Atkin et al., 2021)
Cold shock - (Holland, Roberts, Wood, & Cunliffe, 1993) & (Sonna et al., 2002)	**Inflammation** - (van Eden, 2015) & (Pockley, 2002)
Viral Infection - (Pockley, 2002), (Merkling et al., 2015)	**Hypoxia -** (Gobbel et al., 1995) & (Baird, Turnbull, & Johnson, 2006)
UV Radiation - (Jonak, Constanze et al., 2009) & (Jonak, Klosner, & Trautinger, 2006)	**Nutritional Deficiency** - (Kaul & Thippeswamy, 2009) & (Pockley, 2002)
Increase in Blood Pressure (Xu, Schett, Li, Hu, & Wick, 2000)	**Osmotic Shock** (Sheikh-Hamad, Garcia-Perez, Ferraris, Peters, & Burg, 1994) & (Beck, Grunbein, Lugmayr, & Neuhofer, 2000)
Amino Acid analogues - (Li, G. C. & Laszlo, 1985)	**Bacterial Products -** (Deitch, Beck, Cruz, & De Maio, 1995) & (Varano Della Vergiliana, J. F. et al., 2013)
Alcohol - (Tóth et al., 2014) (Muralidharan & Mandrekar, 2013)	**Intracellular Hypercalcaemia -** (Lu, T. et al., 2012) & (Wakita, Tokura, Furukawa, & Takigawa, 1994)
Radiation - (Lee, S. J. et al., 2001) & (Multhoff, Pockley, Schmid, & Schilling, 2015)	**Arsenide -** (Khalil et al., 2006; Wijeweera et al., 1995)

Environmental stressors which have been proven to alter the expression of heat shock proteins as a response to the insulting stress, as part of a cytoprotective response

1.13. Cellular Ageing and senescence

Ageing is a time-dependent complex chronic change in the physiology of a biological system and its impact is rising more than ever before to the forefront due to an ever increasing life expectancy and the sheer number of pathologies directly resultant of, or attributed to the temporally challenged biologically systems within the aging individual. Biologically it boils down to the temporal-associated cellular functional decay centred around proteostasis dysregulation often secondary to DNA damage which on accumulation leads to an increased chance or morbidity and mortality (Höhn et al., 2017). The process of aging involves a number of hallmark on molecular, cellular and organ level, however a major factor is the development of cellular senescence an irreversible process of cell cycle arrest of which there may be many aetiologies (Figure 1.10) and cellular features (Figure 1.11). Accumulation of senescent cell en masse is believed to be a principle player of biological ageing as it leads to functional tissue disruption and adult stem cells stunting (Mylonas & O'Loghlen, 2022).

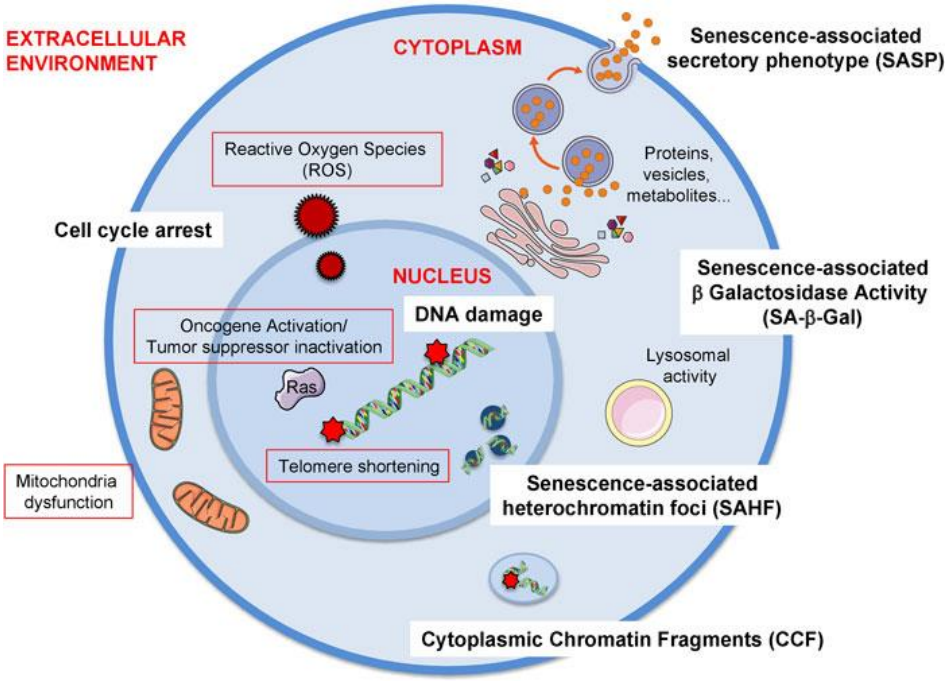

Figure 1.10: Trigger and biomarkers of cellular senescence.
Numerous instigators of the onset of cellular senescence (red outline) and markers that indicate senescence (white box). Triggers include Reactive ROS arising from both exogenous and endogenous sources, expression of specific oncogenes such as RAS (Rat sarcoma virus) or the loss of tumor suppressor genes like PTEN (Phosphatase and Tensin Homolog), mitochondrial dysfunction and telomere shortening. Adapted with permission from Cellular Senescence and Ageing: Mechanisms and Interventions, Mylonas & O'Loghlen, 2022, Frontiers in Aging, 3, p. 866718. Copyright 2022 by authors.

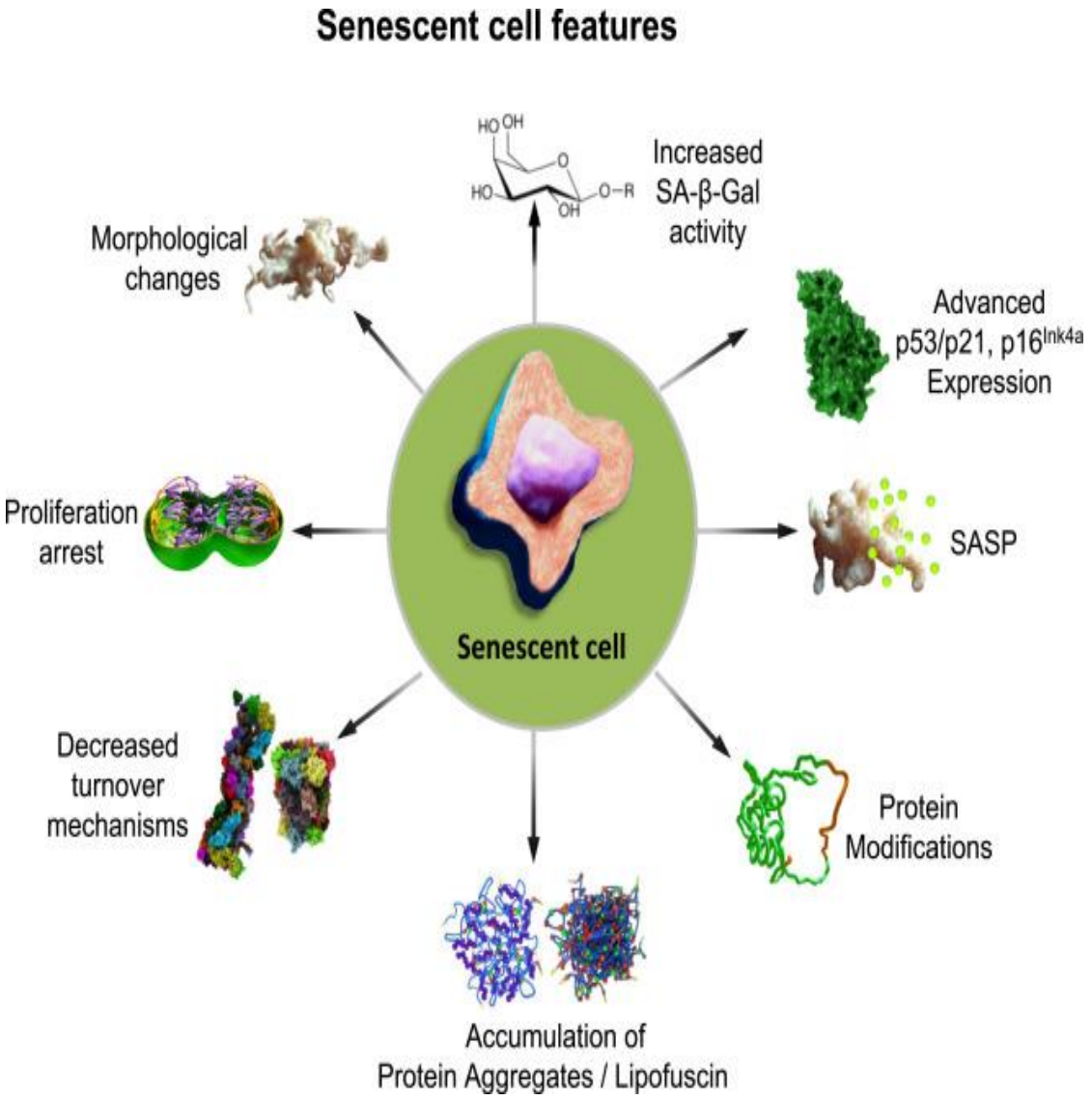

Figure 1.11: Features of senescent cells
Several markers have been identified to characterize the state of cellular senescence in terms of both morphology and proteostasis. As cells undergo senescence, they undergo noticeable morphological alterations, including an increase in size, protein content, and nuclear size. The lysosomes undergo an increase in magnitude, resulting in heightened SA-β-Gal activity, a widely used indicator of senescence. Cells experience a cessation in proliferation, marked by elevated levels of cell cycle inhibitors such as p53/p21 and the tumor suppressor p16INK4a. Senescent cells also release cytokines, chemokines, growth factors, proteases, fibronectin, as well as reactive oxygen species (ROS) and reactive nitrogen species (RNS). This combined secretion is referred to as the senescence-associated secretory phenotype (SASP). Furthermore, senescence involves changes in proteostasis, characterized by an upsurge in modified proteins, accumulation of protein aggregates, and reduced functionality of the proteasomal and autophagy systems. Adapted with permission Happily (n)ever after: Aging in the context of oxidative stress, proteostasis loss and cellular senescence, Höhn et al., 2017, Redox Biology, 11, p. 482 - 501. Copyright 2017 by Elsevier.

It is well established that oxidative stress is a key event in the development and progression of senescence. This is supported principally by two lines of thought, that the levels of oxidative stress products are elevated in senescent cells and aged organisms and that submitting cells to hyperoxia has been shown to present with a gene expression profile comparable to aged fibroblasts (Warraich et al., 2020). Heat stress (45 °C for 30 min) has also been observed to induced p21 dependant senescence-like cell cycle arrest particularly in S-phase cells on human dermal fibroblasts (Velichko et al., 2015). Furthermore numerous models have indicated that exposure to subcytotoxic level of UV radiation (UVA/UVB) to human fibroblasts and keratinocytes can result in the characteristic hallmarks of senescence (Debacq-Chainiaux et al., 2012).

1.14. Skin Ageing

The skin is comprised of a multitude of specialised cells each with a targeted function and each with different proliferative capacities. Skin aging occurs with advancement of age and upon exposure to intrinsic and extrinsic factors similar as Section 1.13 (Ho & Dreesen, 2021). Principle intrinsic risk factors include age, gender and ethnicity while extrinsic include pollution, nutrition, chemicals, smoking, and UV exposure (Wong & Chew, 2021). These induce skin aging, where in essence senescent cells accumulate with the human skin, leading to impaired skin physiology (Figure 1.12) and results in slower regenerative capabilities and eventual deterioration of skin microarchitecture and physiology. This altered pathological physiology leads to a compromised skin paradigm resulting in varying degrees of diversion from standard and can result in morbidity such as impaired wound healing, increased inflammation, loss of thermoregulation and carcinogenesis (Ganceviciene et al., 2012).

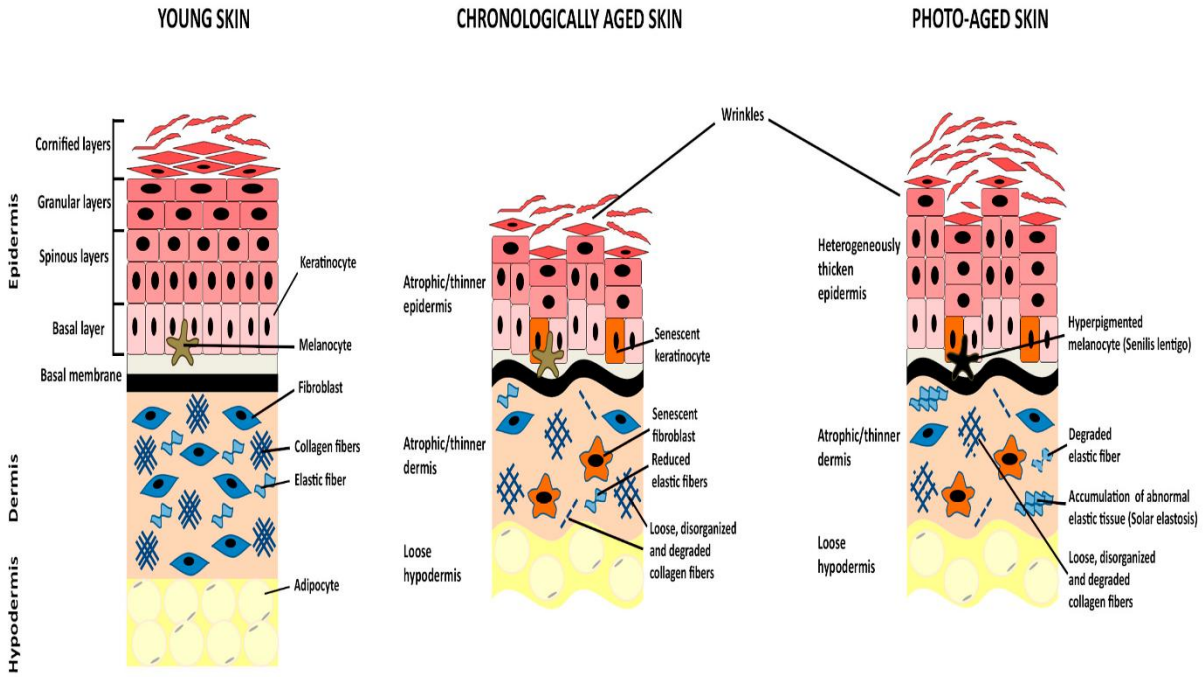

Figure 1.12: Morphological features of different forms of skin
The epidermis is a layered epithelial tissue consisting of keratinocytes arranged into four primary strata representing progressive stages of maturation, along with the presence of melanocytes. The dermis hosts fibroblasts interwoven with extracellular matrix elements like collagen, elastic fibres, glycoproteins, and proteoglycans. The hypodermis is predominantly occupied by adipocytes. Adapted with permission Epigenetic Regulation of Skin Cells in Natural Aging and Premature Aging Diseases, Orioli et al., Cells, 7 (12), p. 268. Copyright 2018 by Authors

Skin ageing occurs naturally however the effect of UVR on the skin is considered to be the most consequential extrinsic factor and is superimposed chronologically aged skin and is known as photo-aging. Photo-aging is a multistep systematic degenerative process that involves the skin and results from photo-damage resultant from exposure to UVR as seen in Figure 1.13 (Tobin, 2017). Chronological skin aging is dominated by fine lines and tissue laxity while photo-aged skin manifests as rhytids, mottled pigmentation, lentigines, coarse texture, sallow colour, deep furrows and leathery appearance amongst other visual characteristics (Han et al., 2014). Heat stress occurs quickly on direct exposure to solar plexus of summer sun where the skin can heat up to about 40 °C within 15 minutes through infrared light absorption and is now being considered as a contributing factor for sun-induced skin aging coined at thermal aging although this avenue of research is still at its infancy (Seo & Chung, 2006). Oxidative stress is also a major factor towards skin aging and ROS production is generally secondary to an insulting stimuli and possess a diverse aetiology as previously discussed (Section 1.9) (Chen et al., 2021).

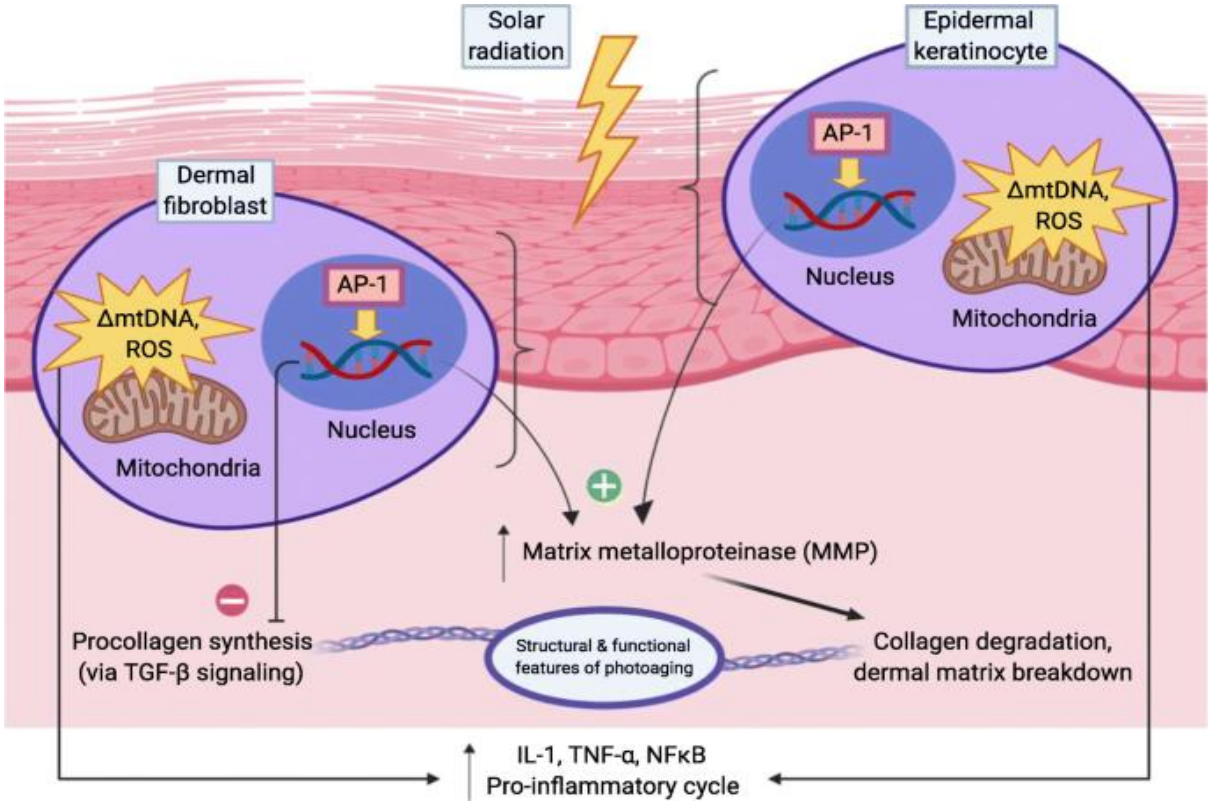

Figure 1.13: Pathogenesis of photo-aging
This is a basic diagrammatic representation of the pathogenesis of photo-aging after UVR exposure. Adapted with permission Photoaging: A Review of Current Literature, Huang et al., 2020, Current Dermatology Reports, 9, p. 22 - 29. Copyright 2020 by Springer Nature

1.15. Carcinogenesis

It is estimated that there were at least 19.3 million new cases of cancer and subsequently 10 million deaths from cancer in 2020, making it a leading cause of morbidity and mortality worldwide (Sung et al., 2021). In mature adults, cellular replication, and differentiation, in most circumstances is limited to normal turnover constrained to simple cellular replacement which is vital to repopulate tissues and organs (He et al., 2007). The human body demonstrates elegant control over cell numbers maintaining a delicate balance between cell formation and removal, one which if not maintained has the potential to increase the total number of cells in a particular tissue or organ, resulting in neoplasia (Bertram, 2000).

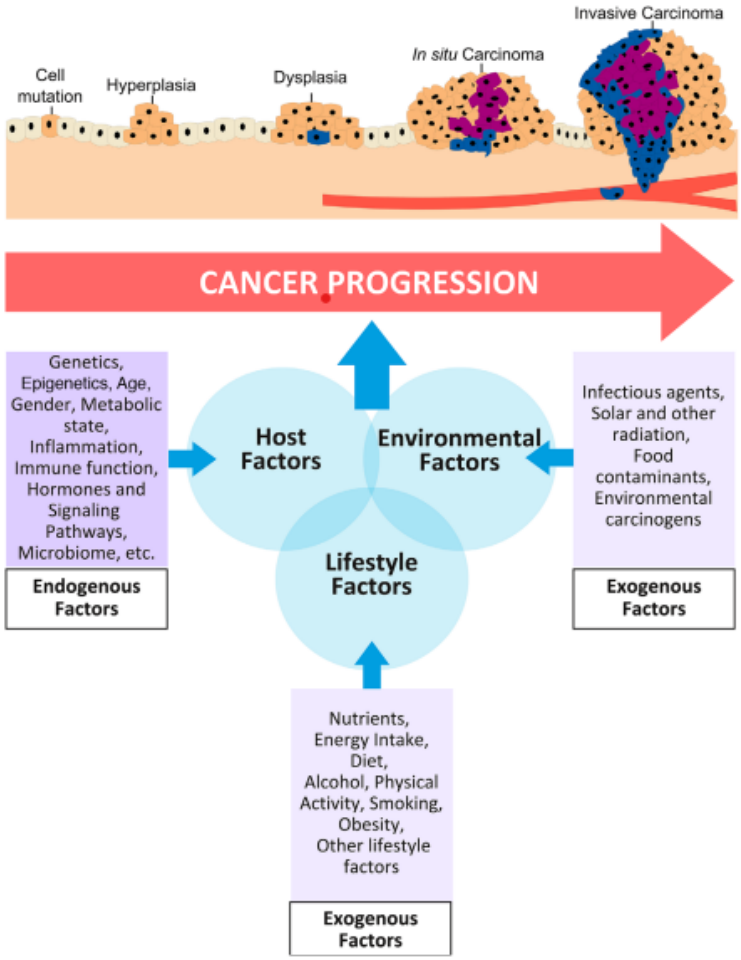

Figure 1.14: Risk factors for carcinogenesis.
The progression of cancer is influenced by an intricate interplay of inherent host elements (endogenous risk factors) like genetic predispositions and epigenetic markers, alongside exogenous factors that can heighten the risk of mutations over time, such as exposure to UV radiation, alcohol intake and infectious agents. Adapted with permission from Berry chemoprevention: Do berries decrease the window of opportunity for tumorigenesis, by May et al., 2020, Food Frontiers, 1(3), p. 260-275. Copyright 2020 by the authors.

A neoplasm (tumor) is any abnormal proliferation of cells, which many be benign (non-invasive) and remain localised or malignant (invasive) and possess the ability to invade tissue, metastasize and proliferate (Couch, 1996). Carcinogenesis occurs because of somatic mutations being passed on to a daughter cell bypassing defence procedures and forming the cell-of-origin possessing tumorigenic transformation because of these genetic mutations (Rycaj & Tang, 2015) and (Blanpain, 2013). These mutations can occur spontaneously or be induced directly/indirectly through exogenous factors (Figure 1.14) which may include Heat stress (Section 1.10), Oxidative Stress (Section 1.9) and UV (Section 1.6). From a functional perspective, mutations can have two distinct consequential targets; oncogenes, whose activation results in amplification of signalling pathways related to proliferation and tumor suppressor genes, whose deactivation results in the lack of coded proteins that serve as checkpoints for cell proliferation and death. Thus, tumor suppressor gene inactivation and/or oncogene activation results in the phenotypic properties in the cancer genesis, simply put; resistance to apoptosis, infinite proliferative capacity, angiogenic potential, independence to growth stimulatory signals and resistance to growth inhibitory signals (Bertram, 2000).

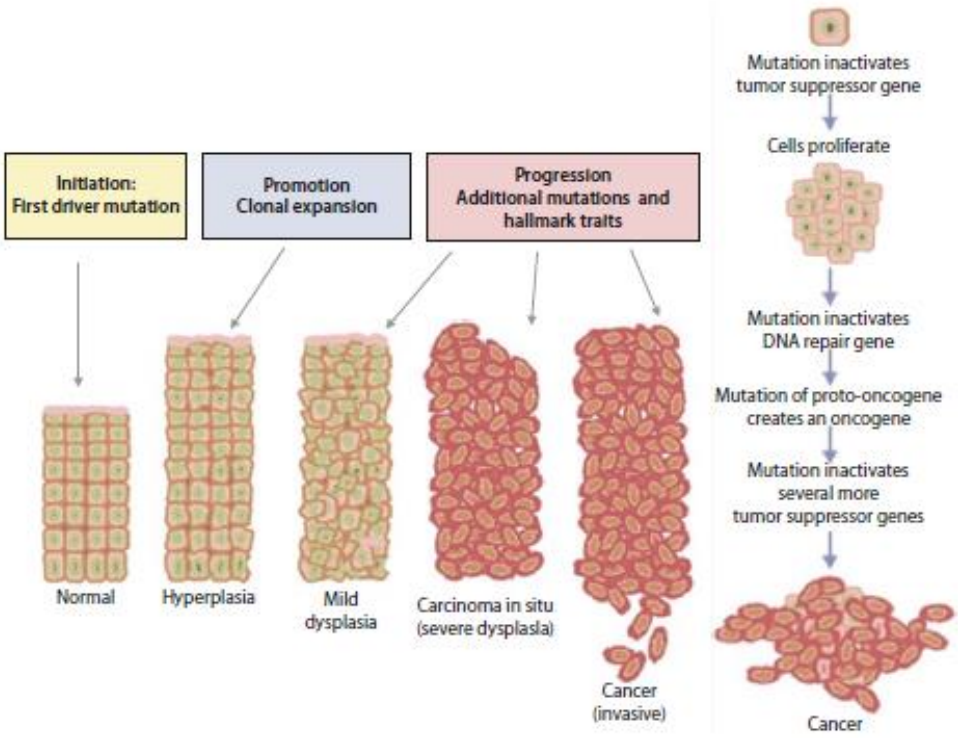

Figure 1.15: Basic Scheme of cancer progression
This is a basic diagrammatic representation of the progression of cancer from normal to invasive. Adapted with permission Cancer Initiation, Promotion, and Progression and the Acquisition of Key Behavioural Traits, by Compton, 2020, In Cancer: The Enemy from Within, Copyright 2020 by Springer, Cham.

Cancer is an umbrella term for any form of abnormal growth of the cell types within the body, resulting in over a hundred distinct cancer types which can be thought of as a unique diseases and exhibit diverse behaviours and responses to treatments. Cancer can be seen as multistep process (Figure 1.15) where its origin does not occur instantaneously but rather insidiously over temporal distance along a succession of genetic and molecular changes, where each change enables a further change, tallying up more and more abnormalities that lead to the creation of malignant growth, often over an extensive time frame that can normally take decades. This is the reason why cancer incidence increases with age, carcinogens exposure and predisposing mutations which defiantly move the bar towards increasing the probability of developing cancer during a normal life span (Hassanpour & Dehghani, 2017). Apart from the regulatory functions provided by proto-oncogenes and tumor suppressor genes to control cell proliferation which have previously been mentioned, cells possess at least three additional mechanisms to prevent uncontrolled cell division.

The first of these mechanisms is the DNA repair system, active in almost all cells. It identifies and rectifies DNA errors caused by exogenous carcinogens, internally generated chemicals, and replication mishaps. Generally, these errors are swiftly repaired. However, if the system fails, the error transforms into a permanent mutation, persisting in the cell and its descendants. The system's effective operation explains why a significant amount of time is usually required for the accumulation of mutations necessary for cancer development in a single cell. Mutations in DNA repair genes can critically impair this repair process, significantly elevating the frequency of mutations, including those in cell growth control genes (Hoeijmakers, 2001; Jakóbisiak et al., 2003).

A second safeguarding mechanism in cells triggers programmed cell death (apoptosis) upon damage to essential components or deregulation of control systems. The observation indicates that tumours arise from cells that have evaded this self-destruction process. An example of this evasion involves the P53 protein. Normally, P53 not only halts cell division but also induces apoptosis in abnormal cells. However, P53, a product of a tumor suppressor gene, is deactivated in many cancer types. The evasion of apoptosis poses two risks for cancer patients. Firstly, it promotes tumor growth, and secondly, it renders cancer cells resistant to treatment. Formerly, it was believed that therapies like radiation and chemotherapy directly killed cancer cells by harming their DNA. However, these treatments actually induce slight DNA damage, prompting the damaged cells to self-destruct. This realization indicates that cancer cells capable of

evading apoptosis will respond less effectively to treatments compared to other cells (Hoeijmakers, 2001; Jakóbisiak et al., 2003).

The third backup system curbs the number of cell divisions, ensuring that cells can't proliferate endlessly. This mechanism relies on a counting process involving DNA segments at chromosome ends known as telomeres. These segments shorten with each chromosome replication. When telomeres become shorter than a certain threshold, they trigger an internal signal causing the cell to halt division. If division continues, further telomere shortening can lead to chromosome breakage or fusion, culminating in cell death. Early observations of cultured cancer cells unveiled their ability to proliferate without limits, in contrast to normal cells. Recently, the molecular basis for this trait has been elucidated: an enzyme called telomerase. This enzyme is largely absent in mature cells but is prevalent in most cancer cells (Hoeijmakers, 2001; Jakóbisiak et al., 2003).

All in all, cancer is a multifaceted series of related diseases that require a series of molecular and genetic events, possibly intertwined with exogenous and endogenous risk factors that through time lead to the emergence of potential life threatening pathologies. Although remarkable progress has occurred in the field of cancer research, with significant breakthroughs in the understanding, prevention, and treatment of cancer, the disease continues to affect millions of people worldwide.

1.16. Aims and Objectives

The aim of this study is to analyse the effectiveness and mechanisms of action of the selected plant extract – prickly pear extract – as a mode of protection against the cellular damage induced by cellular stressors on human dermal fibroblasts. This extract was produced from a local cultivar of *Opuntia ficus-indica*, by Nutribiotech Services Limited, Malta. Specifically, the cellular stressors optimised in this study were, heat stress, oxidative stress and UV irradiation that may result in numerous deleterious effects on the cellular microarchitecture and cellular physiology thereby the biological system and organism as a whole. A successful conclusion to the study would lead to the development and understanding of a novel innovative approach to the protection against cellular damage incurred by these cellular stressors facilitated through the application of the prickly pear extract. Thus, resulting in a cytoprotective mechanism, that can protect against UV, heat stress and oxidative stress and resultant pathologies secondary to the effect of these injurious stimuli including but is not limited to, sunburn, cellular aging, and carcinogenesis, and will keep Malta at the forefront of this field of research as well as enhance the country's international scientific credentials. The objectives of this study were as follows;

- To review and consolidate existing literature around cellular stressors and their effect on cellular physiology, resultant pathologies and the influence of similar prickly pear extracts on counteracting cellular stress.
- To establish a cell culture model for human dermal fibroblasts with optimised growth and maintenance conditions for experimentation.
- To assess the cytotoxicity and biocompatibility of the prickly pear extract on human dermal fibroblasts with a range on concentrations and durations of exposure times and the impact of these cellular stressors on human dermal fibroblasts with and without the optimised prickly pear extracts treatment time, evaluating change using cell viability assays.
- To quantify potentially bioactive components within the prickly pear extract through the use of chemical analysis.
- To elucidate the underlying mechanisms by which the prickly pear extract mitigates the deleterious effect of cellular stress on human dermal fibroblasts through the use of transcriptome analysis using RNA sequencing.

All this was carried out in parallel with the prickly pear extract carrier – propylene glycol in order to normalise findings. This approach will provide a comprehensive and thorough analysis of the cellular changes that occur in response to stress and how these changes are altered by the protective action of the bioactive molecules in the prickly pear extract.

Chapter 2 Materials and Methods

2.1. Materials

2.1.1. General materials

A wide array of materials were utilised for the various methodologies carried out in this study. These included; EDTA (Sigma-Aldrich, Germany), Sodium Hydrogen Carbonate (Roth, Germany), Menadione (Sigma-Aldrich, Germany), 70% Ethanol (Sigma-Aldrich, Germany) Dimethyl sulfoxide (DMSO) (Sigma-Aldrich, Germany), Hydrochloric acid (Sigma-Aldrich, Germany), Gallic acid (Sigma-Aldrich, Germany), Folin-ciocalteu reagent (Sigma-Aldrich, Germany), TPTZ (Sigma-Aldrich, Germany), Iron(III) chloride (Sigma-Aldrich, Germany), Sodium carbonate (Sigma-Aldrich, Germany), Protocatechuic acid (Sigma-Aldrich, Germany), QIAzol Lysis Reagent (QIAGEN, Germany), Absolute Ethanol (Carlo Erba, Italy), , Chloroform (Sigma Aldrich, Germany), Sodium Molybate (Sigma-Aldrich, Germany), Sodium Nitrite (Sigma-Aldrich, Germany), Sodium Hydroxide (Sigma-Aldrich, Germany), Quercetin (Sigma-Aldrich, Germany), Aluminium chloride (Sigma-Aldrich, Germany), Copper Chloride (Sigma-Aldrich, Germany), Ammonium Acetate (Sigma-Aldrich, Germany), Neocuproine (Sigma-Aldrich, Germany), Absolute Methanol, DPPH (Sigma-Aldrich, Germany), Ascorbic Acid (Sigma-Aldrich, Germany), ABTS (Sigma-Aldrich, Germany) and 5x HOT FIREpol® EvaGreen® qPCR mix plus (ROX) (Solis BioDyne, Tartu, Estonia)

2.1.2. Kits

Several kits were utilized for the various methodologies and unless otherwise stated all materials were provided by said kit. These include; Cell Titre Glo® Luminescent cell viability Assay (Promega, USA), PrestoBlue™ Cell Viability Reagent (ThermoFisher Scientific, USA), RevertAid first stand cDNA synthesis kit (ThermoFisher Scientific, USA) and RNeasy® Plus Mini (Qiagen, Germany).

2.1.3. Cell Culture Preparations

The methods of preparation of the solutions pertaining to the cell culture experiments conducted in this study are detailed in Table 2.1.

Table 2.1: The list of cell culture specific materials utilised, and manipulations required.

Materials	Preparation Carried out
Dulbecco`s Modified Eagle Medium/ F12 (1:1) (DMEM) (Pan Biotech, Germany)	DMEM powder (11.70 g) and $NaHCO_3$ (1.2 g) were dissolved in 1000 ml of distilled water (pH of 7.4) and was filter sterilised using 0.2 µm Sterivex™ Filter units (Millipore, Germany). The DMEM was completed through the addition of 10 % (v/v) foetal bovine serum and 0.2 % (v/v) penicillin-streptomycin.
Dulbecco`s Phosphate Buffered Saline (PBS) (Sigma-Aldrich, Germany)	PBS powder (9.6 g) was dissolved in 1000 ml distilled water and the solution was autoclaved
Foetal Bovine Serum (FBS) (Gibco®, USA)	Thawed, and stored at -20 °C in 20 ml
Menadione (Sigma-Aldrich, Germany)	Dilutions of menadione (100 µM, 50 µM, 25 µM, 12.5 µM, 6.25 µM and 3.125 µM) were prepared through the appropriate dilution of the stock solution of menadione in DMEM (0.1 M) and filter sterilised (0.2 µm).
Penicillin-Streptomycin (Sigma-Aldrich, Germany)	Thawed, aliquoted (2 ml) and stored (-20 °C) until use.
Trypsin - EDTA Solution 10× (Sigma Aldrich, Germany)	Thawed, aliquoted (5 ml) and frozen until use. It was then diluted 10× with PBS in a sterile environment and stored (2 – 8 °C) until use.
Trypan Blue 0.4 % (ThermoFisher Scientific, USA)	Filter sterilised (0.2 µm) and stored in a sterile environment at room temperature.
EDTA (pH 8) (Sigma-Aldrich, Germany)	2.922 g EDTA powder was added to 50 ml Deionized Water Filter Sterilised

This shows all the various reagents, buffer, solutions, and media that were used throughout this study, their manufacturer, any in-lab preparation carried out and the sterilization techniques utilized to ensure an effective aseptic technique and/or to prevent contamination. Filter sterilisation was carried out 0.2-micron filters. All autoclaving was carried out at 121°C, 15 psi for 20min.

2.1.4. Chemical Assay Specific Preparations

The methods of preparation of the solutions pertaining to the chemical assay experiments conducted in this study are detailed in Table 2.2.

Table 2.2: The list of general materials utilised, and manipulations required.

Materials	Preparation Carried out
Methanolic DPPH (2,2-Diphenyl-1-picrylhydrazyl) Reagent	Made fresh by preparing a 60 µM DPPH solution in absolute methanol. Following preparation it was kept in the dark at 4 °C
ABTS (2,20 -Azino-bis(3-ethylbenzothiazoline-6-sulfonic acid) Radical Solution	Prepared by mixing a 7 mM stock of ABTS with 2.45 mM potassium persulfate.
Neocuproine Ethanolic Solution	Prepared a 7.5 mM neocuproine solution in absolute ethanol.
FRAP Reagent	Prepared by mixing 25 mL of 300 mmol/L acetate buffer, 2.5 mL of 10 mmol/L TPTZ solution dissolved in 300 mmol/L HCL and 2.5 mL of 20 mmol/L $FeCl_3$ solution in a 10:1:1 ratio.
Arnow`s Reagent	Prepared through the addition of 10 g of sodium molybdate and 10 g sodium nitrite to 100 ml of a 1:1 (v/v) ethanol: water.

This shows all the various reagents, buffer and solutions that were used throughout this study in relation to chemical assays and any in-lab preparation carried out.

2.2. Cell culture

Fundamental to successful cell culture is the strict adherence to aseptic technique which in the totality of procedures must be stringently followed in order to provide a comprehensive barrier between infectious agents from the non-sterile external environment and the uncontaminated culture within a sterile environment such as flask, dish or multiwell plate (Phelan & May, 2016). Successful cell culture is fundamentally reliant on preventing all kinds of contamination and was achieved by adhering to the following elements while carrying out all tissue culture related procedures.

2.2.1. Sterile Work Area

Cell culture experiments were conducted according to the codes of practice of the Centre of Molecular Medicine and Biobanking. A SafeFAST Elite laminar flow hood (FASTER, Italy) ideally positioned in a climate-controlled room was used for all tissue culture related activities. The laminar flow hood is an ideal work area for cell culture as a stable flow of high-efficiency particulate air (HEPA) filtered air and physical glass barrier ensure a work surface that is separated from the external environment and thus provides a steadfast form of protection from aerosols, dust, and infectious agents. Ultraviolet lights (UVC 200 – 280 nm) bulbs were utilized to provide biocidal protection of exposed work surfaces through 30-minute exposure prior to activation of laminar-flow hood (Meechan & Wilson, 2006). Following activation, the decontamination procedure was completed through the cleaning of the interior work surfaces within the laminar flow hood with a chemical disinfectant namely 70 % ethanol. Any subsequent spillages were immediately handled in the same manner. Strict protocols of personal hygiene were adhered to. Hands and forearms were washed thoroughly with water followed by 70 % ethanol and personal protective equipment in the form of gloves and a lab coat were worn prior to the commencement of cell culture work.

The external surface of all the materials that were placed inside the operational laminar flow hood, including gloved hands, were thus swabbed in 70 % ethanol. All media, cell suspension, and reagent transfers were carried out with the use of single use disposable plastic pipettes of various sizes including 2, 5, 10 ml. Pouring from one sterile container into another was absolutely avoided as this increases the likelihood of contamination through the generation of a bridge between the outside and inside of a sterile vessel. All protocols were carried out

expeditiously and sterile vessels were uncapped/uncovered for the slightest amount of time, and covers were placed with the internal surface facing downwards, all in an effort to reduce the possibility of contamination (Phelan & May, 2016).

2.3. Primary Cell Culture Management

Primary cells were used in this project and included Human Dermal Fibroblasts (HDFs) which were isolated (Section 2.3.1) and Human Neonatal Dermal Fibroblasts (nHDFs) - ATCC PCS-201-010 (LCG Standards, Germany) which were purchased. When referring to both HDFs and nHDFs in tandem these shall be referred to as fibroblasts.

2.3.1. Primary Human Dermal Fibroblast Isolation

The arrival of a recently deceased cadaver (24 – 48 h post-mortem) signalled the start of the isolation process. HDFs were derived from skin biopsy specimens obtained from the trunk of donated cadavers. The resection site surface was chemically sterilised using 70 % ethanol and a tissue section was resected and transferred aseptically to the tissue culture laboratory in a sterile centrifuge tube in complete DMEM. Once in the laminar flow hood the skin resection was placed in a petri dish and was rapidly washed in a bath of 70 % ethanol followed by PBS. The biopsy was then minced into small fragments using sterile disposable scalpels, which were transferred to T25 flasks (CytoOne, UK), using a disposable Pasteur pipette to evenly distribute the fragments over the bottom surface of the flask. The flasks were then passed rapidly through a Bunsen flame to evaporate the medium and thus firmly adhere the minced tissue pieces to the plastic surface of the bottom of the T25 flasks. To each T25 flask, 2 ml of fresh complete DMEM solution was added, and these were firmly closed and placed inside an incubator. The following day the lid of each flask was loosened to facilitate gaseous exchange. The culture medium was changed every three days and fibroblast growth was observed from the minced fragments after 2-3 days. When sufficient cells had proliferated to occupy the available substrate in the T25 flask these were subcultured (*passaged*) into individual T75 flasks (Orange Scientific, Belgium) to create a primary cell culture identified as *Passage 1*. Thus, from a very heterogeneous primary culture containing many cell types,

homogenous primary culture emerged, which is a critical transition period in cell culture biology (Besta, 2014).

2.3.2. Standard Culture Conditions

All cultures derived from HDFs and nHDFs were cultured in sterile tissue culture flasks containing complete DMEM. All fibroblast cell cultures were maintained as monolayers in incubators (LEEC, UK) and (ESCO, USA) at 37 °C and 5 % CO_2 and were studied between the sixth and twelfth subpassage for HDFs and twentieth and thirtieth subpassage for nHDFs. All experimentation was carried out under the same conditions within multiwell plates or appropriate tissue culture vessels unless otherwise explicitly stated.

2.3.3. Routine Maintenance and Subculturing

Cell morphology was microscopically examined at different stages to check the status of the cells and to confirm the absence of contamination. The goal of routine maintenance and subculturing was to prevent cellular deterioration, to proliferate the cell line and to seed for further experimentation.

2.3.3.1. Routine Maintenance

The medium of a T75 flask was replaced approximately every 4 days or when a drop in pH (orange coloration), or higher cellular density was observed. This was done by removing the old medium in the T75 flask and replacing it with 12 ml of complete DMEM. In situations where the cells were growing sub-optimally, a partial media change was carried out (half the medium removed and replaced) or the length of time between one media change and another was extended.

2.3.3.2. Subculturing

The fibroblasts were subcultured in accordance to the procedure described by Hayflick & Moorhead (1961) in a 1:2 ratio (1 flask subcultured into 2 flasks) which ensures that the passage number and the generation time were approximately equal. This is important as the

finite primary cell cultures can only be grown to a limited number of generations before senescence and thus keeping track of the passage number was an important factor. When the cells in the T75 flasks appeared to reach over 70 % confluency (~ 5 days), they were subcultured. The medium was replaced with 3 ml of PBS to eliminate any serum residue that could lead to the inactivation of the trypsin. After a couple of minutes, the PBS was aspirated with a fresh sterile pipette and 3 ml of pre-warmed (37°C) trypsin were added. The flasks were then placed horizontally in the incubator (37 °C) for 3-5 minutes or the length of time required for the majority of the cells appear rounded and detached under the AE2000 inverted microscope (Motic, Hong Kong) and the EVOS™ XL Core Imaging System microscope (ThermoFisher scientific, USA), under 4x objective lens. A volume of pre-warmed (37 °C) complete DMEM (3 ml) equal to the amount of trypsin was then added to each flask to inhibit any further enzyme activity. The cell suspension was then aspirated and placed into a sterile 50 ml centrifuge tube. The flasks were then washed with 3 ml of PBS which was then transferred to the same centrifuge tube. This tube was then centrifuged at 1500 rpm for 5 min to collect a cell pellet. The resultant supernatant gently discarded, not to disturb the cell pellet. The cell pellet was resuspended in an appropriate volume of pre-warmed (37 °C) complete DMEM assisted by gentle agitation. Those cellular suspensions, that were earmarked for propagation of the cell line, were added to each flask followed by an amount of fresh complete medium to a total volume of 12 ml, and the passage number was noted. On the other hand, cellular suspensions that were used for experimentation underwent cellular quantification (Section 2.4) (Freshney, 2010).

2.3.4. Cell Management

To ensure the preservation of the primary cells generated during this project and to prevent the deleterious effects of senescence, genetic/phenotypic instability, and contamination, the cell lines were cryopreserved when they reached passage six for HDFs and passage twenty for nHDFs and were only thawed depending on requirements.

2.3.4.1. Cryopreservation

The cells to be cryopreserved were subcultured in a standard manner, however the cell pellet obtained following centrifugation (1500 rpm for 5 minutes at room temperature) was resuspended in 1.5 ml of FBS. This cellular suspension of high cellular concentration ($10x10^5$

or greater) was then transferred to a labelled plastic cryotube. To this 150 µl of DMSO as a cryoprotectant, was added to give a final concentration of 10 %. The cell suspension was then cooled at an approximate rate of at 1 °C/min by placing the cryotubes in polystyrene foam box of approximate 15 mm thickness inside a -80 °C freezer, thus reducing ice crystal growth and increasing cell viability post-cryopreservation. For long-term storage, the cryotubes were transferred to a liquid nitrogen freezer (Freshney, 2010).

2.3.4.2. Thawing

When required, the cryopreserved cells were thawed and seeded at a relatively high concentration to optimise cellular recovery. The cryotube was thawed rapidly by placing it in a beaker containing water at 37 °C, as to minimize intracellular ice crystal formation. Simultaneously 5 ml of complete medium (DMEM) was added to a centrifuge tube, followed by 50 µL EDTA (200 mM) pH 8.0 to avoid cellular clumping. Once thawed, the cellular suspension was immediately transferred to the prepared 15 ml centrifuge tube. The suspension was then centrifuged at 1500 rpm for 5 minutes, and the supernatant was discarded. The process was repeated. The pellet was then resuspended in 5 ml complete medium (DMEM) and was transferred to the T25 tissue culture flasks, which were subsequently incubated under standard culture conditions (Freshney, 2010).

2.4. Cell Quantification

Cell quantification is necessary to ensure experimental reproducibility and accuracy, thus it is vital that cellular quantification is accurate, consistent, and fast particularly in quantitative cellular responses (Ongena et al., 2010). Thus prior to seeding, the concentration of the cell suspension of fibroblasts needed to be quantified and this was done using the Countess™ II Automated Cell Counter (ThermoFisher scientific, USA) (Section 2.4.1) or a haemocytometer (Section 2.4.2).

2.4.1. Countess™ II Automated Cell Counter

The Countess™ II Automated Cell Counter a fully automated cell counter which utilises optics and image analysis algorithms to analyse trypan blue-stained cells in suspension (ThermoFisher Scientific, 2019).

2.4.1.1. Standard Operation of Countess™ II Automated Cell Counter

The fibroblasts were trypsinised (Section 2.3.3.2), and the sample prepared by mixing equal quantities of cell suspension and 0.4 % (w/v) trypan blue stain. The trypan blue-stained sample (10 µl) was pipetted gently into the sample loading area on the Countess™ loading slide (ThermoFisher scientific, USA). The sample was allowed to settle (30 seconds). The slide was inserted into the instrument for automated run-through under the pre-prepared optimised profile (Section 2.4.1.2). The results were saved, interpreted, and the automated dilution factor provided utilised. Finally, the volume of the cellular suspension was adjusted using pre-warmed (37 °C) complete DMEM to achieve the desired cellular density for the protocol to be carried out (ThermoFisher Scientific, 2019).

2.4.1.2. Calibration of Countess™ II Automated Cell Counter

The sample was prepared (Section 2.4.1.1) and analysed by the Countess™ II Automated Cell Counter (brightfield settings) according to manufacturer instruction The count parameters (size, brightness, circularity) were manually adjusted post-capture to optimise the algorithmic efficiency at cellular quantification for the cells under study. Thus, ensuring that algorithmic selection of cells accurately quantifies and differentiates debris, living cells and dead cells. Furthermore, the optimisation was carried out in such a way so that the readings given for samples provided comparable counts using the haemocytometer (Section 2.4.2) and Countess™ II Automated Cell Counter. The profile was saved following the review of 6 separate samples on both the haemocytometer and Countess™ II Automated Cell Counter and was used from then on for the quantification of fibroblasts as it was optimised.

2.4.2. Haemocytometer

This method was chosen as it is a widely accepted, cost-effective and simple technique which gives the opportunity to visualise cells that are being quantified (Freshney, 2010). Firstly, the glass haemocytometer and coverslip were then cleaned with 70 % (v/v) ethanol. The coverslip was then moistened with deionised water and properly affixed to the haemocytometer as indicated by the presence of Newton`s refraction rings. The cells were handled as done for subculturing (Section 2.3.3.2) however the cell suspension was preserved within a known homogenous volume. From this, 10 µl was aspirated and loaded under the coverslip by gentle expulsion and capillary action. All excess fluid was blotted off with tissue paper while ensuring that fluid was not drawn out from under the coverslip. The loaded haemocytometer visualised using by the microscope with a standard 10x objective lens. The count was carried out as shown in using a hand tally counter moving from the first counting grid square to the next. The same procedure was carried out on the second grid of the haemocytometer amounting to 4 grid squares in total (Fuentes, 2010). Once the cell counting was carried out the following formula (Equation 3.1) was used to adjust the volume of original cellular suspension through the addition of the determined volume of pre-warmed (37 °C) complete DMEM to achieve the desired cellular density for the protocol to be carried out (Grigoryev, 2014).

Equation 2.1

$$\underline{\text{Part A}}\ \text{Total cells/ml} = \frac{\text{total cells counted} \times \text{sample dilution factor}}{\text{number of grid squares counted}} \times 10{,}000$$

$$\underline{\text{Part B}}\ \text{Needed dilution factor} = \frac{\text{total cells/ml}}{\text{desired cell density/ml}}$$

$$\underline{\text{Part C}}\ \text{Total Volume} = \text{volume of cell suspension} \times \text{needed dilution factor}$$

$$\underline{\text{Part D}}\ \text{Volume to be added} = \text{total volume} - \text{volume of cell suspension}$$

2.5. Prickly Pear Extract and Carrier Preparation

The Prickly Pear Extract (PPE)/ Prickly Pear Extract Carrier (PPEC) were provided by Nutribiotech Services Limited, Malta and as such are proprietary and limited information was provided. The PPE is a total solvent extraction of the prickly pear *Opuntia ficus-indica* fruit particularly the skin extracted through low pressure distillation to produce a concentrated extract, while the PPEC – 'vehicle' utilised is 100 % propylene glycol (PG). The ratio by volume of PPE with PPEC is 1:9.

2.5.1. Prickly Pear Extract and Carrier Sterilisation

Sterilisation was not required. This was determined through a standard sterility test through the inoculation of DMEM with PPE or prickly PPEC followed by incubation (37 °C and 5 % CO_2) for a period of 7 days following which no microbial growth was observed.

2.5.2. Prickly Pear Extract and Carrier Preparation

A 50 % (v/v) stock solution of PPE and PPEC was prepared through the 1:1 addition of complete DMEM with PPE or PPEC respectively, using aseptic technique. At this point, several dilutions in complete DMEM were made to prepare working solutions of the concentrations shown in Table 2.3. These dilutions were made fresh on the day of use.

2.5.3. Prickly Pear Extract and Carrier Treatment

To test the effects of PPE/PPEC on the fibroblasts, these cells were treated with the PPE/PPEC for 1 h / 24 h prior to exposure to the respective stress protocol through the replacement of DMEM media with appropriate concentrations of PPE/PPEC in complete DMEM. Those cells that were not subjected to treatment also had their media replaced to avoid the introduction of a confounding factor. During PPE/PPEC treatment, the cells were placed inside an incubator at 37 °C and 5 % CO_2.

Table 2.3: The concentrations of prickly pear extract and prickly pear extract carrier used.

Prickly pear extract and carrier concentration
PPE/PPEC 0.002 %
PPE/PPEC 0.004 %
PPE/PPEC 0.01 %
PPE/PPEC 0.02 %
PPE/PPEC 0.04 %
PPE/PPEC 0.08 %
PPE/PPEC 0.16 %
PPE/PPEC 0.32 %
PPE/PPEC 0.64 %
PPE/PPEC 1.28 %
PPE/PPEC 2.56 %
PPE/PPEC 5.12 %
PPE/PPEC 10.24 %
PPE/PPEC 20.48 %
PPE/PPEC 40.96 %

2.6. Stress Protocols

The fibroblasts were exposed to three stress stimuli: heat stress, oxidative stress and ultraviolet stress. The following protocols were established to assess the cellular response to these stress factors.

2.6.1. Heat Stress Protocol

The heat stress protocols that were designed to induce heat stress in fibroblasts can be seen described below and represented Figure 2.1.

Heat Stress Protocol A - To induce a heat shock response, tissue culture flasks/plates were transferred from an incubator (37 °C) to a waterbath pre-set to 42 °C. The tissue culture flask/plates were exposed to this thermal stress for 1 h(Henderson et al., 2022; Jonak et al., 2006). The tissue culture plates/flasks were placed on a stand in the waterbath in a manner so that the bottom on the plate/flask was in contact with the water, without letting water seep into and compromise the sterility of the culture. The tissue culture flasks/plates were then returned to the incubator (37 °C) for a minimum of 1 h for recovery, before being processed further.

Heat Stress Protocol B - To prompt this thermally induced heat shock response, the medium replaced of the flask/plates was replaced with complete DMEM pre-warmed to 42 °C and were transferred from an incubator (37 °C) to a waterbath pre-set to 42 °C(Henderson et al., 2022; Jonak et al., 2006). The tissue culture flask/plates were exposed to this thermal stress 1 h. The tissue culture plates/flasks were placed on a stand in the waterbath in a manner so that the bottom on the plate/flask was in contact with the water, without letting water seep into and compromise the sterility of the culture. The tissue culture flasks/plates were then returned to the incubator (37 °C) for a minimum of 1 h for recovery, before being processed further.

Heat Stress Protocol C - To prompt this thermally induced heat shock response, tissue culture flasks/plates were transferred from an incubator (37 °C) to a waterbath pre-set to 44 °C. The tissue culture flask/plates were exposed to this thermal stress for 1 h (Henderson et al., 2022; Pedersen & Gregersen, 2010). The tissue culture plates/flasks were placed on a stand in the waterbath in a manner so that the bottom on the plate/flask was in contact with the water,

without letting water seep into and compromise the sterility of the culture. The tissue culture flasks/plates were then returned to the incubator (37 °C) for a minimum of 1 h for recovery, before being processed further.

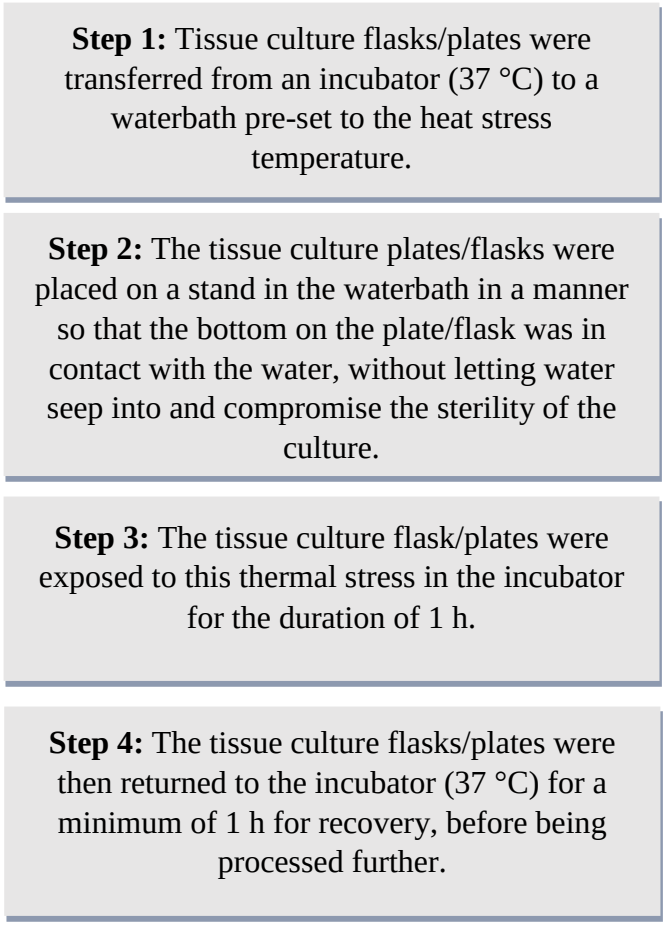

Figure 2.1: Heat stress protocol
This is a diagrammatic representation showing the heat stress protocol guidelines followed throughout experimentation.

2.6.2. Oxidative stress protocol

Oxidative stress is caused by the generation of free radicals such as superoxide and hydroxyl radicals that cause damage to membranes, proteins, and nucleic acids, which may result in induced apoptosis/necrosis. To prompt this oxidative- induced response, the complete medium (DMEM) was supplemented with a working concentration of 100 µM, 50 µM, 25 µM, 12.5 µM, 6.25 µM and 3.125 µM Menadione, respectively. The tissue culture flasks/plates were then returned to the incubator (37 °C and 5% CO_2) for a minimum of 1 h, before being processed in accordance with the experimental protocol (Loor et al., 2010).

2.6.3. Ultraviolet radiation stress protocol

The Stratalinker® UV Crosslinker 2400 (Stratagene, USA) with 254-nm (UVC) 15 W/365-nm (UVA) 15 W bulbs was used as a self-contained source of UV radiation with an in-build light detector reporting in µJ/cm^2 × 100. The protocol as shown in Figure 2.2 was used to expose fibroblasts to UV radiation and was adapted from work carried out by Crowley & Waterhouse, 2016, with UVC doses (10 µJ/m^2 or 25 µJ/m^2) utilised following a similar range to that of work carried out by Latonen, Taya, & Laiho, 2001 / Gentile, Latonen, & Laiho, 2003 and with UVA doses (5 J/cm^2 or 10 J/cm^2) utilised following a similar range to that of work carried out by Zhang et al., 2020 / Scharffetter et al., 1991. To prompt the efficient UV irradiation of cells, tissue culture plates/ petri dishes had the medium replaced with an adequate volume of PBS to cover the cells. The media was removed as DMEM contains phenol red which partially blocks UV light and may become photoactivated. The lid of the tissue culture plate/ petri dish was removed to ensure unobstructed UV transmission, while control cells were covered with cardboard to prevent exposure. The uncovered tissue culture plates/ petri dishes were then placed in the centre of the Stratalinker, and this was programmed with the desired dose setting and started. On conclusion of UV exposure, the tissue culture plates/ petri dishes were removed from the Stratalinker, the PBS removed, the media added, and the lids replaced. The tissue culture plates/ petri dishes were then returned to the incubator (37 °C) for recovery, before being processed further (Crowley & Waterhouse, 2016; Gentile et al., 2003; Latonen et al., 2001; Scharffetter et al., 1991; Zhang, M. et al., 2020).

Step 1: Media was replaced with PBS.

Step 2: Control cells not to be irradiated were covered.

Step 3: Cells were placed in the center of the Stratalinker.

Step 4: The door was closed and the exposure set.

Step 5: The PBS was removed.

Step 6: The media was replaced, and cells were incubated at 37°C.

Figure 2.2: Ultraviolet radiation protocol
This is a diagrammatic representation showing the ultraviolet radiation stress protocol guidelines followed throughout experimentation.

2.7. Scratch Assay

The *in vitro* scratch assay is well-developed method used to measure the effect of cellular migration *in vitro* (Liang et al., 2007). The scratch assay involved seeding and interval for confluent monolayer formation (Section 2.7.1), treatment and exposure (Section 2.7.2), scratch and image acquisition (Section 2.7.3). The chronology of the whole procedure can be seen in Figure 2.3.

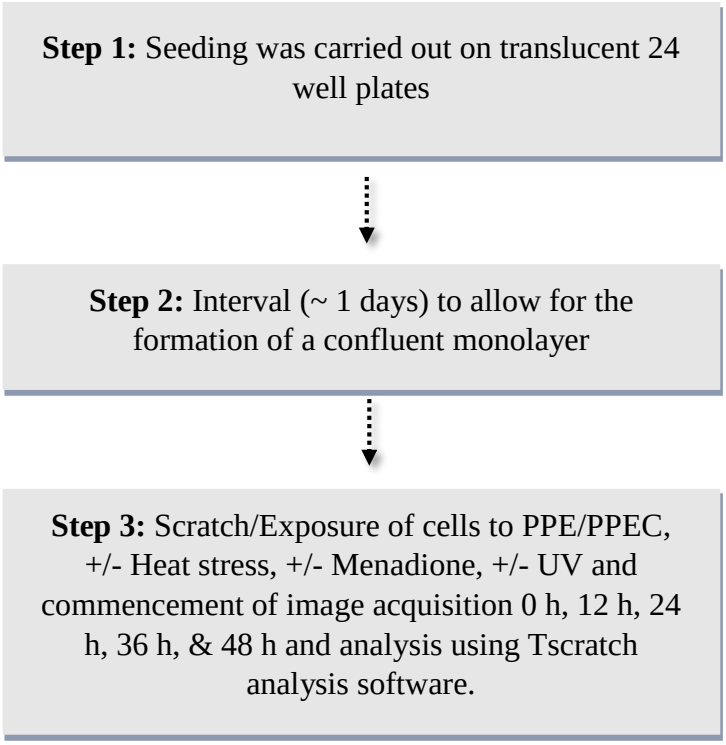

Figure 2.3: The chronology for the *in vitro* scratch assay experiment.

2.7.1. Seeding for scratch assay and Interval

The cells cultured in T75 flasks were harvested and following cell quantification (Section 2.4), the cell suspension was diluted to $5x10^4$ cells/ml. A micropipette was then utilised to dispense 0.5 ml of this cell suspension to each well utilized in the twenty-four-well plates (Orange Scientific, Belgium), to provide a final seeding density of $2.5x10^4$ cells/well (determined through optimisation). All plates were seeded in manner to reduce edge effect, by surrounding test wells with one row/column of blank wells filled with PBS and utilizing a

humidified incubator. The microtitre plates were placed in the incubator and the cells were allowed to adhere and form a confluent monolayer (~ 1 days).

2.7.2. Treatment and stress exposure

The scratch assay was conducted in combination with each of the following stresses: the heat stress exposure / oxidative stress or UV stress exposure as described below.

For heat stress, the media (0.5 ml) was aspirated and replaced by 0.25 ml of complete DMEM (Condition: Negative control and 10% DMSO), except for the wells to be treated with PPE (Condition: PPE) or PPEC (condition: PPEC) where 0.25 ml of PPE or PPEC solution respectively. The plates were returned to the incubator to allow for 1 h pre-treatment prior to heat stress exposure. Following this, the plates were removed from the incubator and the scratch (Section 2.7.3) was performed. The wells were "completed" through the addition of 0.25 ml of the respective solutions to bring the concentrations to working levels; Negative Control (addition of 0.25 ml complete DMEM), DMSO 10 % (addition of 0.25 ml 10 % DMSO) and PPE/PPEC (addition of 0.25 ml 1x PPE/PPEC). All conditions were tested in triplicate. The plates were removed from the incubator and the cells were then exposed in accordance with the heat stress protocol C (Section 2.6.1). A parallel set of plates were not exposed to heat stress and were left in the incubator (37°C).

For oxidative stress, the media (0.5 ml) was aspirated and discarded. The cells were then treated depending on test condition being analysed, through the addition of 0.25 ml of complete DMEM (Conditions: Negative control, menadione and 10 % DMSO), except for the wells to be treated with PPE (Condition: PPE and menadione/PPE) and PPEC (Condition: PPEC and Menadione/PPEC), where 0.25 ml of their respective solution was added. The plates were returned to the incubator to allow for 1 h treatment prior to oxidative stress exposure. Following this the plates were removed from the incubator and the scratch (Section 2.7.3) was performed. The wells were "completed" through the addition of 0.5ml of the respective solutions to bring the concentrations to working levels, negative control (addition of 0.25 ml complete DMEM), DMSO 10 % (addition of 0.25 ml 20 % DMSO), PPE/PPEC (addition of 0.25 ml PPEC), menadione (addition of 0.25 ml menadione) or menadione with PPE/PPEC (addition of 0.125 ml 4x menadione + 0.125 ml 2x PPE/PPEC premixed) in accordance with the oxidative stress protocol (Section 2.6.2).

For UV stress, the media (0.5 ml) was replaced by the addition of 0.25 ml of complete DMEM (Condition: Negative control and 10% DMSO), except for the wells to be treated with PPE (Condition: PPE) or PPEC (condition PPEC) where 0.25 ml of their respective solution was added. The plates were returned to the incubator to allow for 1 h treatment prior to UV stress exposure. Following this, the plates were removed from the incubator and the scratch (Section 2.7.3) was performed. The wells were "completed" through the addition of 0.25 ml of the respective solutions to bring the concentrations to working levels; negative control (addition of 0.25 ml complete DMEM), DMSO 10 % (addition of 0.25 ml 20 % DMSO) and PPE/PPEC (addition of 0.25 ml 1x PPE/PPEC). All conditions were tested in triplicate. The plates were removed from the incubator and the cells were then exposed in accordance with the ultraviolet radiation protocol (Section 2.6.3). A parallel set of plates were not exposed to ultraviolet radiation and removed from incubator but not exposed to UV radiation.

2.7.3. Scratch Procedure and image acquisition

A sterile P200 pipette tip was used to create a scrape in the cell monolayer. This forming a cell free or denuded area, where the HDF could migrate to. The media was then slowly aspirated and discarded from the wells. The wells were then washed twice with 0.5 ml of PBS to remove any cellular debris and to smooth the edges of the scratch. The cells were then re-treated in accordance with the condition being tested. All conditions were tested in triplicate. To ensure the same field during image acquisition, reference points were made using an ultra-fine tip marker just outside the image capture field but within eye-piece field of view. The first image of the scratch was then obtained at 0 h which was taken to be the point immediately following the scratch. The plates were then returned to the incubator and were checked at 12, 24, 36, 48 h post scratch to observe the resultant cellular migration/proliferation.

After each respective incubation period, the plate was observed using an EVOS™ XL Core Imaging System microscope (ThermoFisher scientific, USA) under 40 × magnification with phase contrast and a photograph was taken of each well ensuring that the reference points were appropriately aligned. The images acquired for each sample were then analysed quantitatively using Tscratch analysis software (Geback et al., 2009), which was utilized to determine the degree of inter-scratch variation.

2.8. Cell Viability Assays

Viability in a cellular biology context can be simply defined as the ability of a cell to retrain the faculty to both grow and develop (Pegg, 1989). The measurements of cell viability equate to number of healthy/viable cells within a sample and is generally expressed as a percentage of the control (Fang & Trewyn, 2012). Cell viability assays are in general used as a screen for the effect of physical and chemical agents on cell proliferation or to indicate direct cytotoxic effects via mechanistically diverse means (Aslantürk, 2018).

2.8.1. Prickly Pear Extract and Carrier Treatment

The viability assays that were conducted followed seeding, exposure, and testing. The chronology of the whole experimental procedure can be seen in Figure 2.4.

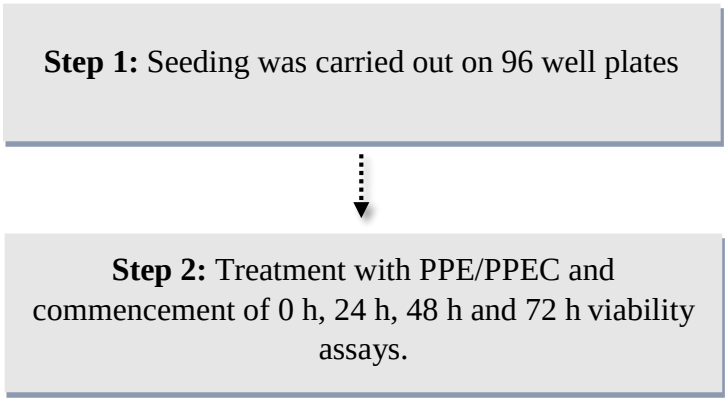

Figure 2.4: The chronology of the CellTitre-Glo assay/Presto Blue Assay for PPE and PPEC testing.

The appropriate number of T75 flasks were harvested in accordance with the subculture protocol (Section 2.3.3.2). Following cellular quantification (Section 2.4), the cell suspension was diluted to give a solution containing $1.25x10^4$ cells/ml (CellTitre-Glo Assay) / $2.5x10^4$ cells/ml (Presto Blue Assay), 100 µl of this quantified cellular suspension was then dispensed to the appropriate wells of the ninety-six well plates, to provide a final seeding density of $1.25x10^3$ cells/well (CellTitre-Glo Assay) / $2.5x10^3$ cells/well (Presto Blue Assay), both determined through optimisation. All plates were seeded in a manner to reduced edge effect, by surrounding test wells with one row/column of blank wells filled with sterile PBS and utilising a humidified incubator (37 °C / 5% CO_2). The cells were then treated with PPE/PPEC (Section 2.5.3), firstly the media (100 µl) was aspirated and discarded followed by the addition of 100 µl

of the respective concentrations of PPE/PPEC in complete DMEM. This media replacement was also done for the negative control (replaced with fresh complete DMEM) and DMSO 10% (replaced with DMEM supplemented with 10% DMSO). The plates were returned to the incubator (37 °C and 5 % CO_2) until analysis. Morphological observations were noted for any acute crude cellular structural abnormalities or signs of infection, which if noted would halt experiment run. The CellTitre-Glo Assay / Presto Blue Assay was carried out (Section 2.8.5) and all results were shown as the percentage change in metabolic activity relative to baseline, the baseline being the median CellTitre-Glo Assay Value / normalised Presto Blue Assay Value for negative control at 0 h, where 0 h was the moment PPE/PPEC treatment had begun. In the case of PPE values these were also normalised to PPEC.

2.8.2. CellTitre-Glo Assay/Presto Blue Assay – Heat Stress

The viability assay that was conducted followed seeding, exposure, and testing. The chronology of the whole experimental procedure can be seen in Figure 2.5.

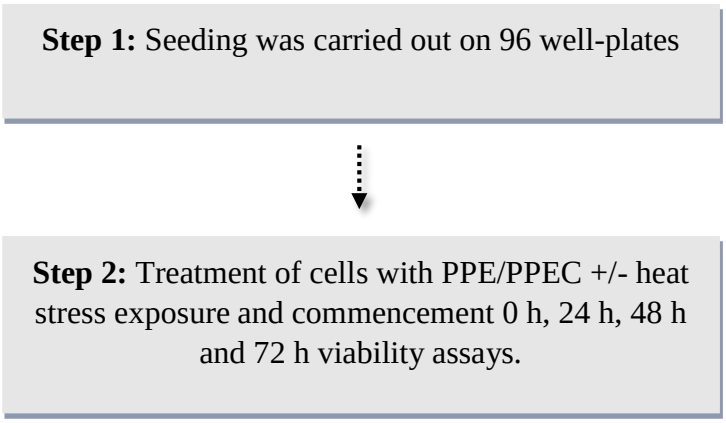

Figure 2.5: The chronology of the CellTitre-Glo assay/Presto Blue Assay for heat stress testing fibroblasts with/without PPE/PPEC.

The appropriate number of T75 flasks were harvested in accordance with the subculture protocol (Section 2.3.3.2) Following cellular quantification (Section 2.4), the cell suspension was diluted to give a solution containing $1.25x10^4$ cells/ml (CellTitre-Glo Assay) / $2.5x10^4$ cells/ml (Presto Blue Assay), 100 µl of this quantified cellular suspension was then dispensed to the appropriate wells of the ninety-six well plates, to provide a final seeding density of $1.25x10^3$ cells/well (CellTitre-Glo Assay) / $2.5x10^3$ cells/well (Presto Blue Assay), both

determined through optimisation. To permit parallel runs, these plates were seeded in duplicate, one to be exposed to heat stress (Section 2.6.1) while the other to be always kept in the incubator serving as the thermal control (37 °C), with each condition being seeded in triplicate. These were incubated for 24 h at (37 °C and 5 % CO_2) to allow time for the fibroblasts to adhere and recover. All plates were seeded in a manner to reduced edge effect, by surrounding test wells with one row/column of blank wells filled with PBS and utilising a humidified incubator (37 °C / 5% CO_2). The cells were then treated in accordance with test condition being analysed, firstly the media (100 µl) was aspirated and discarded followed by the addition of 50 µl of complete DMEM (Conditions: Negative control and 10 % DMSO) except for the wells to be treated with PPE/PPEC where 50 µl of their respective solution was added (Condition: PPE/PPEC). The plates were returned to the incubator (37 °C and 5 % CO_2) to allow for a 1 h PPE/PPEC treatment. Following the conclusion of the treatment, the plates were removed from the incubator and the assay mixture was completed through the addition of 50 µl of the respective solutions to bring the concentrations to working levels; Negative Control (addition of 50 µl complete DMEM), DMSO 10 % (addition of 50 µl of 20 % DMSO) and PPE/PPEC (addition of 50 µl of 1x PPE/PPEC). All conditions were tested in triplicate. The plates were removed from the incubator and the cells were then exposed in accordance with the heat stress (Section 2.6.1) parallel set of plates were not exposed to heat stress and were left in the incubator (37°C) and served as a thermal control. Morphological observations were noted for any acute crude cellular structural abnormalities or signs of infection, which if noted would halt experiment run. The CellTitre-Glo Assay / Presto Blue Assay was carried out (Section 2.8.5) and all results were shown as the percentage change in metabolic activity relative to baseline, the baseline being the median CellTitre-Glo Assay Value / normalised Presto Blue Assay Value for negative control at 0 h, where 0 h was the moment PPE/PPEC treatment had begun. In the case of PPE values these were also normalised to PPEC.

2.8.3. CellTitre-Glo Assay/Presto Blue Assay – Oxidative Stress

The viability assay was carried out to observe effect of menadione-induced oxidative stress. The chronology of the whole experimental procedure can be seen in Figure 2.6.

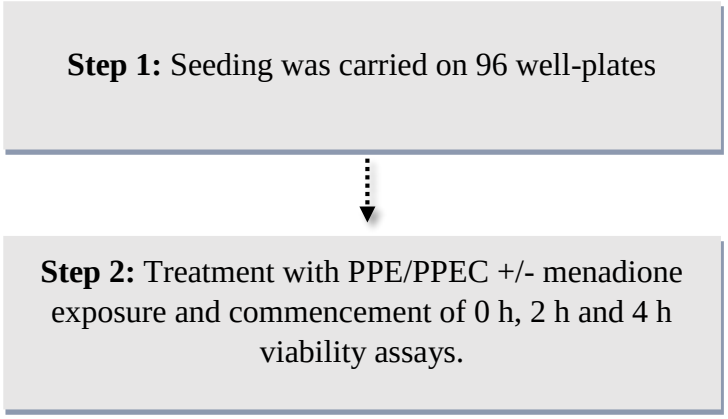

Figure 2.6: The chronology of the CellTitre-Glo assay/Presto Blue Assay for oxidative stress testing fibroblasts with/without PPE/PPEC.

The appropriate number of T75 flasks were harvested in accordance with the subculture protocol (Section 2.3.3.2). Following cellular quantification (Section 2.4), the cell suspension was diluted to give a solution containing $1.25x10^4$ cells/ml (CellTitre-Glo Assay) / $2.5x10^4$ cells/ml (Presto Blue Assay), 100 µl of this quantified cellular suspension was then dispensed to the appropriate wells of the ninety-six well plates, to provide a final seeding density of $1.25x10^3$ cells/well (CellTitre-Glo Assay) / $2.5x10^3$ cells/well (Presto Blue Assay), both determined through optimisation. These were incubated for 24 h to allow time for the fibroblasts to adhere and recover. In addition, one transparent ninety-six well plate was used for microscopic interpretations. All plates were seeded in a manner to reduced edge effect, by surrounding test wells with one row/column of blank wells filled with PBS and utilizing a humidified incubator. The media (100 µl) was aspirated and discarded. The cells were then treated in accordance with the below depending on experimental condition being analysed, through the addition of 50 µl of complete DMEM (Conditions: Negative control, Menadione and 10% DMSO), except for the wells to be treated with PPE/PPEC (Conditions: PPE/PPEC, Menadione/PPE and Menadione/PPEC) were 50 µl of their respective solution was added. The plates were returned to the incubator to allow for 1 h PPE/PPEC treatment. Following this, the plates were removed from the incubator and the viability assay mixture was completed through the addition of 50 µl of the respective solutions to bring the concentrations to working levels; Negative Control (addition of 50 µl complete DMEM), DMSO 10% (addition of 50 µl 20 %

DMSO) PPE/PPEC (addition of 50 µl 1× PPE/PPEC), Menadione (addition of 50 µl 2× Menadione) or Menadione with PPE/PPEC (addition of 25 µl 4× Menadione + 25 µl 2× PPE/PPEC pre-mixed) in accordance to the oxidative stress protocol (Section 2.6.2). All conditions were tested in triplicate. Microscopic observations were noted for any acute crude cellular structural abnormalities or signs of infection, which if noted would halt experiment run. The CellTitre-Glo Assay / Presto Blue Assay was carried out (Section 2.8.5) and all results were shown as the percentage change in metabolic activity relative to baseline, the baseline being the median CellTitre-Glo Assay Value / normalised Presto Blue Assay Value for negative control at 0 h, where 0 h was the moment PPE/PPEC treatment had begun. In the case of PPE values these were also normalised to PPEC.

2.8.4. CellTitre-Glo® Assay/Presto Blue Assay – Ultraviolet Light

The viability assay that was conducted followed seeding, exposure, and testing. The chronology of the whole experimental procedure can be seen in Figure 2.7.

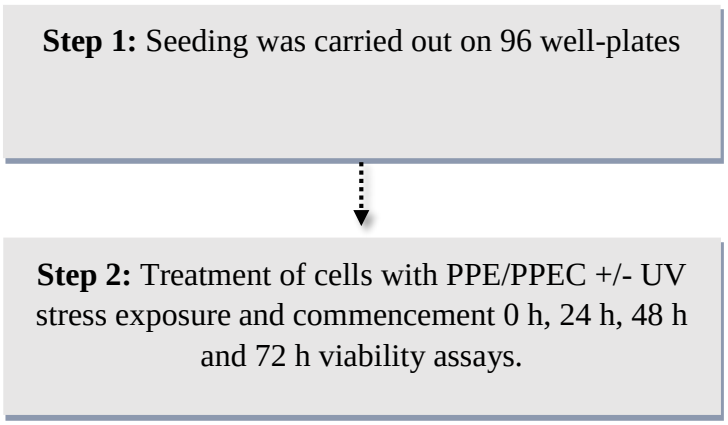

Figure 2.7: The chronology of the CellTitre-Glo assay/Presto Blue Assay for UV testing fibroblasts with/without PPE/PPEC.

The appropriate number of T75 flasks were harvested in accordance with the subculture protocol (Section 2.3.3.2). Following cellular quantification (Section 2.4), the cell suspension was diluted to give a solution containing $1.25x10^4$ cells/ml (CellTitre-Glo Assay) / $2.5x10^4$ cells/ml (Presto Blue Assay), 100 µl of this quantified cellular suspension was then dispensed to the appropriate wells of the ninety-six well plates, to provide a final seeding density of $1.25x10^3$ cells/well (CellTitre-Glo Assay) / $2.5x10^3$ cells/well (Presto Blue Assay), both determined through optimisation. To permit parallel runs, these plates were seeded in duplicate,

one to be exposed to Ultraviolet stress (Section 2.6.3) while the other not exposed to UV and thus serving as the UV control with each condition being seeded in triplicate. These were incubated for 24 h at (37 °C and 5 % CO_2) to allow time for the fibroblasts to adhere and recover. In addition, one transparent ninety-six well plate was used for microscopic interpretations. All plates were seeded in a manner to reduced edge effect, by surrounding test wells with one row/column of blank wells filled with PBS and utilising a humidified incubator (37 °C / 5% CO_2). The cells were then treated in accordance with test condition being analysed, firstly the media (100 µl) was aspirated and discarded followed by the addition of 50 µl of complete DMEM (Conditions: Negative control and 10 % DMSO) except for the wells to be treated with PPE/PPEC where 50 µl of their respective solution was added (Condition: PPE/PPEC). The plates were returned to the incubator (37 °C and 5 % CO_2) to allow for a 1 h PPE/PPEC treatment. Following the conclusion of the treatment, the plates were removed from the incubator and the assay mixture was completed through the addition of 50 µl of the respective solutions to bring the concentrations to working levels; Negative Control (addition of 50 µl complete DMEM), DMSO 10 % (addition of 50 µl of 20 % DMSO) and PPE/PPEC (addition of 50 µl of 1x PPE/PPEC). All conditions were tested in triplicate. The plates were removed from the incubator and the cells were then exposed in accordance with the UV stress protocol (Section 2.6.3) A parallel set of plates was not exposed to UV stress and were removed from incubator but not exposed to UV. Morphological observations were noted for any acute crude cellular structural abnormalities or signs of infection, which if noted would halt experiment run. The CellTitre-Glo Assay / Presto Blue Assay was carried out (Section 2.8.5) and all results were shown as the percentage change in metabolic activity relative to baseline, the baseline being the median CellTitre-Glo Assay Value / normalised Presto Blue Assay Value for negative control at 0 h, where 0 h was the moment PPE/PPEC treatment had begun. In the case of PPE values these were also normalised to PPEC.

2.8.5. Viability Assays

The CellTitre-Glo® luminescent cell viability assay (Invitrogen, USA) was the selected as ATP detection assays are described as the most sensitive, least prone to inference, and are the fastest to perform (Riss, 2014). The viability assay was conducted in a Nunc™ ninety-six MicroWell™ White Polystyrene plates (ThermoFisher scientific, USA) that had been prepared appropriately for experimentation (Sections 2.8.1 – 2.8.4). In addition, one transparent ninety-six well plate (Orange scientific, Belgium) was used for microscopic interpretations. The assay was done in accordance with the CellTitre-Glo® Luminescent Cell Viability Assay protocol. The reagent, and the cells to be tested were equilibrated to room temperature for 30 minutes. To each well, a volume of 100 µl of CellTitre-Glo reagent was added and the contents were mixed on an orbital shaker at 400 rpm at room temperature for 2 minutes to ensure complete cell lysis. The plates were then allowed to incubate at room temperature for 10 minutes and the luminescence was then recorded using the Mithras LB 940 Microplate reader (Berthold Technologies, Germany).

The PrestoBlue™ Cell Viability Assay (Invitrogen, USA) is a vital stain based on resazurin as a functional viability indicator that is reduced by active cellular respiration to resorufin that allows for spectrophotometric quantification(Xu et al., 2015). The viability assay was conducted in ninety-six microwell transparent plates that had been prepared appropriately for experimentation (Sections 2.8.1 – 2.8.4). The assay was done in accordance with the PrestoBlue™ Cell Viability Assay protocol, the reagent, and the cells to be tested were equilibrated to room temperature. To each microtitre plate well, a volume of 10 µl of PrestoBlue™ Reagent was added and the contents were mixed on an orbital shaker at 400 rpm at room temperature for 2 minutes. The plates were then allowed to incubate at room temperature for 4 hours to ensure adequate sensitivity and the absorbance was then recorded using the Mithras LB 940 Microplate reader (Berthold Technologies, Germany) with 570nm experimental wavelength and 600nm reference wavelength for normalisation.

2.9. Chemical Composition Assays

A number of experiments were carried in order to uncover different consequential aspects of the chemical composition of the PPE/PPEC and how this composition could have a visible effect on *in vitro* results taking into consideration the past literature. These assays include; Folin-Ciocalteu assay (Section 2.9.1), Arnow`s assay (Section 2.9.2), Aluminium chloride assay (Section 2.9.3), Cupric Reducing Antioxidant Capacity (CUPRAC) assay (Section 2.9.4), DPPH (2,2-Diphenyl-1-picrylhydrazyl) Radical Scavenging Activity assay (Section 2.9.5), Ferric Reducing Antioxidant Power (FRAP) assay (Section 2.9.6) and the ABTS (2,20 -Azino-bis(3-ethylbenzothiazoline-6-sulfonic acid) assay (Section 2.9.7).

2.9.1. Folin-Ciocalteu Assay – Total phenolic content

The total phenolic content of the PPE/PPEC was determined using the method of Slinkard and Singleton, with reduction of volumes as described by Waterhouse using varying concentration of gallic acid (Sigma-Aldrich, Germany) standards for the creation of standard curve (Slinkard & Singleton, 1977) & (Waterhouse, 2003). To each well, 20 µl of gallic acid standard or PPE/PPEC sample was added followed by 80 µl of 5-fold diluted Folin-Ciocalteu reagent (Sigma-Aldrich, Germany). This was followed by the addition of 80 µl of 7.5 % Na_2CO_3 which was homogenised and incubated at room temperature for 2 h in the dark. The absorbance was read for each condition in triplicate at 630 nm using a UV/Visible microtitre plate reader spectrophotometer (BioTek ELx800, Gen5^{TM}, Friedrchshall, Germany). The value of total phenolic content for PPE was normalised from PPEC following extrapolation from the gallic acid standard curve.

2.9.2. Arnow`s Assay – Ortho-Diphenolic content

The Arnow`s colorimetric assay was modified from work done by Woisky and Salatino (Woisky & Salatino, 1998) using protocatechuic acid (Sigma-Aldrich, Germany) standards for the creation of standard curve. In a 96 well plate 20 µL of each protocatechuic acid standard or PPE/PPEC sample was pipetted followed by the addition of 20 µL 1M HCl and 20 µL of Arnow's reagent. The plate was shaken for 5 minutes at 500 rpm and then incubated at room temperature for 15 minutes. This was followed by the addition of 80 µL of deionised water and 40 µL of 1M NaOH and the reading of the absorbance for each condition in triplicate at 405

nm using a UV/Visible microplate reader. The value of total flavanoid content for PPE was normalised from PPEC following extrapolation from the protocatechuic acid standard curve.

2.9.3. Aluminium Chloride Assay – Total Flavonoid content

The aluminium chloride assay was used to determine the total flavonoid content of PPE/PPEC using quercetin (Sigma-Aldrich, Germany) as a standard for calibration curve (Attard et al., 2022). In a 96 well plate, 25 µl standard or PPE/PPEC sample was pipetted followed by the addition of 10 µl of 10 % (w/v) aluminium chloride, 10 µl of a 7 % (w/v) sodium nitrite and 80 µl distilled water. The plate was taken to an orbital shaker and mixed for 5 minutes at 500 rpm, followed by incubation at room temperature for 30 minutes. Following this, 100 µl of 1M NaOH was added to each well and the absorbance was read at for each condition in triplicate at 415 nm, using a UV/Visible microplate reader. The value of Ortho-Diphenolic content for PPE was normalised from PPEC following extrapolation from the quercetin standard curve.

2.9.4. Cupric reducing antioxidant capacity Assay – Reducing capacity

The reducing capacity of PPE/PPEC was determined using the CUPRAC assay using gallic acid as a standard for calibration curve (Apak et al., 2016). In a 96 well plate, 20 µl of standard or PPE/PPEC sample was pipetted followed by 100 µl of 10 mM $CuCl_2$ solution, followed by 100 µl of 1M ammonium acetate buffer at pH of 7.0. Subsequently, 100 µl of 7.5 mM neocuproine ethanolic solution was added and the reaction was allowed to proceed for 30 minutes following which the absorbance for all conditions in triplicate was read at 405 nm using a UV/Visible microplate reader. The value of CUPRAC assay for PPE was normalised from PPEC following extrapolation from the gallic acid standard curve.

2.9.5. DPPH Assay - Radical Scavenging Activity

The DPPH Radical Scavenging activity of PPE/PPEC was determined using Rahman et al. method, with minor modifications (Rahman et al., 2015). In a 96 well plate, 50 µL of PPE/PPEC was added into the well, along with two-fold serial dilution of PPE/PPEC. A row of negative DPPH controls was added in the same 96 well plate by adding 50 µL of methanol

into each well. An amount of 150 µL of fresh methanolic DPPH was added into each well, and the reaction was allowed to proceed for 30 min in the dark, following which the absorbance was measured at 560 nm using UV/Visible microplate reader. For each sample, all parameters were determined in triplicate. The value of DPPH assay for PPE was normalised from PPEC.

2.9.6. FRAP Assay – Reducing capacity activity

The Ferric Reducing Antioxidant Power (FRAP) was evaluated employing the method previously outlined by Benzie and Strain, 1996 with ascorbic acid (Sigma Aldrich, Germany) serving as the standard for generating the calibration curve. In a 96-well plate, 10 µL of either the standard or PPE/PPEC was combined with 200 µL of the FRAP reagent. The mixture was vigorously agitated, and subsequently, the absorbance was measured at 630 nm in triplicate for each condition using a UV/Visible microplate reader. The value of FRAP assay for PPE was normalised from PPEC following extrapolation from the ascorbic acid standard curve.

2.9.7. ABTS Assay – Radical scavenging

The ABTS radical scavenging activity was assessed following the method outlined by Rajurkar and Hande, 2011. In a 96-well plate, 50 µL of concentrated stock solution of PPE/PPEC was dispensed into each well, alongside a series of two-fold dilutions of PPE/PPEC. A set of negative ABTS controls was also established in the same plate by introducing 50 µL of methanol into each well. Subsequently, 280 µL of ABTS radical solution was introduced into each well, and the reaction was left to incubate for 5 minutes at 30 ◦C. The absorbance was then recorded at 450 nm in triplicate for each condition using a UV/Visible microplate reader. The value of ABTS assay for PPE was normalised from PPEC.

2.10. RNA Analysis

Following RNA extraction (Section 2.10.1) this high quality isolated and purified RNA was then used in a number of downstream application including; Complementary DNA (cDNA) synthesis (Section 2.10.2), real-time polymerase chain reaction (RT-PCR) (Section 2.10.3) and RNA sequencing (RNA-seq) (Section 2.10.4). This allows for the unravelling of information regarding gene expression and regulation through RNA which is the vital information bridge between DNA following transcription and through to the functional product know as proteins following translation (Shi & Bressan, 2006).

2.10.1. RNA Extraction

The RNeasy® Plus Mini (Qiagen, Germany) was used to isolate high quality mRNA samples for RNA sequencing. Furthermore, RNaseZap solution (Invitrogen, USA) was used on labware as a special measure to ensure an RNase-free environment. The fibroblasts were cultured to a cell density of at least 5×10^6 cells in T75 flasks and were treated in accordance to PPE/PPEC treatment protocol (Section 2.5) and stress protocol (Section 2.6) prior to typsinisation (Section 2.3.3.2) and quantification (Section 2.4). The cells were pelleted at 1500 rpm for 5 minutes and the supernatant discarded. A volume of 300 µl Qiazol was dispensed into the fibroblasts cell pellet which was then mixed thoroughly to ensure proper resuspension and lysis. The lysate was then transferred to an appropriately sized RNase-free tube and stored at -80°C for at least 1 week. These lysates were then thawed slowly on ice. Subsequently, 140 µl of chloroform was added and the resultant mixture was pulse vortexed. The samples were then incubated at room temperature for 2 minutes and centrifuged at 12,000 g for 15 minutes at 4°C. The upper aqueous phase was then transferred to a new RNase-free tube, ensuring no contamination with interphase occurred. To this aqueous phase 350 µl of absolute ethanol was added and this was transferred to an RNeasy mini spin column with a 2ml collection tube attached. The RNA extraction was conducted according to the manufacturers' protocol. The quantity and quality the purified RNA sample was determined using the NanoDrop™ 2000 spectrophotometer (ThermoFisher Scientific, USA) where 1 µl of sample was added and the absorbance read at 260 nm / 280 nm. The purified RNA was then stored at -80°C for long-term storage.

2.10.2. Complementary DNA Synthesis

RevertAid first stand cDNA synthesis kit (ThermoFisher Scientific, USA) was utilised as it is a complete system for the synthesis of first stand cDNA from mRNA and total RNA templates and is ideal for creation of templates for qPCR. The needed components of the cDNA synthesis kit were thawed, mixed, briefly centrifuged and stored on ice until use. In a sterile nuclease free tube which was kept on ice the reaction mix for cDNA synthesis was prepared as shown in Table 2.4 and includes 2 steps. The completed mix in the reaction vessel was then incubated at 42°C for 60 minutes which permitted cDNA synthesis. The synthesis was then terminated by heating the reaction vessel 70°C for 5 minutes. The product of the cDNA synthesis was either kept on ice if it was to be used within a few hours of synthesis or/and was then stored at -80°C for long-term storage.

Table 2.4: Recommended cDNA synthesis reaction mix.

Component	Volume
Step 1	
Total RNA (concentration 0.1 ng – 5 µg)	up to 11 µl
Oligo $(dT)_{18}$ Primer	1 µl
Water PCR grade	to 12 µl
Total Volume	**12 µl**
Step 2	
5x Reaction mix	4 µl
RiboLock RNase Inhibitor (20 U/µL)	1 µl
10 mM dNTP Mix	2 µl
RevertAid M-MuLV RT (200 U/µL)	1 µl
Total Volume	**20 µl**

2.10.3. Quantitative Polymerase Chain Reaction

The 5x HOT FIREpol® EvaGreen® qPCR mix plus (ROX) (Solis BioDyne, Tartu, Estonia) was utilised as it is an optimised ready-to-use solution for real time quantitative PCR assays, incorporating the EvaGreen® dye. This mix comprises of all the components necessary for effective qPCR: HOT FIREPol® DNA polymerase, ultrapure deoxyribonucleotide triphosphates (dNTPs), $MgCl_2$, EvaGreen® dye (DNA binding dye) and ROX dye (Internal passive fluorescent reference). The PCR reaction mix recommended by Solis BioDyne was followed and can be seen in Table 2.5 The forward and reverse primers used in complete reaction mix can be seen in Table 2.7. This completed reaction mix was then transferred PCR Strip Tubes 0.1 ml (QIAGEN, Valencia, California) which were then loaded on the Rotor-Gene Q series software 2.1.0 (QIAGEN, Valencia, California) and qPCR cycles were performed as described in Table 2.6.

Table 2.5: Recommended qPCR reaction mix.

Component	Volume	Final concentration
5x HOT FIREpol® EvaGreen® qPCR mix plus	4 µl	1x
Primer Forward (10pmol/µl)	0.16 – 0.5 µl	80 – 250 nM
Primer Reverse (10pmol/µl)	0.16 – 0.5 µl	80 – 250 nM
cDNA template	1 – 5 µl	1 – 50 ng/µl
Water PCR grade	Up to 20 µl	
Total	**20 µl**	

Table 2.6: Recommended qPCR cycles.

Cycle Step	Temperature	Time	Cycles
Initial Denaturation	95 °C	15 min	1x
Denaturation	95 °C	15 s	40x
Annealing	60 – 65 °C	30 s	
Elongation	72 °C	30 s	

Table 2.7: Primer sequences and amplicon sizes for each gene analysed.

Gene	Forward Primer (5'-3')	Reverse Primer (5'-3')	Fragment size
CD90	TGCTCTTTGGCACTGTGG	CTGCTCCTGCTCTCCCTCT	248 bp
CD105	GGGGTCAACACCACAGAG	CACATCCTGAGGGTCCTG	261 bp
ACTB	AGTCCTAGCTACTCCGGAGGC	CGGCTATTCTCGCAGCTCAC	113 bp

2.10.4. RNA sequencing

RNA sequencing provides in-depth knowledge on the transcriptome of the biological system under study. RNA sequencing was conducted by Genewiz™ RNA sequencing services by Azenta Life Sciences using an Illumina NovaSeq platform with a 2x150bp configuration. It was ensured that samples met the minimum stringent requirements for RNA Seq analysis by Genewiz™ as seen in Table 2.8. The bioinformatics carried out by Genewiz™ included; quality report, FASTQ files, data QC, trimming, mapping, differential gene expression, alternative splicing, and gene ontology analysis. Further analysis was carried out using iDEP which aids in creating actionable insights on transcriptomic results(Ge et al., 2018).

Table 2.8: Requirements for samples sent for RNA sequencing

Sample Type	Quantity	Sample Quality
Total RNA	≥ 50 ng/µl & ≥ 250 ng	RIN > 6.0 A260/280 = 1.8 - 2.2 DNA free Nuclease-free water

2.11. Statistical Analysis

The Statistical Package for the Social Sciences (SPSS) software Version 20 was used to perform all statistical analysis related to viability assay and scratch assay. The Shapiro-Wilk Test was utilized to check for normality as it is the most appropriate test for small sample sizes < 50 samples. It is important to note that the small sample sizes make the normality results low power, nevertheless data distribution using Shapiro-Wilk test show non normal distribution which should be assumed since small sample sizes violate fundamental normality assumption. The Kruskal-Wallis (KW) test on standard SPSS settings was then used to analyse statistically significance between the various conditions with an ideal for low quantity data analysis. The error was deduced to 95 % confidence. The Standard error was determined through standard deviation divided by the square root of n = x and were used compile the error bars. A general null and alternative hypothesis were assumed as displayed below.

H_0: There is no significant difference between the test variable under study and the control it is compared too.

H_1: There is a significant difference between the test variable under study and the control it is compared too.

RNA-seq analysis is a process that involves a multi-step workflow which culminates in the identification of differentially expressed genes (DEGs) and the inferring of biological meaning to the findings (Corchete et al., 2020). The iDEP96 (integrated differential expression and pathway analysis) web app was chosen for its user-friendly yet in-depth approach to RNA-seq analysis. The raw counts table containing the processed raw read data for each condition being investigated is uploaded to iDEP to start the process of analysis. The raw counts table contains the raw reads for each gene per sample. Two replicates were used for each condition being investigated. The uploaded data is processed automatically by the iDEP program, with the raw read data being changed to transformed data by converting any gene IDs into gene names as well as applying a filter of 0.5 million counts per million (CMP) for each gene. The CMPs are calculated by iDEP through a process of normalization of the read counts uploaded by the total counts per sample. Genes which were expressed in low levels were filtered out. The two replicates for each condition are combined automatically by the iDEP program by averaging both readings to obtain a single expression value (Ge, S. X. et al., 2018a; Ge, X., 2021; Koch et al., 2018). The DESeq2 package integrated in iDEP, the upregulated and downregulated genes for each comparison were identified. A FDR (false discovery rate) of <0.05 was used to

ensure statistical significance and a fold-change of >1 was applied. The top up and down regulated DEGs were then investigated to start identifying links between DEGs. The genes can be visualized in a gene plot, with the expression of each gene in CPM for each condition. The DEGs were then subjected to enrichment analysis according to biological process (gene-accomplished biological objectives), cellular component (location of gene activation in the cell) and molecular function (biological activation on gene products) (Ashburner et al., 2000). DESeq2 is the method adopted by iDEP (Ge, S. X. et al., 2018a; Ge, X., 2021) to identify DEGs. The Benjamin and Hochberg approach is the method applied by the program to ensure that the p-values (attained by the Wald test automatically) are corrected by multiple testing. Significant genes can be identified using adjusted p values. By having a false discovery rate (FDR) cut off < 0.05, a limit is set for the percentage of anticipated false positives to be 5%. Therefore, the lower the FDR/adjusted p-value past the cutoff point of 0.05, the more statistically significant they are and the less likely it is the occurrence of false positives (Benjamini & Hochberg, 1995). iDEP presents DEGs according to their log2fold. This shows the fold change between two sets of groups in terms of gene expression. Fold change is a measure that expresses how the level of a gene's expression has changed when one set of experiments is compared to another. It is calculated automatically by iDEP by taking the ratio of the two conditions in terms of gene expression. It gives insight not only to the magnitude of the change but also shows whether each gene has been up or downregulated. In this study, genes were often sorted by their log2fold to visualise the top DEGs in each comparison.

Chapter 3 Results

The experimental conditions were assessed thoroughly to identify the optimal conditions to conduct the analysis of the effect that the PPE may exert on the HDFs. The following are the parameters that were tested and/or optimised: Characterisation of growth profile of HDFs; characterisation of pHDFs with PCR, the potential cytotoxicity of PPE at a range of concentrations on the viability of HDFs at 24, 48 and 72-h; the potential cytotoxicity of PPEC at a range of concentrations on the viability of HDFs at 24, 48 and 72-h; the effect of heat stress (42˚C 1 h) on HDFs in the presence or absence of PPE at 24, 48 and 72-h ; the effect of pre-warming the media on the effect of heat stress (42˚C 1 h); the effect of heat stress (44˚C 1 h) on HDFs in the presence or absence of PPE at 24, 48 and 72-h; the establishment of the optimal concentration of menadione to induce oxidative stress as well as the establishment of the optimal concentrations of PPE for HDF maintenance of viability from the menadione-induced oxidative stress after 2-h and 4-h- exposure; the effect of UVC (2500 and 1000) and UVA (5) on HDF viability with and without PPE and PPEC, the effect of PPE on cell migration and proliferation following heat stress (44˚C 1 h) in the presence of absence of PPE at a range of concentrations and RNA sequencing and transcriptome analysis on the target concentration of PPE and PPEC 0.04 %.

3.1. Cell culture basics

Through a prolonged period of primary HDF isolation and expansion a bank of frozen primary HDFs was created and utilised. Furthermore, Human Neonatal Dermal Fibroblasts (nHDFs) - ATCC PCS-201-010 (LCG Standards, Germany) were purchased and utilised in conjunction as a biological replicate.

3.1.1. Cell culture microscopic analysis

The fibroblasts (Figure 3.1) were continuously monitored visually/morphologically through all phases of experimentation to ensure no drift into senescence or other forms of cellular transformation. During the duration of experimentation, no aberrations were observed and the cultures had retained their standard growing pattern and elongated spindle shape morphology.

Figure 3.1: The primary human dermal fibroblasts at ×40 magnification.

Fibroblasts in culture visualized under ×40 magnification using an EVOS™ XL Core Imaging System microscope (ThermoFisher scientific, USA).

3.1.2. Quantitative Polymerase Chain Reaction

The qPCR (Section 3.2) was performed utilising B-actin as housekeeping gene to normalize the expression levels of the two genes (CD105, CD90) used to characterize the cultured fibroblasts. In addition to morphology (Figure 3.1), the positive expression of CD90 and CD105 are affirmative indicators that the HDFs were correctly isolated into a homogenous primary culture as seen in Figure 3.2.

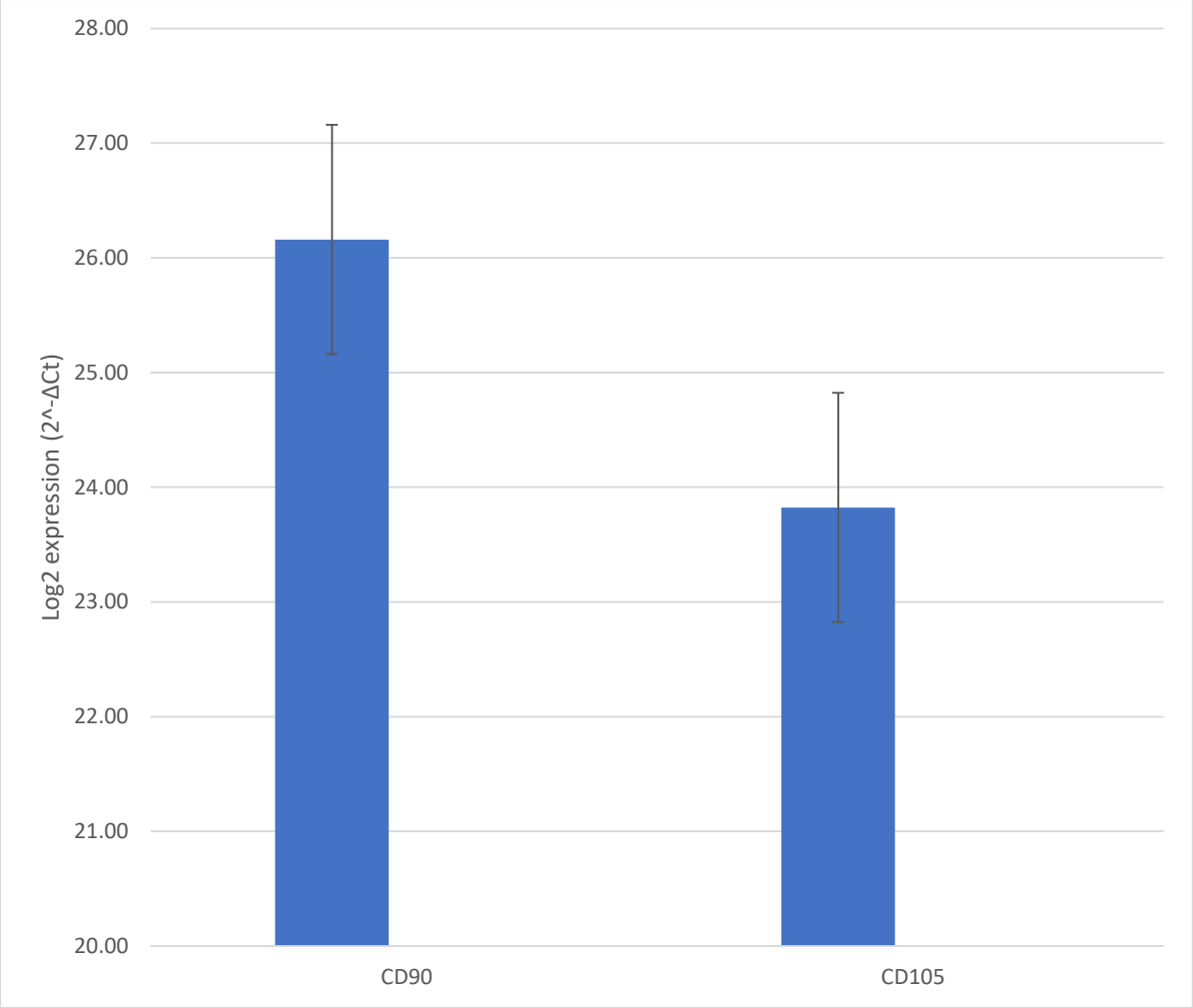

Figure 3.2: The qPCR results for the expression of CD90 and CD105 on the pHDFs used in this study.

The pHDFs were cultured, underwent RNA extraction, cDNA synthesis and finally qPCR targeting the CD90 and CD105 while utilising B-actin as housekeeping gene to normalize the expression levels of the three aforementioned genes. The concentration of cDNA utilised was 5 ng/replicate. The results are shown as the Log2 expression (2^-ΔCt) which represents the expression level of target genes. The values shown are the median of 3 technical replicates. Standard error was determined through Standard deviation divided by the Square root of n=3.

3.2. CellTitre-glo Assay

The CellTitre-Glo® Luminescent cell viability Assay (Invitrogen) was selected as ATP (Adenosine Triphosphate) detection assays are the most sensitive, least prone to interference, and are the fastest to perform (Riss, 2014). Following the optimisation of the CellTitre-glo assay, several avenues of experimentation were taken to analyse the effect of test conditions on HDF viability (Section 3.2.1) as well as the effect on HDF viability following the exposure to heat stress (Section 3.2.2), oxidative stress (Section 3.2.3 – 3.2.4) and ultraviolet radiation (Section 3.2.5 – 3.2.7) with and without prior treatment for 1 h with PPE and PPEC. The results can be found below. Additionally, data is not shown for work carried out with heat stress protocol A / B as these were not sufficient to result in loss of pHDF viability as well as for 24 h PPE and PPEC treatment as no difference was seen when compared to 1 h treatment.

3.2.1. Prickly Pear Extract and Carrier Effect on Viability

In accordance to the protocol shown in Section 2.8.1 the CellTitre-Glo assay was performed to analyse the effect of PPE and PPEC exposure on HDFs for a duration of 72 h. Firstly, as expected 10 % DMSO serving as the positive cytotoxic control showed a significant (KW $p = <0.05$) negative effect on viability when compared to the negative control. Figures 3.3 – 3.5 demonstrate that the PPEC concentrations (0.002, 0.004, 0.01, 0.02, 0.04 and 0.08 %) at 24 h, 48 h and 72 h, exhibited no significant (KW $p = >0.05$) effect on viability of HDFs when compared to the negative control in the same time frame. PPEC concentration 0.16% was seen to have a significant negative (KW $p = <0.05$) effect on viability of HDFs when compared to negative control after 48 h while the rest (0.64, 2.56, 10.24 and 40.96 %) showed this after just 24 h and persisted for 72 h. Furthermore, PPE at all concentration tested when added to HDFs in culture for 24 h, 48 h and 72 h, exhibited no significant (KW $p = >0.05$) effect on viability of HDFs when compared to the negative control in the same time frame and normalised to PPEC relative to the change from the baseline. The results indicate that *in vitro* the PPEC has no effect of the viability of HDFs up to a concentration of 0.08% and thus the range of PPE / PPEC concentrations (0.002, 0.004, 0.01, 0.02, 0.04 and 0.08 %) were used.

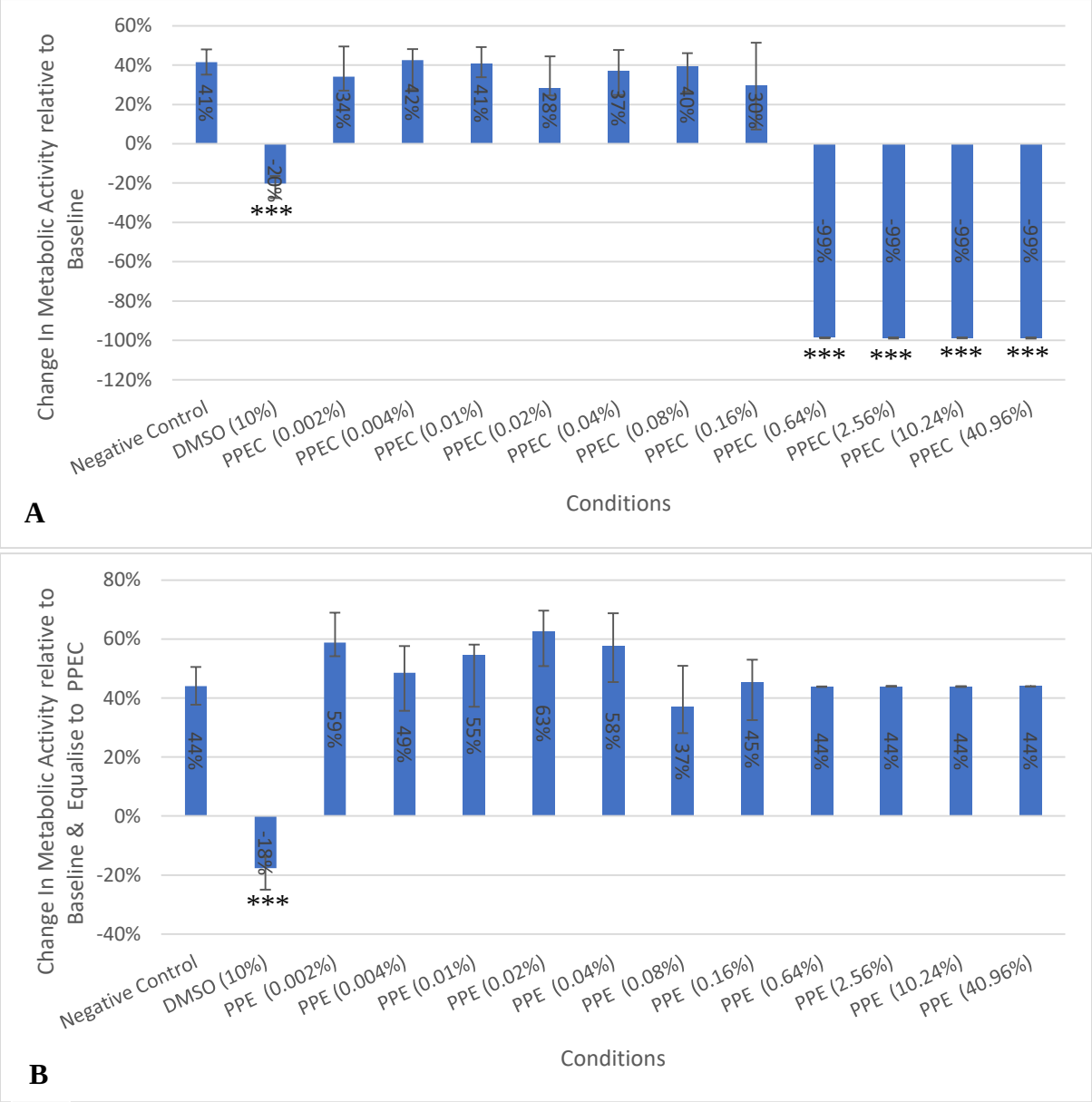

Figure 3.3: The effect of PPEC (**A**) and PPE (**B**) on the viability of HDFs after 24 h exposure.

The HDFs were seeded at $1.25x10^3$ cells/well in 96 well-plates and were allowed to recover overnight under standard culture conditions (37°C / 5 % CO_2). Post-recovery at 0 h the HDFs were exposed to a range of conditions. A CellTitre-Glo assay was performed 24 h post exposure and the results are represented as a percentage change in metabolic activity relative to the activity observed at 0 h and in the case of PPE also equalised to PPEC. The values shown are the median 2 biological replicates with 9 technical replicates each. Postitve/negative error was determined by difference of median to upper/lower quartiles. The KW was a comparison between the various conditions in relation to the negative control and any significant difference was apporopriately indicated p <0.05 */<0.01 **/<0.001 ***.

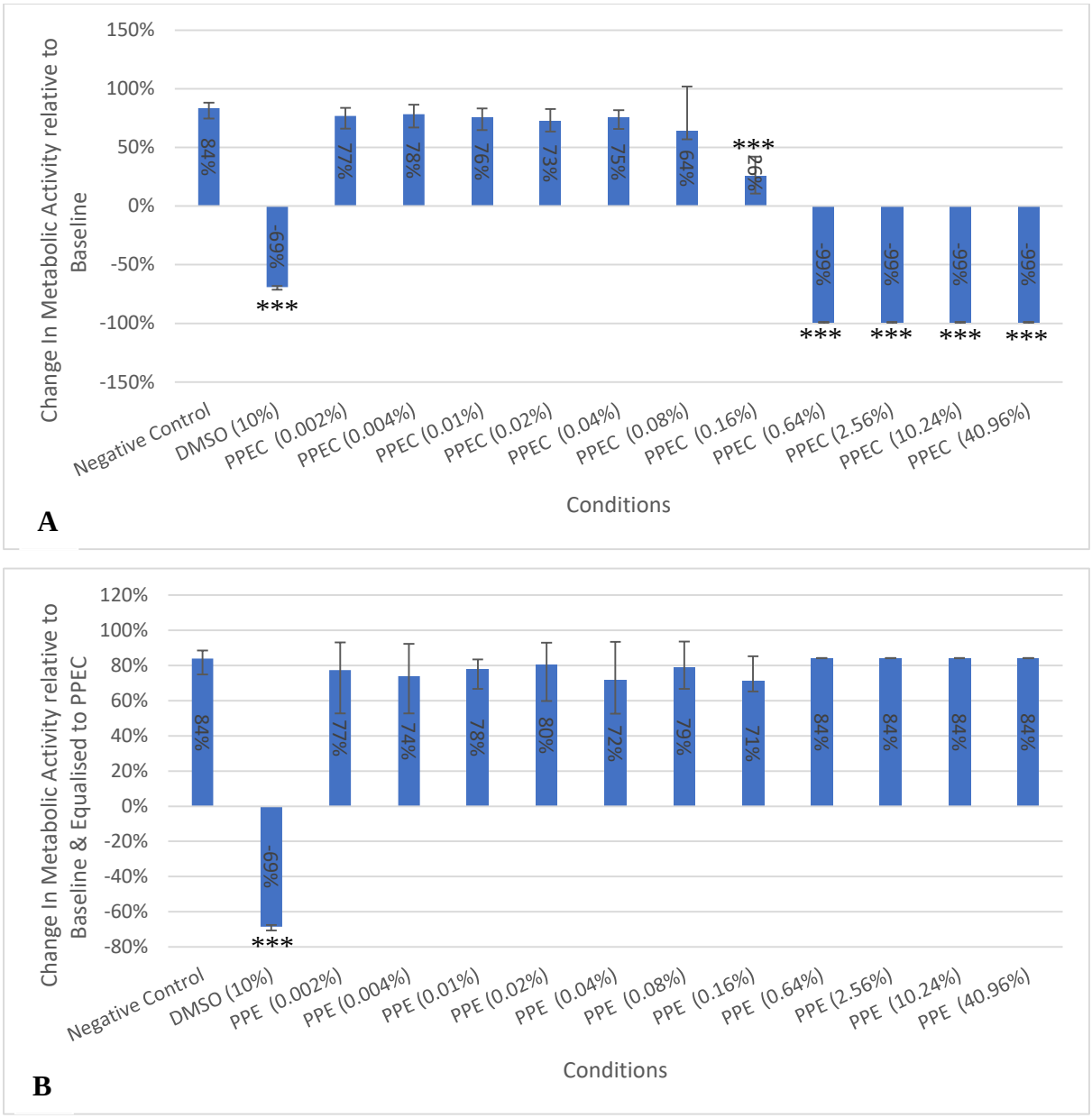

Figure 3.4: The effect of PPEC (**A**) and PPE (**B**) on the viability of HDFs after 48 h exposure. The HDFs were seeded at $1.25x10^3$ cells/well in 96 well-plates and were allowed to recover overnight under standard culture conditions (37°C / 5 % CO_2). Post-recovery at 0 h the HDFs were exposed to a range of conditions. A CellTitre-Glo assay was performed 48 h post exposure and the results are represented as a percentage change in metabolic activity relative to the activity observed at 0 h and in the case of PPE also equalised to PPEC. The values shown are the median 2 biological replicates with 9 technical replicates each. Postitve/negative error was determined by difference of median to upper/lower quartiles. The KW was a comparison between the various conditions in relation to the negative control and any significant difference was apporopriately indicated p <0.05 */<0.01 **/<0.001 ***.

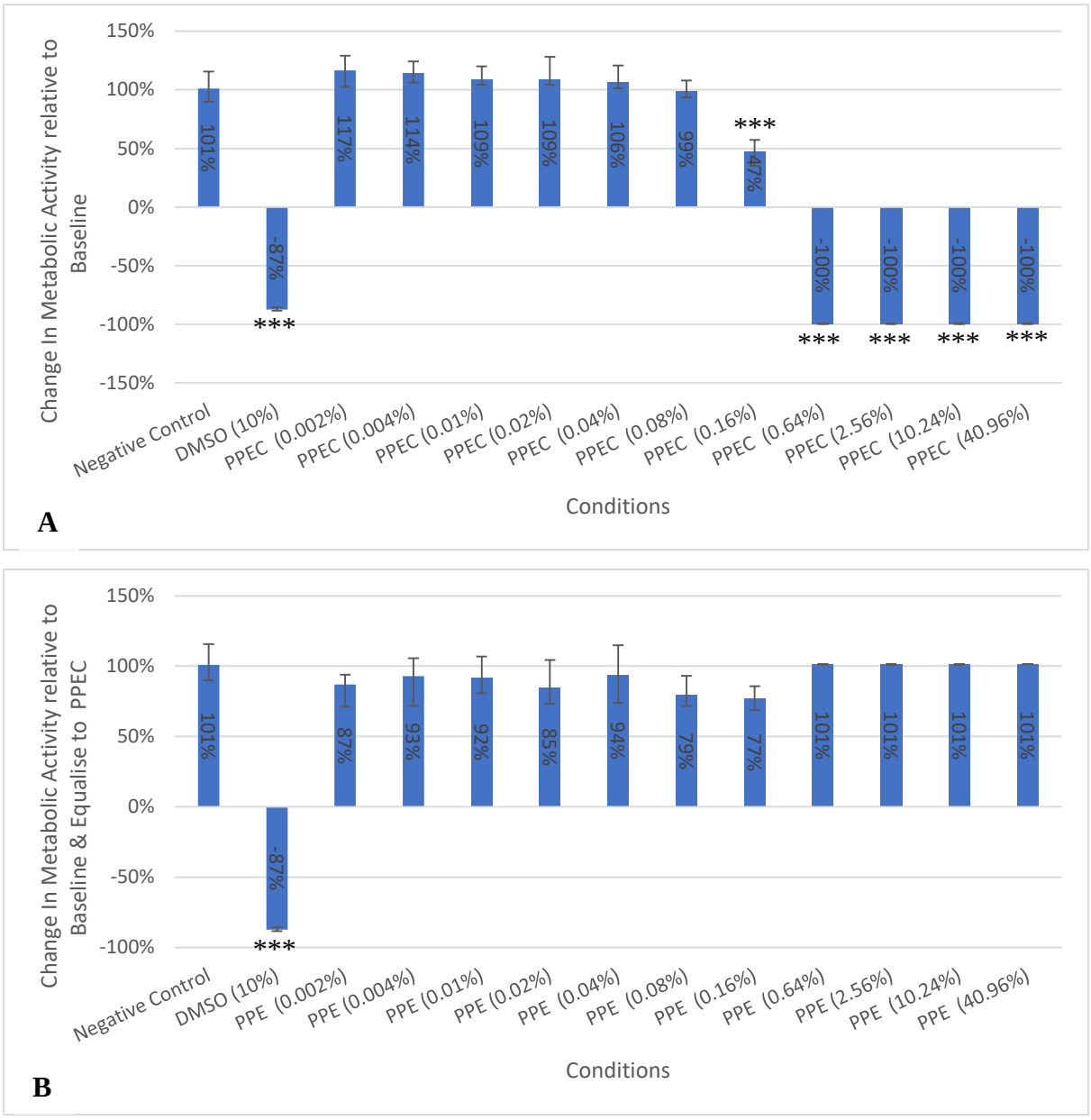

Figure 3.5: The effect of PPEC (**A**) and PPE (**B**) on the viability of HDFs after 72 h exposure. The HDFs were seeded at $1.25x10^3$ cells/well in 96 well-plates and were allowed to recover overnight under standard culture conditions (37°C / 5 % CO_2). Post-recovery at 0 h the HDFs were exposed to a range of conditions. A CellTitre-Glo assay was performed 72 h post exposure and the results are represented as a percentage change in metabolic activity relative to the activity observed at 0 h and in the case of PPE also equalised to PPEC. The values shown are the median 2 biological replicates with 9 technical replicates each. Postitve/negative error was determined by difference of median to upper/lower quartiles. The KW was a comparison between the various conditions in relation to the negative control and any significant difference was apporopriately indicated p <0.05 */<0.01 **/<0.001 ***.

3.2.2. Heat stress (44°C) effect on viability with or /without prickly pear extract /carrier

Figures 3.6 – 3.8, in accordance to the protocol shown in Section 2.8.2 the CellTitre-Glo assay was performed in conjunction with heat stress protocol C were a parallel run with both heat stress (+ HS 44°C for 1 h) and non-heat stress control (- HS 37°C for 1 h) were tested with varying concentrations of PPE and PPEC (0.002, 0.004, 0.01, 0.02, 0.04 and 0.08 %) for 72 h, with a reading taken every 24 h. Firstly, as expected 10 % DMSO serving as the positive cytotoxic control showed a significant (KW p = <0.05) negative effect on viability when compared to the negative control. A significant difference was observed between the Negative control with Heat stress and the Negative control without Heat stress at 24 h and 48 h but did not persist to 72 h which indicates a deleterious effect to viability by the heat stress treatment (44°C) which is then overcome. The PPE/PPEC (0.002, 0.004, 0.01, 0.02, 0.04 and 0.08 %) when in direct contact with HDFs in culture for duration without heat stress (- HS 37°C for 1hr) were seen to have no significant (KW p = >0.05) effect on viability of HDFs when compared to the negative control in the same time frame. Furthermore, the PPEC (0.002, 0.004, 0.01, 0.02, 0.04 and 0.08 %) with heat stress (+ HS 44°C for 1 h) was also seen to have no significant (KW p = >0.05) effect on viability of HDF when compared to the negative control under the same conditions in the same time frame during all time points (24, 48, 72 h).

The interpretation of Figure 3.6 shows that the PPE (0.002, 0.004, 0.01, 0.02, 0.04 and 0.08 %), at 24 h following heat stress (+ HS 44°C for 1 h), had a significant (KW p = <0.05) positive protective effect on viability of HDFs when compared to the negative control in the same time frame amounting to 66 %, 44 %, 48 %, 50 %, 82 % and 55 % respectively. The interpretation of Figure 3.7 shows that the PPE (0.04 and 0.08 %) at 48 h following heat stress (+ HS 44°C for 1 h) had a significant (KW p = <0.05) positive protective effect on viability of HDFs when compared to the negative control in the same time frame amounting to 55% and 55 % respectively. Furthermore, PPE (0.002, 0.004, 0.01, 0.02 %) when in direct contact with HDFs in culture for 48 h following heat stress (+ HS 44°C for 1 h) were seen to have no significant (KW p = >0.05) effect on viability of HDFs when compared to the negative control in the same time frame. The interpretation of Figure 3.8 shows that the PPE (0.002, 0.004, 0.01, 0.02, 0.04 and 0.08 %) at 72hr following heat stress (+ HS 44°C for 1hr) had no significant (KW p = >0.05) effect on viability of HDFs when compared to the negative control in the same time frame.

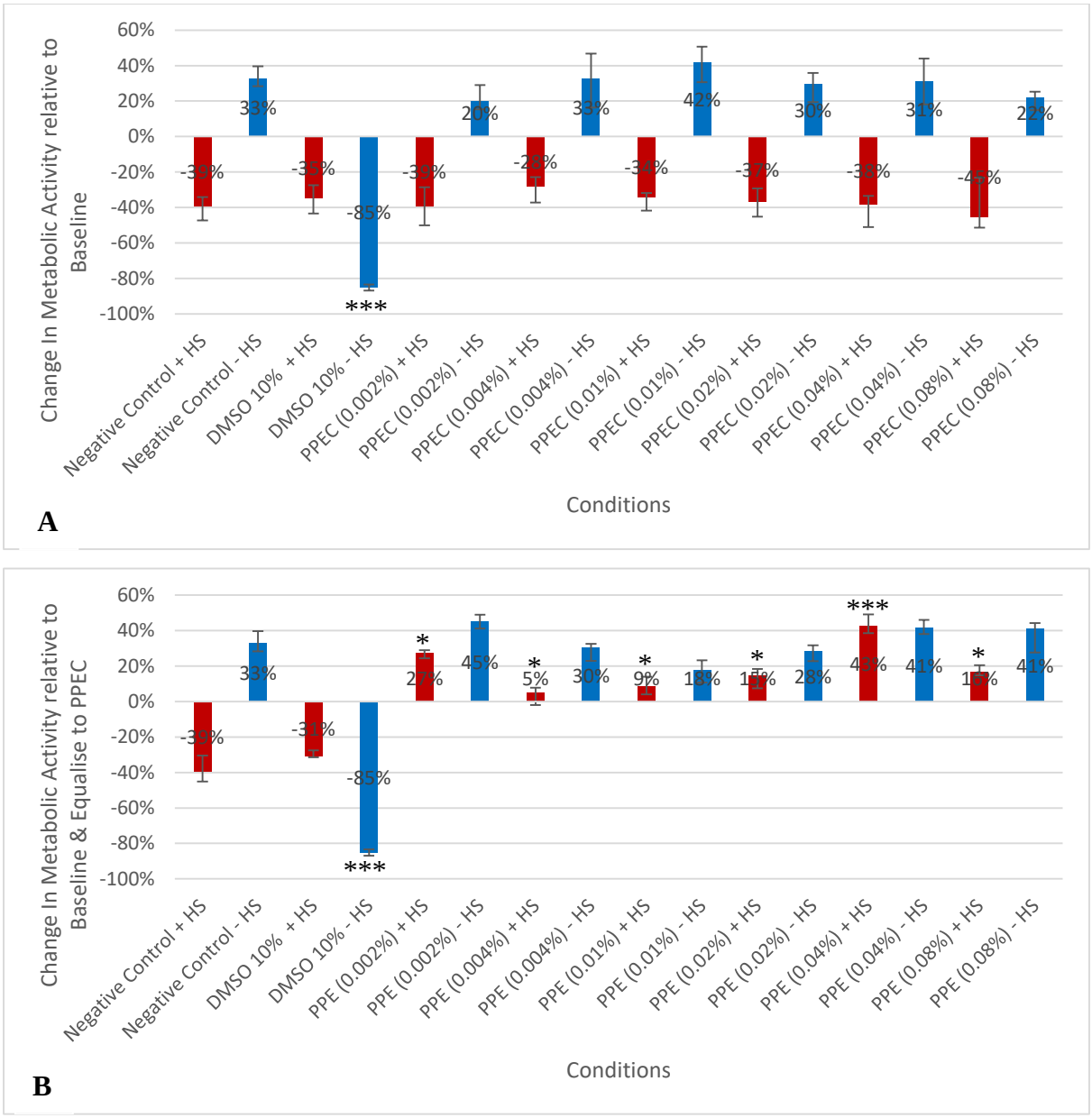

Figure 3.6: The effect of heat stress (44°C for 1 h) with/without PPEC (**A**) or PPE (**B**) on the viability of HDFs after 24 h post-exposure.

The HDFs were seeded at $1.25x10^3$ cells/well in 96 well-plates and were allowed to recover overnight (24 h) in standard culture conditions (37°C / 5 % CO_2). At this point (0 h) the HDFs were treated to a range of PPE/PPEC concentrations (0.002 %, 0.004 %, 0.04 %, 0.08 %) and were returned to standard culture conditions for 1 h. Following treatment half the plates were exposed to heat stress (+ HS) while the other half were left in the incubator (- HS). Following exposure, the plates were subsequently return to standard culture conditions until analysis. A CellTitre-Glo assay was performed 24 h post exposure and the results are represented as a percentage change in metabolic activity relative to the activity observed at 0 h and in the case of PPE also equalised to PPEC. The values shown are the median 2 biological replicates with 9 technical replicates each. Postitve/negative error was determined by difference of median to upper/lower quartiles. The KW was a comparison between the various conditions in relation to the negative control within group (+ HS or – HS) and any significant difference was apporopriately indicated p <0.05 */<0.01 **/<0.001 ***.

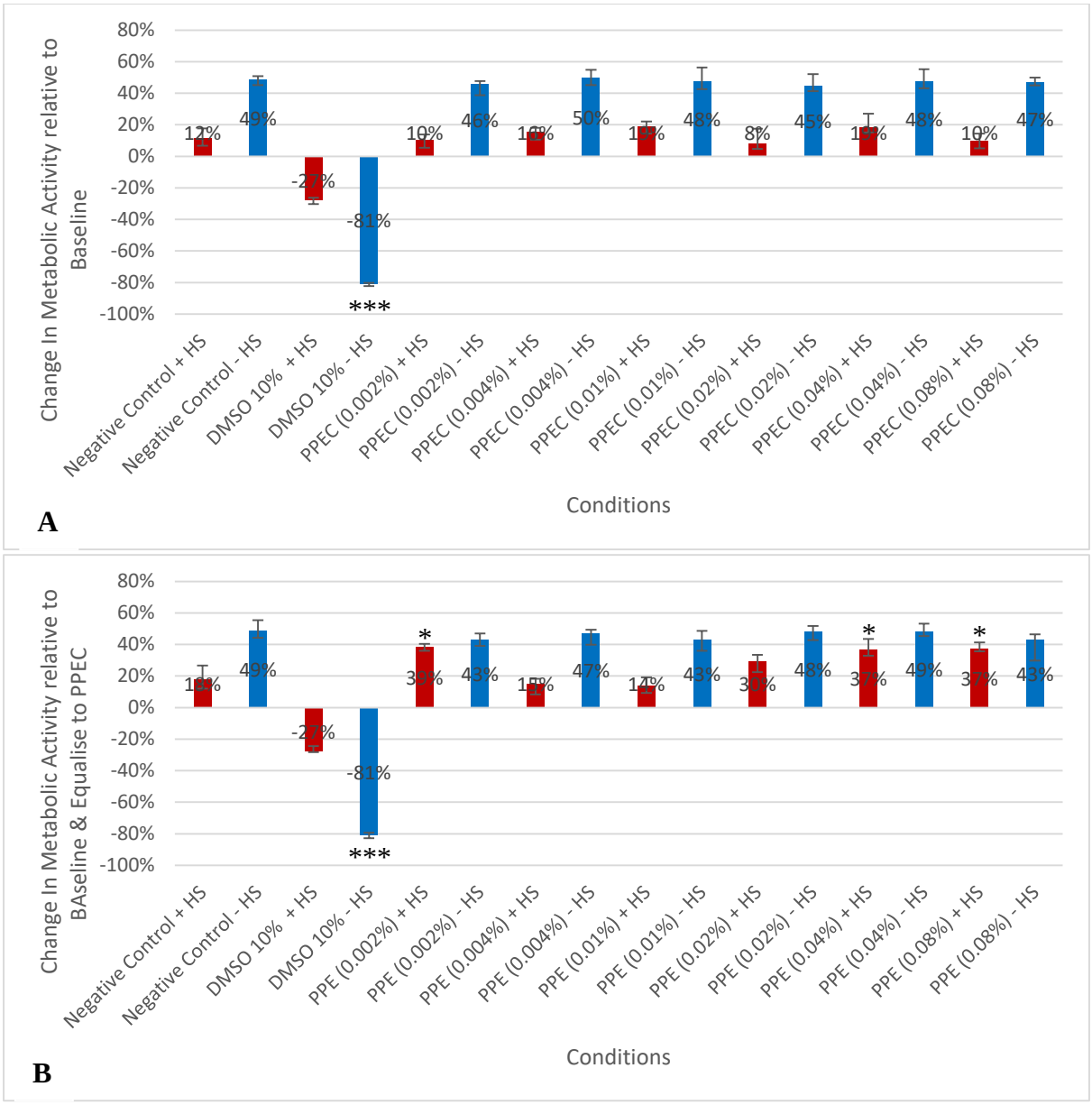

Figure 3.7: The effect of heat stress (44°C for 1 h) with/without PPEC (**A**) or PPE (**B**) on the viability of HDFs after 48 h post-exposure.

The HDFs were seeded at $1.25x10^3$ cells/well in 96 well-plates and were allowed to recover overnight (24 h) in standard culture conditions (37°C / 5 % CO_2). At this point (0 h) the HDFs were treated to a range of PPE/PPEC concentrations (0.002 %, 0.004 %, 0.04 %, 0.08 %) and were returned to standard culture conditions for 1 h. Following treatment half the plates were exposed to heat stress (+ HS) while the other half were left in the incubator (- HS). Following exposure, the plates were subsequently return to standard culture conditions until analysis. A CellTitre-Glo assay was performed 48 h post exposure and the results are represented as a percentage change in metabolic activity relative to the activity observed at 0 h and in the case of PPE also equalised to PPEC. The values shown are the median 2 biological replicates with 9 technical replicates each. Postitve/negative error was determined by difference of median to upper/lower quartiles. The KW was a comparison between the various conditions in relation to the negative control within group (+ HS or – HS) and any significant difference was apporopriately indicated p <0.05 */<0.01 **/<0.001 ***.

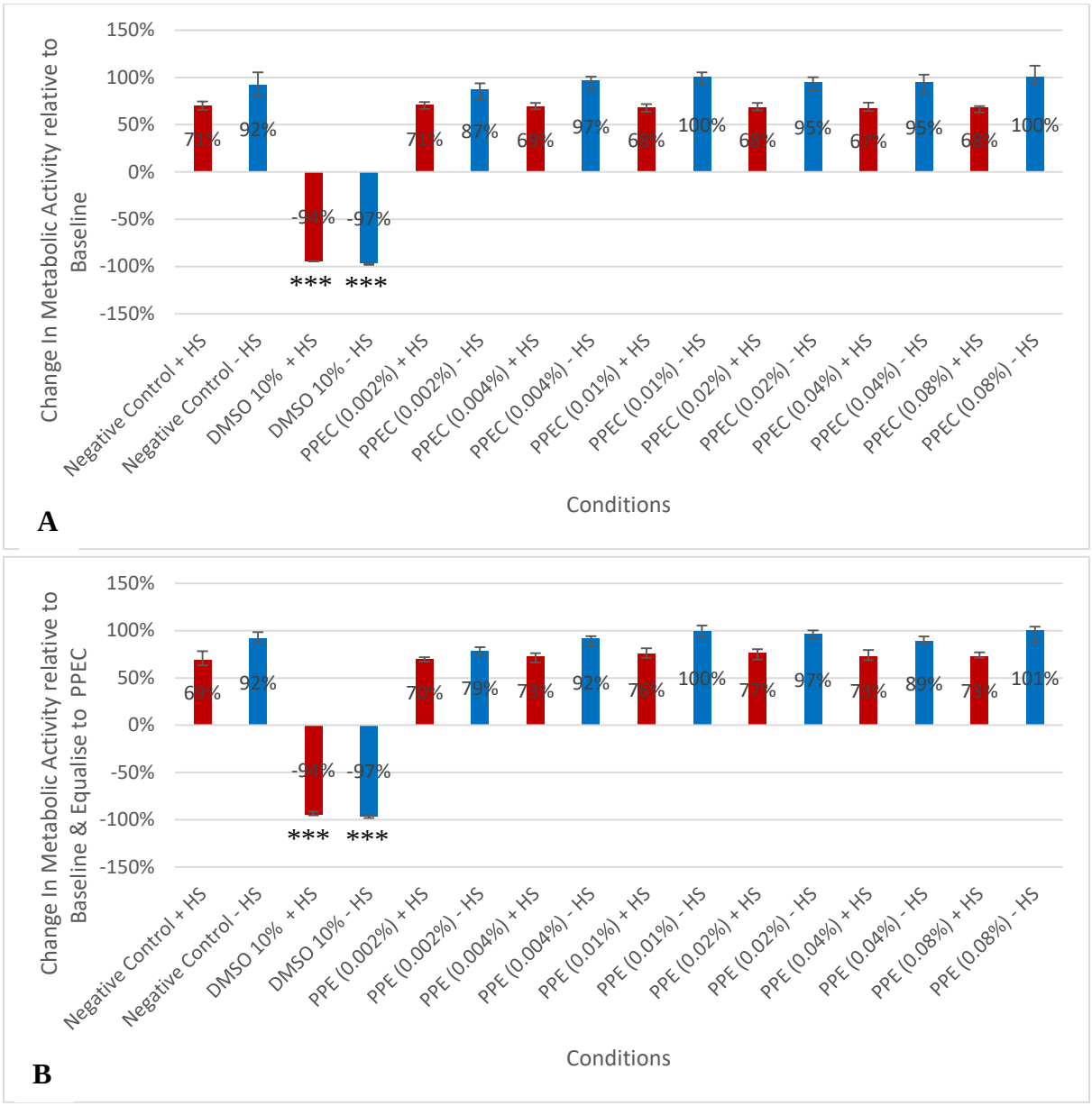

Figure 3.8: The effect of heat stress (44°C for 1 h) with/without PPEC (**A**) or PPE (**B**) on the viability of HDFs after 72 h post-exposure.

The HDFs were seeded at $1.25x10^3$ cells/well in 96 well-plates and were allowed to recover overnight (24 h) in standard culture conditions (37°C / 5 % CO_2). At this point (0 h) the HDFs were treated to a range of PPE/PPEC concentrations (0.002 %, 0.004 %, 0.04 %, 0.08 %) and were returned to standard culture conditions for 1 h. Following treatment half the plates were exposed to heat stress (+ HS) while the other half were left in the incubator (- HS). Following exposure, the plates were subsequently return to standard culture conditions until analysis. A CellTitre-Glo assay was performed 72 h post exposure and the results are represented as a percentage change in metabolic activity relative to the activity observed at 0 h and in the case of PPE also equalised to PPEC. The values shown are the median 2 biological replicates with 9 technical replicates each. Postitve/negative error was determined by difference of median to upper/lower quartiles. The KW was a comparison between the various conditions in relation to the negative control within group (+ HS or – HS) and any significant difference was apporopriately indicated p <0.05 */<0.01 **/<0.001 ***.

3.2.3. Oxidative Stress effect on viability with or /without prickly pear extract carrier

Following the protocol described in Section 2.8.3 the oxidative stress viability was performed to test the effect of various concentrations of menadione (25 µM, 12.5 µM and 6.25 µM) on the viability of HDFs in the presence/absence of PPE/PPEC (0.002, 0.004, 0.01, 0.02, 0.04 and 0.08 %) for 4 h, with a reading taken every 2 h. The results are presented in Figures 3.9 – 3.15. The deleterious effect of menadione (25 µM, 12.5 µM and 6.25 µM) on the viability of HDFs when compared to the negative control within the same time frame at both 2 h and 4 h post exposure is undeniable. Furthermore, the PPE/PPEC (0.002, 0.004, 0.01, 0.02, 0.04 and 0.08 %) appeared to have no significant (KW $p = >0.05$) effect on the viability of HDFs when in direct contact with HDFs for 2 and 4 h respectively. Finally, PPEC (0.002, 0.004, 0.01, 0.02, 0.04 and 0.08 %) were shown to significantly preserve HDFs viability, thus conferring protection to HDFs against oxidative stress (Menadione 25 µM, 12.5 µM and 6.25 µM) at both 2 h and 4 h post exposure to varying degrees however to a lesser extent than the corresponding PPE.

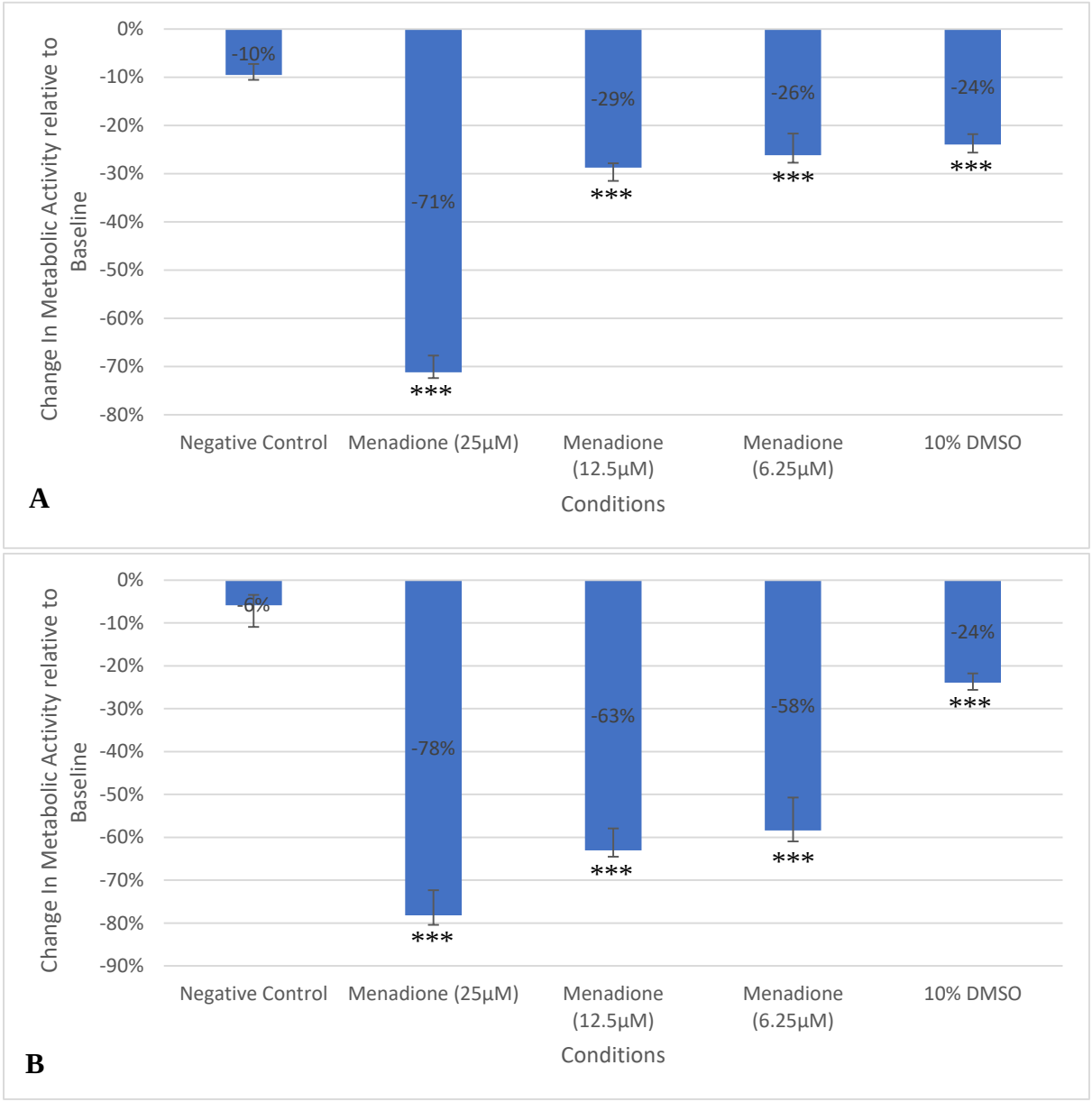

Figure 3.9: The effect of menadione (25 µM, 12.5 µM and 6.25 µM) on HDFs viability in 2 [**A**] or 4 [**B**] h post-exposure.
The HDFs were seeded at $1.25x10^3$ cells/well in 96 well-plates and were allowed to recover overnight under standard culture conditions (37°C / 5 % CO_2). Post-recovery at 0 h the HDFs were exposed to a range of conditions principally, menadione (25 µM, 12.5 µM and 6.25 µM). Following exposure, the plates were subsequently return to standard culture conditions (37°C / 5 % CO_2) until analysis. A CellTitre-Glo assay was performed 2 h [**A**] & 4 [**B**] h post exposure and the results are represented as a percentage change in metabolic activity relative to the activity observed at 0 h. The values shown are the median 2 biological replicates with 9 technical replicates each. Postitve/negative error was determined by difference of median to upper/lower quartiles. The KW was a comparison between the various conditions in relation to the negative control and any significant difference was apporopriately indicated $p < 0.05$ */<0.01 **/<0.001 ***.

The interpretation of figure 3.9 [**A**] and show the effect on viability of HDFs after 2 h exposure to varying concentrations of Menadione compared to the negative control.

- Negative Effect – Menadione (25 µM), Menadione (12.5 µM), Menadione (6.25 µM), when in direct contact with HDFs for 2hr, was seen to have significant (KW p = <0.05) negative effect on viability of HDFs when compared to the negative control in the same time frame, to the tune of ~61 %, 19 % and 16 % respectively.

The interpretation of Figure 3.9 [**B**] show the effect on viability of HDFs after 4 h exposure to varying concentrations of Menadione compared to the negative control.

- Negative Effect – Menadione (25 µM), Menadione (12.5 µM), Menadione (6.25 µM), when in direct contact with HDFs for 4 h, was seen to have significant (KW p = <0.05) negative effect on viability of HDFs when compared to the negative control in the same time frame, to the tune of ~72 %, 57 % and 52 % respectively.

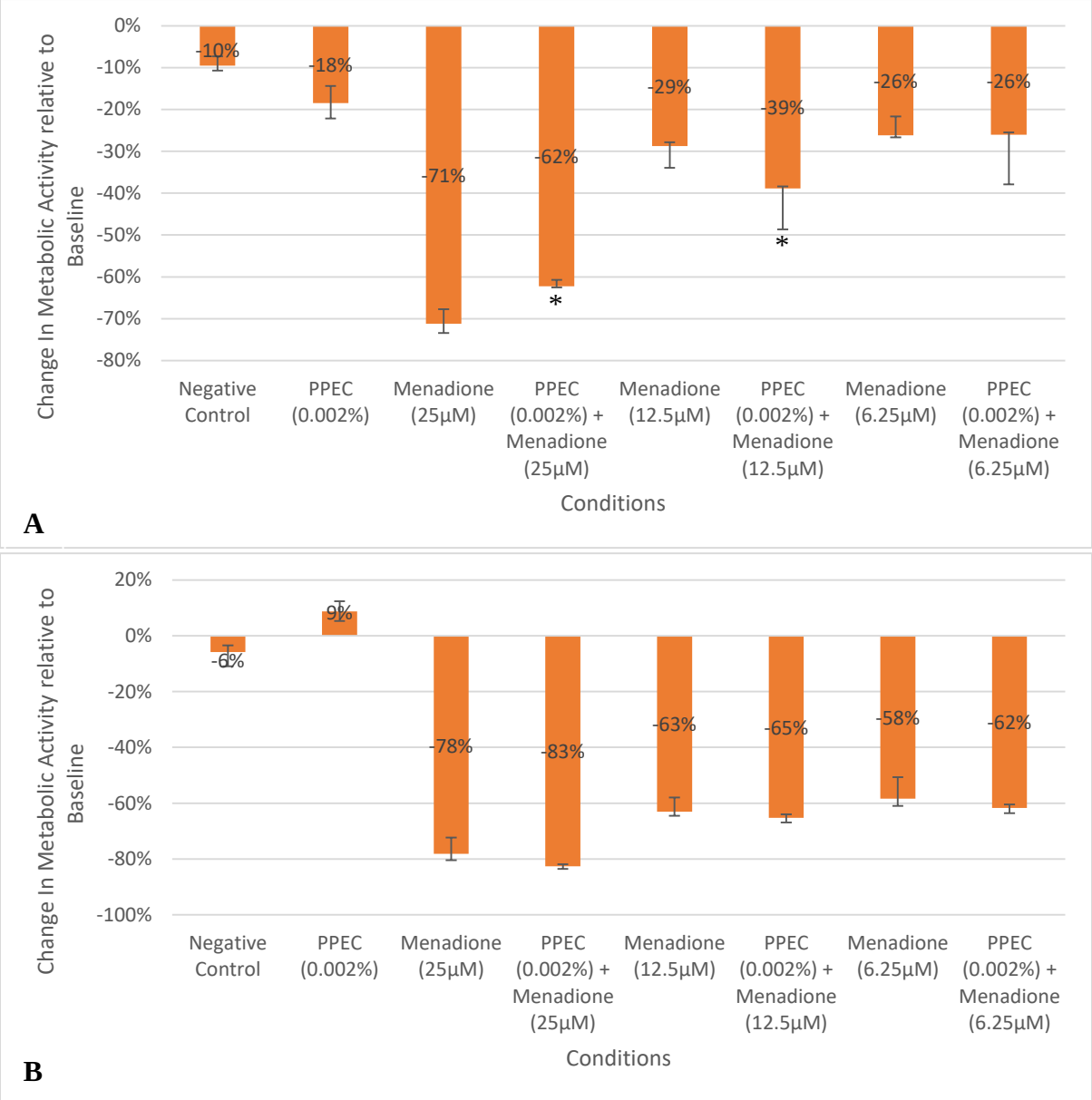

Figure 3.10: The effect menadione (25 µM, 12.5 µM and 6.25 µM) on HDFs viability in presence/absence of prickly pear extract carrier (PPEC) at 0.002% concentration, 2 [**A**] or 4 [**B**] h post-exposure.

The HDFs were seeded at $1.25x10^3$ cells/well in 96 well-plates and were allowed to recover overnight under standard culture conditions (37°C / 5 % CO_2). Post-recovery at 0 h the HDFs were exposed to a range of conditions principally, PPEC (0.002%) or menadione (25 µM, 12.5 µM and 6.25 µM) in conjunction. The PPEC was added 1 hour prior to the menadione as part of pre-exposure treatment. Following exposure, the plates were subsequently return to standard culture conditions (37°C / 5 % CO_2) until analysis. A CellTitre-Glo assay was performed 2 h [**A**] & 4 [**B**] h post exposure and the results are represented as a percentage change in metabolic activity relative to the activity observed at 0 h. The values shown are the median 2 biological replicates with 9 technical replicates each. Postitve/negative error was determined by difference of median to upper/lower quartiles. The KW was a comparison between the conditions in relation relevant menadione (25 12.5 or 6.25 µM) exposure control and any significant difference was apporopriately indicated p <0.05 */<0.01 **/<0.001 ***.

The interpretation of Figure 3.10 [**A**] show the effect on viability of HDFs after 2 h exposure to varying concentrations of menadione with and without PPEC 0.002 %.

- Positive Effect – Menadione 25 µM/ PPEC 0.002 % when in direct contact with HDFs for 4hr, were seen to have significant (KW p = <0.05) positive effect on viability of HDFs when compared to the Menadione 25 µM alone in the same time frame to the tune of ~9 % respectively. This is indicative of a protective effect provided by the PPEC 0.002 %.
- Neutral Effect – Menadione 6.25 µM/ PPEC 0.002 % when in direct contact with HDFs for 4 h was seen to have no significant (KW p = >0.05) effect on viability of HDFs when compared in the same time frame to menadione 6.25 µM.
- Negative Effect - Menadione 12.5 µM/ PPEC 0.002% when in direct contact with HDFs for 4 h was seen to have was seen to have significant (KW p = <0.05) negative effect on viability of HDFs when compared to the Menadione 12.5 µM alone to the tune of 10 %.

The interpretation of Figure 3.10 [**B**] show the effect on viability of HDFs after 4 h exposure to varying concentrations of Menadione with and without PPEC (0.002 %).

- Neutral Effect – Menadione 25 µM/ PPEC, Menadione 12.5 µM/ PPEC 0.002 % and menadione 6.25 µM/ PPEC 0.002 % when in direct contact with HDFs for 2 h was seen to have no significant (KW p = >0.05) effect on viability of HDFs when compared in the same time frame to menadione 25 µM, menadione 12.5 µM and menadione 6.25 µM respectively.

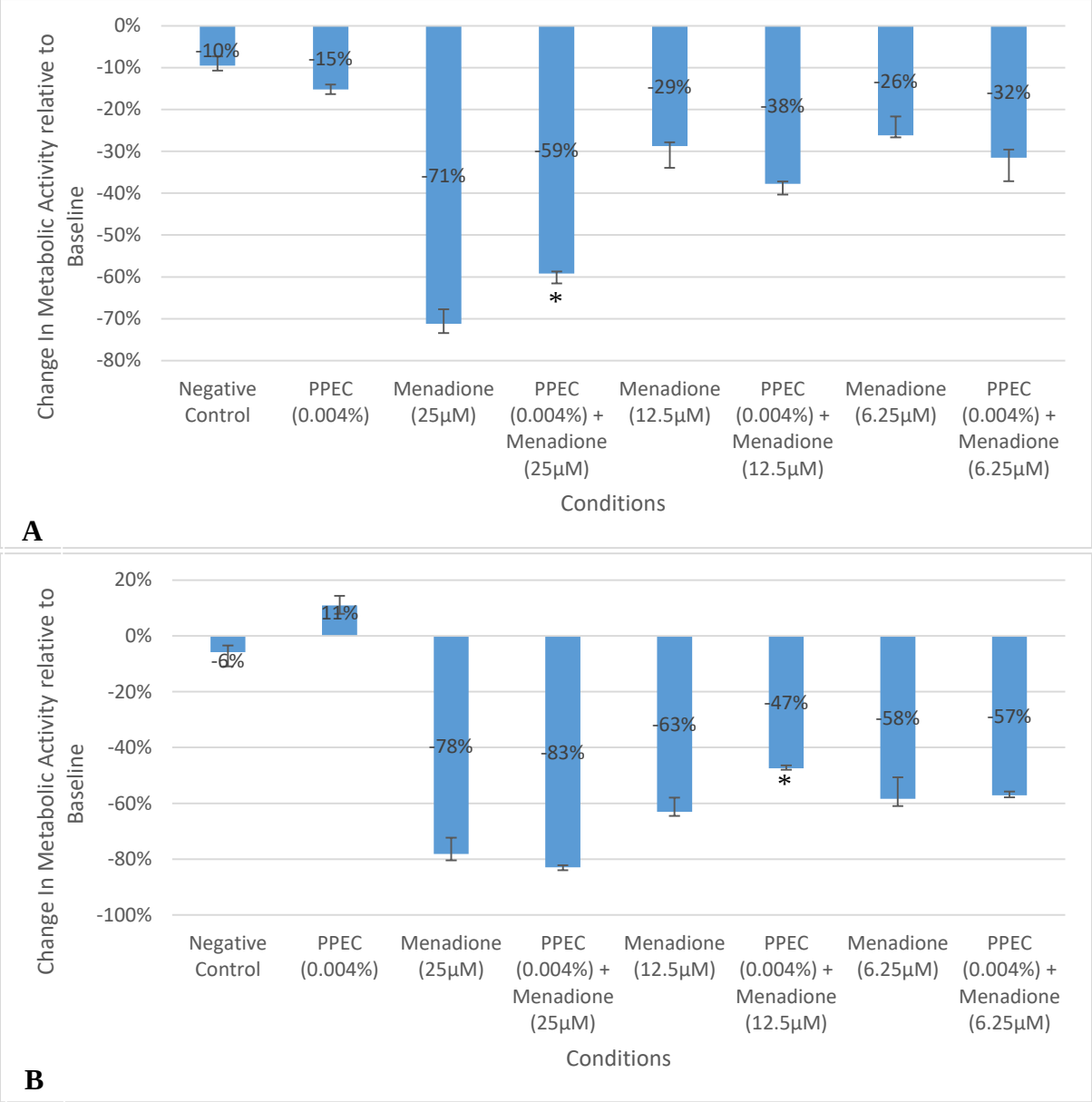

Figure 3.11: The effect of menadione (25 µM, 12.5 µM and 6.25 µM) on HDFs viability in presence/absence of prickly pear extract carrier (PPEC) at 0.004% concentration, 2 [**A**] or 4 [**B**] h post-exposure.
The HDFs were seeded at $1.25x10^3$ cells/well in 96 well-plates and were allowed to recover overnight under standard culture conditions (37°C / 5 % CO_2). Post-recovery at 0 h the HDFs were exposed to a range of conditions principally, PPEC (0.004%) or menadione (25 µM, 12.5 µM and 6.25 µM) in conjunction. The PPEC was added 1 hour prior to the menadione as part of pre-exposure treatment. Following exposure, the plates were subsequently return to standard culture conditions (37°C / 5 % CO_2) until analysis. A CellTitre-Glo assay was performed 2 h [**A**] & 4 [**B**] h post exposure and the results are represented as a percentage change in metabolic activity relative to the activity observed at 0 h. The values shown are the median 2 biological replicates with 9 technical replicates each. Postitve/negative error was determined by difference of median to upper/lower quartiles. The KW was a comparison between the conditions in relation relevant menadione (25 12.5 or 6.25 µM) exposure control and any significant difference was apporopriately indicated p <0.05 */<0.01 **/<0.001 ***.

The interpretation of figure 3.11 [**A**] shows the effect on viability of HDFs after 2 h exposure to varying concentrations of Menadione with and without PPEC 0.004 %.

- Positive Effect – Menadione 25 µM/ PPEC 0.004 % when in direct contact with HDFs for 4hr, were seen to have significant (KW p = <0.05) positive effect on viability of HDFs when compared to the Menadione 25 µM alone respectively in the same time frame to the tune of ~12 %. This is indicative of a protective effect provided by the PPEC 0.004 %.
- Neutral Effect – Menadione 12.5 µM/ PPEC 0.004 % and menadione 6.25 µM/ PPEC when in direct contact with HDFs for 4 h was seen to have no significant (KW p = >0.05) effect on viability of HDFs when compared in the same time frame to Menadione 12.5 µM and menadione 6.25 µM respectively.

The interpretation of Figure 3.11 [**B**] show the effect on viability of HDFs after 4 h exposure to varying concentrations of Menadione with and without PPEC 0.004 %.

- Positive Effect – Menadione 12.5 µM/ PPEC 0.004 % when in direct contact with HDFs for 2 h, were seen to have significant (KW p = <0.05) positive effect on viability of HDFs when compared to the Menadione 12.5 µM alone in the same time frame to the tune of 16 % respectively. This is indicative of a protective effect provided by the PPEC 0.004 %.
- Neutral Effect – Menadione 25 µM/ PPEC 0.004 % and Menadione 6.25 µM/ PPEC 0.004 % when in direct contact with HDFs for 2hr, were seen to have no significant (KW p = >0.05) positive effect on viability of HDFs when compared to the Menadione 25 µM and menadione 6.25 µM alone in the same time frame.

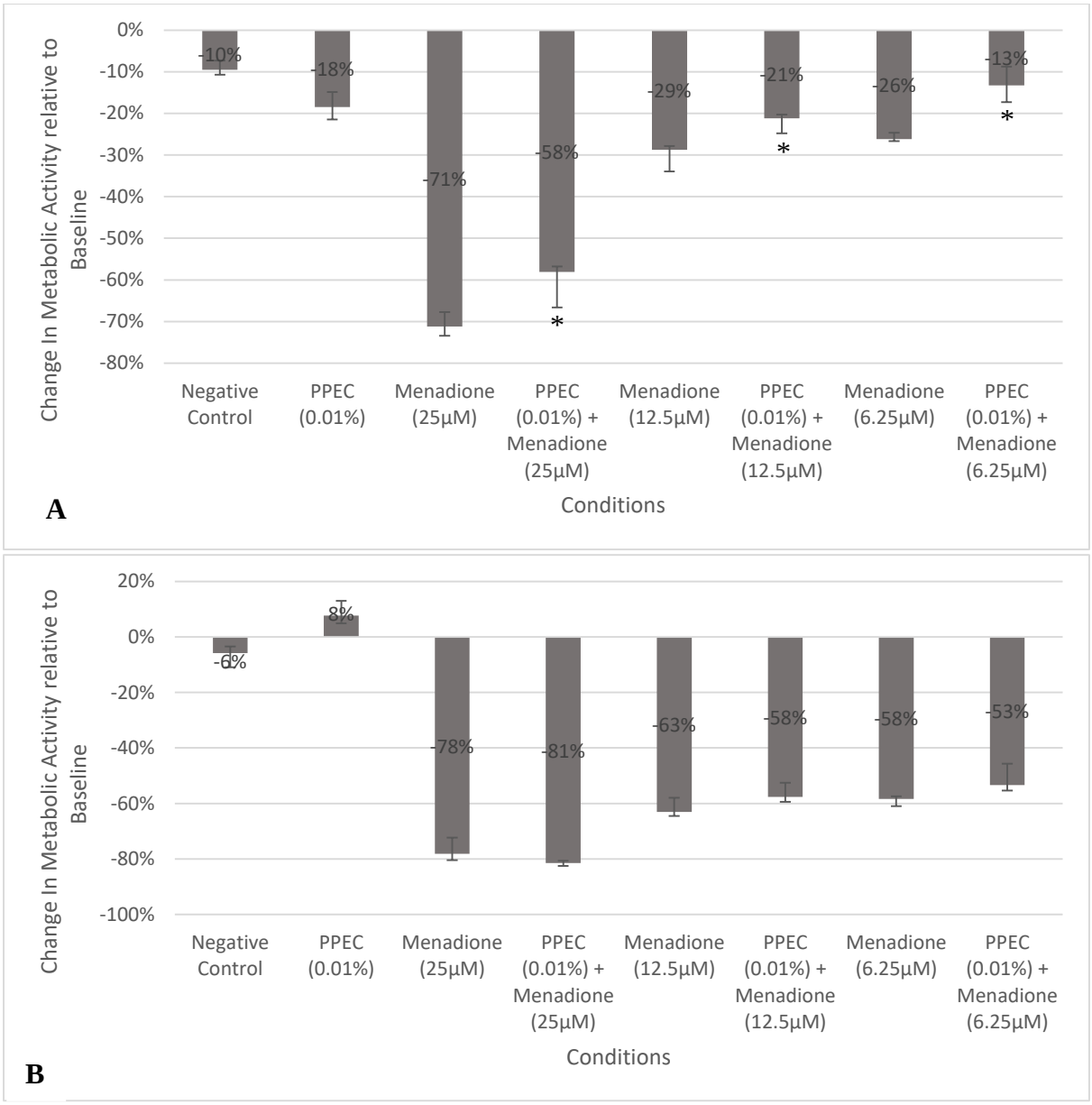

Figure 3.12: The effect menadione (25 µM, 12.5 µM and 6.25 µM) on HDFs viability in presence/absence of prickly pear extract carrier (PPEC) at 0.01% concentration, 2 [**A**] or 4 [**B**] h post-exposure.

The HDFs were seeded at $1.25x10^3$ cells/well in 96 well-plates and were allowed to recover overnight under standard culture conditions (37°C / 5 % CO_2). Post-recovery at 0 h the HDFs were exposed to a range of conditions principally, PPEC (0.01%) or menadione (25 µM, 12.5 µM and 6.25 µM) in conjunction. The PPEC was added 1 hour prior to the menadione as part of pre-exposure treatment. Following exposure, the plates were subsequently return to standard culture conditions (37°C / 5 % CO_2) until analysis. A CellTitre-Glo assay was performed 2 h [**A**] & 4 [**B**] h post exposure and the results are represented as a percentage change in metabolic activity relative to the activity observed at 0 h. The values shown are the median 2 biological replicates with 9 technical replicates each. Postitve/negative error was determined by difference of median to upper/lower quartiles. The KW was a comparison between the conditions in relation relevant menadione (25 12.5 or 6.25 µM) exposure control and any significant difference was apporopriately indicated p <0.05 */<0.01 **/<0.001 ***.

The interpretation of Figure 3.12 [**A**] show the effect on viability of HDFs after 2 h exposure to varying concentrations of Menadione with and without PPEC 0.01 %.

- Positive Effect - Menadione 25 µM/ PPEC 0.01 %, Menadione 12.5 µM/ PPEC 0.01 % and Menadione 6.25 µM/ PPEC 0.01 % when in direct contact with HDFs for 2 h, were seen to have significant (KW p = <0.05) positive effect on viability of HDFs when compared to the Menadione 25 µM, Menadione 12.5 µM and Menadione 6.25 µM alone in the same time frame to the tune of ~13 %, ~8 % and ~13 % respectively. This is indicative of a protective effect provided by the PPEC 0.01 %.

The interpretation of Figure 3.12 [**B**] show the effect on viability of HDFs after 4 h exposure to varying concentrations of Menadione with and without PPEC (0.01 %).

- Neutral Effect – Menadione 25 µM/ PPEC 0.01%, Menadione 12.5 µM/ PPEC 0.01 % and Menadione 6.25 µM/ PPEC 0.02 % when in direct contact with HDFs for 4hr, were seen to have no significant (KW p = >0.05) positive effect on viability of HDFs when compared to the Menadione 25 µM, menadione 12.5 µM and menadione 6.25 µM alone in the same time frame.

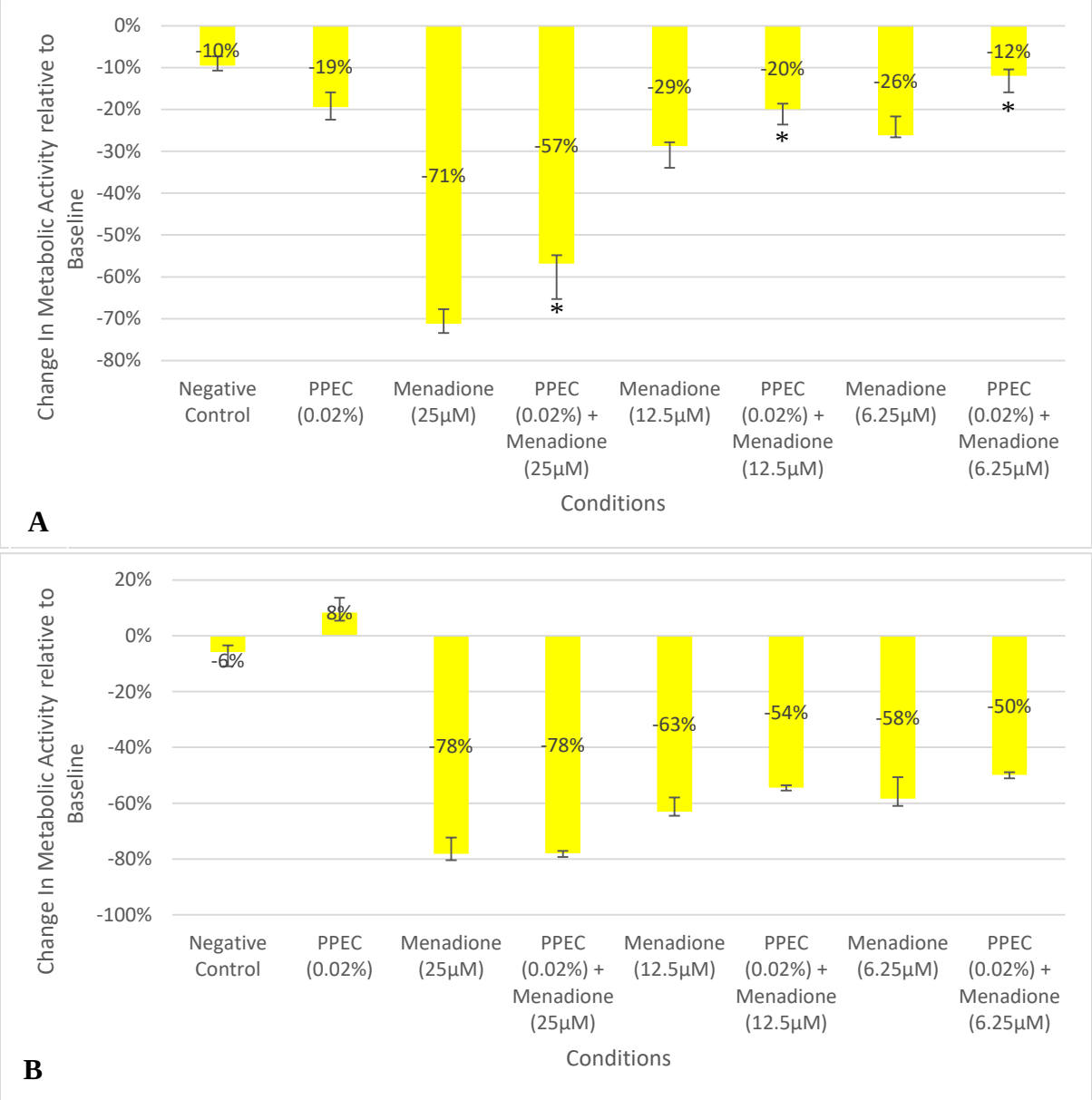

Figure 3.13: The effect menadione (25 µM, 12.5 µM and 6.25 µM) on HDFs viability in presence/absence of prickly pear extract carrier (PPEC) at 0.02% concentration, 2 [**A**] or 4 [**B**] h post-exposure.

The HDFs were seeded at $1.25x10^3$ cells/well in 96 well-plates and were allowed to recover overnight under standard culture conditions (37°C / 5 % CO_2). Post-recovery at 0 h the HDFs were exposed to a range of conditions principally, PPEC (0.02%) or menadione (25 µM, 12.5 µM and 6.25 µM) in conjunction. The PPEC was added 1 hour prior to the menadione as part of pre-exposure treatment. Following exposure, the plates were subsequently return to standard culture conditions (37°C / 5 % CO_2) until analysis. A CellTitre-Glo assay was performed 2 h [**A**] & 4 [**B**] h post exposure and the results are represented as a percentage change in metabolic activity relative to the activity observed at 0 h. The values shown are the median 2 biological replicates with 9 technical replicates each. Postitve/negative error was determined by difference of median to upper/lower quartiles. The KW was a comparison between the conditions in relation relevant menadione (25 12.5 or 6.25 µM) exposure control and any significant difference was apporopriately indicated p <0.05 */<0.01 **/<0.001 ***.

The interpretation of Figure 3.13 [**A**] shows the effect on viability of HDFs after 2 h exposure to varying concentrations of Menadione with/without PPEC 0.02 %.

- Positive Effect – Menadione 25 µM/ PPEC 0.02 %, Menadione 12.5 µM/ PPEC 0.02 % and Menadione 6.25 µM/ PPEC 0.02 % when in direct contact with HDFs for 2 h, were seen to have significant (KW p = <0.05) positive effect on viability of HDFs when compared to the Menadione 25 µM, Menadione 12.5 µM and Menadione 6.25 µM alone in the same time frame to the tune of ~14 %, ~9 % and ~12 % respectively. This is indicative of a protective effect provided by the PPEC 0.02 %.

The interpretation of Figure 3.13 [**B**] shows the effect on viability of HDFs after 4 h exposure to varying concentrations of Menadione with and without PPEC (0.02 %).

- Neutral Effect – Menadione 25 µM/ PPEC 0.02 %, Menadione 12.5 µM/ PPEC 0.02 % and Menadione 6.25 µM/ PPEC 0.02 % when in direct contact with HDFs for 4hr, were seen to have no significant (KW p = >0.05) positive effect on viability of HDFs when compared to the Menadione 25 µM, Menadione 12.5 µM and Menadione 6.25 µM alone in the same time frame.

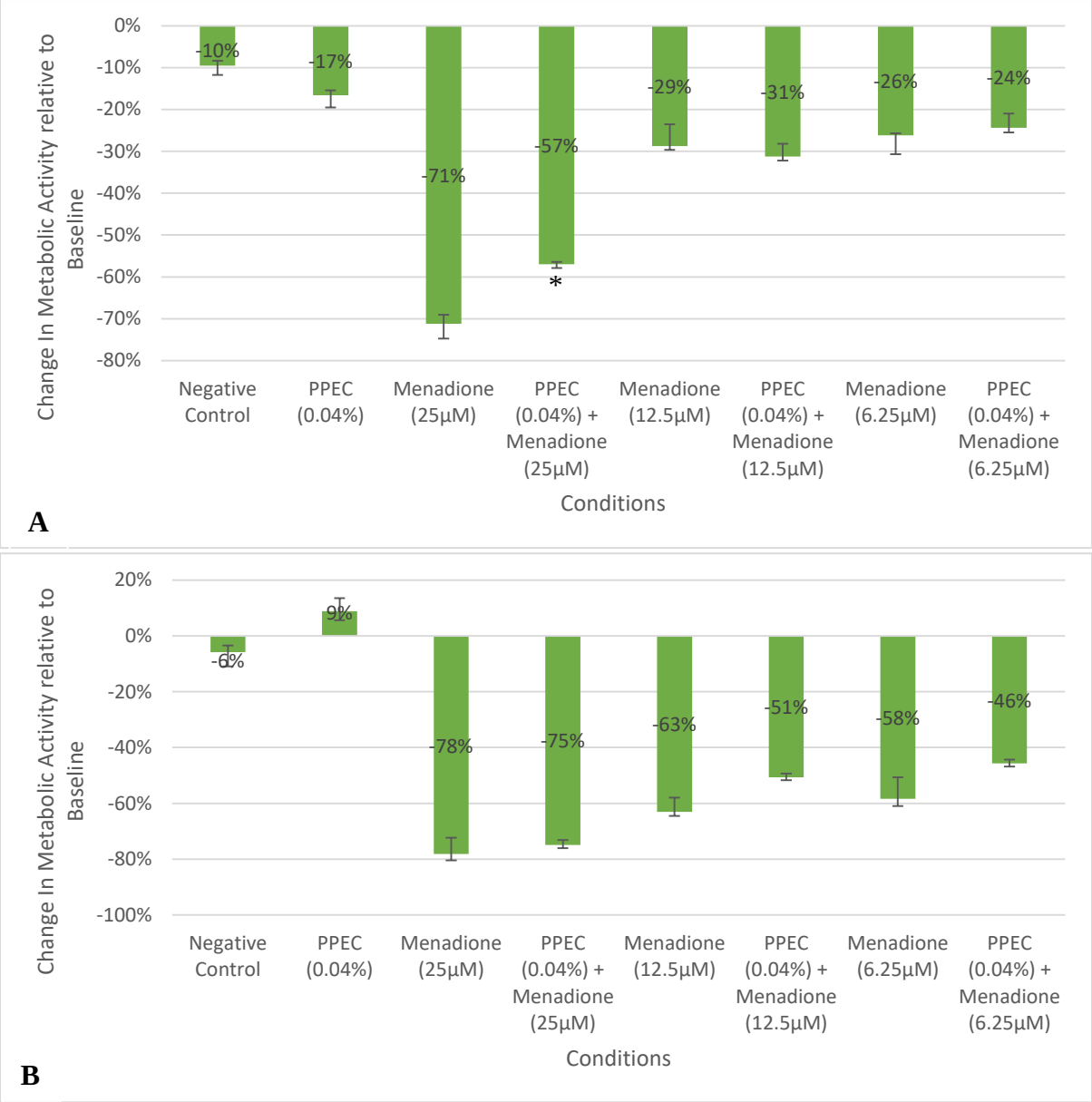

Figure 3.14: The effect menadione (25 µM, 12.5 µM and 6.25 µM) on HDFs viability in presence/absence of prickly pear extract (PPEC) at 0.04% concentration, 2 [**A**] or 4 [**B**] h post-exposure.

The HDFs were seeded at $1.25x10^3$ cells/well in 96 well-plates and were allowed to recover overnight under standard culture conditions (37°C / 5 % CO_2). Post-recovery at 0 h the HDFs were exposed to a range of conditions principally, PPEC (0.04%) or menadione (25 µM, 12.5 µM and 6.25 µM) in conjunction. The PPEC was added 1 hour prior to the menadione as part of pre-exposure treatment. Following exposure, the plates were subsequently return to standard culture conditions (37°C / 5 % CO_2) until analysis. A CellTitre-Glo assay was performed 2 h [**A**] & 4 [**B**] h post exposure and the results are represented as a percentage change in metabolic activity relative to the activity observed at 0 h. The values shown are the median 2 biological replicates with 9 technical replicates each. Postitve/negative error was determined by difference of median to upper/lower quartiles. The KW was a comparison between the conditions in relation relevant menadione (25 12.5 or 6.25 µM) exposure control and any significant difference was apporopriately indicated p <0.05 */<0.01 **/<0.001 ***.

The interpretation of Figure 3.14 [**A**] show the effect on viability of HDFs after 2 h exposure to varying concentrations of Menadione with/without PPEC 0.04 %.

- Positive Effect – Menadione 25 µM/ PPEC 0.04 % when in direct contact with HDFs for 2 h, were seen to have significant (KW p = <0.05) positive effect on viability of HDFs when compared to the Menadione 25 µM alone in the same time frame to the tune of ~14 %. This is indicative of a protective effect provided by the PPEC 0.04 %.
- Neutral Effect – Menadione 12.5 µM/ PPEC 0.04 % and menadione 6.25/ PPEC – 'Vehicle' when in direct contact with HDFs for 2 h was seen to have no significant (KW p = >0.05) effect on viability of HDFs when compared in the same time frame to Menadione 12.5 µM and menadione 6.25 µM respectively.

The interpretation of Figure 3.14 [**B**] shows the effect on viability of HDFs after 4 h exposure to varying concentrations of Menadione with and without PPEC (0.04 %).

- Neutral Effect – Menadione 25 µM/ PPEC 0.04 %, Menadione 12.5 µM/ PPEC 0.04 % and Menadione 6.25 µM/ PPEC 0.04 % when in direct contact with HDFs for 4hr, were seen to have no significant (KW p = <0.05) effect on viability of HDFs when compared to the Menadione 25 µM, Menadione 12.5 µM and Menadione 6.25 µM alone in the same time frame.

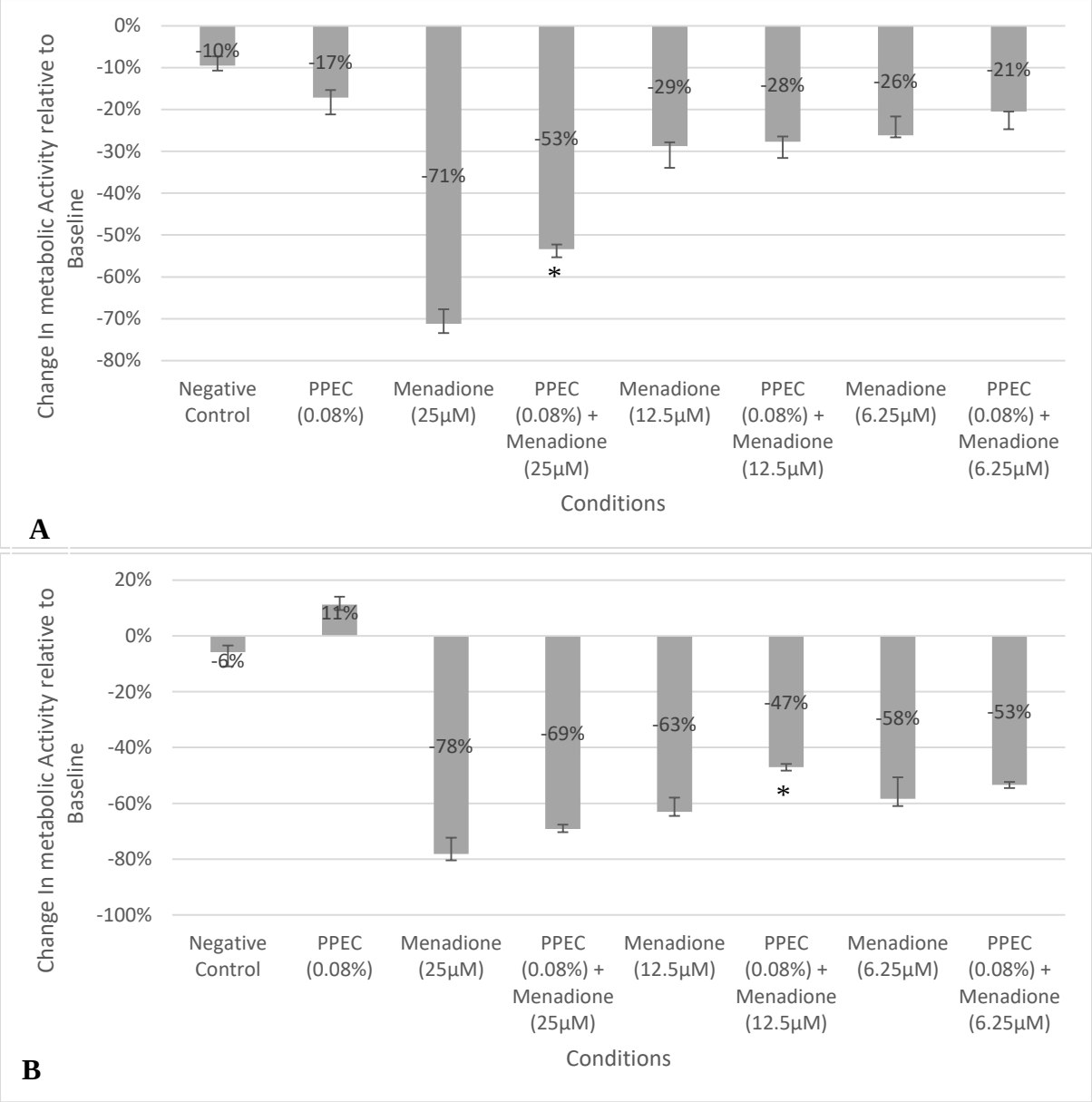

Figure 3.15: The effect menadione (25 µM, 12.5 µM and 6.25 µM) on HDFs viability in presence/absence of prickly pear extract carrier (PPEC) at 0.08% concentration, 2 [**A**] or 4 [**B**] h post-exposure.

The HDFs were seeded at $1.25x10^3$ cells/well in 96 well-plates and were allowed to recover overnight under standard culture conditions (37°C / 5 % CO_2). Post-recovery at 0 h the HDFs were exposed to a range of conditions principally, PPEC (0.08%) or menadione (25 µM, 12.5 µM and 6.25 µM) in conjunction. The PPEC was added 1 hour prior to the menadione as part of pre-exposure treatment. Following exposure, the plates were subsequently return to standard culture conditions (37°C / 5 % CO_2) until analysis. A CellTitre-Glo assay was performed 2 h [**A**] & 4 [**B**] h post exposure and the results are represented as a percentage change in metabolic activity relative to the activity observed at 0 h. The values shown are the median 2 biological replicates with 9 technical replicates each. Postitve/negative error was determined by difference of median to upper/lower quartiles. The KW was a comparison between the conditions in relation relevant menadione (25 12.5 or 6.25 µM) exposure control and any significant difference was apporopriately indicated p <0.05 */<0.01 **/<0.001 ***.

The interpretation of Figure 3.15 [**A**] shows the effect on viability of HDFs after 2 h exposure to varying concentrations of Menadione with and without PPEC 0.08 %.

- Positive Effect - Menadione 25 µM/ PPEC 0.08 % when in direct contact with HDFs for 2 h, were seen to have significant (KW p = <0.05) positive effect on viability of HDFs when compared to the Menadione 25 µM alone in the same time frame to the tune of ~18 %. This is indicative of a protective effect provided by the PPEC 0.08 %.
- Neutral Effect – Menadione 12.5 µM/ PPEC 0.08 % and Menadione 6.25 µM/ PPEC 0.08 % when in direct contact with HDFs for 2 h was seen to have no significant (KW p = >0.05) effect on viability of HDFs when compared in the same time frame to Menadione 12.5 µM and Menadione 6.25 µM alone.

The interpretation of Figure 3.15 [**B**] show the effect on viability of HDFs after 4 h exposure to varying concentrations of Menadione with and without PPEC (0.08 %).

- Positive Effect – Menadione 12.5 µM/ PPEC 0.08 % when in direct contact with HDFs for 4 h, were seen to have significant (KW p = <0.05) positive effect on viability of HDFs when compared to the Menadione 12 µM alone in the same time frame to the tune of ~16 %. This is indicative of a protective effect provided by the PPEC 0.08 %.
- Neutral Effect – Menadione 25 µM/ PPEC 0.08 % and Menadione 6.25 µM/ PPEC 0.08 % when in direct contact with HDFs for 4 h, were seen to have no significant (KW p = >0.05) effect on viability of HDFs when compared in the same time frame to Menadione 25 µM and menadione 6.25 µM respectively.

3.2.4. Oxidative stress effect on viability with or /without prickly pear extract

Following the protocol described in Section 2.8.3, the oxidative stress viability was performed to test the effect of various concentrations of menadione (25 µM, 12.5 µM and 6.25 µM) on the viability of HDFs in the presence/absence of PPEC (0.002, 0.004, 0.01, 0.02, 0.04 and 0.08 %) for 4 h, with a reading taken every 2 h. The results are presented in Figures 3.16 – 3.21. The deleterious effect of menadione (25 µM, 12.5 µM and 6.25 µM) on the viability of HDFs when compared to the negative control within the same time frame at both 2 h and 4 h post exposure is undeniable. Furthermore, the PPEC (0.002, 0.004, 0.01, 0.02, 0.04 and 0.08 %) were exhibited no significant (KW p = >0.05) effect on the viability of HDFs when in direct contact with HDFs for 2 and 4 h respectively. Finally, and interestingly, PPEC (0.002, 0.004, 0.01, 0.02, 0.04 and 0.08 %) were shown to significantly preserve HDFs viability, thus conferring protection to HDFs against oxidative stress (Menadione 25 µM, 12.5 µM and 6.25 µM) at both 2 h and 4 h post exposure to varying degrees however to a lesser extent than the corresponding PPE.

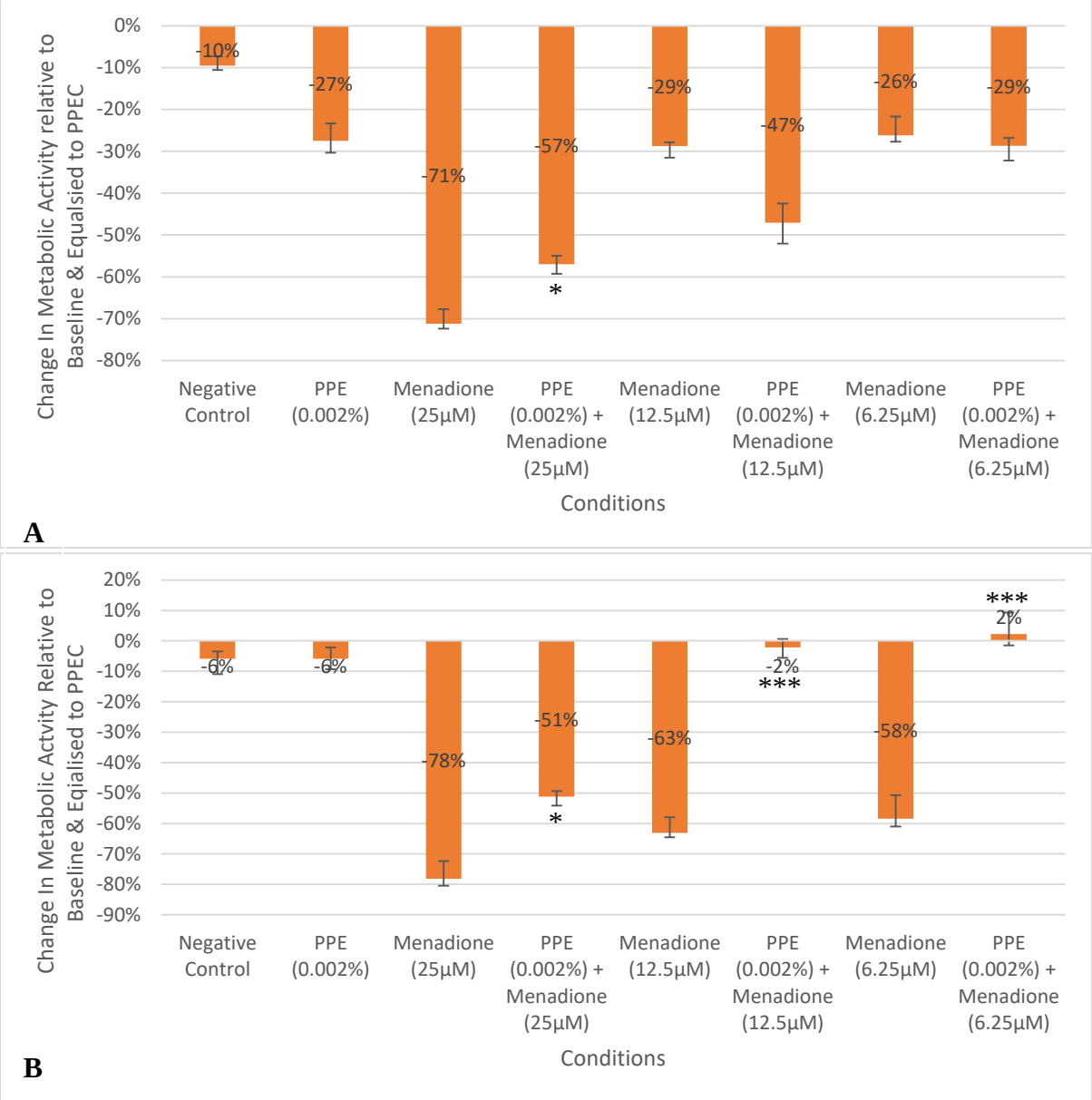

Figure 3.16: The effect menadione (25 µM, 12.5 µM and 6.25 µM) on HDFs viability in presence/absence of prickly pear extract (PPE) at 0.002% concentration, 2 [**A**] or 4 [**B**] h post-exposure.

The HDFs were seeded at $1.25x10^3$ cells/well in 96 well-plates and were allowed to recover overnight under standard culture conditions (37°C / 5 % CO_2). Post-recovery at 0 h the HDFs were exposed to a range of conditions principally, PPE (0.002%) or menadione (25 µM, 12.5 µM and 6.25 µM) in conjunction. The PPE was added 1 hour prior to the menadione as part of pre-exposure treatment. Following exposure, the plates were subsequently return to standard culture conditions (37°C / 5 % CO_2) until analysis. A CellTitre-Glo assay was performed 2 h [**A**] & 4 [**B**] h post exposure and the results are represented as a percentage change in metabolic activity relative to the activity observed at 0 h and equalised to PPEC. The values shown are the median 2 biological replicates with 9 technical replicates each. Postitve/negative error was determined by difference of median to upper/lower quartiles. The KW was a comparison between the conditions in relation relevant menadione (25 12.5 or 6.25 µM) exposure control and any significant difference was apporopriately indicated p <0.05 */<0.01 **/<0.001 ***.

The interpretation of Figure 3.16 [**A**] show the effect on viability of HDFs after 2 h exposure to varying concentrations of menadione with and without PPE 0.002 %.

- Positive Effect – Menadione 25 µM/ PPE 0.002 % when in direct contact with HDFs for 2hr, was seen to have significant (KW p = <0.05) positive effect on viability of HDFs when compared to the Menadione 25 µM alone in the same time frame to the tune of ~14 %. This is indicative of a protective effect provided by the PPE 0.002 %.
- Neutral Effect – Menadione 12.5 µM/ PPE 0.002 % and menadione 6.25 µM/ PPE 0.002 % when in direct contact with HDFs for 2 h was seen to have no significant (KW p = >0.05) effect on viability of HDFs when compared in the same time frame to menadione 12.5 µM and Menadione 6.25 µM respectively.

The interpretation of Figure 3.16 [**B**] shows the effect on viability of HDFs after 4 h exposure to varying concentrations of Menadione with and without PPE (0.002 %).

- Positive Effect – Menadione 25 µM/ PPE 0.002 %, Menadione 12.5 µM/ PPE 0.002% and Menadione 6.25 µM/ PPE 0.002 % when in direct contact with HDFs for 4hr, were seen to have significant (KW p = <0.05) positive effect on viability of HDFs when compared to the Menadione 25 µM, Menadione 12.5 µM and Menadione 6.25 µM alone in the same time frame to the tune of ~27 %, ~61 % and ~60 % respectively. This is indicative of a protective effect provided by the PPE 0.002 %.

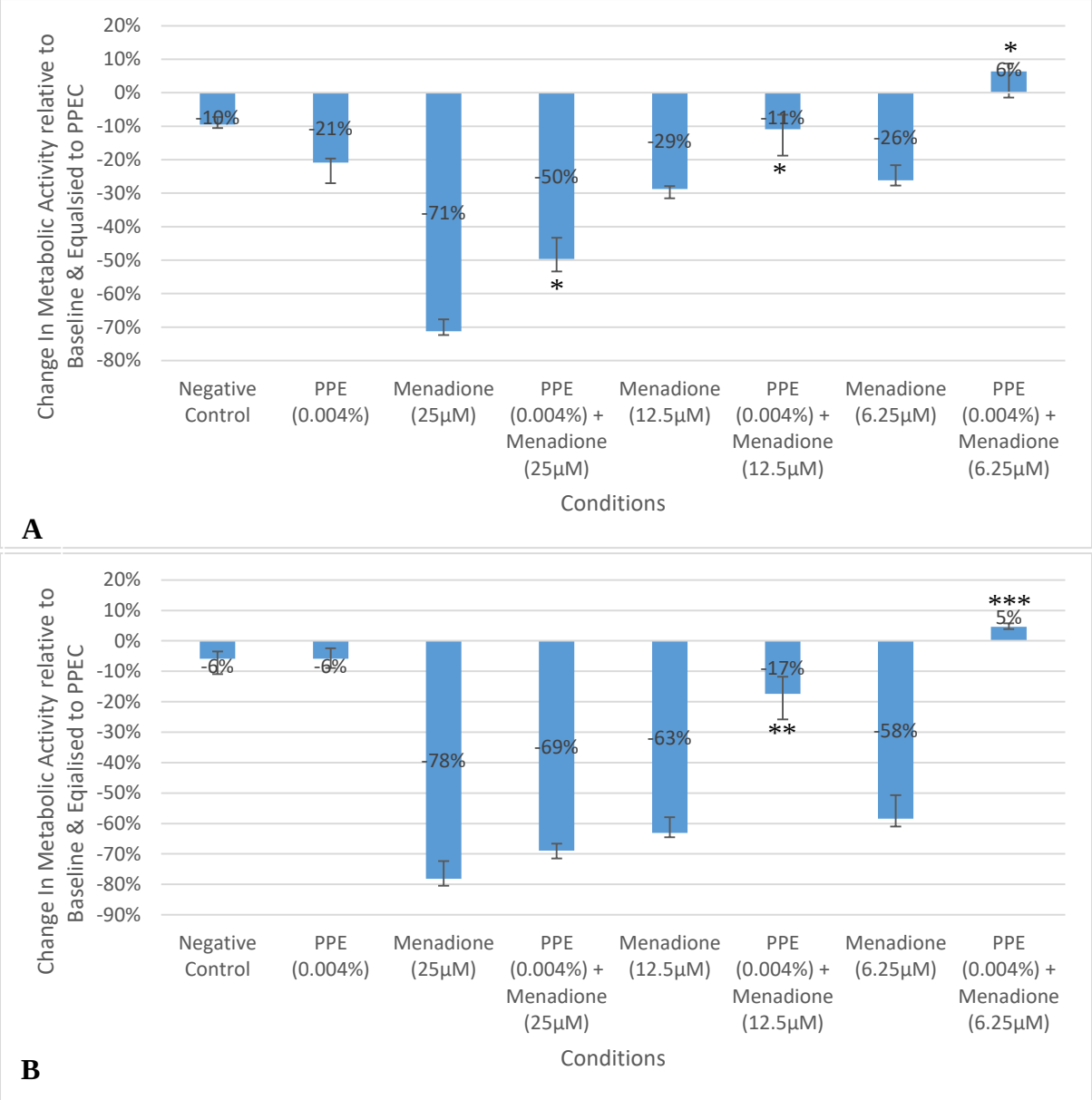

Figure 3.17: The effect menadione (25 µM, 12.5 µM and 6.25 µM) on HDFs viability in presence/absence of prickly pear extract (PPE) at 0.004% concentration, 2 [**A**] or 4 [**B**] h post-exposure.
The HDFs were seeded at $1.25x10^3$ cells/well in 96 well-plates and were allowed to recover overnight under standard culture conditions (37°C / 5 % CO_2). Post-recovery at 0 h the HDFs were exposed to a range of conditions principally, PPE (0.004%) or menadione (25 µM, 12.5 µM and 6.25 µM) in conjunction. The PPE was added 1 hour prior to the menadione as part of pre-exposure treatment. Following exposure, the plates were subsequently return to standard culture conditions (37°C / 5 % CO_2) until analysis. A CellTitre-Glo assay was performed 2 h [**A**] & 4 [**B**] h post exposure and the results are represented as a percentage change in metabolic activity relative to the activity observed at 0 h and equalised to PPEC. The values shown are the median 2 biological replicates with 9 technical replicates each. Postitve/negative error was determined by difference of median to upper/lower quartiles. The KW was a comparison between the conditions in relation relevant menadione (25 12.5 or 6.25 µM) exposure control and any significant difference was apporopriately indicated p <0.05 */<0.01 **/<0.001 ***.

The interpretation of Figure 3.17 [**A**] shows the effect on viability of HDFs after 2 h exposure to varying concentrations of Menadione with and without PPE 0.004 %.

- Positive Effect – Menadione 25 µM/ PPE 0.004 %, Menadione 12.5 µM/ PPE 0.004 % and Menadione 6.25 µM/ PPE 0.004 % when in direct contact with HDFs for 2hr, were seen to have significant (KW p = <0.05) positive effect on viability of HDFs when compared to the Menadione 25 µM, Menadione 12.5 µM and Menadione 6.25 µM alone in the same time frame to the tune of ~21 %, ~18 % and ~32 % respectively. This is indicative of a protective effect provided by the PPE 0.004 %.

The interpretation of Figure 3.17 [**B**] show the effect on viability of HDFs after 4 h exposure to varying concentrations of Menadione with and without PPE 0.004 %.

- Positive Effect –Menadione 12.5 µM/ PPE 0.004 % and Menadione 6.25 µM/ PPE 0.004 % when in direct contact with HDFs for 4hr, were seen to have significant (KW p = <0.05) positive effect on viability of HDFs when compared to the Menadione 12.5 µM and Menadione 6.25 µM alone in the same time frame to the tune of ~46 %, ~63 % respectively. This is indicative of a protective effect provided by the PPE 0.004 %.
- Neutral Effect – Menadione 25 µM/ PPE 0.004 %, when in direct contact with HDFs for 4 h was seen to have no significant (KW p = >0.05) effect on viability of HDFs when compared in the same time frame to Menadione 25 µM alone

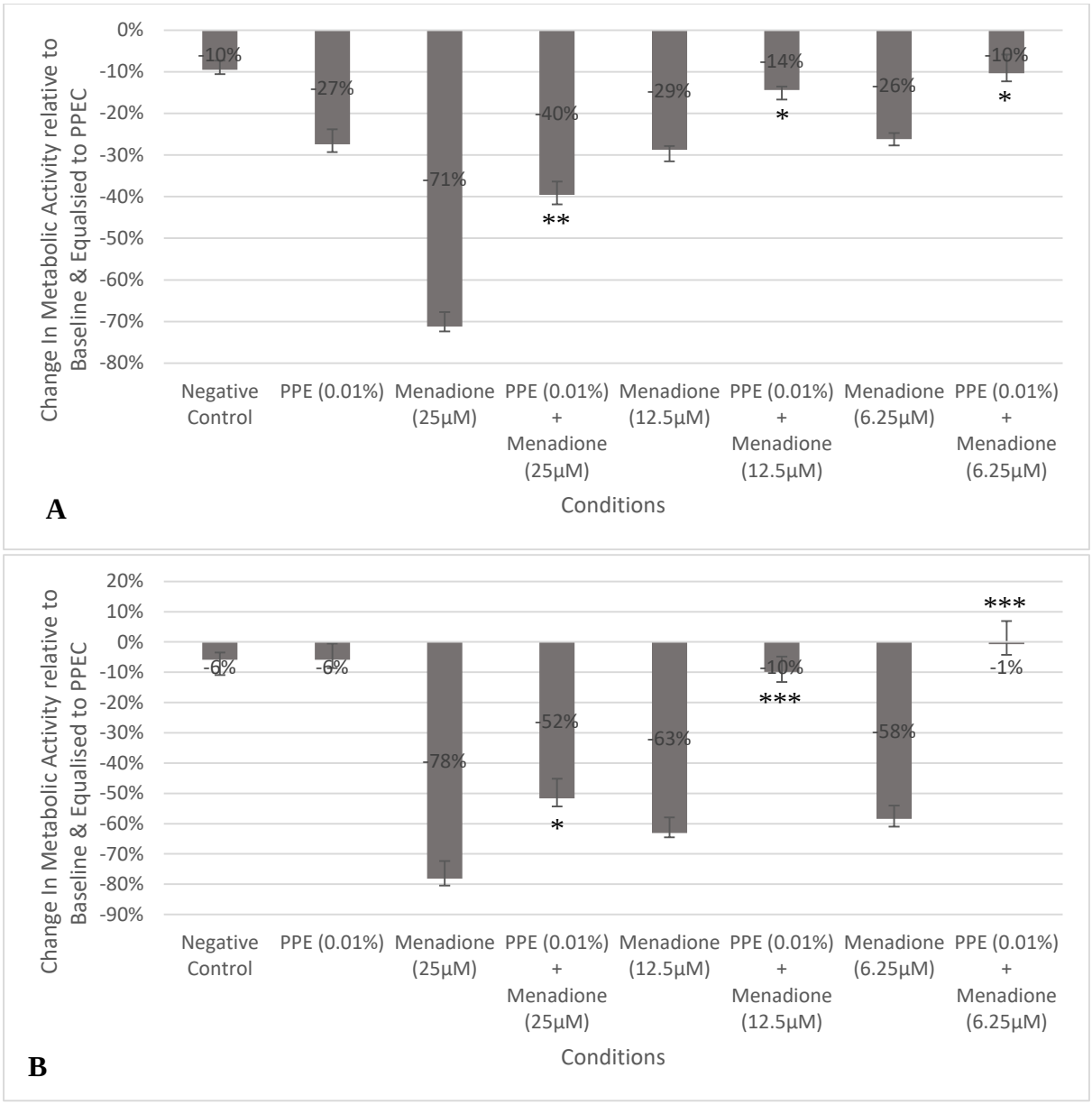

Figure 3.18: The effect menadione (25 µM, 12.5 µM and 6.25 µM) on HDFs viability in presence/absence of prickly pear extract (PPE) at 0.01% concentration, 2 [**A**] or 4 [**B**] h post-exposure.

The HDFs were seeded at $1.25x10^3$ cells/well in 96 well-plates and were allowed to recover overnight under standard culture conditions (37°C / 5 % CO_2). Post-recovery at 0 h the HDFs were exposed to a range of conditions principally, PPE (0.01%) or menadione (25 µM, 12.5 µM and 6.25 µM) in conjunction. The PPE was added 1 hour prior to the menadione as part of pre-exposure treatment. Following exposure, the plates were subsequently return to standard culture conditions (37°C / 5 % CO_2) until analysis. A CellTitre-Glo assay was performed 2 h [**A**] & 4 [**B**] h post exposure and the results are represented as a percentage change in metabolic activity relative to the activity observed at 0 h and equalised to PPEC. The values shown are the median 2 biological replicates with 9 technical replicates each. Postitve/negative error was determined by difference of median to upper/lower quartiles. The KW was a comparison between the conditions in relation relevant menadione (25 12.5 or 6.25 µM) exposure control and any significant difference was apporopriately indicated p <0.05 */<0.01 **/<0.001 ***

The interpretation of Figure 3.18 [**A**] show the effect on viability of HDFs after 2 h exposure to varying concentrations of Menadione with and without PPE 0.01 %.

- Positive Effect - Menadione 25 µM/ PPE 0.01 %, Menadione 12.5 µM/ PPE 0.01 % and Menadione 6.25 µM/ PPE 0.01 % when in direct contact with HDFs for 2 h, were seen to have significant (KW p = <0.05) positive effect on viability of HDFs when compared to the Menadione 25 µM, Menadione 12.5 µM and Menadione 6.25 µM alone in the same time frame to the tune of ~21 %, ~15 % and ~16 % respectively. This is indicative of a protective effect provided by the PPE 0.01 %.

The interpretation of Figure 3.18 [**B**] show the effect on viability of HDFs after 4 h exposure to varying concentrations of Menadione with and without PPE (0.01 %).

- Positive Effect – Menadione 25 µM/ PPE 0.01 %, Menadione 12.5 µM/ PPE 0.01 % and Menadione 6.25 µM/ PPE 0.01 % when in direct contact with HDFs for 4 h, were seen to have significant (KW p = <0.05) positive effect on viability of HDFs when compared to the Menadione 25 µM, Menadione 12.5 µM and Menadione 6.25 µM alone in the same time frame to the tune of ~26 %, ~53 % and ~57 % respectively. This is indicative of a protective effect provided by the PPE 0.01 %.

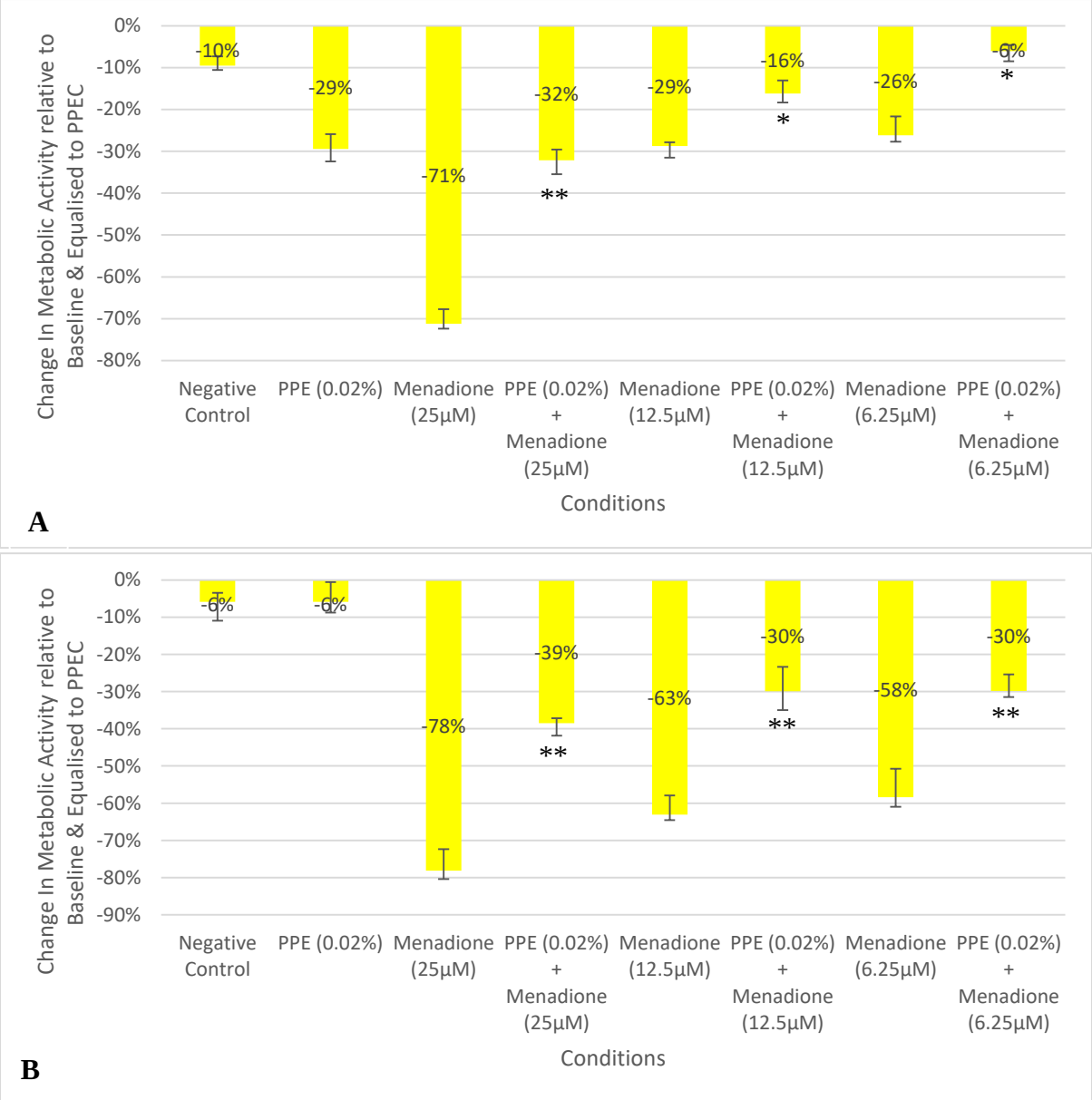

Figure 3.19: The effect menadione (25 µM, 12.5 µM and 6.25 µM) on HDFs viability in presence/absence of prickly pear extract (PPE) at 0.02% concentration, 2 [**A**] or 4 [**B**] h post-exposure.
The HDFs were seeded at $1.25x10^3$ cells/well in 96 well-plates and were allowed to recover overnight under standard culture conditions (37°C / 5 % CO_2). Post-recovery at 0 h the HDFs were exposed to a range of conditions principally, PPE (0.02%) or menadione (25 µM, 12.5 µM and 6.25 µM) in conjunction. The PPE was added 1 hour prior to the menadione as part of pre-exposure treatment. Following exposure, the plates were subsequently return to standard culture conditions (37°C / 5 % CO_2) until analysis. A CellTitre-Glo assay was performed 2 h [**A**] & 4 [**B**] h post exposure and the results are represented as a percentage change in metabolic activity relative to the activity observed at 0 h and equalised to PPEC. The values shown are the median 2 biological replicates with 9 technical replicates each. Postitve/negative error was determined by difference of median to upper/lower quartiles. The KW was a comparison between the conditions in relation relevant menadione (25 12.5 or 6.25 µM) exposure control and any significant difference was apporopriately indicated p <0.05 */<0.01 **/<0.001 ***.

The interpretation of Figure 3.19 [**A**] shows the effect on viability of HDFs after 2 h exposure to varying concentrations of Menadione with/without PPE 0.02 %.

- Positive Effect – Menadione 25 µM/ PPE 0.02 %, Menadione 12.5 µM/ PPE 0.02 % and Menadione 6.25 µM/ PPE 0.02 % when in direct contact with HDFs for 2 h, were seen to have significant (KW p = <0.05) positive effect on viability of HDFs when compared to the Menadione 25 µM, Menadione 12.5 µM and Menadione 6.25 µM alone in the same time frame to the tune of ~39 %, ~13 % and ~20 % respectively. This is indicative of a protective effect provided by the PPE 0.02 %.

The interpretation of Figure 3.19 [**B**] shows the effect on viability of HDFs after 4 h exposure to varying concentrations of Menadione with and without PPE (0.02 %).

- Positive Effect – Menadione 25 µM/ PPE 0.02 %, Menadione 12.5 µM/ PPE 0.02 % and Menadione 6.25 µM/ PPE 0.02 % when in direct contact with HDFs for 4hr, were seen to have significant (KW p = <0.05) positive effect on viability of HDFs when compared to the Menadione 25 µM, Menadione 12.5 µM and Menadione 6.25 µM alone in the same time frame to the tune of ~39 %, ~33 % and ~28 % respectively. This is indicative of a protective effect provided by the PPE 0.02 %.

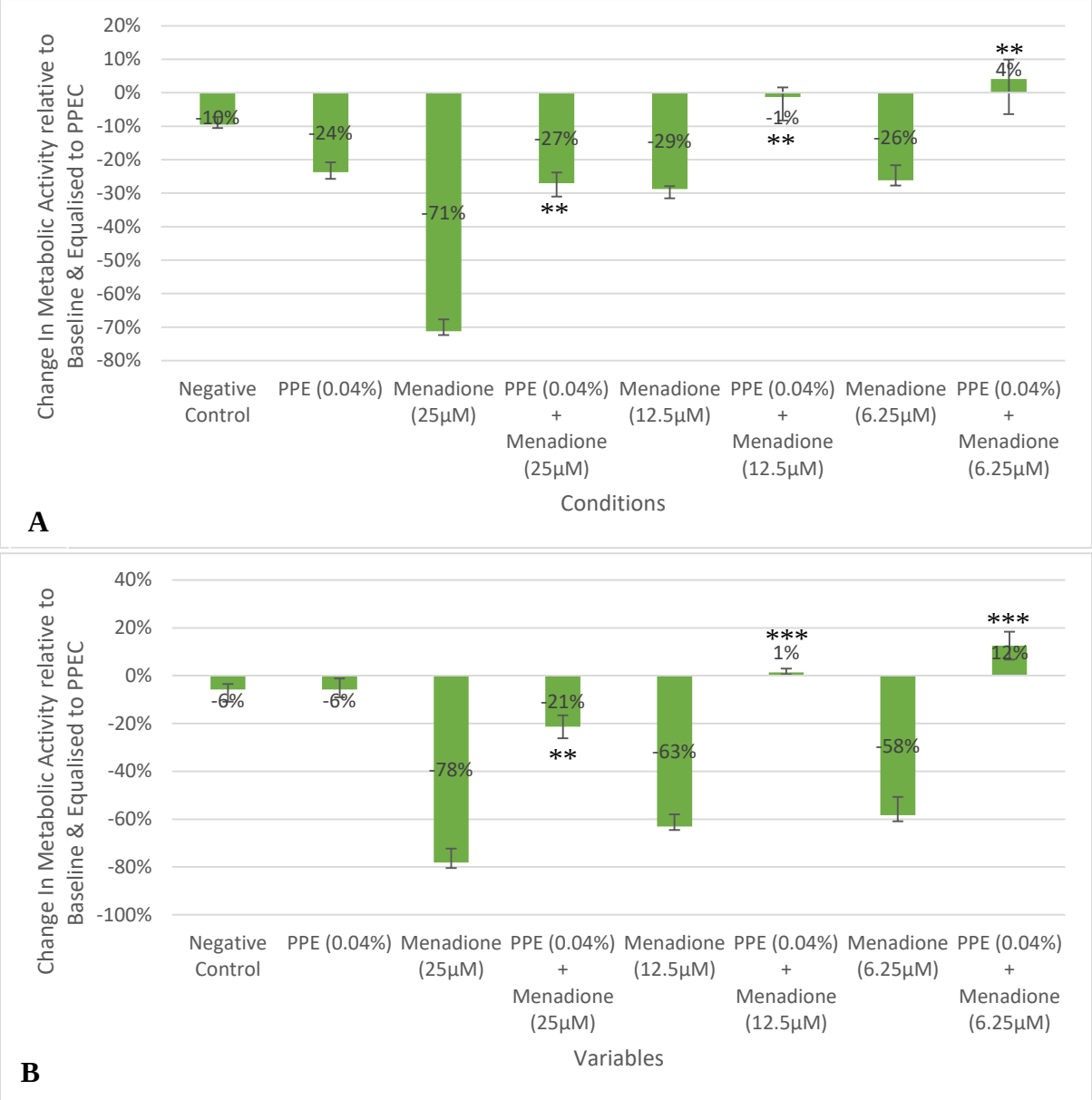

Figure 3.20: The effect menadione (25 µM, 12.5 µM and 6.25 µM) on HDFs viability in presence/absence of prickly pear extract (PPE) at 0.04% concentration, 2 [**A**] or 4 [**B**] h post-exposure.
The HDFs were seeded at $1.25x10^3$ cells/well in 96 well-plates and were allowed to recover overnight under standard culture conditions (37°C / 5 % CO_2). Post-recovery at 0 h the HDFs were exposed to a range of conditions principally, PPE (0.04%) or menadione (25 µM, 12.5 µM and 6.25 µM) in conjunction. The PPE was added 1 hour prior to the menadione as part of pre-exposure treatment. Following exposure, the plates were subsequently return to standard culture conditions (37°C / 5 % CO_2) until analysis. A CellTitre-Glo assay was performed 2 h [**A**] & 4 [**B**] h post exposure and the results are represented as a percentage change in metabolic activity relative to the activity observed at 0 h and equalised to PPEC. The values shown are the median 2 biological replicates with 9 technical replicates each. Postitve/negative error was determined by difference of median to upper/lower quartiles. The KW was a comparison between the conditions in relation relevant menadione (25 12.5 or 6.25 µM) exposure control and any significant difference was apporopriately indicated p <0.05 */<0.01 **/<0.001 ***.

The interpretation of Figure 3.20 [**A**] shows the effect on viability of HDFs after 2 h exposure to varying concentrations of Menadione with/without PPE 0.04 %.

- Positive Effect – Menadione 25 µM/ PPE 0.04 %, Menadione 12.5 µM/ PPE 0.04 % and Menadione 6.25 µM/ PPE 0.04 % when in direct contact with HDFs for 2 h, were seen to have significant (KW p = <0.05) positive effect on viability of HDFs when compared to the Menadione 25 µM, Menadione 12.5 µM and Menadione 6.25 µM alone in the same time frame to the tune of ~44 %, ~28 % and ~30 % respectively. This is indicative of a protective effect provided by the PPE 0.04 %.

The interpretation of Figure 3.20 [**B**] shows the effect on viability of HDFs after 4 h exposure to varying concentrations of Menadione with and without PPE (0.04 %).

- Positive Effect – Menadione 25 µM/ PPE 0.04 %, Menadione 12.5 µM/ PPE 0.04 % and Menadione 6.25 µM/ PPE 0.04 % when in direct contact with HDFs for 4hr, were seen to have significant (KW p = <0.05) positive effect on viability of HDFs when compared to the Menadione 25 µM, Menadione 12.5 µM and Menadione 6.25 µM alone in the same time frame to the tune of ~57 %, ~64 % and ~70 % respectively. This is indicative of a protective effect provided by the PPE 0.04 %.

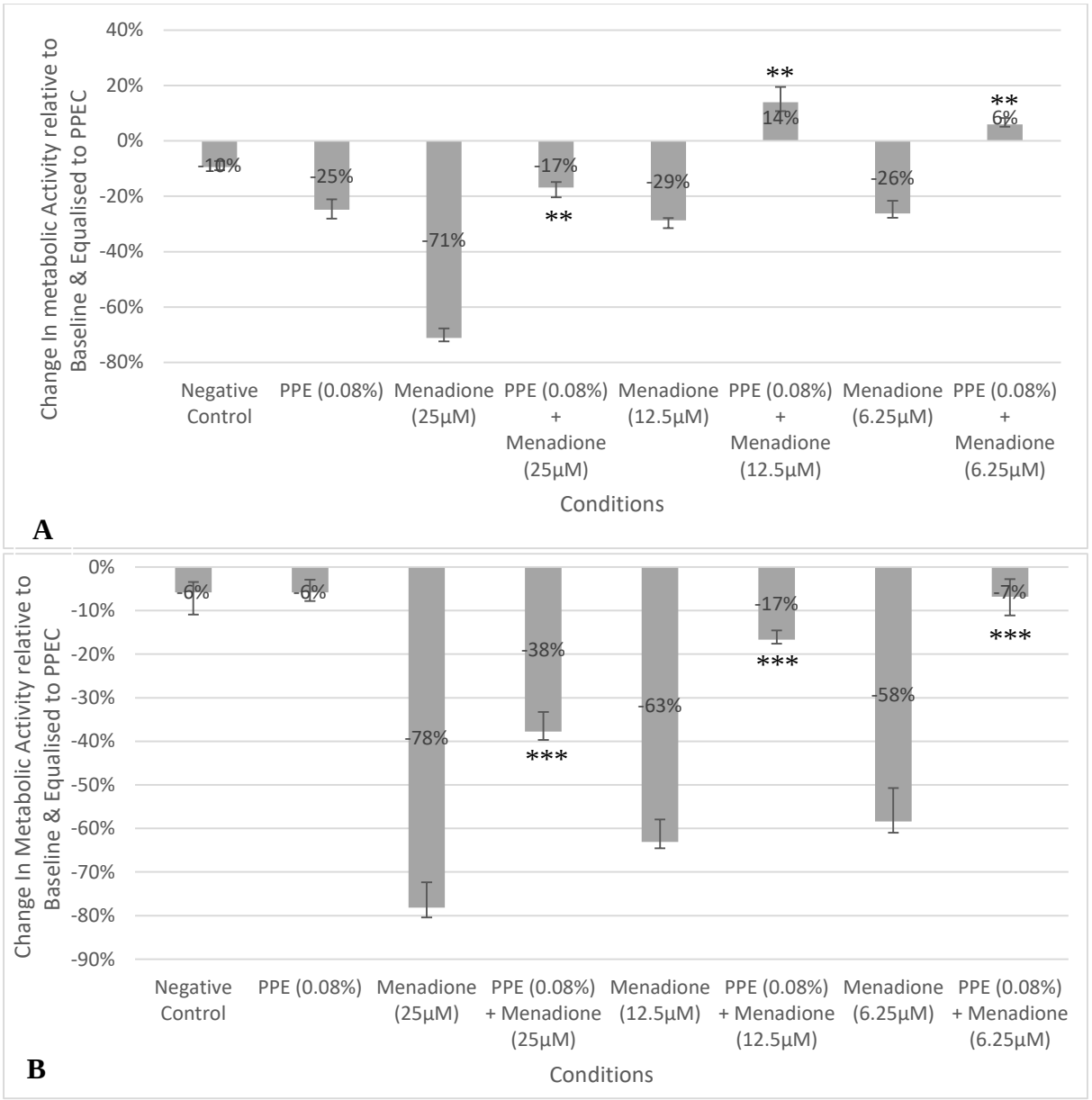

Figure 3.21: The effect menadione (25 µM, 12.5 µM and 6.25 µM) on HDFs viability in presence/absence of prickly pear extract (PPE) at 0.08% concentration, 2 [**A**] or 4 [**B**] h post-exposure.

The HDFs were seeded at $1.25x10^3$ cells/well in 96 well-plates and were allowed to recover overnight under standard culture conditions (37°C / 5 % CO_2). Post-recovery at 0 h the HDFs were exposed to a range of conditions principally, PPE (0.08%) or menadione (25 µM, 12.5 µM and 6.25 µM) in conjunction. The PPE was added 1 hour prior to the menadione as part of pre-exposure treatment. Following exposure, the plates were subsequently return to standard culture conditions (37°C / 5 % CO_2) until analysis. A CellTitre-Glo assay was performed 2 h [**A**] & 4 [**B**] h post exposure and the results are represented as a percentage change in metabolic activity relative to the activity observed at 0 h and equalised to PPEC. The values shown are the median 2 biological replicates with 9 technical replicates each. Postitve/negative error was determined by difference of median to upper/lower quartiles. The KW was a comparison between the conditions in relation relevant menadione (25 12.5 or 6.25 µM) exposure control and any significant difference was apporopriately indicated p <0.05 */<0.01 **/<0.001 ***.

The interpretation of Figure 3.21 [**A**] show the effect on viability of HDFs after 2 h exposure to varying concentrations of Menadione with and without PPE 0.08 %.

- Positive Effect - Menadione 25 µM/ PPE 0.08 %, Menadione 12.5 µM/ PPE 0.08 % and Menadione 6.25 µM/ PPE 0.08 % when in direct contact with HDFs for 2 h, were seen to have significant (KW p = <0.05) positive effect on viability of HDFs when compared to the Menadione 25 µM, Menadione 12.5 µM and Menadione 6.25 µM alone in the same time frame to the tune of ~54 %, ~43 % and ~32 % respectively. This is indicative of a protective effect provided by the PPE 0.08 %.

The interpretation of Figure 3.21 [**B**] shows the effect on viability of HDFs after 4 h exposure to varying concentrations of Menadione with and without PPE (0.08 %).

- Positive Effect – Menadione 25 µM/ PPE 0.08 %, Menadione 12.5 µM/ PPE 0.08 % and Menadione 6.25 µM/ PPE 0.08 % when in direct contact with HDFs for 4 h, were seen to have significant (KW p = <0.05) positive effect on viability of HDFs when compared to the Menadione 25 µM, Menadione 12.5 µM and Menadione 6.25 µM alone in the same time frame to the tune of ~40 %, ~46 % and ~51 % respectively. This is indicative of a protective effect provided by the PPE 0.08 %.

3.2.5. UVA (5 J/cm^2) effect on viability with or /without prickly pear extract / carrier

Following the method described in Section 2.8.4 a parallel run was performed with UVA (5 J/cm^2) exposure (+ UVA 5) and without UVA (5 J/cm^2) exposure (- UVA 5) tested on varying concentrations of PPE /PPEC (0.002, 0.004, 0.01, 0.02, 0.04 and 0.08 %) for 24 h, with a reading taken every 12 h. The results are presented in Figures 3.22 – 3.23. A significant difference (KW p = <0.05) was observed between the Negative control with/without UVA (5 J/cm^2) throughout the course of experimentation indicating the deleterious effects of UVA (5 J/cm^2) on HDFs viability at all time-points, 12 h and 24 h . As expected 10 % DMSO serving as a positive cytotoxic control resulted in a significant (KW p = <0.05) negative effect on viability when compared to the negative control. The interpretation of Figures 3.22 – 3.23 shows that the PPE / PPEC (0.002, 0.004, 0.01, 0.02, 0.04 and 0.08 %), without UVA (5 J/cm^2) exposure (- UVA 5) at 12 h and 24 h, had no significant (KW p = >0.05) effect on viability of HDFs when compared to the negative control in the same timeframe under the same conditions. It also shows that PPE (0.01, 0.02, 0.04 and 0.08 %), when in direct contact with HDFs in culture for 12 h following UVA (5 J/cm^2), did have a significant (KW p = <0.05) protective effect on viability of HDFs when compared to the negative control under the same conditions in the same time frame amounting to 10 %, 8 %, 14 %, 13 % respectively, persisted into 24 h amounting to 6 %, 6 %, 6%, 5 % respectively. PPE (0.002 and 0.004 %) was not observed to show a significant (KW p = >0.05) effect on viability of HDFs when compared to the negative control under UVA (5 J/cm^2) conditions. Lastly it also shows that PPEC (0.002, 0.004, 0.01, 0.02, 0.04 and 0.08 %) that at 12 h and 24 h following UVA (5 J/cm^2) no significant (KW p = >0.05) on viability of HDFs when compared to the negative control in the same time frame.

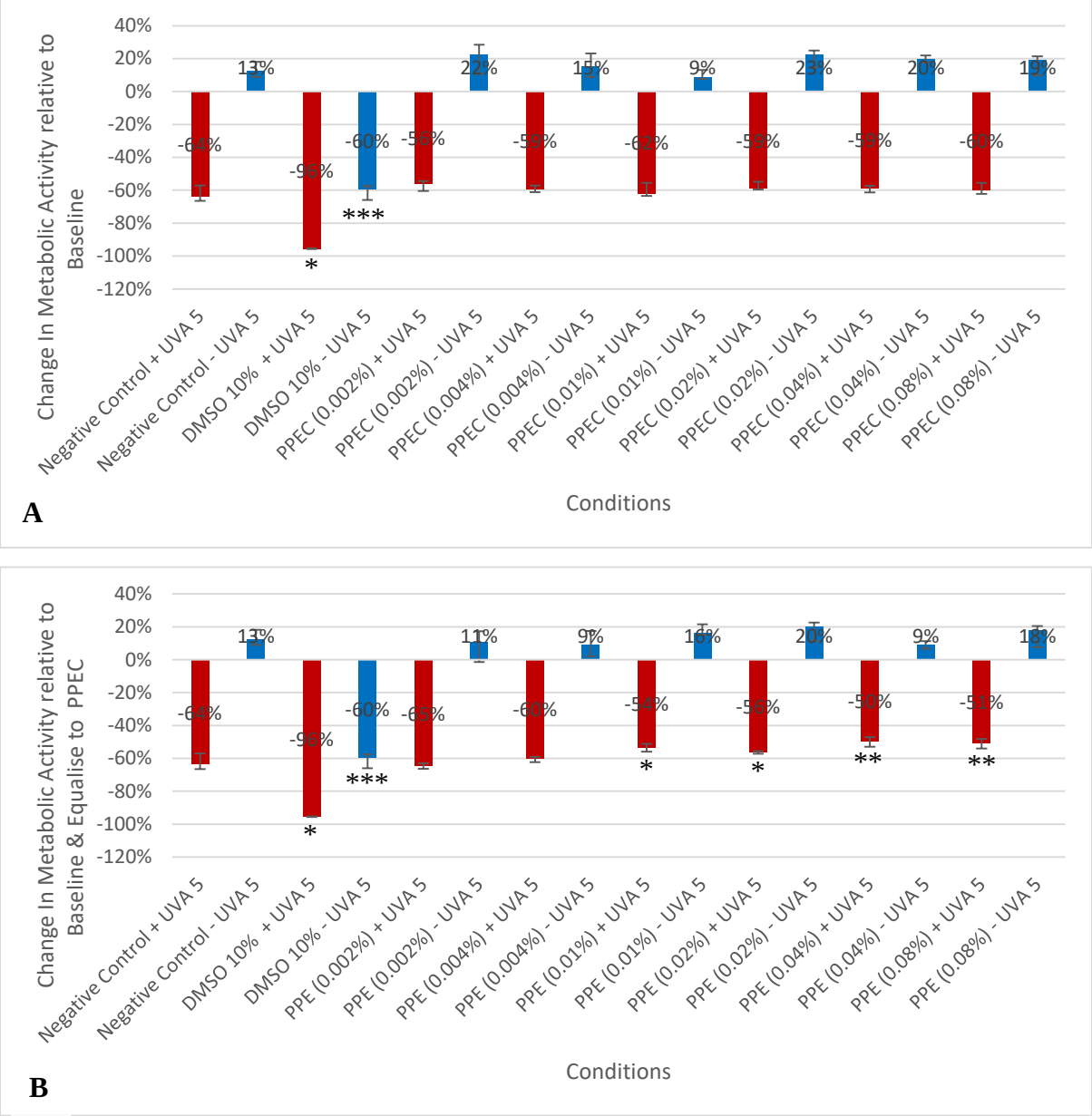

Figure 3.22: The effect of UVA (5 J/cm^2) with/without PPEC (**A**) and PPE (**B**) on the viability of nHDFs after 12 h post-exposure.

The nHDFs were seeded at 1.25x10^3 cells/well in 96 well-plates and were allowed to recover overnight (24 h) in standard culture conditions (37°C / 5 % CO_2). At this point (0 h) the HDFs were treated to a range of PPE and PPEC concentrations (0.002, 0.004, 0.01, 0.02, 0.04 and 0.08 %) and were returned to standard culture conditions for 1 h. Following treatment half the plates were exposed to UVA (5 J/cm^2) radiation (+ UVA 5) while the other half were left in the incubator (- UVA 5). Following exposure, the plates were subsequently return to standard culture conditions until analysis. A CellTitre-Glo assay was performed 12 h post exposure and the results are represented as a percentage change in metabolic activity relative to the activity observed at 0 h and in the case of PPE also equalised to PPEC. The values shown are the median of 9 technical replicates. Postitve/negative error was determined by difference of median to upper/lower quartiles. The KW was a comparison between the various conditions in relation to the negative control within group (+ UVA 5 or – UVA 5) and any significant difference was apporopriately indicated p <0.05 */<0.01 **/<0.001 ***.

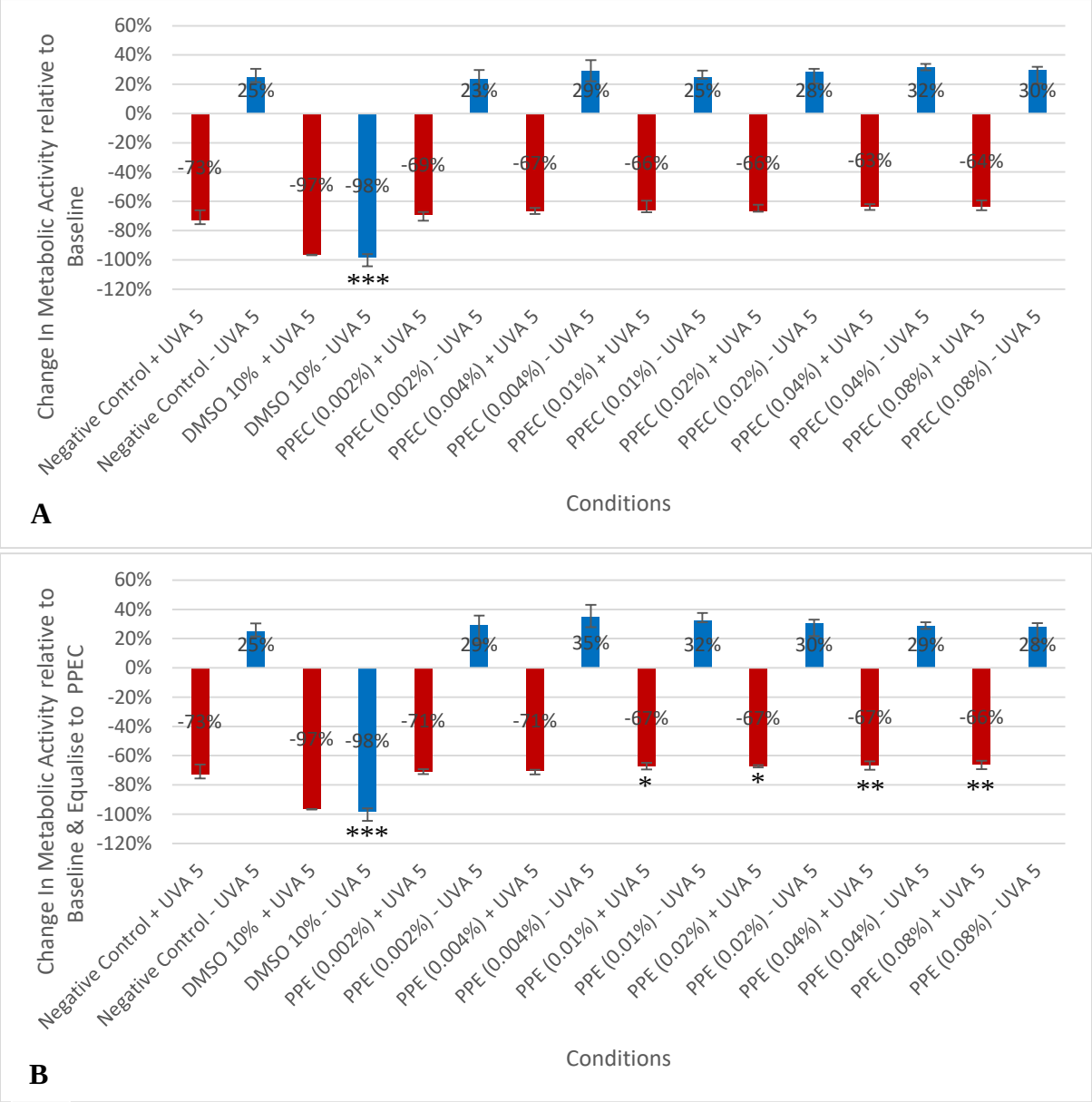

Figure 3.23: The effect of UVA (5 J/cm^2) with/without PPEC (**A**) and PPE (**B**) on the viability of nHDFs after 24 h post-exposure.

The nHDFs were seeded at 1.25x10^3 cells/well in 96 well-plates and were allowed to recover overnight (24 h) in standard culture conditions (37°C / 5 % CO_2). At this point (0 h) the HDFs were treated to a range of PPE and PPEC concentrations (0.002, 0.004, 0.01, 0.02, 0.04 and 0.08 %) and were returned to standard culture conditions for 1 h. Following treatment half the plates were exposed to UVA (5 J/cm^2) radiation (+ UVA 5) while the other half were left in the incubator (- UVA 5). Following exposure, the plates were subsequently return to standard culture conditions until analysis. A CellTitre-Glo assay was performed 24 h post exposure and the results are represented as a percentage change in metabolic activity relative to the activity observed at 0 h and in the case of PPE also equalised to PPEC. The values shown are the median of 9 technical replicates. Postitve/negative error was determined by difference of median to upper/lower quartiles. The KW was a comparison between the various conditions in relation to the negative control within group (+ UVA 1000 or – UVA 1000) and any significant difference was apporopriately indicated p <0.05 */<0.01 **/<0.001 ***.

3.2.6. UVC (10 µJ/m^2) effect on viability with or /without prickly pear extract / carrier

Following the method described in Section 2.8.4 a parallel run was performed with UVC (10 µJ/m^2) exposure (+ UVC 1000) and without UVC (10 µJ/m^2) exposure (- UVC 1000) tested on varying concentrations of PPE /PPEC (0.002, 0.004, 0.01, 0.02, 0.04 and 0.08 %) for 24 h, with a reading taken every 12 h. The results are presented in Figures 3.24 – 3.25. A significant difference (KW p = <0.05) was observed between the Negative control with/without UVC (10 µJ/m^2) throughout the course of experimentation indicating the deleterious effects of UVC (10 µJ/m^2) on HDFs viability at all time-points, 12 h and 24 h. As expected 10 % DMSO serving as a positive cytotoxic control resulted in a significant (KW p = <0.05) negative effect on viability when compared to the negative control. The interpretation of figures 3.24 – 3.25 shows that the PPE / PPEC (0.002, 0.004, 0.01, 0.02, 0.04 and 0.08 %), without UVC (10 µJ/m^2) exposure (- UVC 1000) at 12 h and 24 h, had no significant (KW p = >0.05) effect on viability of HDFs when compared to the negative control in the same timeframe under the same conditions. It also shows that PPE (0.01, 0.02, 0.04 and 0.08 %), when in direct contact with HDFs in culture for 12 h following UVC (10 µJ/m^2), did have a significant (KW p = <0.05) protective effect on viability of HDFs when compared to the negative control under the same conditions in the same time frame amounting to 9 %, 9 %, 14 %, 9 % respectively, but this did not persist into 24 h were no significant (KW p = >0.05) effect on viability of HDFs when compared to the negative control was observed. PPE (0.002 % & 0.004 %) was not observed to show a significant (KW p = >0.05) effect on viability of HDFs when compared to the negative control under UVC (10 µJ/m^2) conditions. Lastly it also shows that PPEC (0.002, 0.004, 0.01, 0.02, 0.04 and 0.08 %) that at 12 h and 24 h following UVC (10 µJ/m^2) no significant (KW p = >0.05) on viability of HDFs when compared to the negative control in the same time frame.

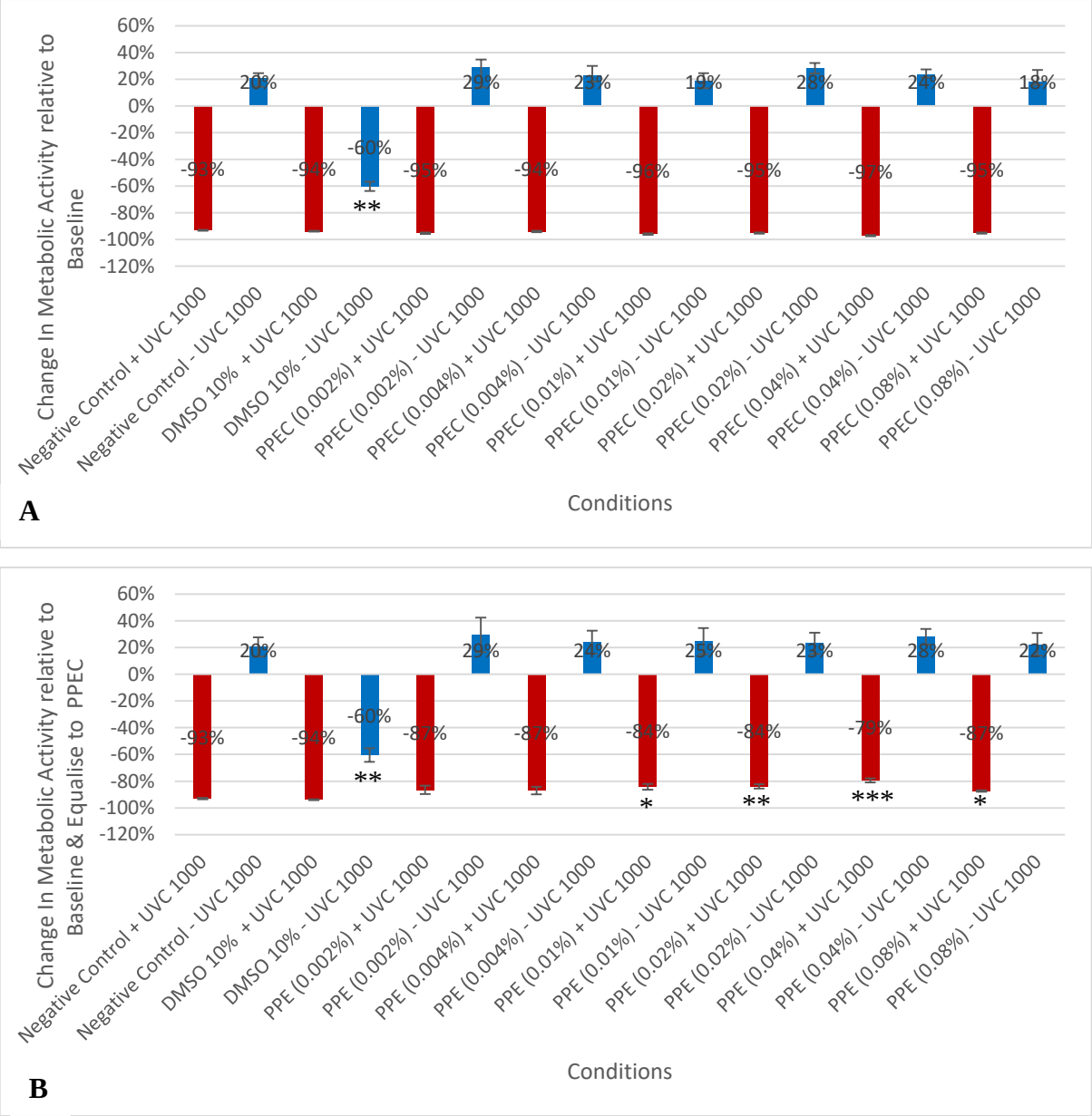

Figure 3.24: The effect of UVC (10 µJ/m^2) with/without PPEC (**A**) and PPE (**B**) on the viability of HDFs after 12 h post-exposure.

The HDFs were seeded at 1.25x10^3 cells/well in 96 well-plates and were allowed to recover overnight (24 h) in standard culture conditions (37°C / 5 % CO_2). At this point (0 h) the HDFs were treated to a range of PPE and PPEC concentration (0.002, 0.004, 0.01, 0.02, 0.04 and 0.08 %) and were returned to standard culture conditions for 1 h. Following treatment half the plates were exposed to UVC (10 µJ/m^2) radiation (+ UVC 1000) while the other half were left in the incubator (- UVC 1000). Following exposure, the plates were subsequently return to standard culture conditions until analysis. A CellTitre-Glo assay was performed 12 h post exposure and the results are represented as a percentage change in metabolic activity relative to the activity observed at 0 h and in the case of PPE also equalised to PPEC. The values shown are the median 2 biological replicates with 9 technical replicates each. Postitve/negative error was determined by difference of median to upper/lower quartiles. The KW was a comparison between the various conditions in relation to the negative control within group (+ UVC 1000 or – UVC 1000) and any significant difference was apporopriately indicated p <0.05 */<0.01 **/<0.001 ***.

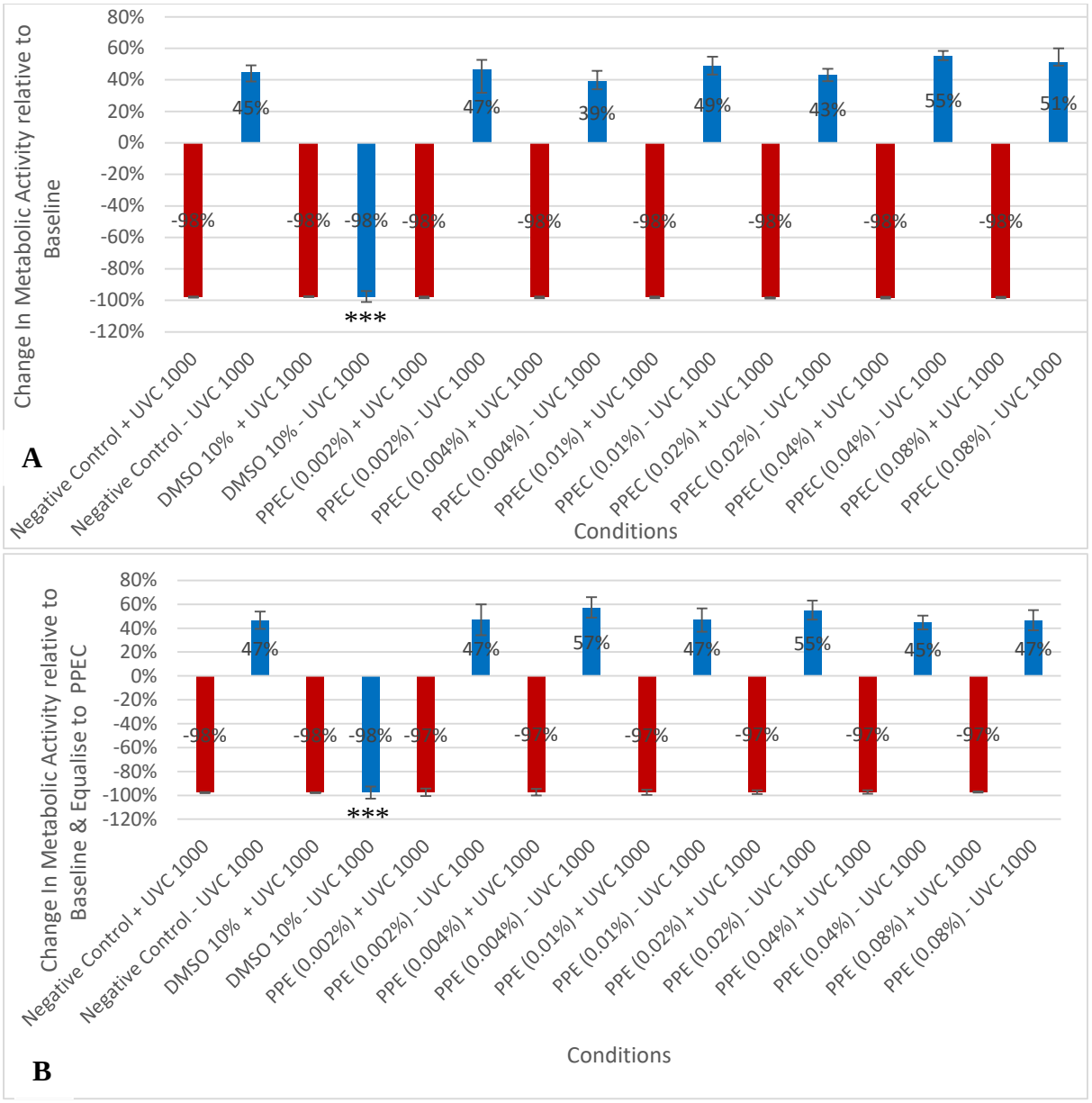

Figure 3.25: The effect of UVC (10 µJ/m^2) with/without PPEC (**A**) and PPE (**B**) on the viability of HDFs after 24 h post-exposure.

The HDFs were seeded at 1.25x10^3 cells/well in 96 well-plates and were allowed to recover overnight (24 h) in standard culture conditions (37°C / 5 % CO_2). At this point (0 h) the HDFs were treated to a range of PPE and PPEC concentration (0.002, 0.004, 0.01, 0.02, 0.04 and 0.08 %) and were returned to standard culture conditions for 1 h. Following treatment half the plates were exposed to UVC (10 µJ/m^2) radiation (+ UVC 1000) while the other half were left in the incubator (- UVC 1000). Following exposure, the plates were subsequently return to standard culture conditions until analysis. A CellTitre-Glo assay was performed 24 h post exposure and the results are represented as a percentage change in metabolic activity relative to the activity observed at 0 h and in the case of PPE also equalised to PPEC. The values shown are the median 2 biological replicates with 9 technical replicates each. Postitve/negative error was determined by difference of median to upper/lower quartiles. The KW was a comparison between the various conditions in relation to the negative control within group (+ UVC 1000 or – UVC 1000) and any significant difference was apporopriately indicated p <0.05 */<0.01 **/<0.001 ***.

3.2.7. UVC (25 µJ/m^2) effect on viability with or /without prickly pear extract / carrier

Following the method described in Section 2.8.4 using CellTitre-glo a parallel run was performed with UVC (25 µJ/m^2) exposure (+ UVC 2500) and without UVC (25 µJ/m^2) exposure (- UVC 2500) tested on varying concentrations of PPE /PPEC (0.002, 0.004, 0.01, 0.02, 0.04 and 0.08 %) for 24 h, with a reading taken every 12 h. The results are presented in Figures 3.26 – 3.27. A significant difference (KW p = <0.05) was observed between the Negative control with/without UVC (25 µJ/m^2) throughout the course of experimentation indicating the deleterious effects of UVC (25 µJ/m^2) on HDFs viability at all time-points, 12 h and 24 h. As expected 10 % DMSO serving as a positive cytotoxic control resulted in a significant (KW p = <0.05) negative effect on viability when compared to the negative control. PPE / PPEC (0.002, 0.004, 0.01, 0.02, 0.04 and 0.08 %), without UVC (25 µJ/m^2) exposure (- UVC 2500) at 12 h and 24 h, had no significant (KW p = >0.05) effect on viability of HDFs when compared to the negative control in the same timeframe under the same conditions. Lastly it also shows that PPE /PPEC (0.002, 0.004, 0.01, 0.02, 0.04 and 0.08 %) at 12 h and 24 h following UVC (25 µJ/m^2) (+ UVC 2500) radiation had no significant (KW p = >0.05) effect on viability of HDFs when compared to the negative control in the same time frame.

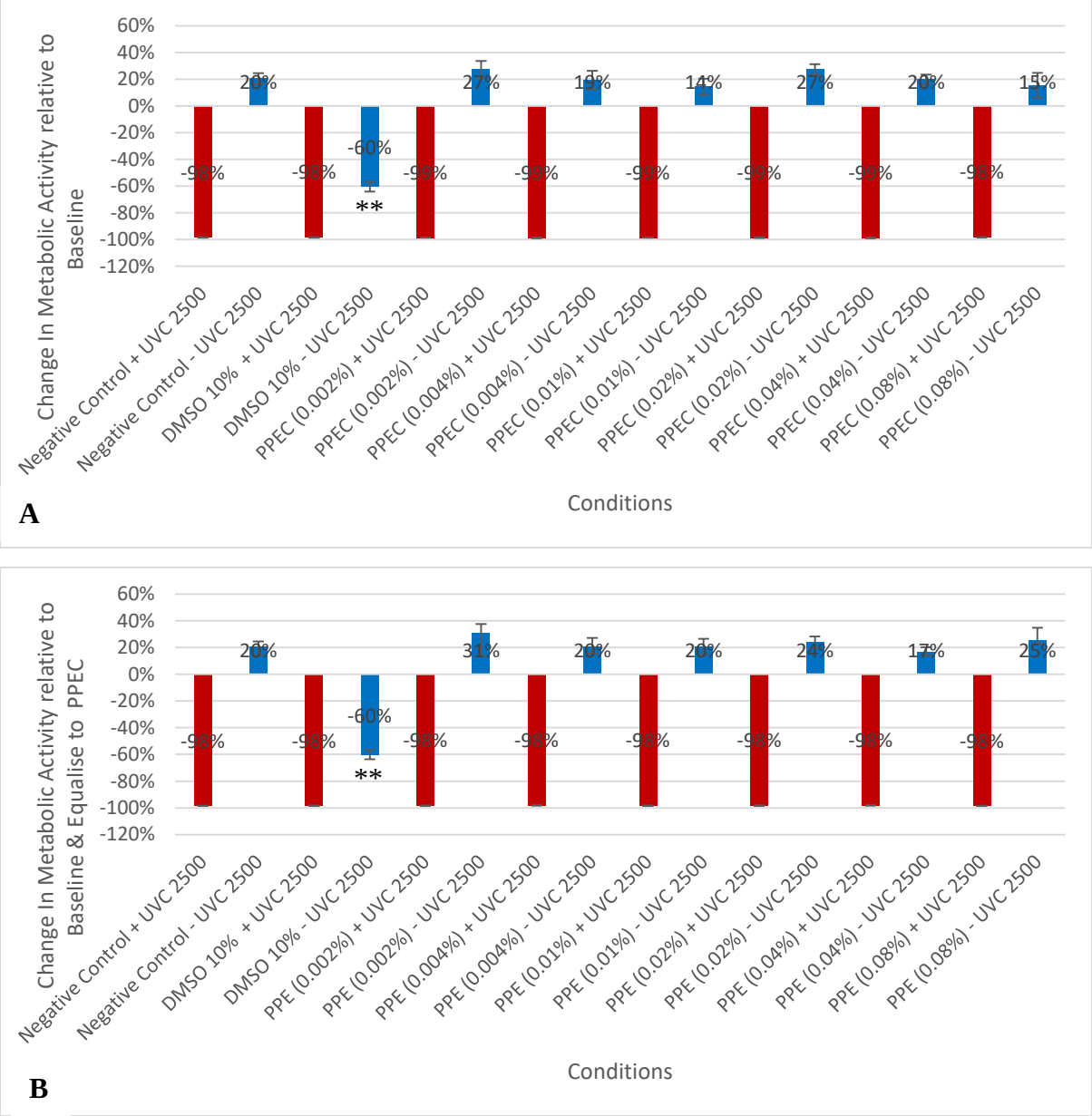

Figure 3.26: The effect of UVC (25 µJ/m^2) with/without PPEC (**A**) and PPE (**B**) on the viability of HDFs after 12 h post-exposure.

The HDFs were seeded at 1.25x10^3 cells/well in 96 well-plates and were allowed to recover overnight (24 h) in standard culture conditions (37°C / 5 % CO_2). At this point (0 h) the HDFs were treated to a range of PPE and PPEC concentration (0.002, 0.004, 0.01, 0.02, 0.04 and 0.08 %) and were returned to standard culture conditions for 1 h. Following treatment half the plates were exposed to UVC (25 µJ/m^2) radiation (+ UVC 2500) while the other half were left in the incubator (- UVC 2500). Following exposure, the plates were subsequently return to standard culture conditions until analysis. A CellTitre-Glo assay was performed 12 h post exposure and the results are represented as a percentage change in metabolic activity relative to the activity observed at 0 h and in the case of PPE also equalised to PPEC. The values shown are the median 2 biological replicates with 9 technical replicates each. Postitve/negative error was determined by difference of median to upper/lower quartiles. The KW was a comparison between the various conditions in relation to the negative control within group (+ UVC 2500 or – UVC 2500) and any significant difference was apporopriately indicated p <0.05 */<0.01 **/<0.001 ***.

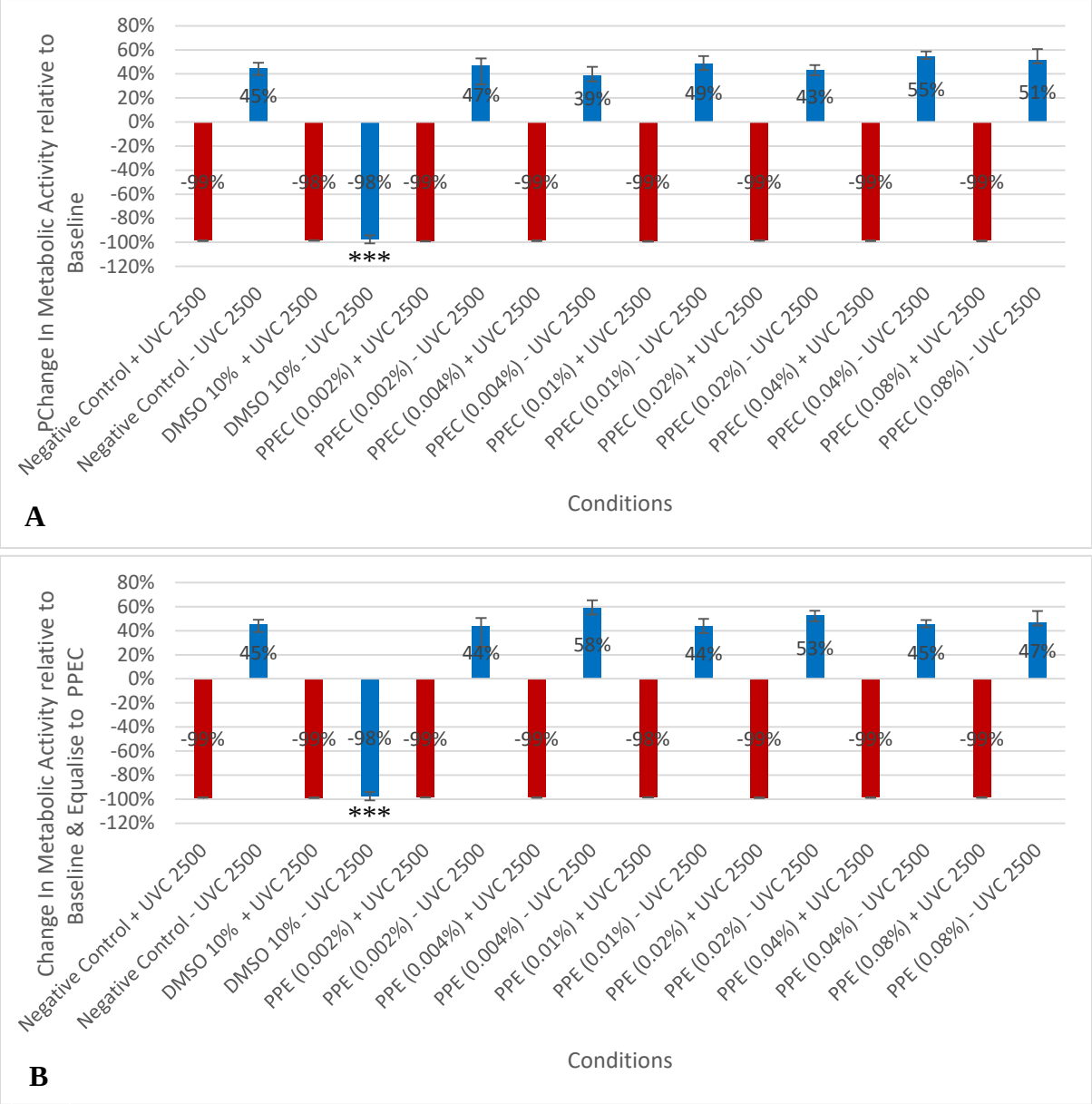

Figure 3.27: The effect of UVC (25 µJ/m^2) with/without PPEC (**A**) and PPE (**B**) on the viability of HDFs after 12 h post-exposure.

The HDFs were seeded at 1.25x10^3 cells/well in 96 well-plates and were allowed to recover overnight (24 h) in standard culture conditions (37°C / 5 % CO_2). At this point (0 h) the HDFs were treated to a range of PPE and PPEC concentration (0.002, 0.004, 0.01, 0.02, 0.04 and 0.08 %) and were returned to standard culture conditions for 1 h. Following treatment half the plates were exposed to UVC (25 µJ/m^2) radiation (+ UVC 2500) while the other half were left in the incubator (- UVC 2500). Following exposure, the plates were subsequently return to standard culture conditions until analysis. A CellTitre-Glo assay was performed 12 h post exposure and the results are represented as a percentage change in metabolic activity relative to the activity observed at 0 h and in the case of PPE also equalised to PPEC. The values shown are the median 2 biological replicates with 9 technical replicates each. Postitve/negative error was determined by difference of median to upper/lower quartiles. The KW was a comparison between the various conditions in relation to the negative control within group (+ UVC 2500 or – UVC 2500) and any significant difference was apporopriately indicated p <0.05 */<0.01 **/<0.001 ***.

3.3. Presto Blue

The Presto Blue assay was utilised to confirm the finding of the celltitre glo and as such several avenues of experimentation were taken to analyse the effect of test conditions on HDF viability (Section 3.3.1 – 3.3.6). The results can be found below.

3.3.1. Prickly Pear Extract and Carrier Effect on Viability

In accordance to the protocol shown in Section 2.8.1 the presto blue assay was performed to analyse the effect of PPE and PPEC exposure on HDFs for a duration of 72 h. Firstly, as expected 10 % DMSO serving as the positive cytotoxic control showed a significant (KW p = <0.05) negative effect on viability when compared to the negative control. The shown in Figures 3.28 – 3.30 demonstrate that the PPEC concentrations (0.002, 0.004, 0.01, 0.02, 0.04 and 0.08 %) when added to HDFs in culture for 24 h, 48 h and 72 h exhibited no significant (KW p = >0.05) effect on viability of HDFs when compared to the negative control in the same time frame. PPEC concentration 0.16% was seen to have a significant negative (KW p = <0.05) effect on viability of HDFs when compared to negative control after 48 h while the rest (0.64, 2.56, 10.24 and 40.96 %) showed this after just 24 h and persisted for 72 h. Furthermore, PPE at all concentration tested when added to HDFs in culture for 24 h, 48 h and 72 h, exhibited no significant (KW p = >0.05) effect on viability of HDFs when compared to the negative control in the same time frame when normalised to PPEC relative from the change from the baseline. The results indicate that *in vitro* the PPEC has no effect of the viability of HDFs up to a concentration of 0.08% and thus the range of PPE / PPEC concentrations (0.002, 0.004, 0.01, 0.02, 0.04 and 0.08 %) were used.

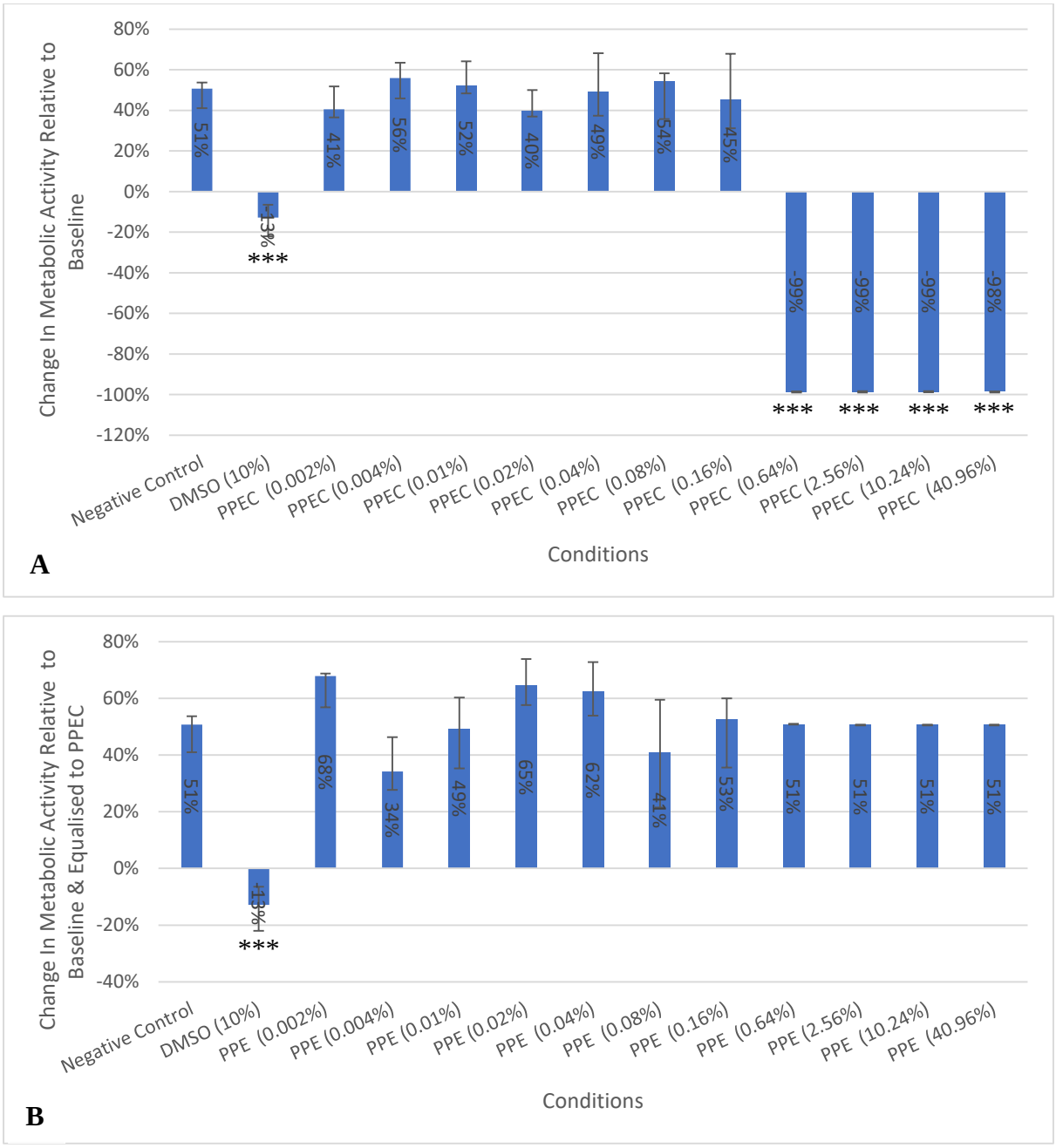

Figure 3.28: The effect of PPEC (**A**) and PPE (**B**) on the viability of HDFs after 24 h exposure.

The HDFs were seeded at $1.25x10^3$ cells/well in 96 well-plates and were allowed to recover overnight under standard culture conditions (37°C / 5 % CO_2). Post-recovery at 0 h the HDFs were exposed to a range of conditions. A Presto Blue assay was performed 24 h post exposure and the results are represented as a percentage change in metabolic activity relative to the activity observed at 0 h and in the case of PPE also equalised to PPEC. The values shown are the median 2 biological replicates with 9 technical replicates each. Postitve/negative error was determined by difference of median to upper/lower quartiles. The KW was a comparison between the various conditions in relation to the negative control and any significant difference was apporopriately indicated p <0.05 */<0.01 **/<0.001 ***.

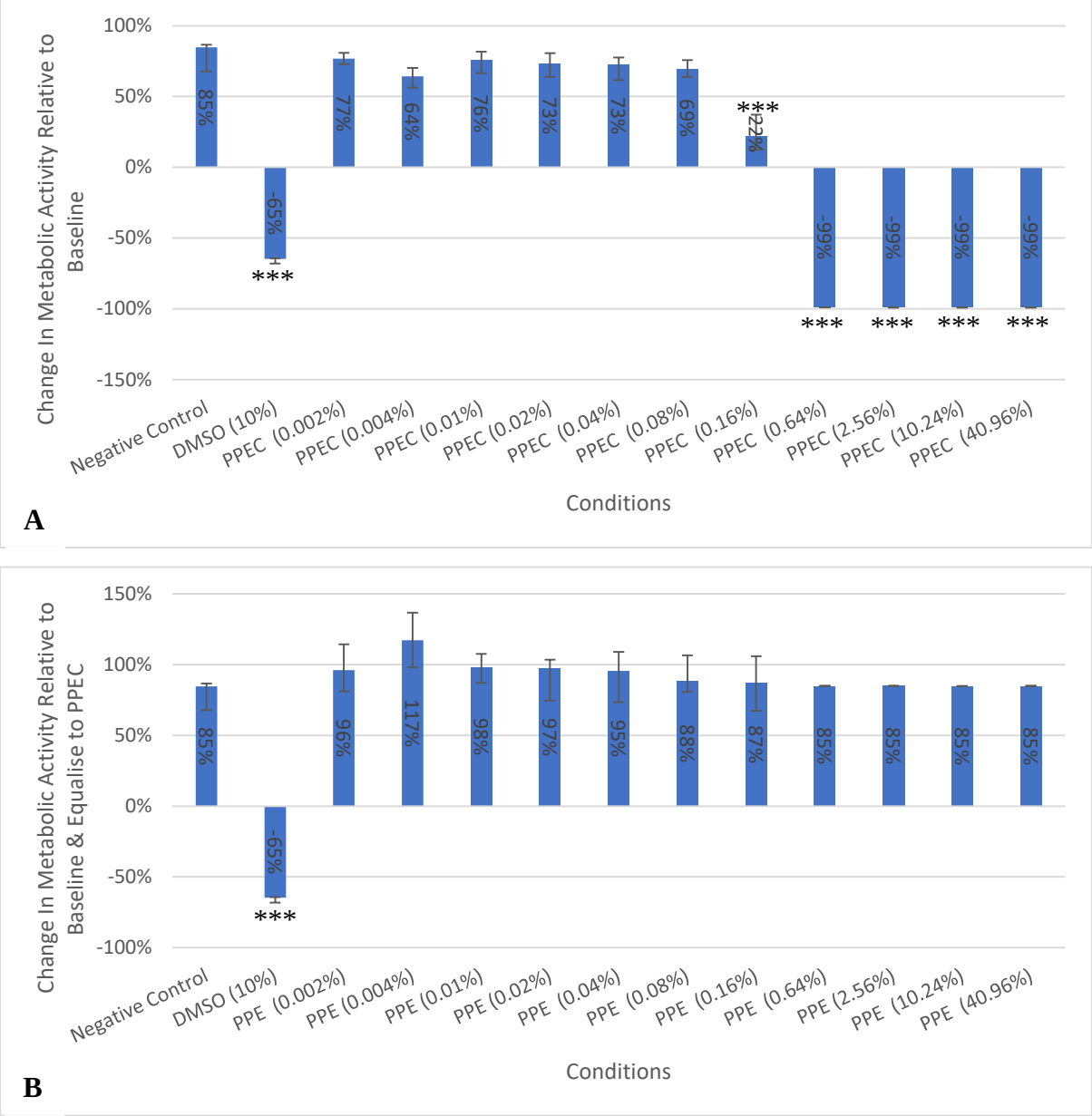

Figure 3.29: The effect of PPEC (**A**) and PPE (**B**) on the viability of HDFs after 24 h exposure.

The HDFs were seeded at 1.25x10^3 cells/well in 96 well-plates and were allowed to recover overnight under standard culture conditions (37°C / 5 % CO_2). Post-recovery at 0 h the HDFs were exposed to a range of conditions. A Presto Blue assay was performed 28 h post exposure and the results are represented as a percentage change in metabolic activity relative to the activity observed at 0 h and in the case of PPE also equalised to PPEC. The values shown are the median 2 biological replicates with 9 technical replicates each. Postitve/negative error was determined by difference of median to upper/lower quartiles. The KW was a comparison between the various conditions in relation to the negative control and any significant difference was apporopriately indicated p <0.05 */<0.01 **/<0.001 ***.

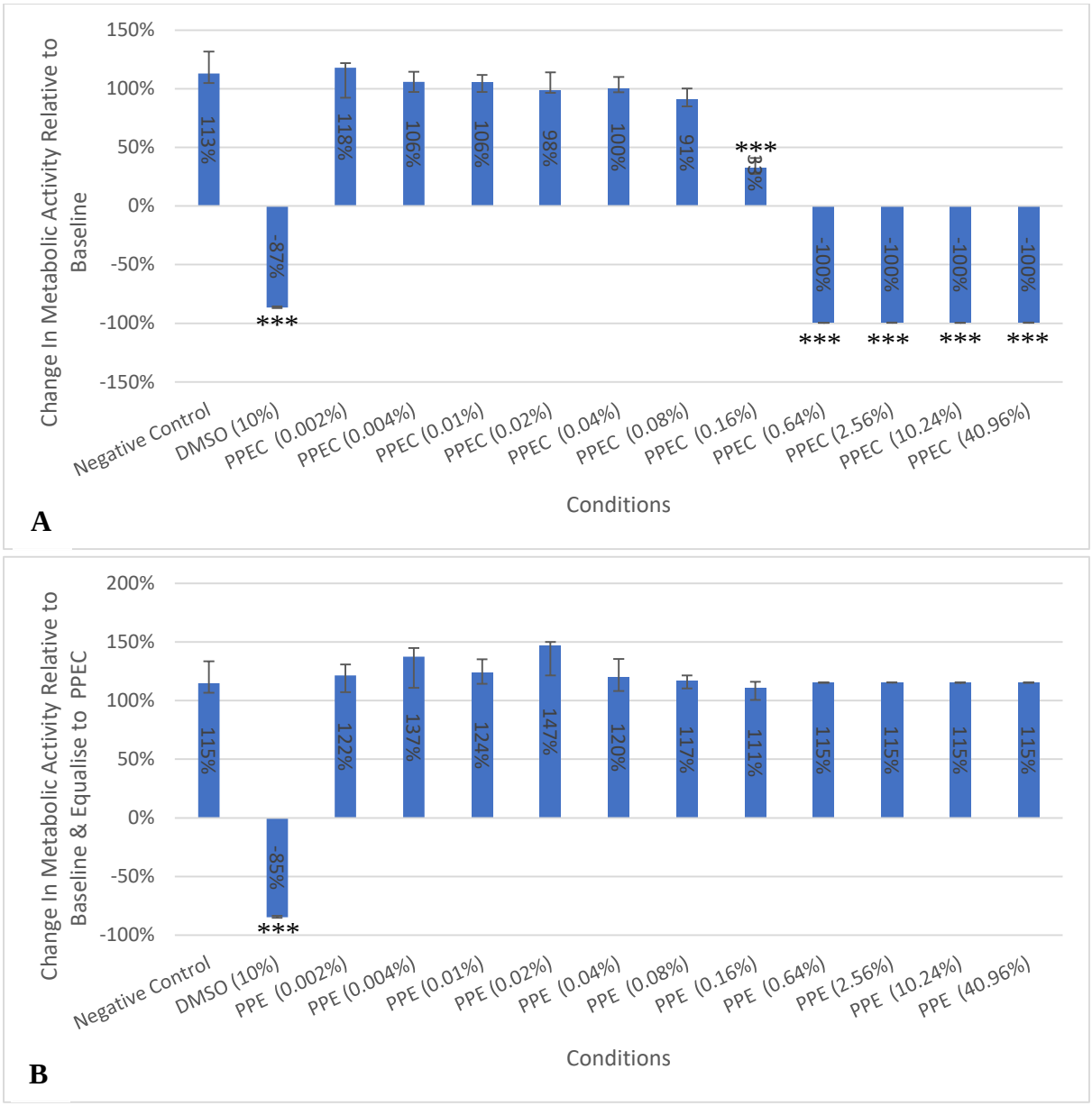

Figure 3.30: The effect of PPEC (**A**) and PPE (**B**) on the viability of HDFs after 72 h exposure.

The HDFs were seeded at $1.25x10^3$ cells/well in 96 well-plates and were allowed to recover overnight under standard culture conditions (37°C / 5 % CO_2). Post-recovery at 0 h the HDFs were exposed to a range of conditions. A Presto Blue assay was performed 72 h post exposure and the results are represented as a percentage change in metabolic activity relative to the activity observed at 0 h and in the case of PPE also equalised to PPEC. The values shown are the median 2 biological replicates with 9 technical replicates each. Postitve/negative error was determined by difference of median to upper/lower quartiles. The KW was a comparison between the various conditions in relation to the negative control and any significant difference was apporopriately indicated p <0.05 */<0.01 **/<0.001 ***.

3.3.2. Heat stress (44°C) effect on viability with or /without prickly pear extract /carrier

Figures 3.31 – 3.33, in accordance to the protocol shown in Section 2.8.2 the Presto Blue assay was performed in conjunction with heat stress protocol C were a parallel run with both heat stress (+ HS 44°C for 1 h) and non-heat stress control (- HS 37°C for 1 h) were tested with varying concentrations of PPE and PPEC (0.002, 0.004, 0.01, 0.02, 0.04 and 0.08 %) for 72 h, with a reading taken every 24 h. Firstly, as expected 10 % DMSO serving as the positive cytotoxic control showed a significant (KW p = <0.05) negative effect on viability when compared to the negative control. A significant difference was observed between the Negative control with Heat stress and the Negative control without Heat stress at 24 h and 48 h but did not persist to 72 h which indicates a deleterious effect to viability by the heat stress treatment (44°C) which is then overcome. The PPE/PPEC (0.002, 0.004, 0.01, 0.02, 0.04 and 0.08 %) when in direct contact with HDFs in culture for duration without heat stress (- HS 37°C for 1hr) were seen to have no significant (KW p = >0.05) effect on viability of HDFs when compared to the negative control in the same time frame. Furthermore, the PPEC (0.002, 0.004, 0.01, 0.02, 0.04 and 0.08 %) with heat stress (+ HS 44°C for 1 h) was also seen to have no significant (KW p = >0.05) effect on viability of HDF when compared to the negative control under the same conditions in the same time frame during all time points (24, 48, 72 h).

The interpretation of Figure 3.31 shows that the PPE (0.002, 0.004, 0.01, 0.02, 0.04 and 0.08 %), at 24 h following heat stress (+ HS 44°C for 1 h), had a significant (KW p = <0.05) positive protective effect on viability of HDFs when compared to the negative control in the same time frame amounting to 79 %, 49 %, 64 %, 62 %, 81 % and 61 % respectively. The interpretation of Figure 3.32 shows that the PPE (0.002, 0.004, 0.01, 0.02, 0.04 and 0.08 %), at 48 h following heat stress (+ HS 44°C for 1 h), had a significant (KW p = <0.05) positive protective effect on viability of HDFs when compared to the negative control in the same time frame amounting to 82 %, 75 %, 67 %, 68 % and 95 %, 87% respectively. The interpretation of Figure 3.33 shows that the PPE (0.002, 0.004, 0.01, 0.02, 0.04 and 0.08 %) at 72hr following heat stress (+ HS 44°C for 1hr) had no significant (KW p = >0.05) effect on viability of HDFs when compared to the negative control in the same time frame.

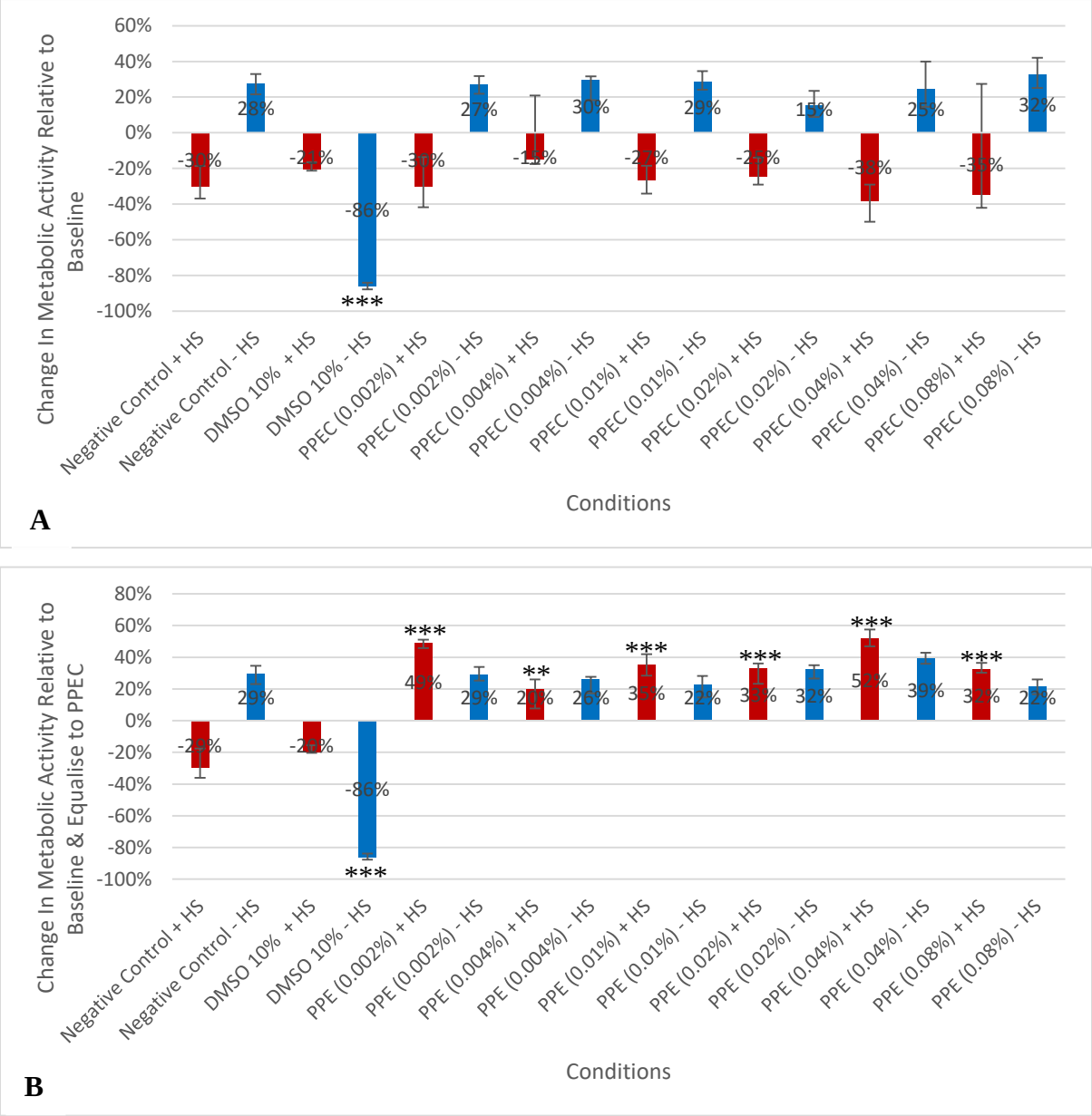

Figure 3.31: The effect of heat stress (44°C for 1 h) with/without PPEC (**A**) or PPE (**B**) on the viability of HDFs after 24 h post-exposure.

The HDFs were seeded at $1.25x10^3$ cells/well in 96 well-plates and were allowed to recover overnight (24 h) in standard culture conditions (37°C / 5 % CO_2). At this point (0 h) the HDFs were treated to a range of PPE/PPEC concentrations (0.002 %, 0.004 %, 0.04 %, 0.08 %) and were returned to standard culture conditions for 1 h. Following treatment half the plates were exposed to heat stress (+ HS) while the other half were left in the incubator (- HS). Following exposure, the plates were subsequently return to standard culture conditions until analysis. A Presto Blue assay was performed 24 h post exposure and the results are represented as a percentage change in metabolic activity relative to the activity observed at 0 h and in the case of PPE also equalised to PPEC. The values shown are the median 2 biological replicates with 9 technical replicates each. Postitve/negative error was determined by difference of median to upper/lower quartiles. The KW was a comparison between the various conditions in relation to the negative control within group (+ HS or – HS) and any significant difference was apporopriately indicated p <0.05 */<0.01 **/<0.001 ***.

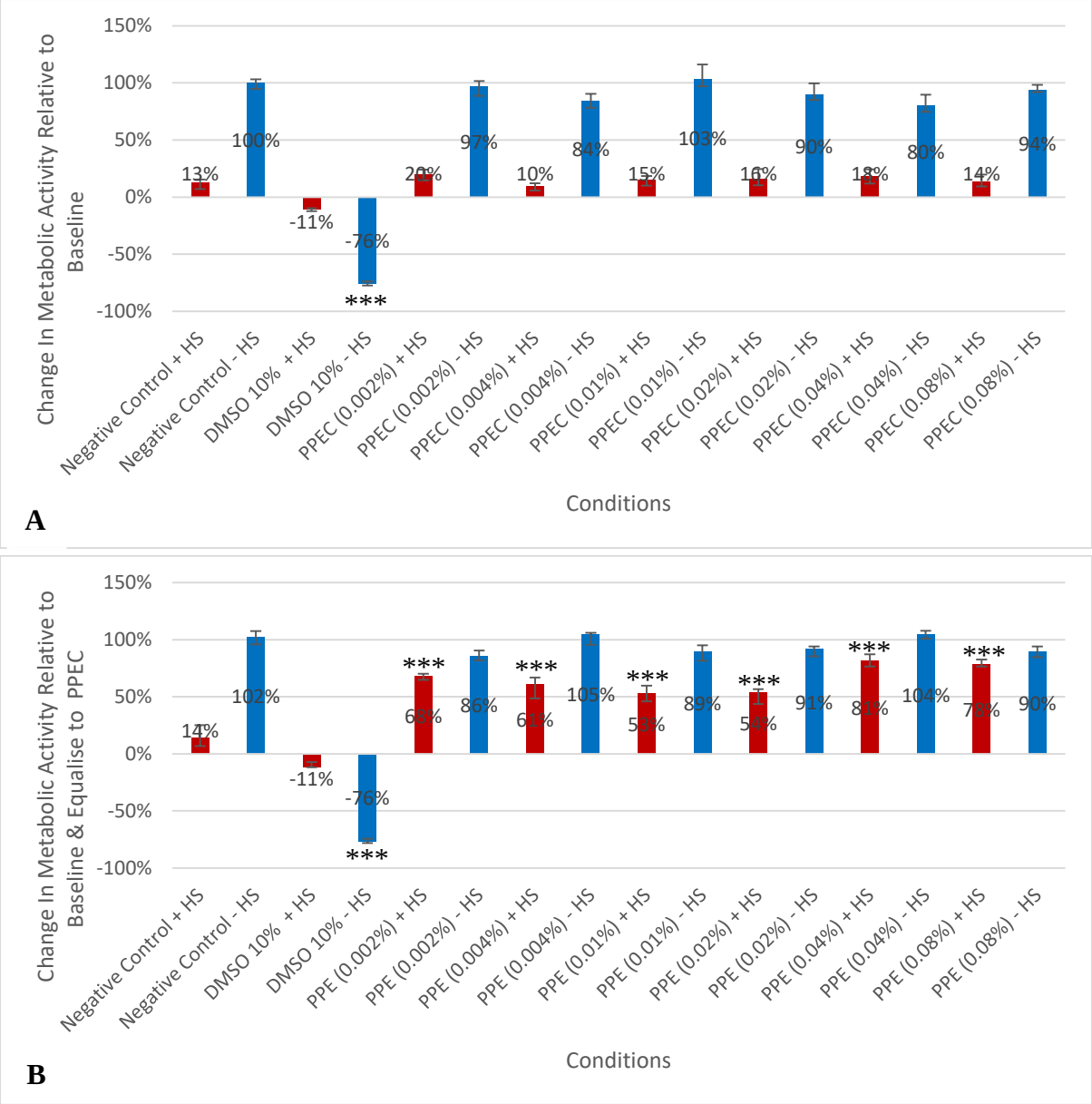

Figure 3.32: The effect of heat stress (44°C for 1 h) with/without PPEC (**A**) or PPE (**B**) on the viability of HDFs after 48 h post-exposure.

The HDFs were seeded at $1.25x10^3$ cells/well in 96 well-plates and were allowed to recover overnight (24 h) in standard culture conditions (37°C / 5 % CO_2). At this point (0 h) the HDFs were treated to a range of PPE/PPEC concentrations (0.002 %, 0.004 %, 0.04 %, 0.08 %) and were returned to standard culture conditions for 1 h. Following treatment half the plates were exposed to heat stress (+ HS) while the other half were left in the incubator (- HS). Following exposure, the plates were subsequently return to standard culture conditions until analysis. A Presto Blue assay was performed 24 h post exposure and the results are represented as a percentage change in metabolic activity relative to the activity observed at 0 h and in the case of PPE also equalised to PPEC. The values shown are the median 2 biological replicates with 9 technical replicates each. Postitve/negative error was determined by difference of median to upper/lower quartiles. The KW was a comparison between the various conditions in relation to the negative control within group (+ HS or – HS) and any significant difference was apporopriately indicated p <0.05 */<0.01 **/<0.001 ***.

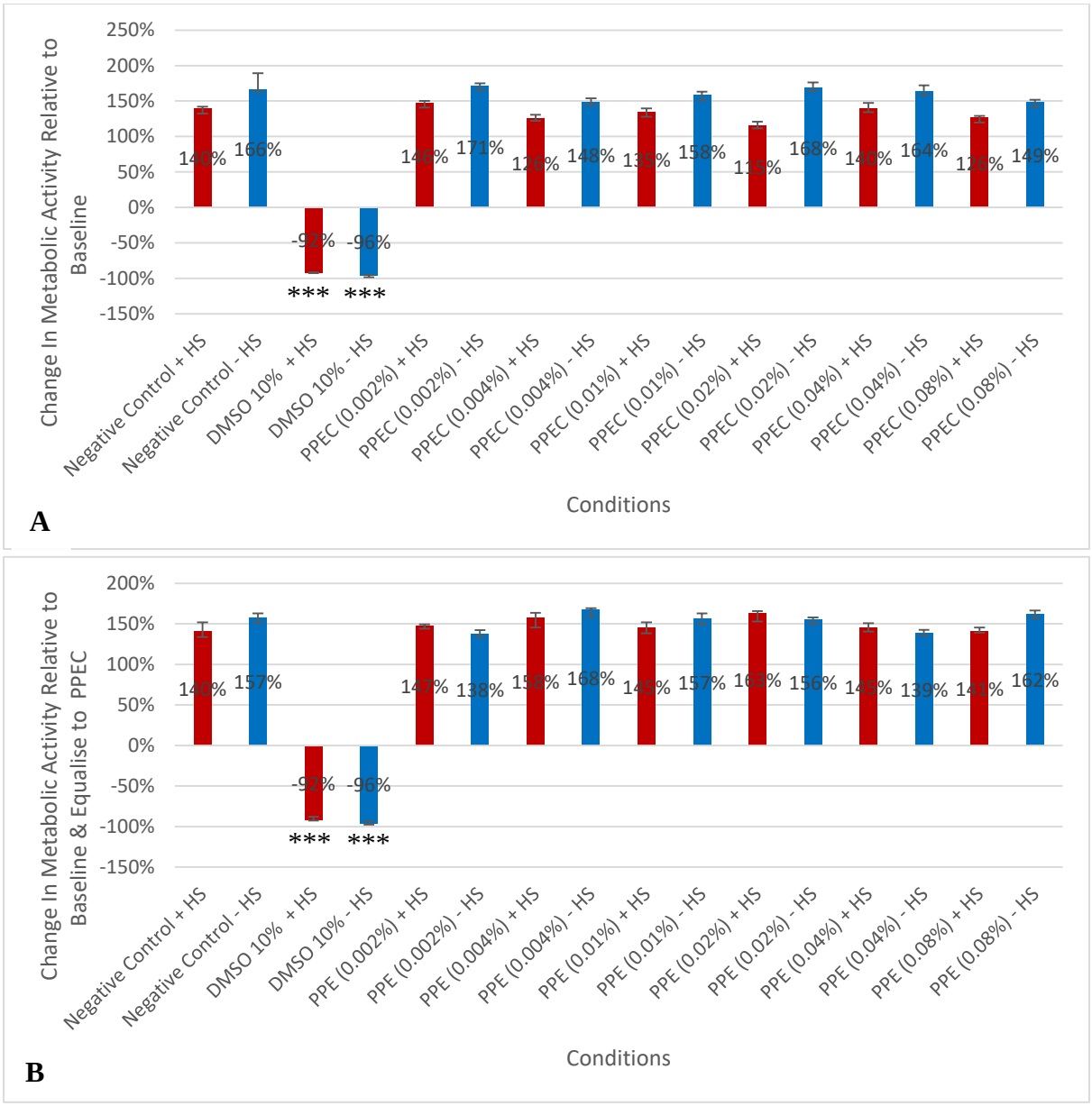

Figure 3.33: The effect of heat stress (44°C for 1 h) with/without PPEC (**A**) or PPE (**B**) on the viability of HDFs after 72 h post-exposure.

The HDFs were seeded at $1.25x10^3$ cells/well in 96 well-plates and were allowed to recover overnight (24 h) in standard culture conditions (37°C / 5 % CO_2). At this point (0 h) the HDFs were treated to a range of PPE/PPEC concentrations (0.002 %, 0.004 %, 0.04 %, 0.08 %) and were returned to standard culture conditions for 1 h. Following treatment half the plates were exposed to heat stress (+ HS) while the other half were left in the incubator (- HS). Following exposure, the plates were subsequently return to standard culture conditions until analysis. A Presto Blue assay was performed 72 h post exposure and the results are represented as a percentage change in metabolic activity relative to the activity observed at 0 h and in the case of PPE also equalised to PPEC. The values shown are the median 2 biological replicates with 9 technical replicates each. Postitve/negative error was determined by difference of median to upper/lower quartiles. The KW was a comparison between the various conditions in relation to the negative control within group (+ HS or – HS) and any significant difference was apporopriately indicated p <0.05 */<0.01 **/<0.001 ***.

3.3.3. Oxidative Stress effect on viability with or /without prickly pear extract carrier

The effect of oxidative stress on the viability of PPE proved impossible to achieved reliable results using the Presto blue assay, partly due to the short time frame of oxidative stress exposure of 2 h / 4 h paired with the incubation time of 4 h for Presto Blue assay.

3.3.4. UVA (5 J/cm^2) effect on viability with or /without prickly pear extract / carrier

Following the method described in Section 2.8.4 a parallel run using the presto blue assay was performed with UVA (5 J/cm^2) exposure (+ UVA 5) and without UVA (5 J/cm^2) exposure (- UVA 5) tested on varying concentrations of PPE /PPEC (0.002, 0.004, 0.01, 0.02, 0.04 and 0.08 %) for 24 h, with a reading taken every 12 h. The results are presented in Figures 3.34 – 3.35. A significant difference (KW p = <0.05) was observed between the Negative control with/without UVA (5 J/cm^2) throughout the course of experimentation indicating the deleterious effects of UVA (5 J/cm^2) on HDFs viability at all time-points, 12 h and 24 h. As expected 10 % DMSO serving as a positive cytotoxic control resulted in a significant (KW p = <0.05) negative effect on viability when compared to the negative control. The interpretation of Figures 3.34 – 3.35 shows that the PPE / PPEC (0.002, 0.004, 0.01, 0.02, 0.04 and 0.08 %), without UVA (5 J/cm^2) exposure (- UVA 5) at 12 h and 24 h, had no significant (KW p = >0.05) effect on viability of HDFs when compared to the negative control in the same timeframe under the same conditions. It also shows that PPE (0.01, 0.02, 0.04 and 0.08 %), when in direct contact with HDFs in culture for 12 h following UVA (5 J/cm^2), did have a significant (KW p = <0.05) protective effect on viability of HDFs when compared to the negative control under the same conditions in the same time frame amounting to 18 %, 14 %, 14 % and 12% respectively, but this did not persist into 24 h were no significant (KW p = >0.05) effect on viability of HDFs when compared to the negative control was observed. PPE (0.002 %) was not observed to show a significant (KW p = >0.05) effect on viability of HDFs when compared to the negative control under UVA (5 J/cm^2) conditions. Lastly it also shows that PPEC (0.002, 0.004, 0.01, 0.02, 0.04 and 0.08 %) that at 12 h and 24 h following UVA (5 J/cm^2) no significant (KW p = >0.05) on viability of HDFs when compared to the negative control in the same time frame.

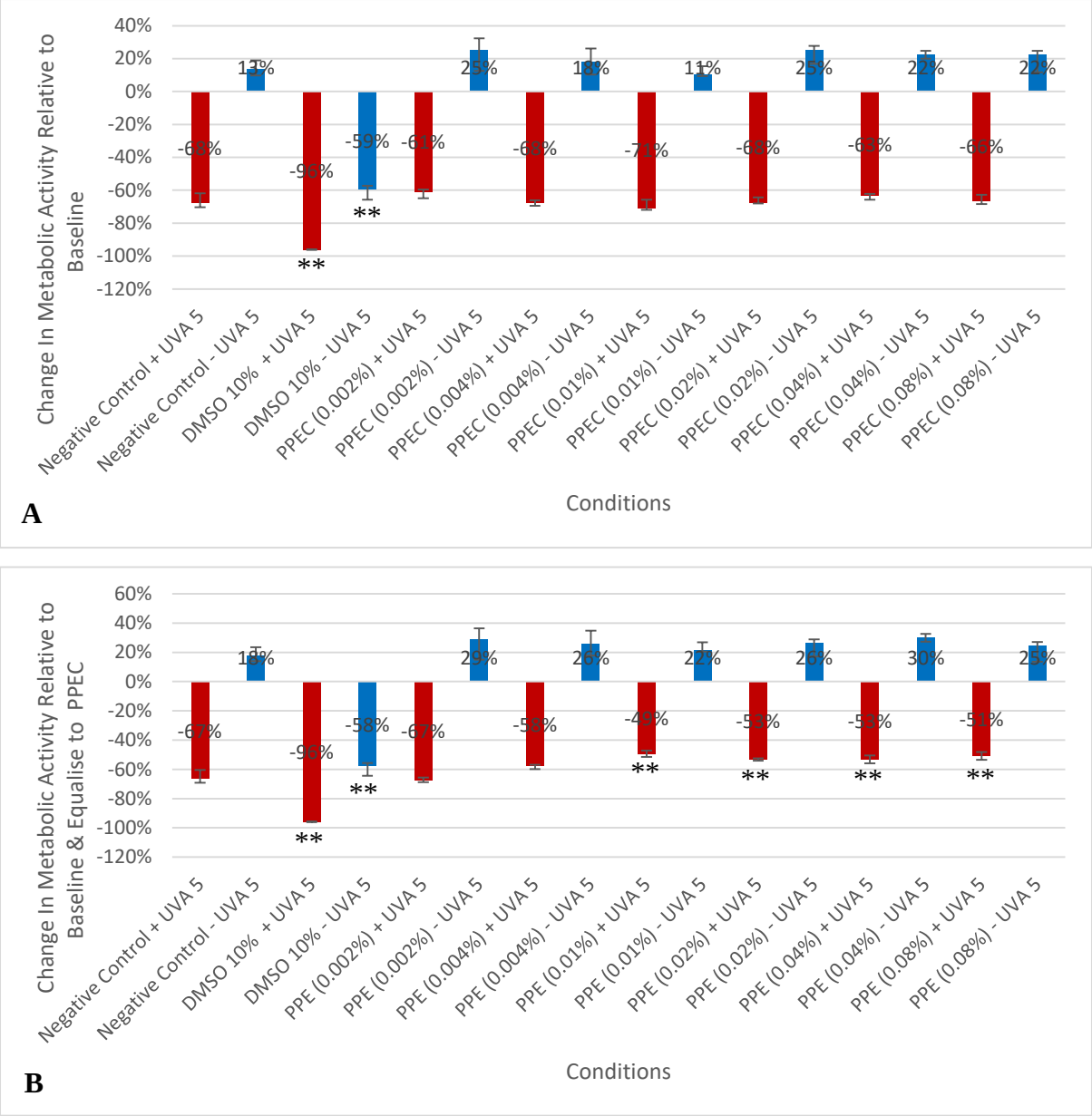

Figure 3.34: The effect of UVA (5 J/cm^2) with/without PPEC (**A**) and PPE (**B**) on the viability of nHDFs after 12 h post-exposure.

The nHDFs were seeded at 1.25x10^3 cells/well in 96 well-plates and were allowed to recover overnight (24 h) in standard culture conditions (37°C / 5 % CO_2). At this point (0 h) the HDFs were treated to a range of PPE and PPEC concentrations (0.002, 0.004, 0.01, 0.02, 0.04 and 0.08 %) and were returned to standard culture conditions for 1 h. Following treatment half the plates were exposed to UVA (5 J/cm^2) radiation (+ UVA 5) while the other half were left in the incubator (- UVA 5). Following exposure, the plates were subsequently return to standard culture conditions until analysis. A Presto Blue assay was performed 12 h post exposure and the results are represented as a percentage change in metabolic activity relative to the activity observed at 0 h and in the case of PPE also equalised to PPEC. The values shown are the median of 9 technical replicates. Postitve/negative error was determined by difference of median to upper/lower quartiles. The KW was a comparison between the various conditions in relation to the negative control within group (+ UVA 5 or – UVA 5) and any significant difference was apporopriately indicated p <0.05 */<0.01 **/<0.001 ***.

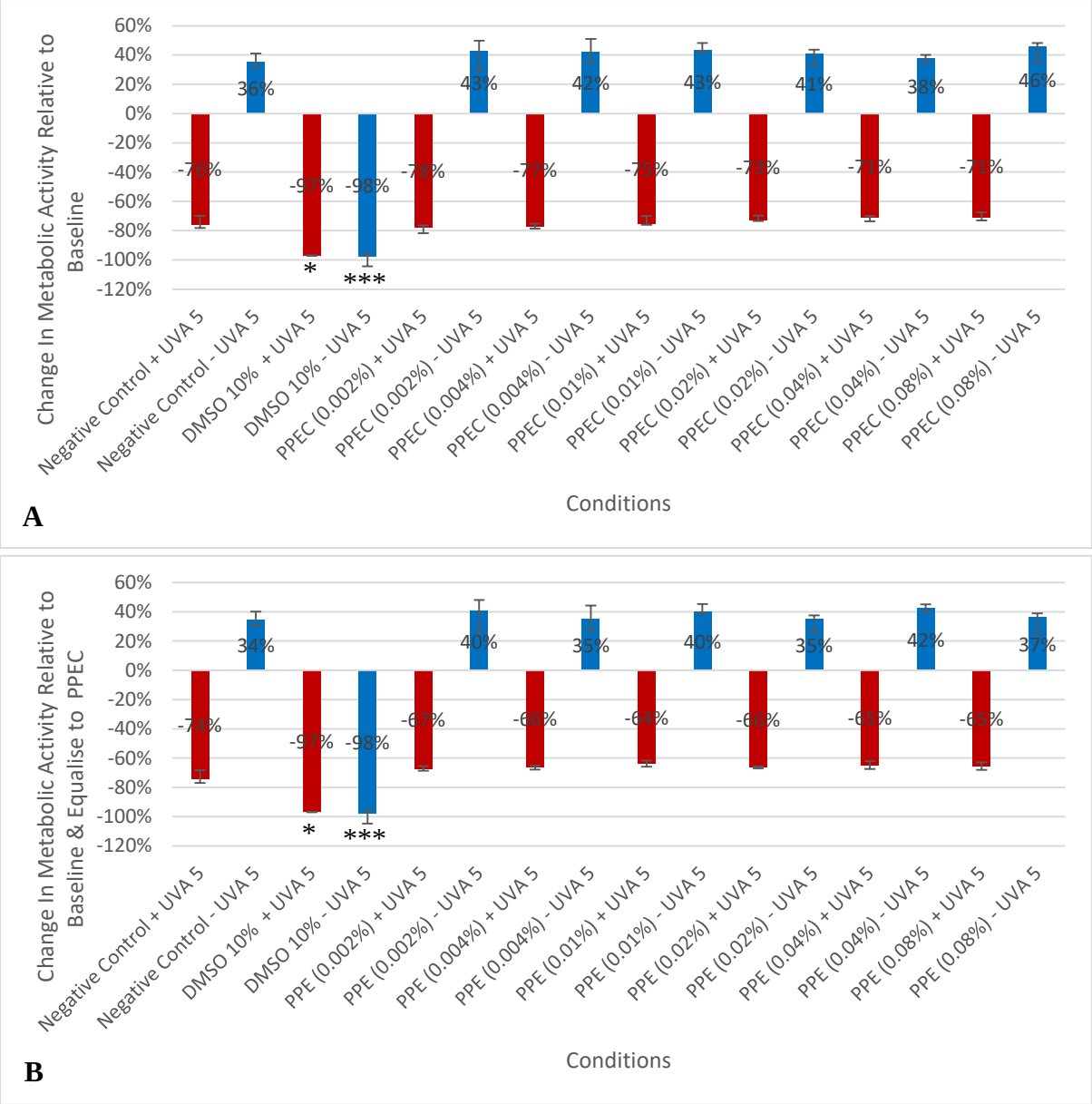

Figure 3.35: The effect of UVA (5 J/cm^2) with/without PPEC (**A**) and PPE (**B**) on the viability of nHDFs after 24 h post-exposure.

The nHDFs were seeded at 1.25x10^3 cells/well in 96 well-plates and were allowed to recover overnight (24 h) in standard culture conditions (37°C / 5 % CO_2). At this point (0 h) the HDFs were treated to a range of PPE and PPEC concentrations (0.002, 0.004, 0.01, 0.02, 0.04 and 0.08 %) and were returned to standard culture conditions for 1 h. Following treatment half the plates were exposed to UVA (5 J/cm^2) radiation (+ UVA 5) while the other half were left in the incubator (- UVA 5). Following exposure, the plates were subsequently return to standard culture conditions until analysis. A Presto Blue assay was performed 24 h post exposure and the results are represented as a percentage change in metabolic activity relative to the activity observed at 0 h and in the case of PPE also equalised to PPEC. The values shown are the median of 9 technical replicates. Postitve/negative error was determined by difference of median to upper/lower quartiles. The KW was a comparison between the various conditions in relation to the negative control within group (+ UVA 5 or – UVA 5) and any significant difference was apporopriately indicated p <0.05 */<0.01 **/<0.001 ***.

3.3.5. UVC (10 µJ/m^2) effect on viability with or /without prickly pear extract / carrier

Following the method described in Section 2.8.4 using Presto Blue a parallel run was performed with UVC (10 µJ/m^2) exposure (+ UVC 1000) and without UVC (10 µJ/m^2) exposure (- UVC 1000) tested on varying concentrations of PPE /PPEC (0.002, 0.004, 0.01, 0.02, 0.04 and 0.08 %) for 24 h, with a reading taken every 12 h. The results are presented in Figures 3.36 – 3.37. A significant difference (KW p = <0.05) was observed between the Negative control with/without UVC (10 µJ/m^2) throughout the course of experimentation indicating the deleterious effects of UVC (10 µJ/m^2) on HDFs viability at all time-points, 12 h and 24 h. As expected 10 % DMSO serving as a positive cytotoxic control resulted in a significant (KW p = <0.05) negative effect on viability when compared to the negative control. PPE / PPEC (0.002, 0.004, 0.01, 0.02, 0.04 and 0.08 %), without UVC (10 µJ/m^2) exposure (- UVC 1000) at 12 h and 24 h, had no significant (KW p = >0.05) effect on viability of HDFs when compared to the negative control in the same timeframe under the same conditions. Lastly it also shows that PPE /PPEC (0.002, 0.004, 0.01, 0.02, 0.04 and 0.08 %) at 12 h and 24 h following UVC (10 µJ/m^2) (+ UVC 1000) radiation had no significant (KW p = >0.05) effect on viability of HDFs when compared to the negative control in the same time frame.

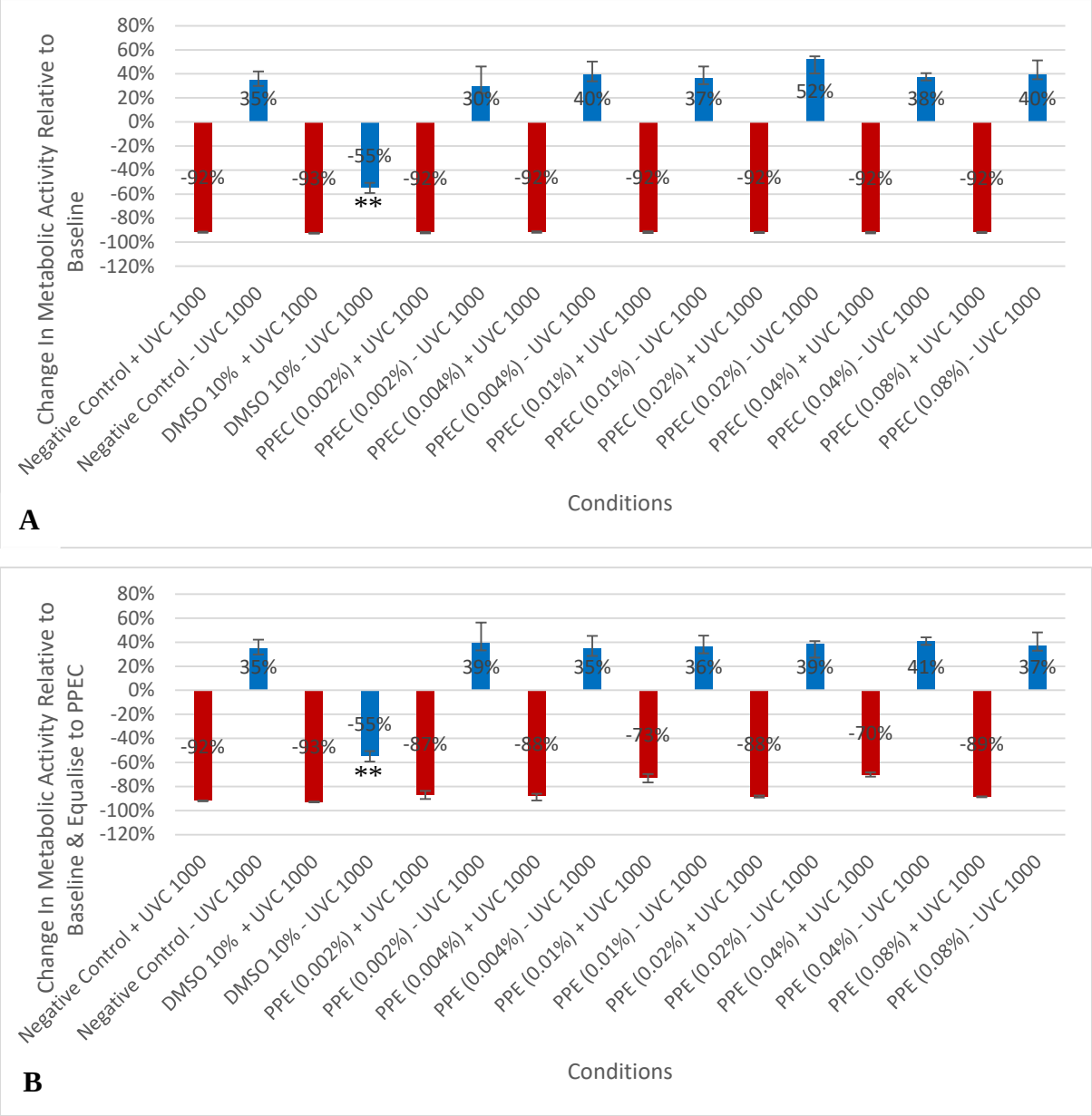

Figure 3.36: The effect of UVC (10 µJ/m^2) with/without PPEC (**A**) and PPE (**B**) on the viability of HDFs after 12 h post-exposure.

The HDFs were seeded at 1.25x10^3 cells/well in 96 well-plates and were allowed to recover overnight (24 h) in standard culture conditions (37°C / 5 % CO_2). At this point (0 h) the HDFs were treated to a range of PPE and PPEC concentration (0.002, 0.004, 0.01, 0.02, 0.04 and 0.08 %) and were returned to standard culture conditions for 1 h. Following treatment half the plates were exposed to UVC (10 µJ/m^2) radiation (+ UVC 1000) while the other half were left in the incubator (- UVC 1000). Following exposure, the plates were subsequently return to standard culture conditions until analysis. A Presto Blue assay was performed 12 h post exposure and the results are represented as a percentage change in metabolic activity relative to the activity observed at 0 h and in the case of PPE also equalised to PPEC. The values shown are the median 2 biological replicates with 9 technical replicates each. Postitve/negative error was determined by difference of median to upper/lower quartiles. The KW was a comparison between the various conditions in relation to the negative control within group (+ UVC 2500 or – UVC 2500) and any significant difference was apporopriately indicated p <0.05 */<0.01 **/<0.001 ***.

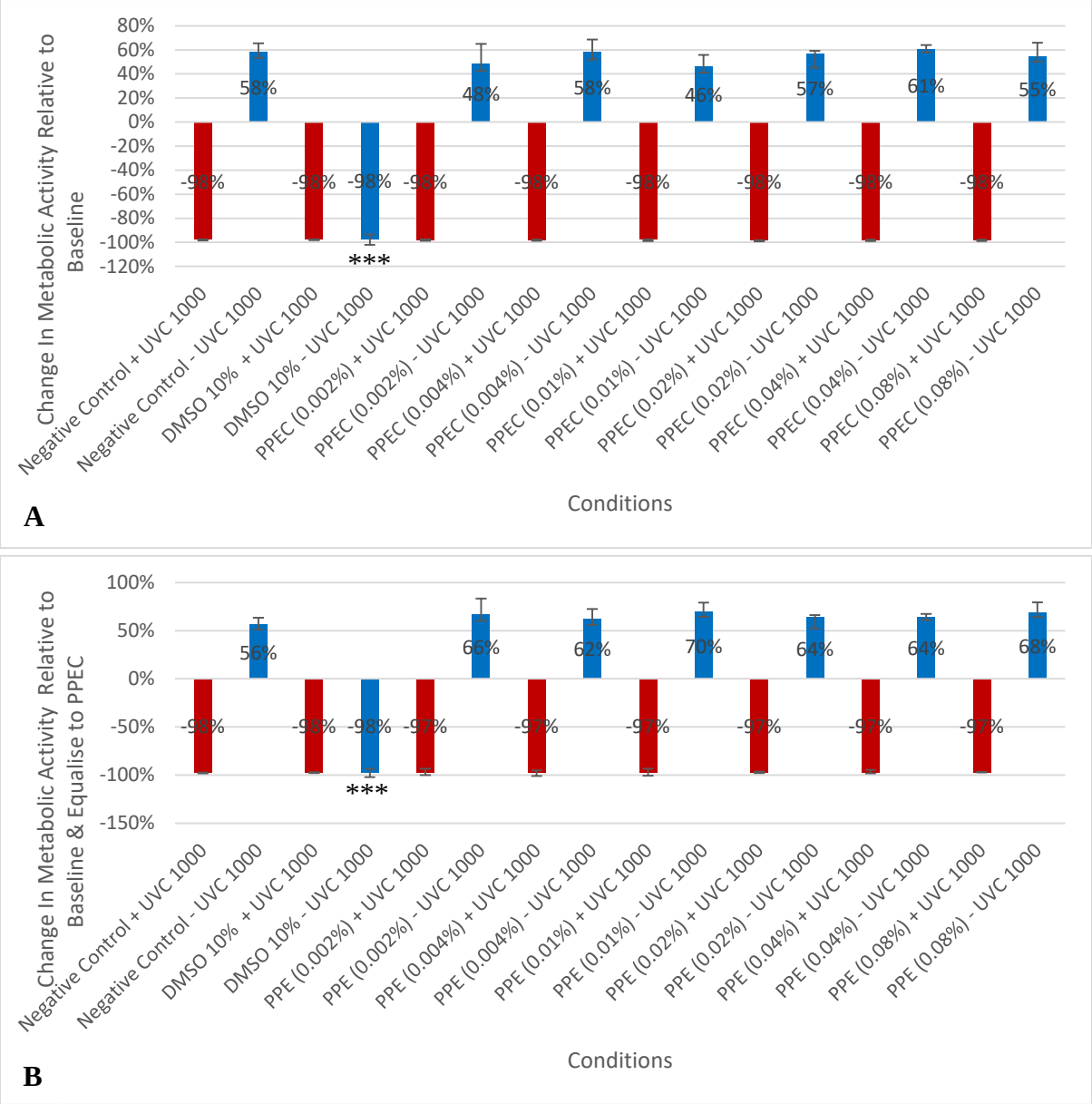

Figure 3.37: The effect of UVC (10 µJ/m^2) with/without PPEC (**A**) and PPE (**B**) on the viability of HDFs after 24 h post-exposure.

The HDFs were seeded at 1.25x10^3 cells/well in 96 well-plates and were allowed to recover overnight (24 h) in standard culture conditions (37°C / 5 % CO_2). At this point (0 h) the HDFs were treated to a range of PPE and PPEC concentration (0.002, 0.004, 0.01, 0.02, 0.04 and 0.08 %) and were returned to standard culture conditions for 1 h. Following treatment half the plates were exposed to UVC (10 µJ/m^2) radiation (+ UVC 1000) while the other half were left in the incubator (- UVC 1000). Following exposure, the plates were subsequently return to standard culture conditions until analysis. A Presto Blue assay was performed 24 h post exposure and the results are represented as a percentage change in metabolic activity relative to the activity observed at 0 h and in the case of PPE also equalised to PPEC. The values shown are the median 2 biological replicates with 9 technical replicates each. Postitve/negative error was determined by difference of median to upper/lower quartiles. The KW was a comparison between the various conditions in relation to the negative control within group (+ UVC 1000 or – UVC 1000) and any significant difference was apporopriately indicated p <0.05 */<0.01 **/<0.001 ***.

3.3.6. UVC (25 µJ/m^2) effect on viability with or /without prickly pear extract / carrier

Following the method described in Section 2.8.4 using Presto Blue a parallel run was performed with UVC (25 µJ/m^2) exposure (+ UVC 2500) and without UVC (25 µJ/m^2) exposure (- UVC 2500) tested on varying concentrations of PPE /PPEC (0.002, 0.004, 0.01, 0.02, 0.04 and 0.08 %) for 24 h, with a reading taken every 12 h. The results are presented in Figures 3.38 – 3.39. A significant difference (KW p = <0.05) was observed between the Negative control with/without UVC (25 µJ/m^2) throughout the course of experimentation indicating the deleterious effects of UVC (25 µJ/m^2) on HDFs viability at all time-points, 12 h (135 %) and 24 h (159 %). As expected 10 % DMSO serving as a positive cytotoxic control resulted in a significant (KW p = <0.05) negative effect on viability when compared to the negative control. PPE / PPEC (0.002, 0.004, 0.01, 0.02, 0.04 and 0.08 %), without UVC (25 µJ/m^2) exposure (- UVC 2500) at 12 h and 24 h, had no significant (KW p = >0.05) effect on viability of HDFs when compared to the negative control in the same timeframe under the same conditions. Lastly it also shows that PPE /PPEC (0.002, 0.004, 0.01, 0.02, 0.04 and 0.08 %) at 12 h and 24 h following UVC (25 µJ/m^2) (+ UVC 2500) radiation had no significant (KW p = >0.05) effect on viability of HDFs when compared to the negative control in the same time frame.

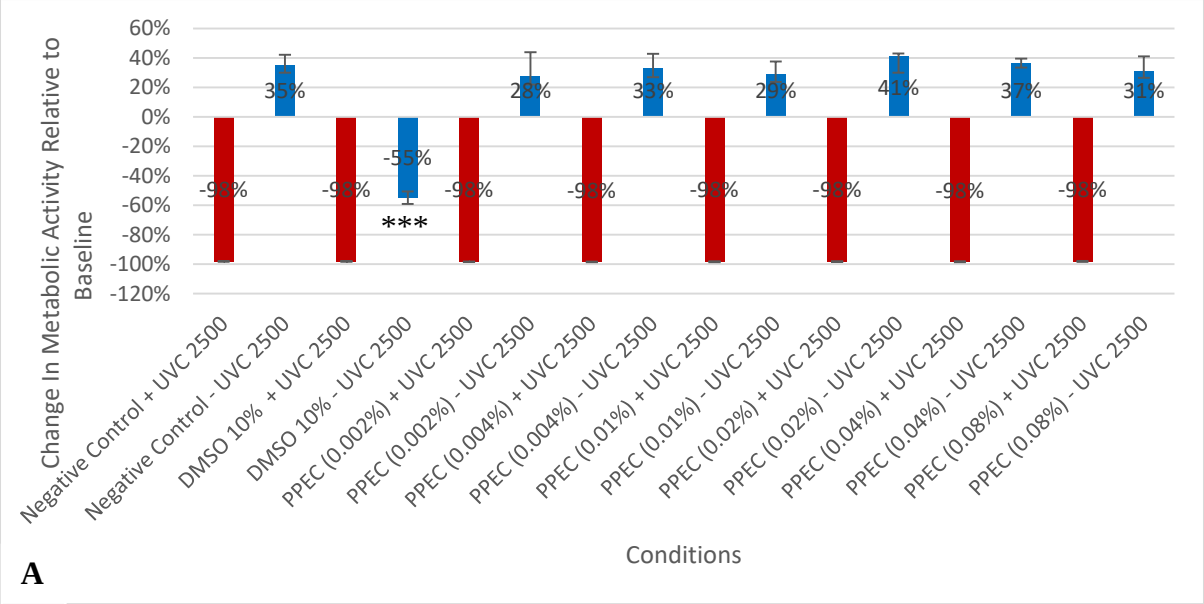

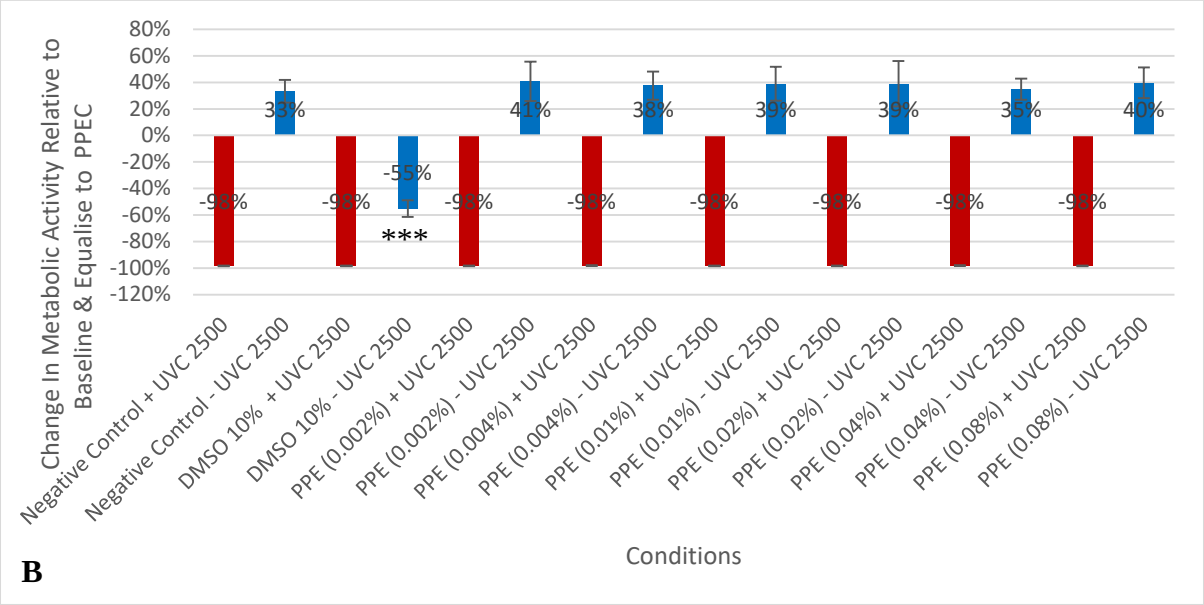

Figure 3.38: The effect of UVC (25 µJ/m^2) with/without PPEC (**A**) and PPE (**B**) on the viability of HDFs after 12 h post-exposure.

The HDFs were seeded at 1.25x10^3 cells/well in 96 well-plates and were allowed to recover overnight (24 h) in standard culture conditions (37°C / 5 % CO_2). At this point (0 h) the HDFs were treated to a range of PPE and PPEC concentration (0.002, 0.004, 0.01, 0.02, 0.04 and 0.08 %) and were returned to standard culture conditions for 1 h. Following treatment half the plates were exposed to UVC (25 µJ/m^2) radiation (+ UVC 2500) while the other half were left in the incubator (- UVC 2500). Following exposure, the plates were subsequently return to standard culture conditions until analysis. A Presto Blue assay was performed 12 h post exposure and the results are represented as a percentage change in metabolic activity relative to the activity observed at 0 h and in the case of PPE also equalised to PPEC. The values shown are the median 2 biological replicates with 9 technical replicates each. Postitve/negative error was determined by difference of median to upper/lower quartiles. The KW was a comparison between the various conditions in relation to the negative control within group (+ UVC 2500 or – UVC 2500) and any significant difference was apporopriately indicated p <0.05 */<0.01 **/<0.001 ***.

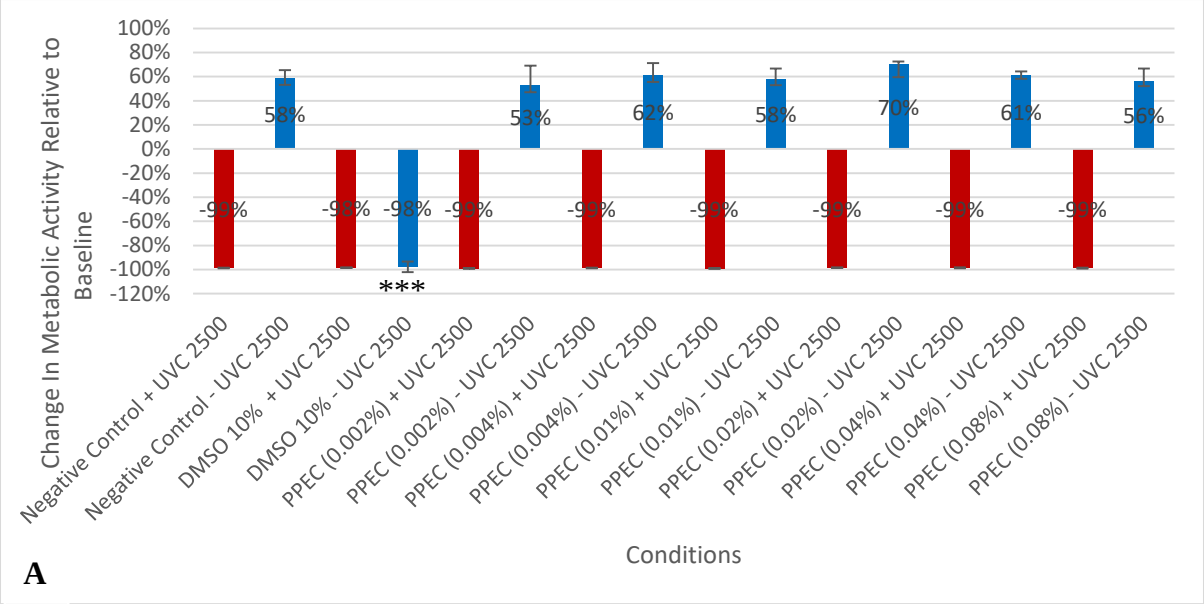

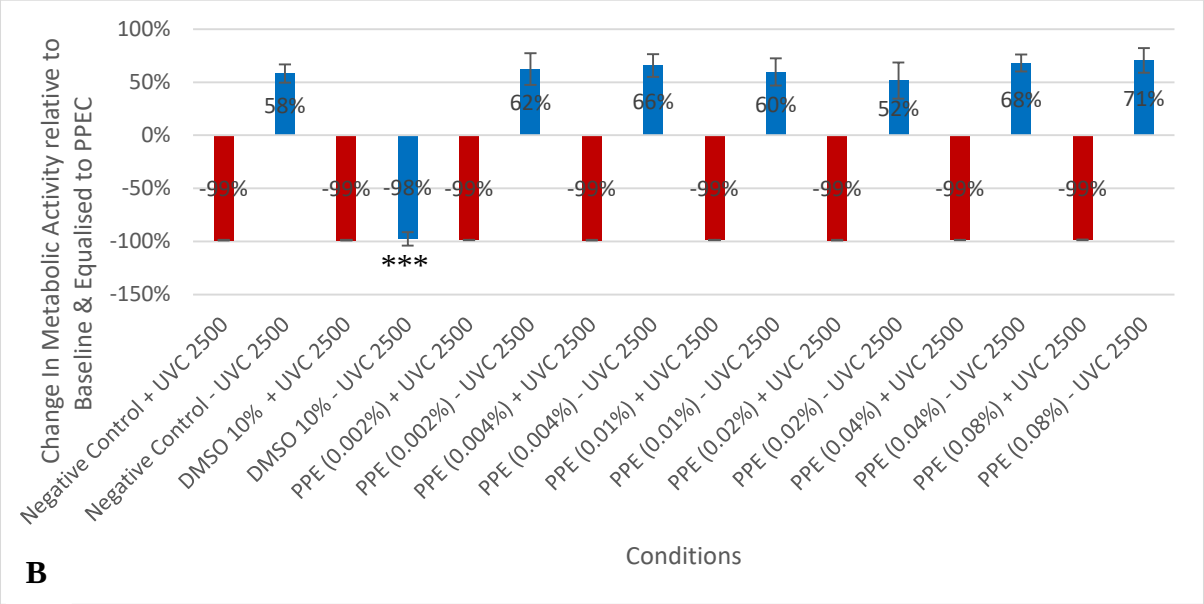

Figure 3.39: The effect of UVC (25 µJ/m^2) with/without PPEC (**A**) and PPE (**B**) on the viability of HDFs after 24 h post-exposure.

The HDFs were seeded at 1.25x10^3 cells/well in 96 well-plates and were allowed to recover overnight (24 h) in standard culture conditions (37°C / 5 % CO_2). At this point (0 h) the HDFs were treated to a range of PPE and PPEC concentration (0.002, 0.004, 0.01, 0.02, 0.04 and 0.08 %) and were returned to standard culture conditions for 1 h. Following treatment half the plates were exposed to UVC (25 µJ/m^2) radiation (+ UVC 2500) while the other half were left in the incubator (- UVC 2500). Following exposure, the plates were subsequently return to standard culture conditions until analysis. A Presto Blue assay was performed 24 h post exposure and the results are represented as a percentage change in metabolic activity relative to the activity observed at 0 h and in the case of PPE also equalised to PPEC. The values shown are the median 2 biological replicates with 9 technical replicates each. Postitve/negative error was determined by difference of median to upper/lower quartiles. The KW was a comparison between the various conditions in relation to the negative control within group (+ UVC 2500 or – UVC 2500) and any significant difference was apporopriately indicated p <0.05 */<0.01 **/<0.001 ***.

3.4. Amalgamation of consequential viability assay findings

Following exhaustive experimentation encompassing two viability assays and three cellular stressors a visual amalgamation was required to deduced the ideal target concentration Table 3.1 is an amalgamation of the most consequential viability assay findings and was utilised to pinpoint the ideal target for continued experimentation which was noted to be PPE 0.04 %

Table 3.1: This is a summary of the results for the CellTitre-glo and Presto blue assays and the values shown are percentage change in metabolic activity relative to the activity observed at 0 h and also equalised to PPEC. The highlighted shows the ideal target concentration.

Conc %	PPE 0.002 %	PPE 0.004 %	PPE 0.01%	PPE 0.02 %	PPE 0.04 %	PPE 0.08 %
Heat Stress (44 °C 1 h) – CellTitre-glo Assay						
24 h	66	44	48	50	82	55
48 h	21	NSD	NSD	NSD	55	55
72 h	NSD	NSD	NSD	NSD	NSD	NSD
Heat Stress (44 °C 1 h) – Presto Blue Assay						
24 h	79	49	64	62	81	61
48 h	82	75	67	68	95	87
72 h	NSD	NSD	NSD	NSD	NSD	NSD
UVA (5 J/cm^2) - CellTitre-glo Assay						
12 h	NSD	NSD	10	8	14	13
24 h	NSD	NSD	6	6	6	5
UVA (5 J/cm^2) – Presto Blue Assay						
12 h	NSD	NSD	18	14	14	12
24 h	NSD	NSD	NSD	NSD	NSD	NSD
UVC (10 µJ/m^2) - CellTitre-glo Assay						
12 h	NSD	NSD	9	9	14	9
24 h	NSD	NSD	NSD	NSD	NSD	NSD
UVC (10 µJ/m^2) – Presto Blue						
12 h	NSD	NSD	NSD	NSD	NSD	NSD
24 h	NSD	NSD	NSD	NSD	NSD	NSD
Menadione 25 µM – CellTitre-glo						
2 h	14	21	21	39	44	54
4 h	27	9	26	39	57	40
Menadione 12.5 µM – CellTitre-glo						
2 h	14	21	21	39	44	54
4 h	27	9	26	39	57	40
Menadione 6.25 µM – CellTitre-glo						
2 h	NSD	32	16	20	30	32
4 h	60	63	57	28	70	51

3.5. Scratch Assay

The Scratch Assay followed the protocol described in Section 2.7 for heat stress, oxidative and UV radiation testing. However only the results of the heat stress experiments are shown as following pHDF exposure to oxidative stress and UV radiation, analysis throughout 48 h time period proved impossible due to high deleterious effects on cellular monolayer and thus subsequent effect on scratch stability. The Scratch Assay followed the protocol described in Section 2.7 and was performed in a parallel run with both heat stress (+ HS 44°C for 1 h) and without heat stress (- HS 37°C for 1 h) being tested at varying concentrations of PPE (0.002 %, 0.004 %, 0.04 % and 0.08%) for 48 Hrs, with a reading taken every 12 h. The results are presented in Figures 3.40 – 3.46. The values are presented as percentage denuded area, for a given time-point the smaller denuded areas are indicators of better pHDF migration and viability.

Following Heat stress (+ HS 44°C for 1 h) PPE had an effect on the migration and viability of pHDF shown as an effect on the percentage denuded area in relation to the corresponding negative control. PPE 0.002 % at 12 h, 24 h and 36 h was seen to have no significant effect (KW p = >0.05) on the percentage denuded area, however at 48 h a significant reduction in the denuded area (KW p = <0.05) was observed. PPE 0.004 % at 12 h was seen to have no significant effect (KW p = >0.05) on the percentage denuded area, however at 24 h, 36 h and 48 h a significant reduction in the denuded area (KW p = <0.05) was observed. PPE 0.04 % at 48 h was seen to have no significant effect (KW p = >0.05) on the percentage denuded area, however at 12 h, 24 h and 36 h a significant reduction in the percentage denuded area (KW p = <0.05) was observed. PPE (0.08 %) was initially (12 h) seen to significant reduce the percentage denuded area (KW p = <0.05), however this effect was subsequently reversed at 36 h and 48 h were it was seen to significantly increase the percentage denuded area. The results here showed no significant inter-scratch variation between the conditions at 0 h. For the parallel run without heat stress (- HS 37 °C for 1 h), the PPE had a concentration-based effect on the migration and viability of HDF shown as an effect on the percentage denuded area in relation to the corresponding negative control. PPE (0.002 %, 0.004 % and 0.04 %) was seen to significantly reduce the percentage denuded area (KW p = <0.05) through course of experimentation.. Furthermore, PPE (0.08 %) was seen to either have no significant effect or significantly increase the percentage denuded area at a given timepoint. The results here show inter – scratch variation a 0 h and thus results should be interpreted as such.

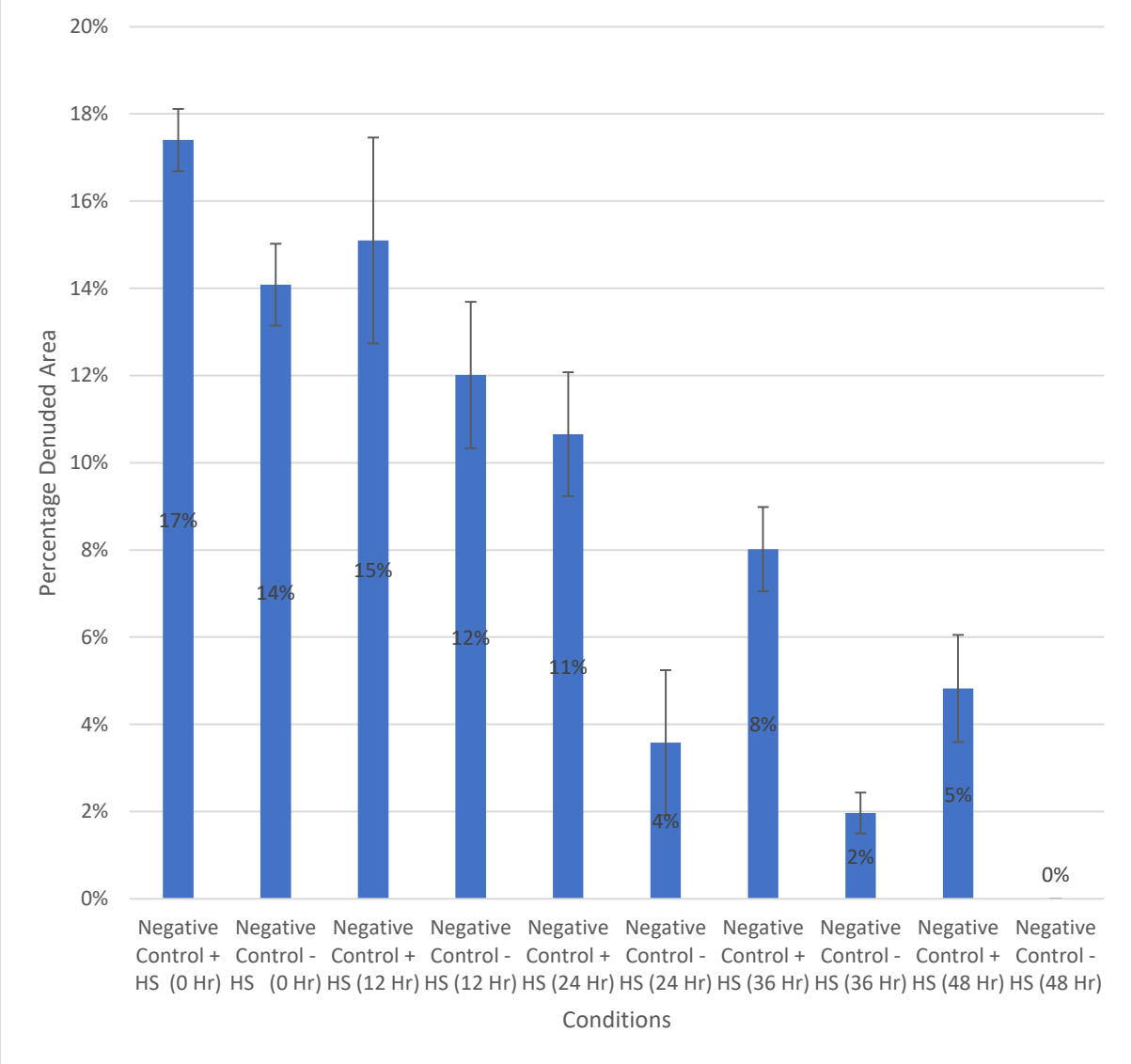

Figure 3.40: The scratch assay results with respect to percentage denuded area for the negative control with heat stress (+ HS) compared to the negative control without heat stress (- HS) over 48 h.

The pHDFs were seeded at $2.5x10^4$ cells/well in 24 well plates which were incubated (37°C / 5 % CO_2) and were allowed to form a confluent monolayer (~ 1 day), which were exposed to test conditions and subsequently scratched to form a denuded area (0 h). Negative control (+ HS) refers to pHDF exposed to heat stress (44°C for 1 h) lacking PPE treatment while negative control (- HS) refers to pHDF lacking exposure to heat stress (37°C for 1 h) lacking PPE treatment. The observed percentage denuded area was then imaged microscopically at x40 magnification at regular time intervals (0 h, 12 h, 24 h, 36 h, and 48 h) and the images acquired were analyzed using Tscratch analysis software. The values shown are the median of 3 technical replicates repeated 3 times. Postitve/negative error was determined by difference of median to upper/lower quartiles.

The interpretation of Figure 3.40 shows a comparison between the Negative control with heat stress (+ HS 44°C for 1 h) and Negative control without heat stress (- HS 37°C for 1 h) as expressed by the percentage denuded area. The less percentage denuded area and quicker the closure is indicative of improved pHDF viability, cell division and migration.

- At 0 h the negative control without heat stress (- HS 37°C for 1 h) was seen to have significantly (KW p = <0.05) less percentage denuded area (~3 %) when compared to the negative control with heat stress (+ HS 44°C for 1 h).
- At 12 h negative control without heat stress (- HS 37°C for 1 h) was seen to have no significantly difference (KW p = <0.05) in the percentage denuded area (~3 %) when compared to negative control with heat stress (+ HS 44°C for 1 h).
- At 24 h, 36 h and 48 h the negative control without heat stress (- HS 37°C for 1 h) was seen to have significantly (KW p = <0.05) less percentage denuded area (~7 %, 6 % and 5 % respectively) when compared to the negative control with heat stress (+ HS 44°C for 1 h).

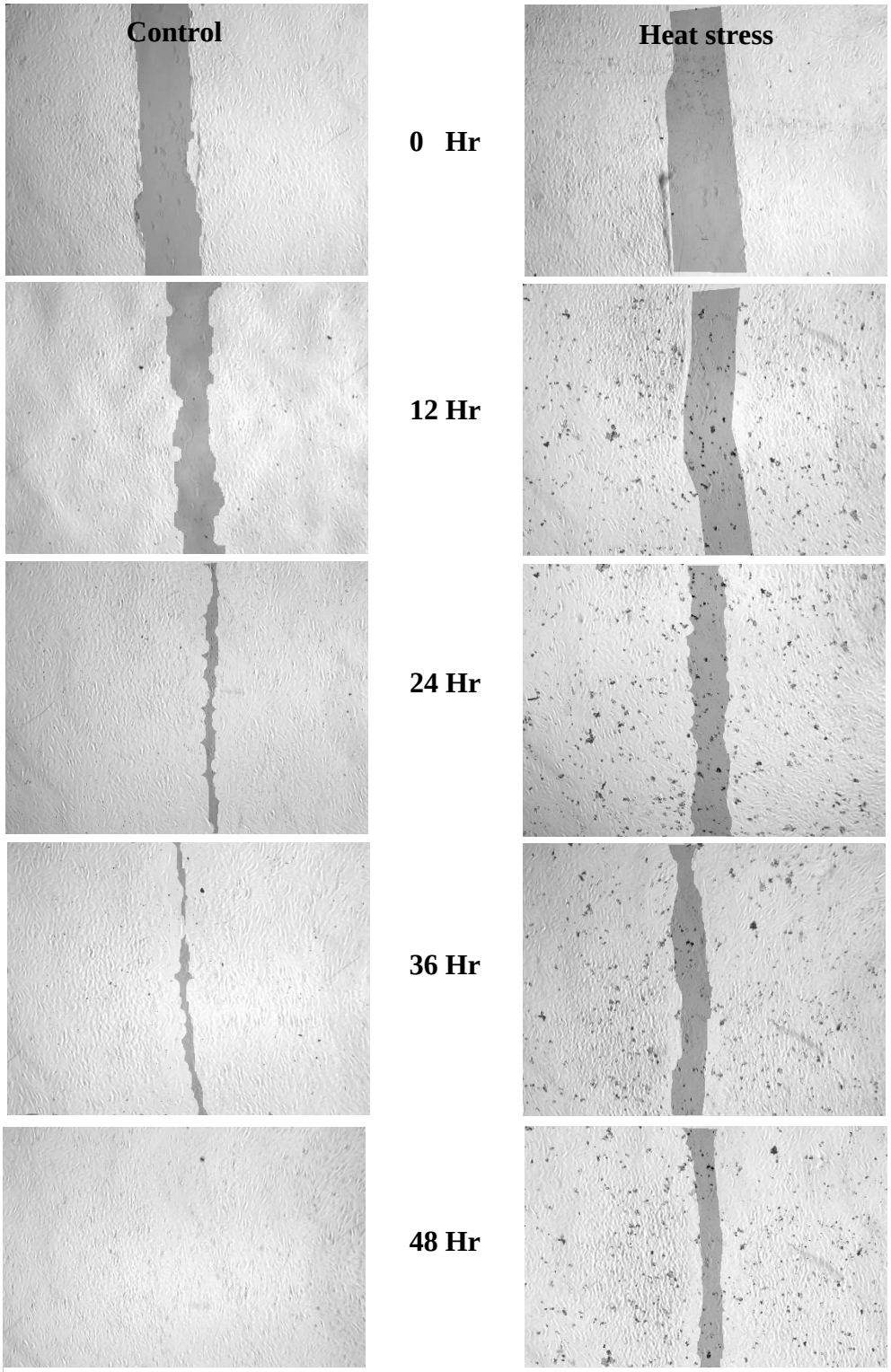

Figure 3.41: A side by side comparison of the denuded area with/without heat stress (44°C 1 h) for the Negative control for the duration of the experiment. Following treatment, scratch and thermal treatment the observed percentage denuded area was imaged microscopically at x40 magnification at regular time intervals (0 h, 12 h, 24 h, 36 h, and 48 h) and the images acquired were analyzed using Tscratch analysis software in a similar fashion as demonstrated above.

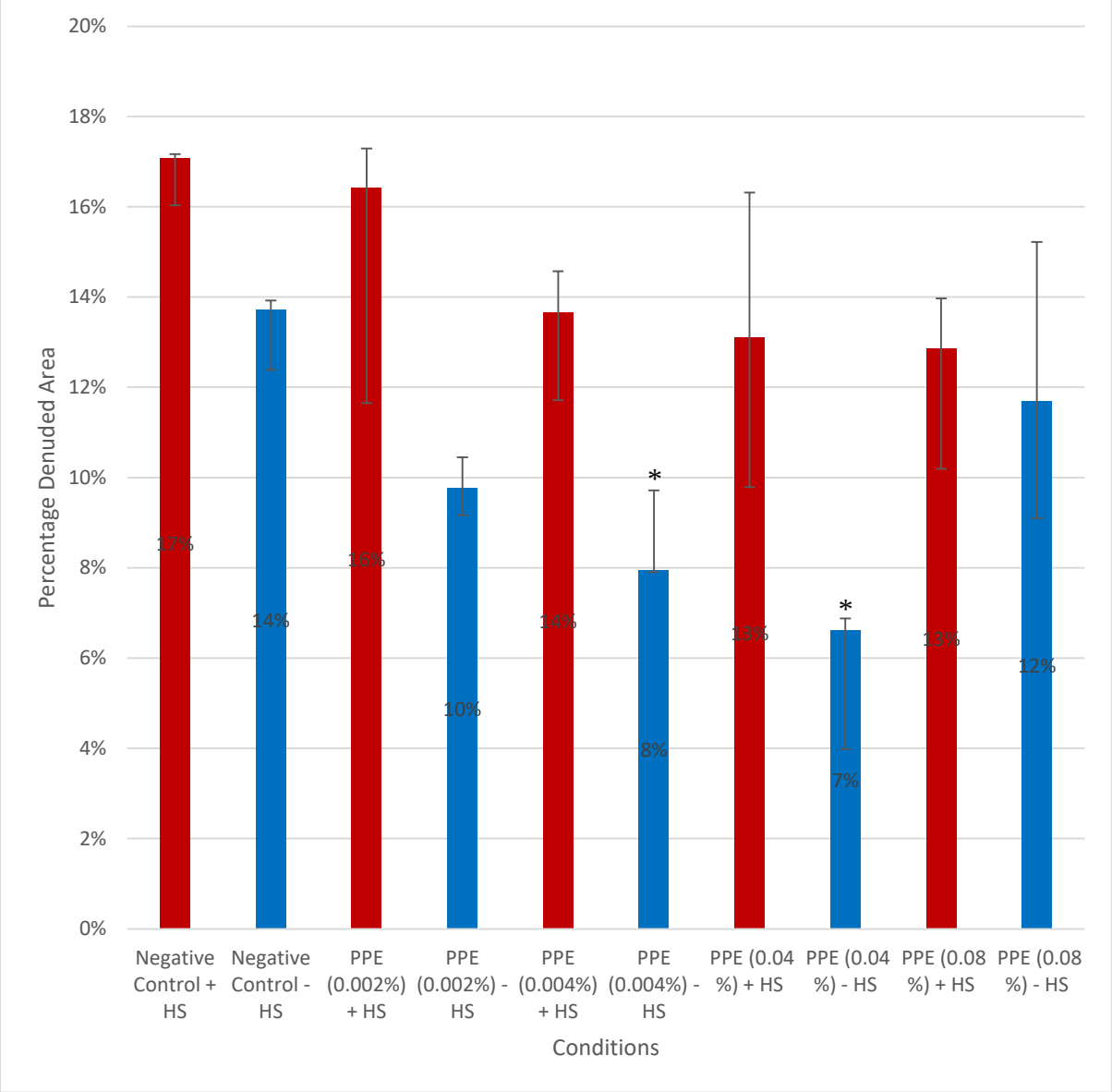

Figure 3.42: The scratch assay results with respect to percentage denuded area for the conditions being tested at 0 h.

The pHDFs were seeded at $2.5x10^4$ cells/well in 24 well plates which were incubated (37°C / 5 % CO_2) and were allowed to form a confluent monolayer (~ 1 day), which were exposed to test conditions and subsequently scratched to form a denuded area (0 h). The pHDFs were exposed to these conditions; Prickly pear extract (PPE) (0.002 %, 0.004 %, 0.04 % and 0.08 %) including a 1hr pre-treatment prior to either Heat Stress (HS) referred to as PPE + HS (44°C for 1 h) or lacking heat stress referred to as PPE - HS (37°C for 1 h), negative control + HS refers to pHDF exposed to heat stress (44°C for 1 h) without PPE, while negative control - HS refers to pHDF not exposed to heat stress (37°C for 1 h) without PPE. The observed percentage denuded area was then imaged microscopically at x40 magnification at regular time intervals (0 h, 12 h, 24 h, 36 h, and 48 h) and the images acquired were analyzed using Tscratch analysis software. The values shown are the median of 3 technical replicates repeated 3 times. Postitve/negative error was determined by difference of median to upper/lower quartiles. The KW was a comparison between the various conditions in relation to the appropriate negative control and any significant difference was apporopriately indicated $p < 0.05$ */<0.01 **/<0.001 ***.

The interpretation of Figure 3.42 show a comparison between the Negative control and various concentrations of PPE (0.002, 0.004, 0.04 and 0.08 %) with Heat stress (+ HS 44°C for 1 h) as well as the Negative control and various concentrations of PPE (0.002, 0.004, 0.04 and 0.08 %) without heat stress (- HS 37°C for 1 h) at 0 h post exposure as expressed by the percentage denuded area. The smaller the percentage denuded area and thus quicker the rate of closure, the greater the indication of improved pHDF viability and migration.

- The PPE (0.002, 0.004, 0.04 and 0.08 %) conditions with heat stress (+ HS 44°C for 1 h) at 0hr were seen to have no significant (KW p = <0.05) effect on viability and migration of pHDF when compared to the corresponding negative control with heat stress (+ HS 44°C for 1 h) in the same time frame. This is indicative of no significant inter-scratch variation.
- The PPE (0.004 and 0.04 %) without heat stress (- HS 37°C for 1 h) at 0 h was seen to have significant (KW p = <0.05) effect on viability and migration of pHDF when compared to the negative control (- HS 37°C for 1 h) in the same time frame, to the tune of 6 % and 7 % respectively. This is indicative of the significant drawback of the scratch assay, the tendency to give inter – scratch variation. Furthermore, PPE (0.002 & 0.08 %) was seen to have no significant (KW p = <0.05) effect on viability and migration of pHDF when compared to the negative control (- HS 37°C for 1 h) in the same time frame.

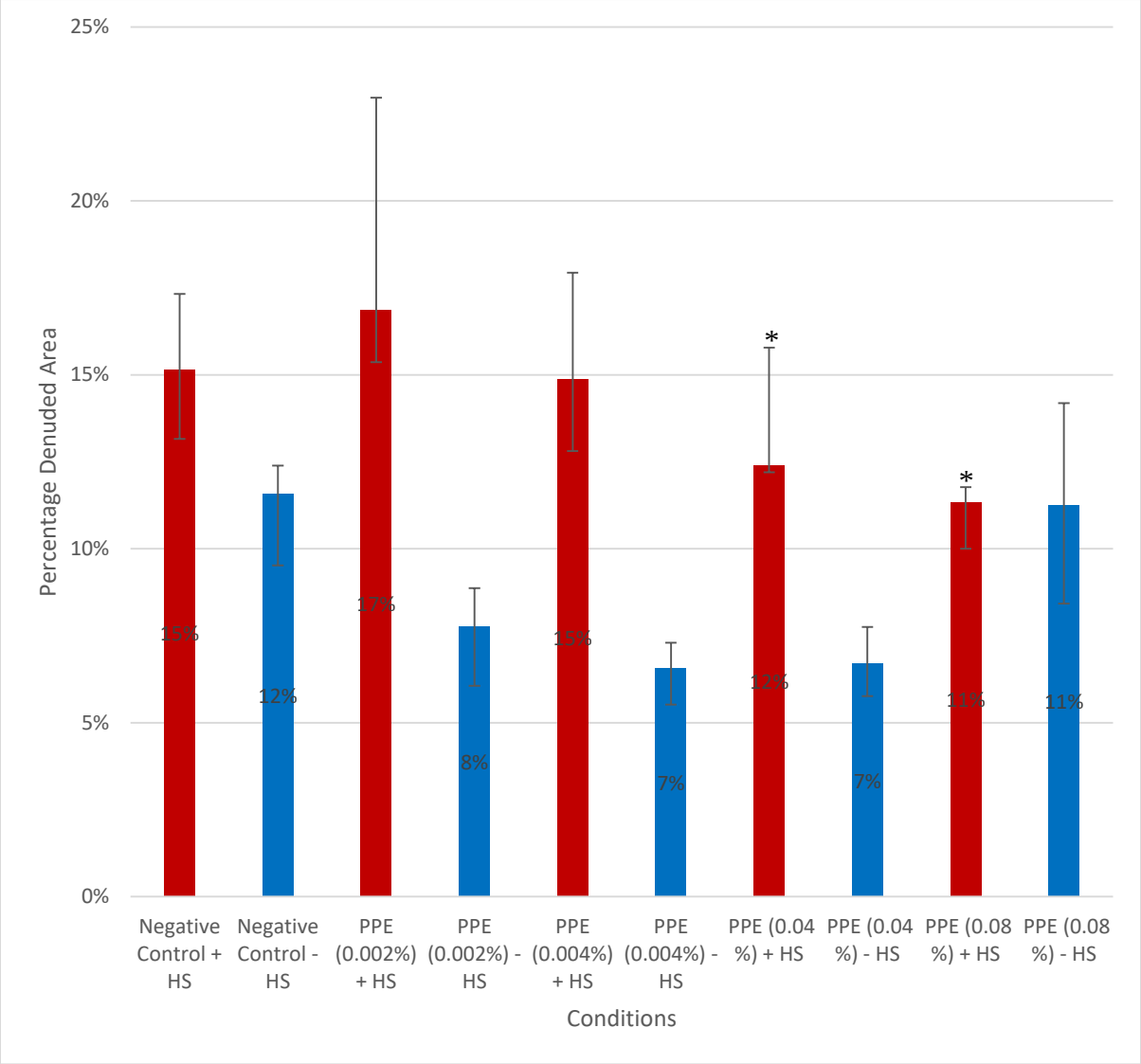

Figure 3.43: The scratch assay results with respect to percentage denuded area for the conditions being tested at 12 h.

The pHDFs were seeded at 2.5x104 cells/well in 24 well plates which were incubated (37°C / 5 % CO_2) and were allowed to form a confluent monolayer (~ 1 day), which were exposed to test conditions and subsequently scratched to form a denuded area (0 h). The pHDFs were exposed to these conditions; Prickly pear extract (PPE) (0.002 %, 0.004 %, 0.04 % and 0.08 %) including a 1hr pre-treatment prior to either Heat Stress (HS) referred to as PPE + HS (44°C for 1 h) or lacking heat stress referred to as PPE - HS (37°C for 1 h), negative control + HS refers to pHDF exposed to heat stress (44°C for 1 h) without PPE, while negative control - HS refers to pHDF not exposed to heat stress (37°C for 1 h) without PPE. The observed percentage denuded area was then imaged microscopically at x40 magnification at regular time intervals (0 h, 12 h, 24 h, 36 h, and 48 h) and the images acquired were analyzed using Tscratch analysis software. The values shown are the median of 3 technical replicates repeated 3 times. Postitve/negative error was determined by difference of median to upper/lower quartiles. The KW was a comparison between the various conditions in relation to the appropriate negative control and any significant difference was apporopriately indicated p <0.05 */<0.01 **/<0.001 ***.

The interpretation of Figure 3.43 show a comparison between the Negative control and various concentrations of PPE (0.002, 0.004, 0.04 and 0.08 %) with Heat stress (+ HS 44°C for 1 h) as well as the Negative control and various concentrations of PPE (0.002, 0.004, 0.04 and 0.08 %) without heat stress (- HS 37°C for 1 h) at 12 h post exposure as expressed by the percentage denuded area.

- The PPE (0.002 and 0.004 %) conditions with heat stress (+ HS 44°C for 1 h) at 12 h were seen to have no significant (KW p = <0.05) effect on viability and migration of pHDF when compared to the corresponding negative control with heat stress (+ HS 44°C for 1 h) in the same time frame. Furthermore, the PPE (0.04 and 0.08 %) conditions with heat stress (+ HS 44°C for 1 h) at 12 h were seen to have a significant (KW p = <0.05) effect on viability and migration of pHDF when compared to the corresponding negative control with heat stress (+ HS 44°C for 1 h) in the same time frame, to the tune of 3 % and 4 % respectively.
- The PPE (0.002, 0.004 and 0.04 %) without heat stress (- HS 37°C for 1 h) at 12 h was seen to have no significant (KW p = <0.05) effect on viability and migration of pHDF when compared to the negative control (- HS 37°C for 1 h) in the same time frame. Furthermore, PPE (0.08 %) was seen to have a significant (KW p = <0.05) effect on viability and migration of pHDF when compared to the negative control (- HS 37°C for 1 h) in the same time frame.

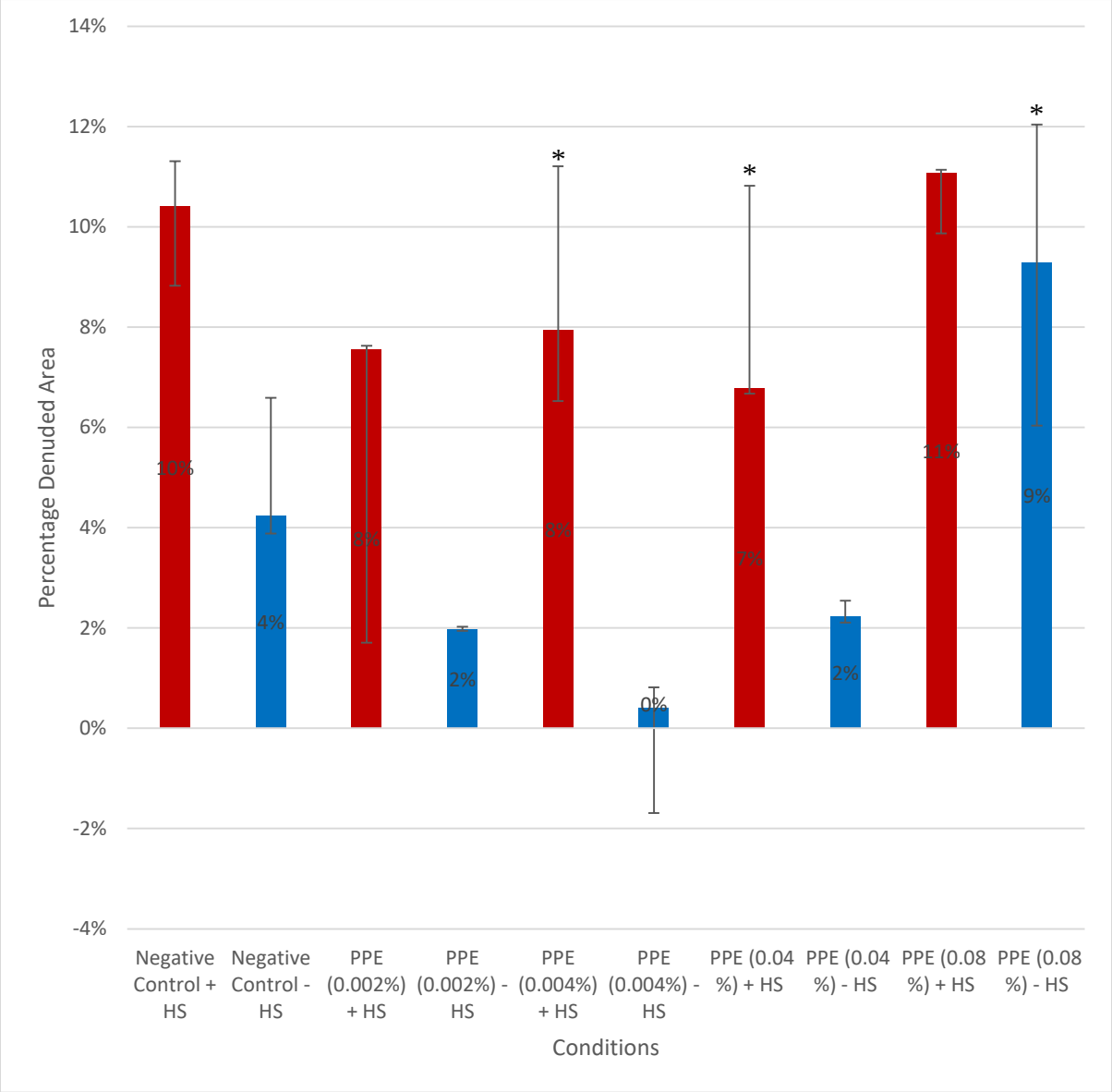

Figure 3.44: The scratch assay results with respect to percentage denuded area for the conditions being tested at 24 h.

The pHDFs were seeded at $2.5x10^4$ cells/well in 24 well plates which were incubated (37°C / 5 % CO_2) and were allowed to form a confluent monolayer (~ 1 day), which were exposed to test conditions and subsequently scratched to form a denuded area (0 h). The pHDFs were exposed to these conditions; Prickly pear extract (PPE) (0.002 %, 0.004 %, 0.04 % and 0.08 %) including a 1hr pre-treatment prior to either Heat Stress (HS) referred to as PPE + HS (44°C for 1 h) or lacking heat stress referred to as PPE - HS (37°C for 1 h), negative control + HS refers to pHDF exposed to heat stress (44°C for 1 h) without PPE, while negative control - HS refers to pHDF not exposed to heat stress (37°C for 1 h) without PPE. The observed percentage denuded area was then imaged microscopically at x40 magnification at regular time intervals (0 h, 12 h, 24 h, 36 h, and 48 h) and the images acquired were analyzed using Tscratch analysis software. The values shown are the median of 3 technical replicates repeated 3 times. Postitve/negative error was determined by difference of median to upper/lower quartiles. The KW was a comparison between the various conditions in relation to the appropriate negative control and any significant difference was apporopriately indicated $p < 0.05$ */<0.01 **/<0.001 ***.

The interpretation of Figure 3.44 show a comparison between the Negative control and various concentrations of PPE (0.002, 0.004, 0.04 and 0.08 %) with Heat stress (+ HS 44°C for 1 h) as well as the Negative control and various concentrations of PPE (0.002, 0.004, 0.04 and 0.08 %) without heat stress (- HS 37°C for 1 h) at 24hr post exposure as expressed by the percentage denuded area.

.

- The PPE (0.002 and 0.08%) conditions with heat stress (+ HS 44°C for 1 h) at 24 h were seen to have no significant (KW p = >0.05) effect on viability and migration of pHDF when compared to the corresponding negative control with heat stress (+ HS 44°C for 1 h) in the same time frame. Furthermore, the PPE (0.004 and 0.04 %) conditions with heat stress (+ HS 44°C for 1 h) at 24 h were seen to have a significant (KW p = >0.05) effect on viability and migration of pHDF when compared to the corresponding negative control with heat stress (+ HS 44°C for 1 h) in the same time frame, to the tune of 2 % and 3 % respectively.
- The PPE (0.002, 0.004 and 0.04 %) without heat stress (- HS 37°C for 1 h) at 24 h was seen to have no significant (KW p = <0.05) effect on viability and migration of pHDF when compared to the negative control (- HS 37°C for 1 h) in the same time frame. Furthermore, PPE (0.08 %) was seen to have a significant (KW p = <0.05) effect on viability and migration of pHDF when compared to the negative control (- HS 37°C for 1 h) in the same time frame.

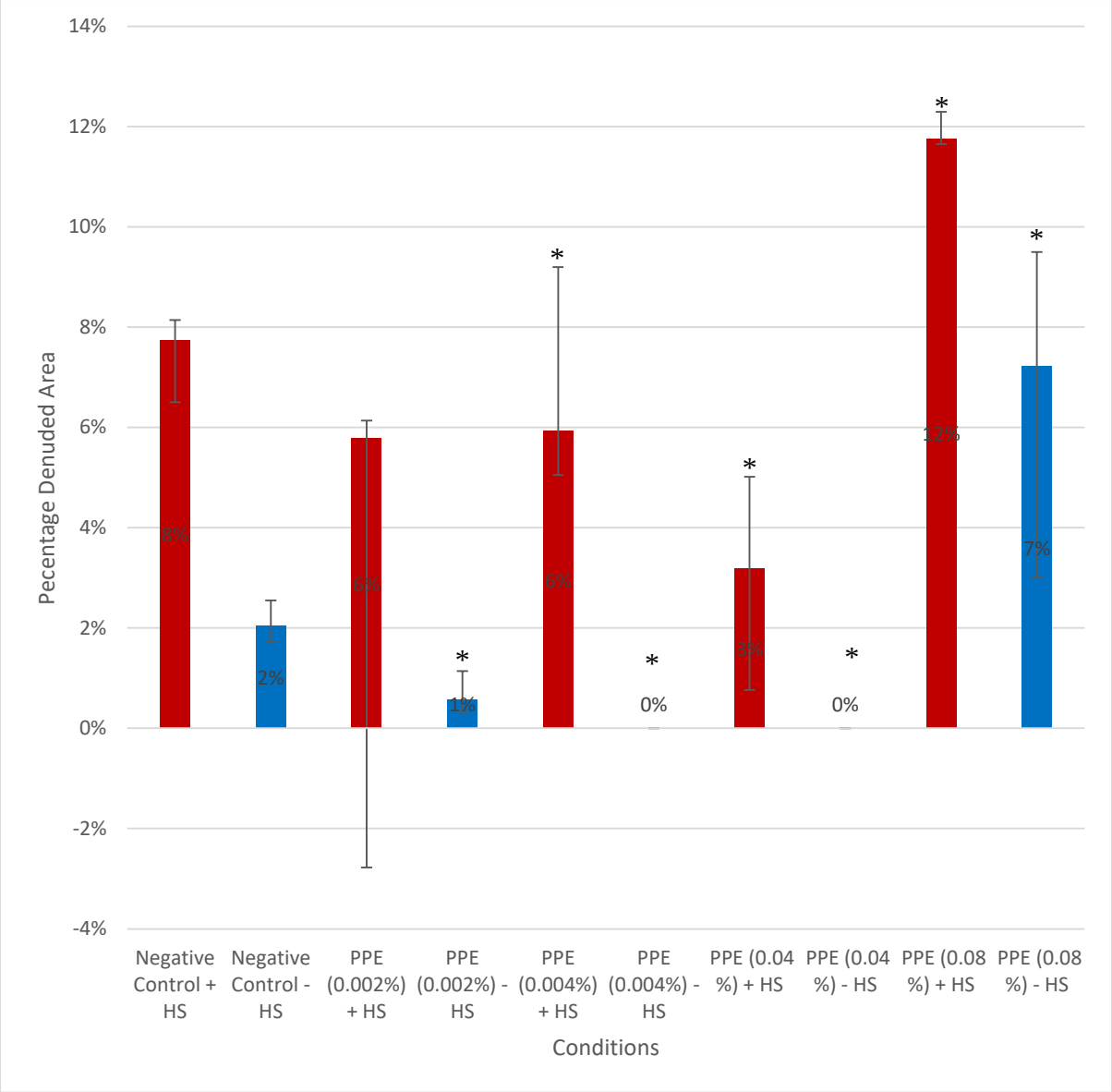

Figure 3.45: The scratch assay results with respect to percentage denuded area for the conditions being tested at 36 h.

The pHDFs were seeded at $2.5x10^4$ cells/well in 24 well plates which were incubated (37°C / 5 % CO_2) and were allowed to form a confluent monolayer (~ 1 day), which were exposed to test conditions and subsequently scratched to form a denuded area (0 h). The pHDFs were exposed to these conditions; Prickly pear extract (PPE) (0.002 %, 0.004 %, 0.04 % and 0.08 %) including a 1hr pre-treatment prior to either Heat Stress (HS) referred to as PPE + HS (44°C for 1 h) or lacking heat stress referred to as PPE - HS (37°C for 1 h), negative control + HS refers to pHDF exposed to heat stress (44°C for 1 h) without PPE, while negative control - HS refers to pHDF not exposed to heat stress (37°C for 1 h) without PPE. The observed percentage denuded area was then imaged microscopically at x40 magnification at regular time intervals (0 h, 12 h, 24 h, 36 h, and 48 h) and the images acquired were analyzed using Tscratch analysis software. The values shown are the median of 3 technical replicates repeated 3 times. Postitve/negative error was determined by difference of median to upper/lower quartiles. The KW was a comparison between the various conditions in relation to the appropriate negative control and any significant difference was apporopriately indicated p <0.05 */<0.01 **/<0.001 ***.

.

The interpretation of Figure 3.45 show a comparison between the Negative control and various concentrations of PPE (0.002, 0.004, 0.04 and 0.08 %) with Heat stress (+ HS 44°C for 1 h) as well as the Negative control and various concentrations of PPE (0.002, 0.004, 0.04 and 0.08 %) without heat stress (- HS 37°C for 1 h) at 36 h post exposure as expressed by the percentage denuded area.

- The PPE (0.002 %) condition with heat stress (+ HS 44°C for 1 h) at 36 h were seen to have no significant (KW p = >0.05) effect on viability and migration of pHDF when compared to the corresponding negative control with heat stress (+ HS 44°C for 1 h) in the same time frame. Furthermore, the PPE (0.004 and 0.04 %) conditions with heat stress (+ HS 44°C for 1 h) at 36 h were seen to have a significant (KW p = >0.05) effect on viability and migration of pHDF when compared to the corresponding negative control with heat stress (+ HS 44°C for 1 h) in the same time frame, to the tune of 2 % and 5 % respectively. Lastly, the PPE (0.08 %) conditions with heat stress (+ HS 44°C for 1 h) at 36 h were seen to have a significant (KW p = >0.05) effect on viability and migration of pHDF when compared to the corresponding negative control with heat stress (+ HS 44°C for 1 h) in the same time frame, to the tune of 4 %.
- The PPE (0.002, 0.004 and 0.04 %) without heat stress (- HS 37°C for 1 h) at 36 h was seen to have no significant (KW p = <0.05) effect on viability and migration of pHDF when compared to the negative control (- HS 37°C for 1 h) in the same time frame. Furthermore, PPE (0.08 %) was seen to have a significant (KW p = <0.05) effect on viability and migration of pHDF when compared to the negative control (- HS 37°C for 1 h) in the same time frame.

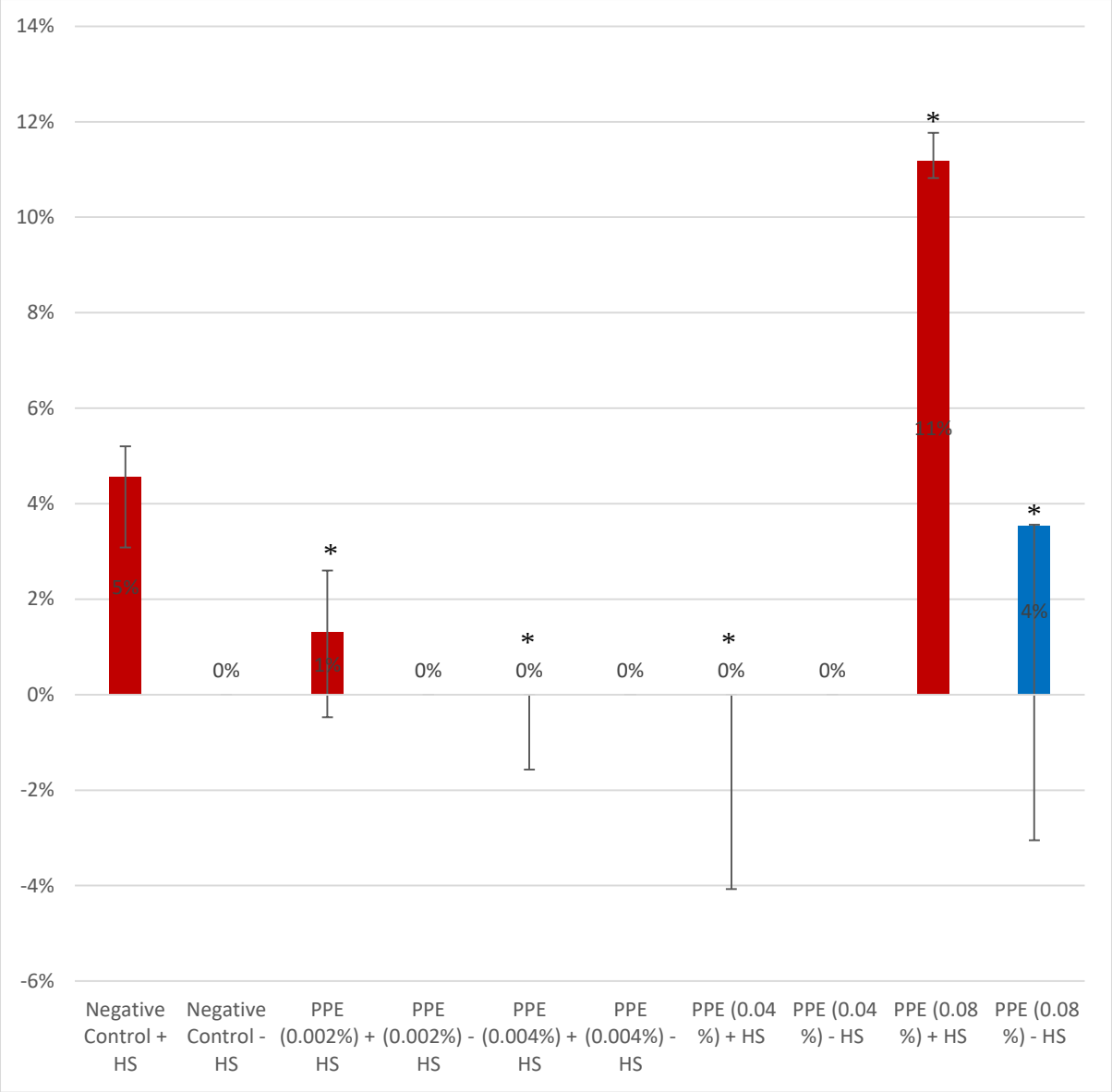

Figure 3.46: The scratch assay results with respect to percentage denuded area for the conditions being tested at 48 h.

The pHDFs were seeded at $2.5x10^4$ cells/well in 24 well plates which were incubated (37°C / 5 % CO_2) and were allowed to form a confluent monolayer (~ 1 day), which were exposed to test conditions and subsequently scratched to form a denuded area (0 h). The pHDFs were exposed to these conditions; Prickly pear extract (PPE) (0.002 %, 0.004 %, 0.04 % and 0.08 %) including a 1hr pre-treatment prior to either Heat Stress (HS) referred to as PPE + HS (44°C for 1 h) or lacking heat stress referred to as PPE - HS (37°C for 1 h), negative control + HS refers to pHDF exposed to heat stress (44°C for 1 h) without PPE, while negative control - HS refers to pHDF not exposed to heat stress (37°C for 1 h) without PPE. The observed percentage denuded area was then imaged microscopically at x40 magnification at regular time intervals (0 h, 12 h, 24 h, 36 h, and 48 h) and the images acquired were analyzed using Tscratch analysis software. The values shown are the median of 3 technical replicates repeated 3 times. Postitve/negative error was determined by difference of median to upper/lower quartiles. The KW was a comparison between the various conditions in relation to the appropriate negative control and any significant difference was apporopriately indicated $p < 0.05$ */<0.01 **/<0.001 ***.

The interpretation of Figure 3.46 show a comparison between the Negative control and various concentrations of PPE (0.002, 0.004, 0.04 and 0.08 %) with Heat stress (+ HS 44°C for 1 h) as well as the Negative control and various concentrations of PPE (0.002, 0.004, 0.04 and 0.08 %) without heat stress (- HS 37°C for 1 h) at 48 h post exposure as expressed by the percentage denuded area.

- The PPE (0.002, 0.004 and 0.04 %) conditions with heat stress (+ HS 44°C for 1 h) at 48 h were seen to have significant (KW p = >0.05) effect on viability and migration of pHDF when compared to the corresponding negative control with heat stress (+ HS 44°C for 1 h) in the same time frame, to the tune of 4, 5 and 5 % respectively. Lastly, the PPE (0.08 %) condition with heat stress (+ HS 44°C for 1 h) at 48 h were seen to have a significant (KW p = >0.05) effect on viability and migration of pHDF when compared to the corresponding negative control with heat stress (+ HS 44°C for 1 h) in the same time frame, to the tune of 6 %.
- The PPE (0.002, 0.004 and 0.04 %) without heat stress (- HS 37°C for 1 h) at 48 h was seen to have no significant (KW p = <0.05) effect on viability and migration of pHDF when compared to the negative control (- HS 37°C for 1 h) in the same time frame. Furthermore, PPE (0.08 %) was seen to have a significant (KW p = <0.05) effect on viability and migration of pHDF when compared to the negative control (- HS 37°C for 1 h) in the same time frame.

3.6. Chemical Assays

A number of experiments were carried in order to better understand the chemical composition of the PPE/PPEC and to discuss whether these molecules (e.g. phenols, flavonoids, ortho-diphenols) may contribute to the effect the PPE and PPEC exhibited on the pHDFs *in vitro.* All readings were carried out within the linear range of the assay carried out. These assays included; Folin-Ciocalteu assay (Section 3.9.1), Arnow`s assay (Section 3.9.2), Aluminium chloride assay (Section 3.9.3), Cupric Reducing Antioxidant Capacity (CUPRAC) assay (Section 3.9.4), DPPH (2,2-Diphenyl-1-picrylhydrazyl) Radical Scavenging Activity assay (Section 3.9.5), Ferric Reducing Antioxidant Power (FRAP) assay (Section 3.9.6) and the ABTS (2,20 -Azino-bis(3-ethylbenzothiazoline-6-sulfonic acid) assay (Section 3.9.7). The values for ABTS and DPPH were negligibly low and data is not shown for these results.

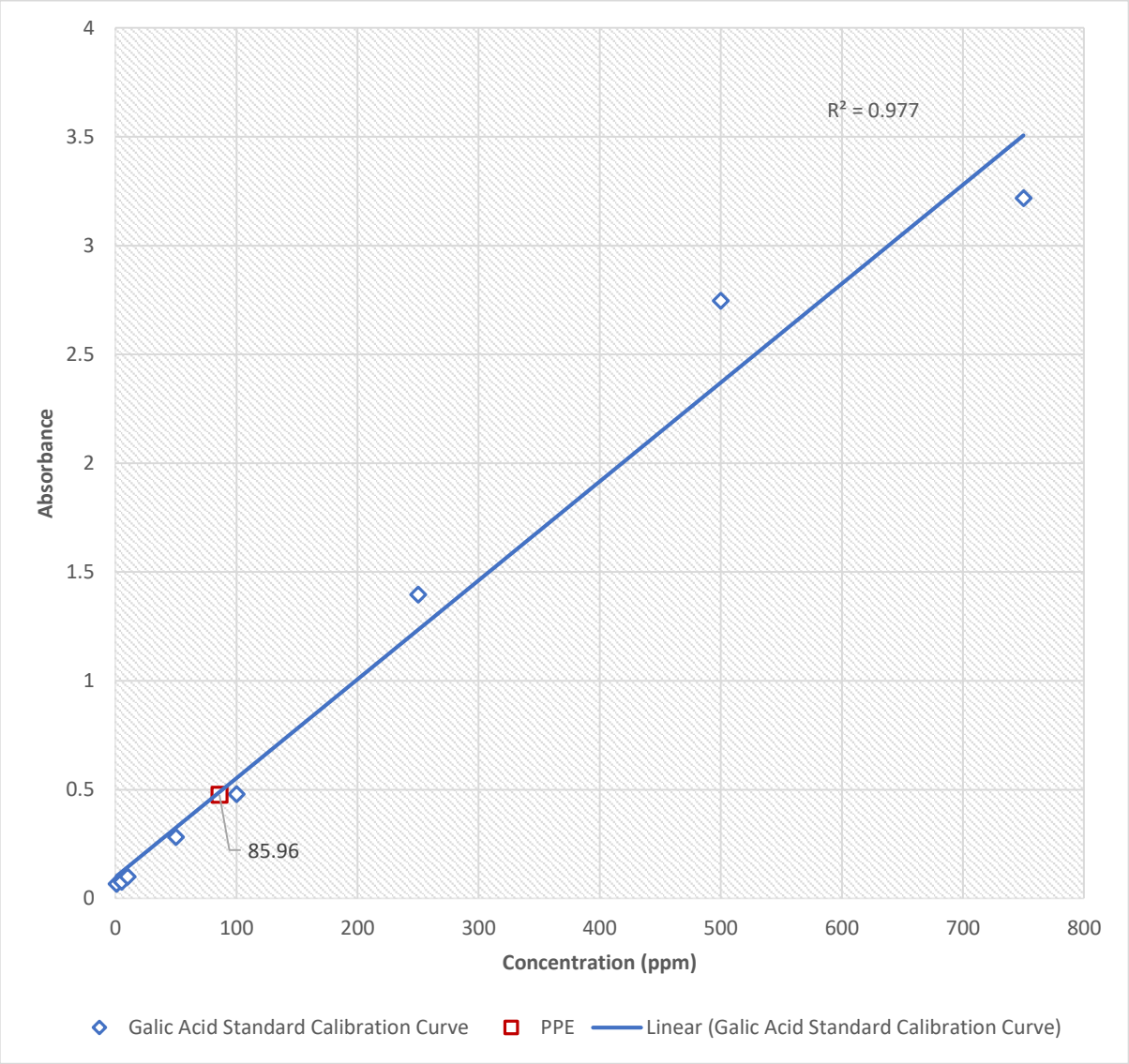

Figure 3.47: Folin-Ciocalteu Assay for total phenolic content of PPE normalised to PPEC.

The Folin-Ciocalteu assay was utilised for the estimation of total phenolic content of the PPE calculated against gallic acid standards which were utlized for the creation of standard curve normalised to PPEC. In a 96 well plate, 20 µl of gallic acid standard or PPE/PPEC sample was added followed by 80 µl of 5-fold diluted Folin-Ciocalteu reagent. This was followed by the addition of 80 µl of 7.5 % Na_2CO_3 which was homogenized and incubated at room temperature for 2 h in the dark. The absorbance was read at 630 nm. For each sample, all parameters were determined in technical triplicate.

From Figure 3.47 the value of total phenolic content for PPE normalised from PPEC extrapolated from the gallic acid standard curve is 85.96 ppm which when expressed in mg GAE / g (gallic acid equivalent) equates to 0.72 mg GAE / g.

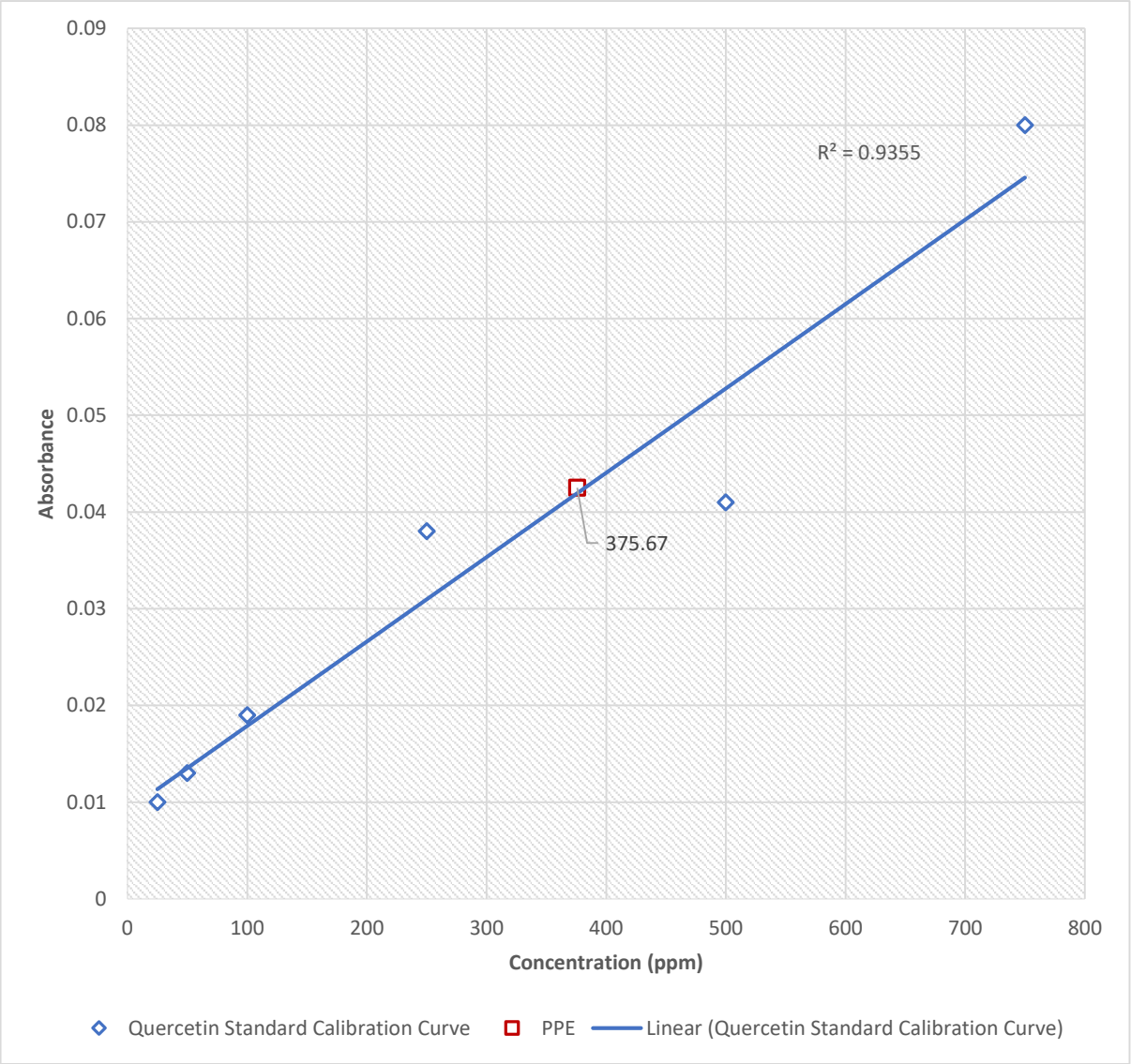

Figure 3.48: Aluminium Chloride Assay for total flavonoid content of PPE/PPEC.

The Aluminium Chloride assay was utilised for the estimation of total flavonoid content of the PPE/PPEC calculated against quercetin standards which were utilised for the creation of standard curve. In a 96 well plate, 25 µl standard or PPE/PPEC sample was pipetted followed by the addition of 10 µl of 10 % (w/v) aluminum chloride, 10 µl of a 7 % (w/v) sodium nitrite and 80 µl distilled water. The plate was taken to an orbital shaker and mixed for 5 minutes at 500 rpm, followed by incubation at room temperature for 30 minutes. Following this, 100 µl of 1M NaOH was added to each well and the absorbance was read at 415 nm. For each sample, all parameters were determined in technical triplicate.

From Figure 3.48 the value of total flavanoid content for PPE normalised from PPEC extrapolated from the quercetin standard curve is 375.67 ppm which when expressed in mg QE / g (Quercetin equivalent) equates to 3.9 mg QE / g.

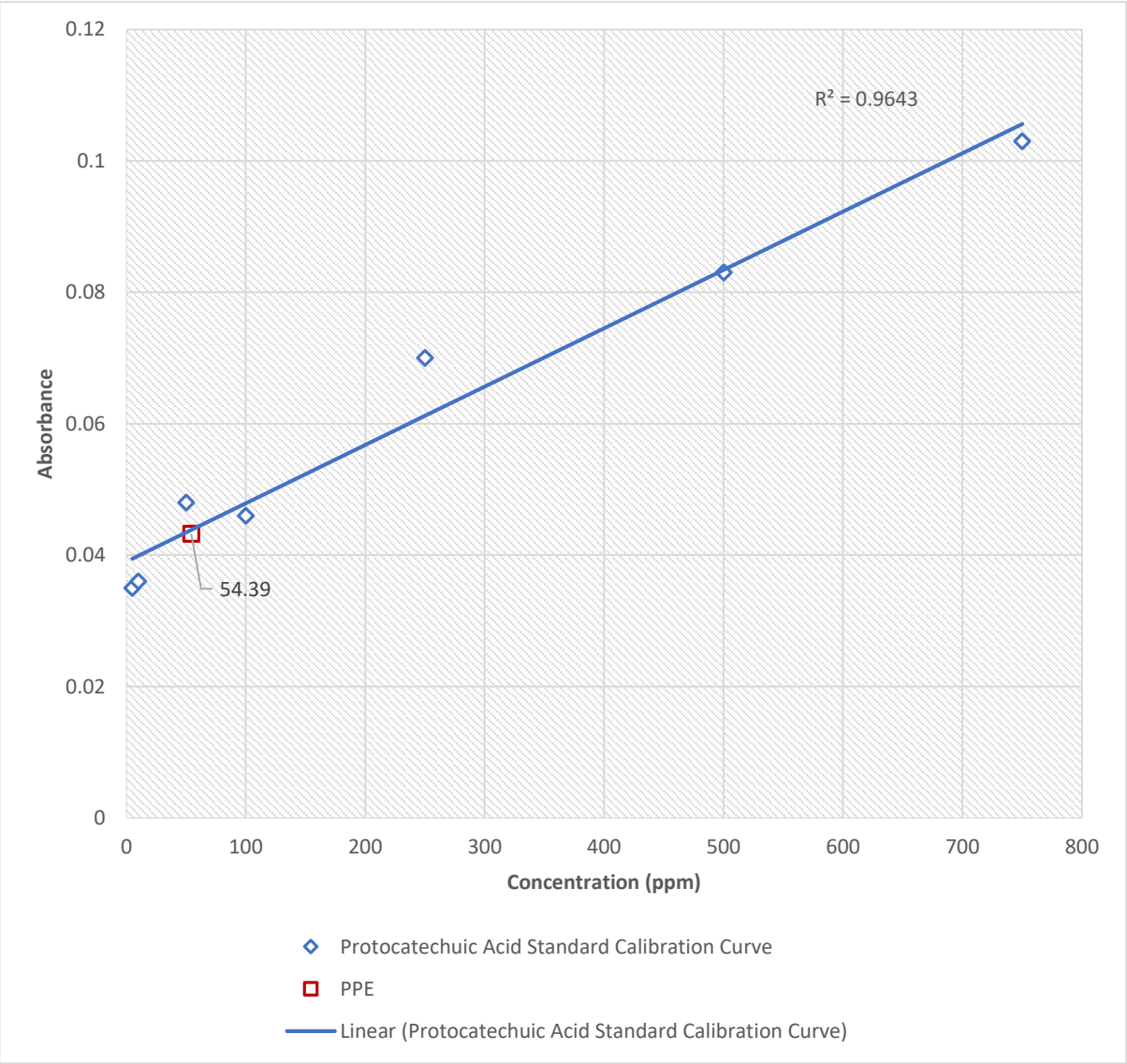

Figure 3.49: Arnow`s Assay for Ortho-Diphenolic content of PPE/PPEC

Arnow`s assay was utilised for the estimation of ortho-diphenolic content of the PPE/PPEC calculated against protocatechuic acid standards which were utilised for the creation of standard curve. In a 96 well plate, 20 µL of each protocatechuic acid standard or PPE/PPEC sample was pipetted followed by the addition of 20 µL 1M HCl and 20 µL of Arnow's reagent. The plate was shaken for 5 minutes at 500 rpm and then incubated at room temperature for 15 minutes. This was followed by the addition of 80 µL of deionised water and 40 µL of 1M NaOH. The absorbance was read at 405 nm. For each sample, all parameters were determined in technical triplicate.

From Figure 3.49 the value of total Ortho-Diphenolic content for PPE normalised from PPEC extrapolated from the protocatechuic acid standard curve is 54.39 ppm which when expressed in mg PE / g (protocatechuic acid equivalent) equates to 0.45 mg PE / g.

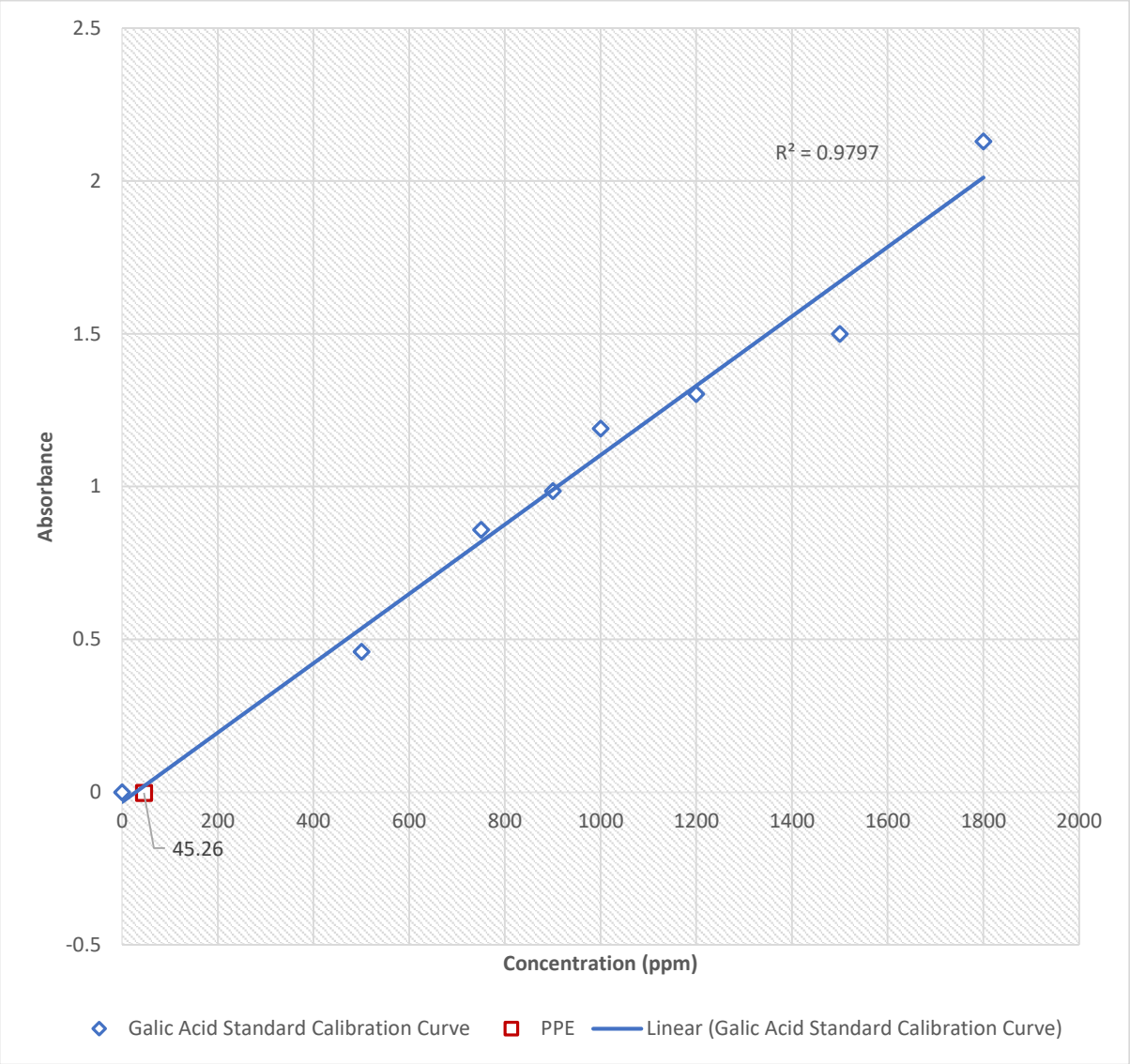

Figure 3.50: CUPRAC Assay for reducing capacity of PPE/PPEC

The CUPRAC assay was utilised for the estimation of reducing capacity of the PPE/PPEC calculated against gallic acid standards which were utilised for the creation of standard curve. The reducing capacity of PPE/PPEC was determined using the CUPRAC assay using gallic acid as a standard for calibration curve. In a 96 well plate, 20 µl of standard or PPE/PPEC sample was pipetted followed by 100 µl of 10 mM CuCl2 solution, followed by 100 µl of 1M ammonium acetate buffer at pH of 7.0. Subsequently, 100 µl of 7.5 mM neocuproine ethanolic solution was added and the reaction was allowed to proceed for 30 minutes following which the absorbance at 405 nm. For each sample, all parameters were determined in technical triplicate

From Figure 3.50 the value of total CUPRAC assay for PPE normalised from PPEC extrapolated from the protocatechuic acid standard curve is 45.2 which when expressed in mg PE / g (gallic acid equivalent) equates to 0.37 mg GAE / g.

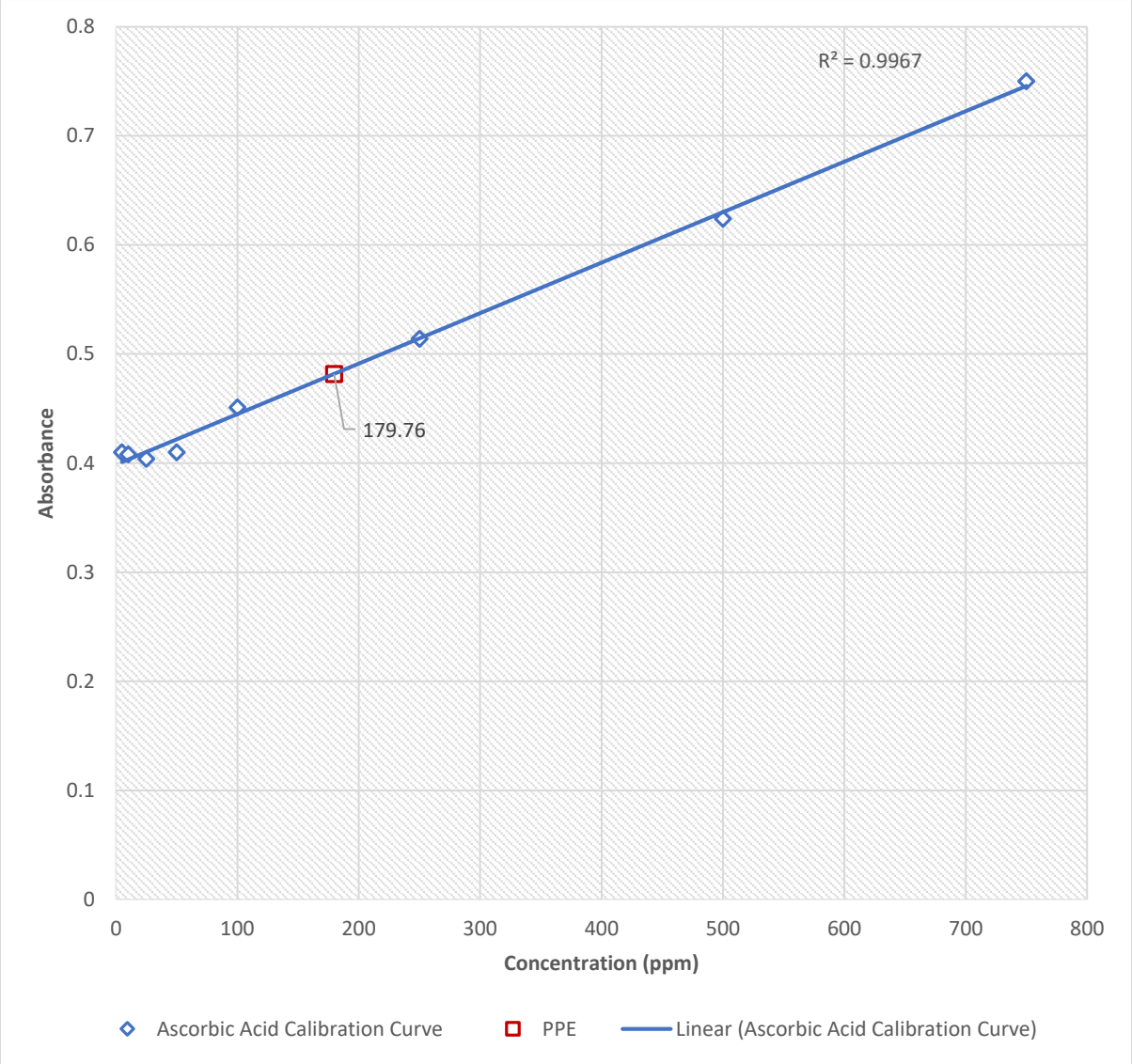

Figure 3.51: FRAP Assay for reducing capacity activity of PPE/PPEC.

The FRAP assay was utilised for the determination of ferric reducing antioxidant power (FRAP) of PPE/PPEC determined against using an ascorbic acid standard calibration curve. In a 96 well plate, 10 µL of standard or PPE/PPEC was mixed with 200 µL of FRAP reagent, and the contents were mixed vigorously, following which the absorbance was read at 630 nm. For each sample, all parameters were determined in technical triplicate.

From Figure 3.51 the value of total FRAP assay for PPE normalised from PPEC extrapolated from the ascorbic acid standard curve is 179.76 which when expressed in mg PE / g (ascorbic acid equivalent) equates to 0.75 mg AAE / g.

3.7. RNA Extraction

RNA was extracted as demonstrated in Section 2.10.1. All samples description with codes are seen in Table 3.2 and Table 3.3 met the stringent requirements for RNA-Seq analysis by Genewiz™ as seen in Section 2.10.4. Prior to RNA-seq analysis, the extracted RNA samples are evaluated for sequence quality and the reads trimmed and then mapped to the genome as discussed in Section 2.10.4. Hit counts for individual genes are generated and a raw counts table is produced. The overall sequencing statistics provided by Azenta show a total of 434,307,956 reads and a mean quality score of 35.19 and 89.87 % of bases with a quality score of 30 or above. Data of high quality is usually required to have a minimum of 80% of bases with a quality score of 30 or higher.

Table 3.2: The samples codes and a brief description of each condition analysed for unstressed nHDFs

Sample Code	Sample Description
C1/2	nHDF cells
E1/2	nHDF treated (1 h) with PPE (0.04 %)
V1/2	nHDF treated (1 h) with PPEC (0.04 %)

Table 3.3: The samples codes and a brief description of each condition analysed for stressed nHDFs

Sample Code	Sample Description
HE1/2	nHDF treated (1 h) with PPE (0.04 %) then exposed to heat stress 44°C (1 h)
HV1/2	nHDF treated (1 h) with PPEC (0.04 %) then exposed to heat stress 44°C (1 h)
O1/2	nHDF exposed to oxidative stress (6.25 µM) for 2hrs
OE1/2	nHDF treated (1hr) with PPE (0.04%) then exposed to oxidative stress (6.25 µM) for 2hrs
OV1/2	nHDF treated (1hr) with PPEC (0.04%) then exposed to oxidative stress (6.25 µM) for 2hrs

3.8. RNA-seq analysis through iDEP

RNA-seq analysis is a process that involves a multi-step workflow which culminates in the identification of differentially expressed genes (DEGs) and the inferring of biological meaning to the findings (Corchete et al., 2020). The iDEP96 (integrated differential expression and pathway analysis) web app was chosen for its user-friendly yet in-depth approach to RNA-seq analysis. The raw counts table containing the processed raw read data for each condition being investigated is uploaded to iDEP to start the process of analysis. The raw counts table contains the raw reads for each gene per sample. Two replicates were used for each condition being investigated. Once the reads counts tables are uploaded to iDEP, analysis of the data can begin using the variety of tools available in the web app. The uploaded data is processed automatically by the iDEP program, with the raw read data being changed to transformed data by converting any gene IDs into gene names as well as applying a filter of 0.5 million counts per million (CMP) for each gene. The CMPs are calculated by iDEP through a process of normalization of the read counts uploaded by the total counts per sample. Genes which were expressed in low levels were filtered out. The two replicates for each condition are combined automatically by the iDEP program by averaging both readings to obtain a single expression value (Ge et al., 2018; Ge, 2021; Koch et al., 2018).

Using the DESeq2 package integrated in iDEP, the upregulated and downregulated genes for each comparison were identified. An FDR (false discovery rate) of <0.05 was used to ensure statistical significance and a fold-change of >2 was applied. The top up and down regulated DEGs were then investigated to start identifying links between DEGs. The genes can be visualized in a gene plot, with the expression of each gene in CPM for each condition. The DEGs were then subjected to enrichment analysis according to biological process (gene-accomplished biological objectives), cellular component (location of gene activation in the cell) and molecular function (biological activation on gene products) (Ashburner et al., 2000). This helped identify the top differentially expressed genes and pathways by summarizing the extensive list of genes into shorter lists related to specific pathways (Reimand et al., 2019). Gene functions were searched on the GeneCards database to further investigate their functions (Stelzer et al., 2016).

The different fold-changes of genes were visualized on their respective KEGG pathways, a feature integrated into iDEP (Kanehisa et al., 2020a; Luo & Brouwer, 2013a). KEGG mapping

helps identify and understand the effect of up and downregulated genes on a cellular level as well as an organism level by looking at a visual representation of the gene pathways.

DESeq2 is the method adopted by iDEP to identify DEGs (Ge et al., 2018; Ge, 2021). The Benjamin and Hochberg approach is the method applied by the program to ensure that the p-values (attained by the Wald test automatically) are corrected by multiple testing. Significant genes can be identified using adjusted p values. By having a false discovery rate (FDR) cut off < 0.05, a limit is set for the percentage of anticipated false positives to be 5%. Therefore, the lower the FDR/adjusted p-value past the cutoff point of 0.05, the more statistically significant they are and the less likely it is the occurrence of false positives (Benjamini & Hochberg, 1995).

iDEP presents DEGs according to their log2fold. This shows the fold change between two sets of groups in terms of gene expression. Fold change is a measure that expresses how the level of a gene's expression has changed when one set of experiments is compared to another. It is calculated automatically by iDEP by taking the ratio of the two conditions in terms of gene expression. It gives insight not only to the magnitude of the change but also shows whether each gene has been up or downregulated. In this study, genes were often sorted by their log2fold to visualise the top DEGs in each comparison. The list of DEGs for each comparison can be compared using the Venn diagram feature integrated in iDEP, providing a visual representation of the up and downregulated genes which are in common between comparisons, those which are not and those that are only expressed in cells subjected to a particular condition. Heat maps can also be used to visualise a set number of variable genes and observe expression trends across different conditions. The use of volcano plots is also useful as a visual representation, with DEGs having an FDR of <0.05 and a log2fold of 1 being selected and shown on the graph. Red and green signify upregulated and downregulated genes respectively, the warmer the colour the greater the differential expression (Koch et al., 2018).

Figure 3.52 shows a bar graph and box plot. The bar graph (A) shows the total number of read counts for each sample. Samples with a higher number of read counts can generally provide a clearer picture of gene expression. A comparable number of read counts between replicates is observed. This ensures that averaging of replicates is valid. The normalized box plot (B) shows uniform read count distribution range and highly similar expression values across samples. Figure 3.53 shows a density plot and gives insight into the gene expression patterns of the different conditions. Two distinct peaks are notably observed, indicating bimodality in gene expression. This could indicate important biological phenomena such as responses to various

stimuli or distinct pathways which are activated within the experimental conditions. Similarity is to be expected in the distribution amongst samples observed in the density plot and boxplot (Ge, 2021).

A. B.

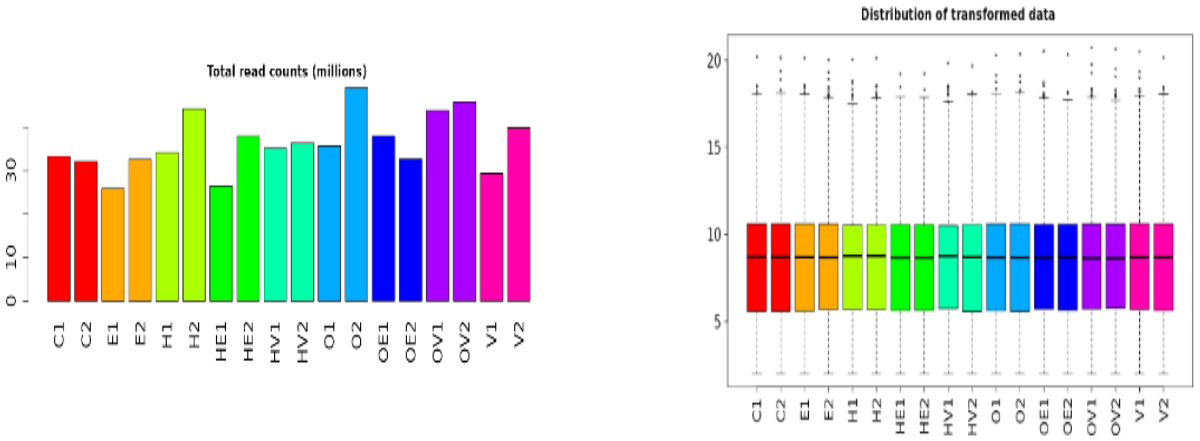

Figure 3.52: Pre-process visual data. **A.** Bar graph showing total read counts for each sample. **B.** Boxplot visualising and comparing distribution of transformed data for each sample.

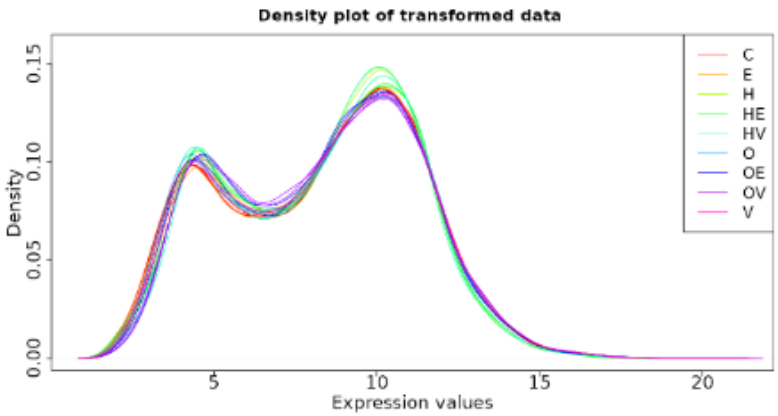

Figure 3.53: Pre-process visual data showing a density plot comparing the count distribution of transformed data for all samples

The heat map in Figure 3.54 comparing the different conditions shows the range of gene expression amongst the various samples. This illustrates the differences due to the different conditions the HDFs were subjected to. An example of this is the highlighted upregulation in the HSPA7 and HSPA6 genes in the samples subjected to heat stress, as well as the upregulation of IL33 in the samples subjected to oxidative stress

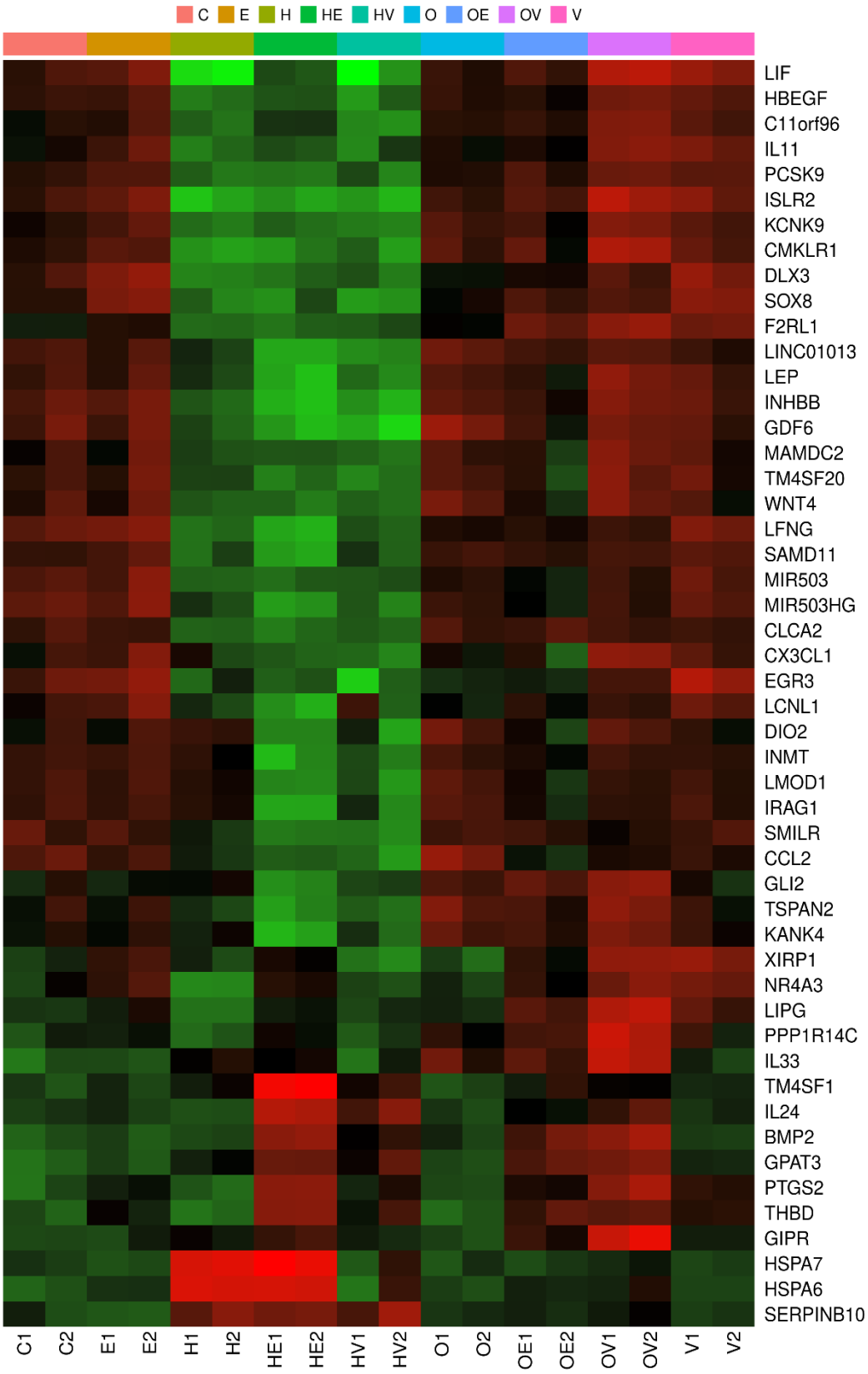

Figure 3.54: Heat map showing hierarchical clustering of top 50 gene showing gene expression patterns across all conditions. Green represents downregulated genes while red represents upregulated genes. The warmer the colour the greater the differential expression.

Scatter plots were generated using iDEP (Ge et al., 2018) to visualise and compare gene expression between both replicates for two conditions (Figure 3.55 – 3.56). Clustering around a diagonal line indicated similarity in the expression of genes between the two conditions and is expected to be observed in scatter plots between two replicates, indicating the similarity and correlation of the two (Koch et al., 2018). A substantial amount of outliers can be observed in the comparison HE-H and to a lesser extent, OE-O. This is suggestive that the of the effects of the PPE on HDFs subjected to heat shock and oxidative stress being picked up by RNA-seq. The outliers observed in the comparisons HE-HV and OE-OV further highlight the effect of the PPE irrespective of the PG it is mixed with.

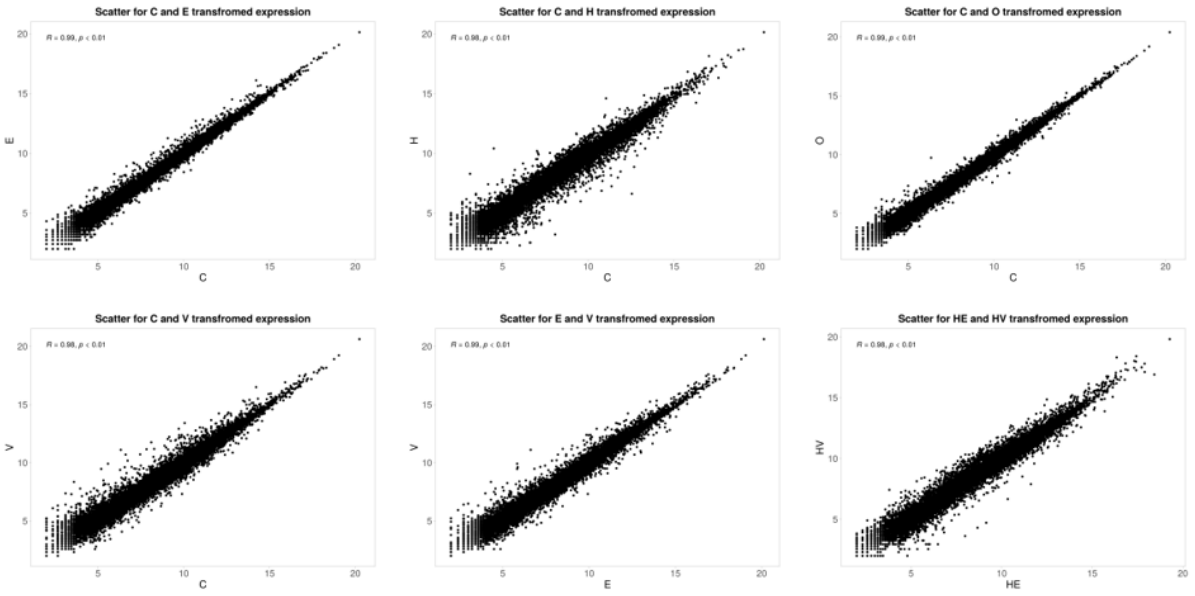

Figure 3.55: Scatter plots showing gene expression changes between different conditions. Clustering around the diagonal line indicates similarity in expression, outliers indicate differentially expressed genes.

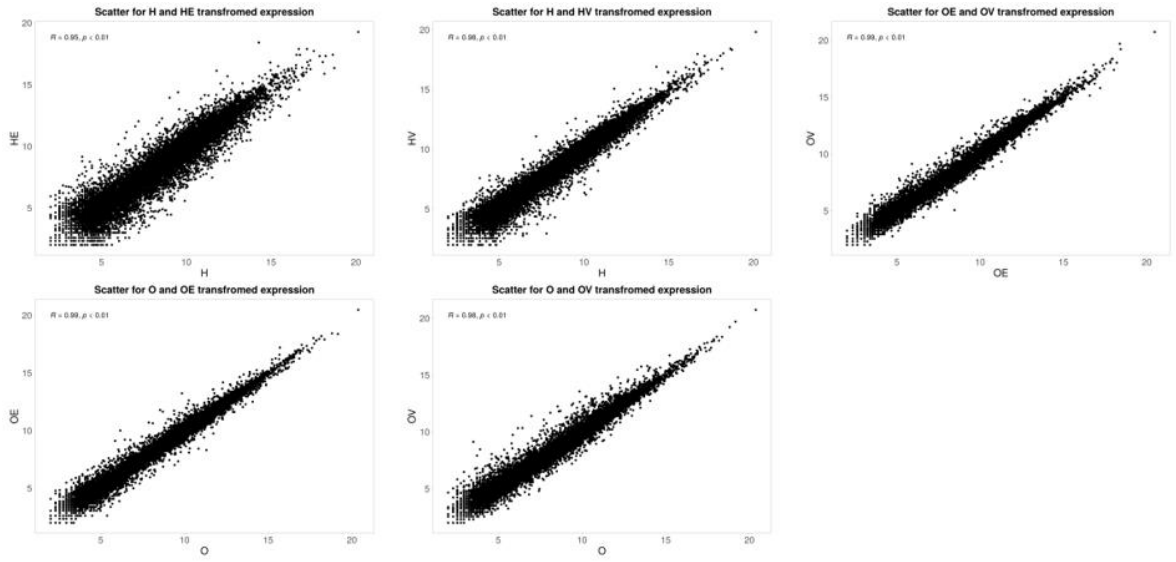

Figure 3.56: Scatter plots showing gene expression changes between different conditions. Clustering around the diagonal line indicates similarity in expression, outliers indicate differentially expressed genes.

3.8.1. RNA-seq analysis on the effect of prickly pear extract / carrier on fibroblasts

The comparison E-V shows 35 downregulated genes and only 2 upregulated genes as seen in Figure 3.57. The Venn diagrams in Figure 3.58 show that the comparisons E-C and V-C share 313 upregulated genes in common. The extract has an effect on 31 genes that are not influenced by the carrier compared to the untreated cells. The comparisons E-C and V-C share 153 downregulated genes in common. There are only 33 significant downregulated genes in E-V. Compared to the control the presence of the extract causes a downregulation of 144 that are different from the genes influenced by the carrier. This shows that the major effect of treatment with PPE on unstressed cells is due to the effect of the vehicle. The expression of genes in the untreated control cells was compared with the expression of genes in the PPE and PPEC treated cells respectively. Both PPE and PPEC had an effect on the cells with the effect of PPEC being more pronounced. Figure 3.59 highlights the top 50 genes whose expression differed between the control and the HDFs treated with PPE or with PG. Although gene expression in HDFs treated with PPE or PG was different than that of the control HDFs, minimal differential gene expression can be observed between the samples treated with PPE and those treated with PG only.

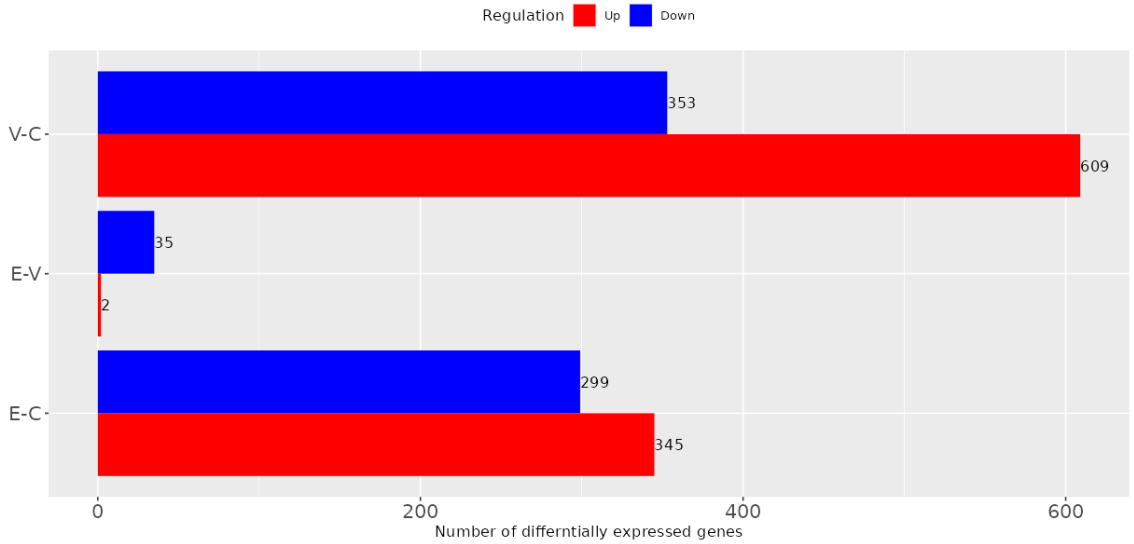

Figure 3.57: A bar graph showing the number of DEGs per comparison, using DESeq2 integrated in iDEP(Ge et al., 2018). A visual overview of the effect of treatment with PPE and PPEC can be seen.

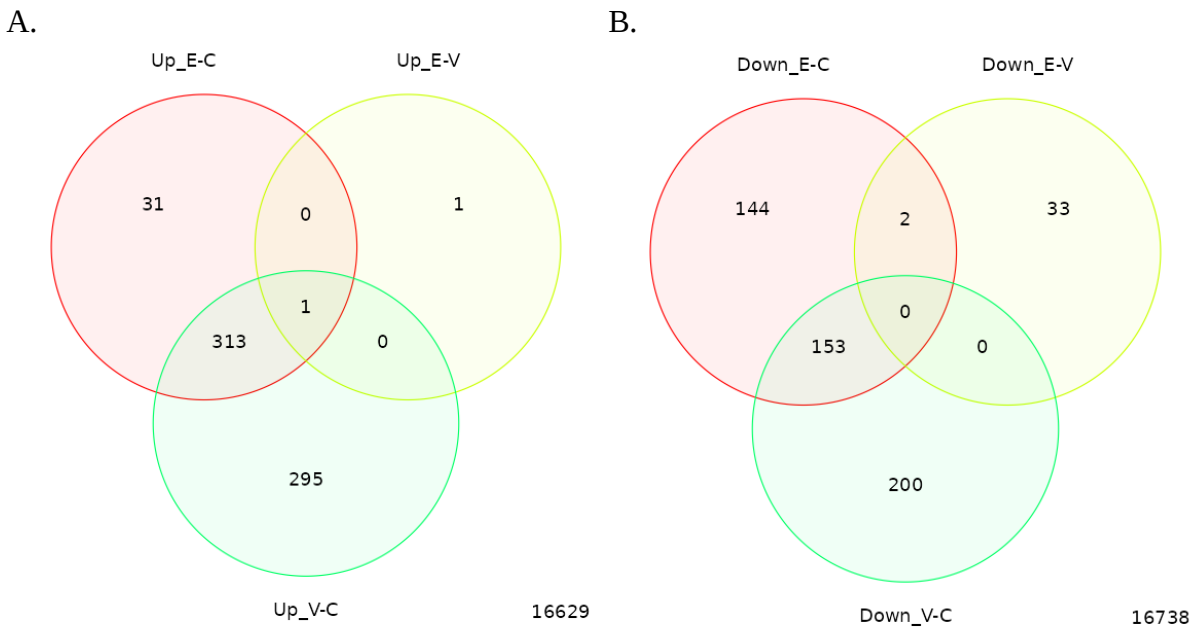

Figure 3.58: Venn diagram showing the upregulated (**A**) and downregulated (**B**) DEGs in common between the comparisons E-C, V-C and E-V.

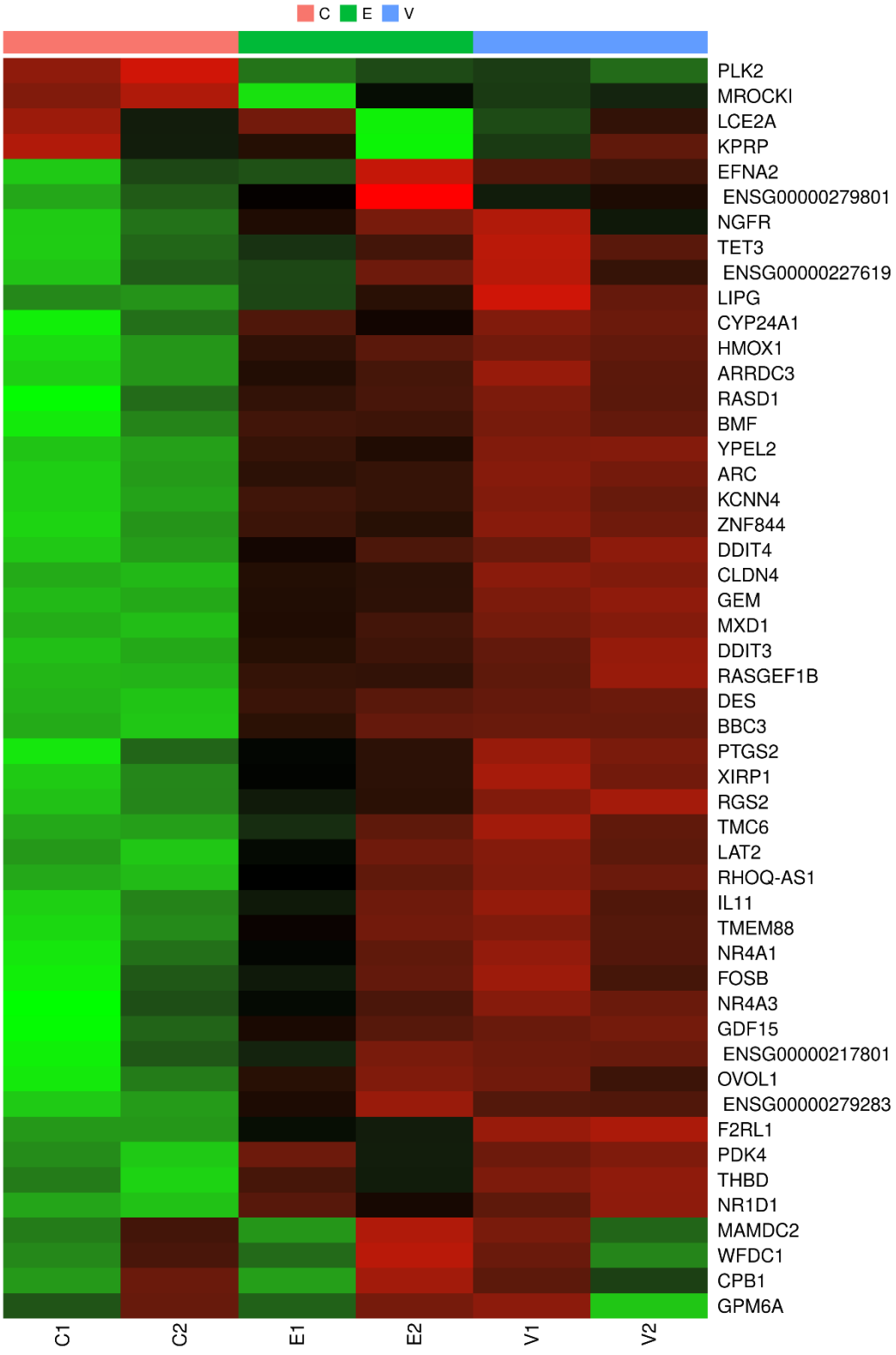

Figure 3.59: Heat map showing hierarchical clustering of top 50 gene showing gene expression patterns across the samples for control, extract and vehicle. Green represents downregulated genes while red represents upregulated genes. The warmer the colour the greater the differential expression.

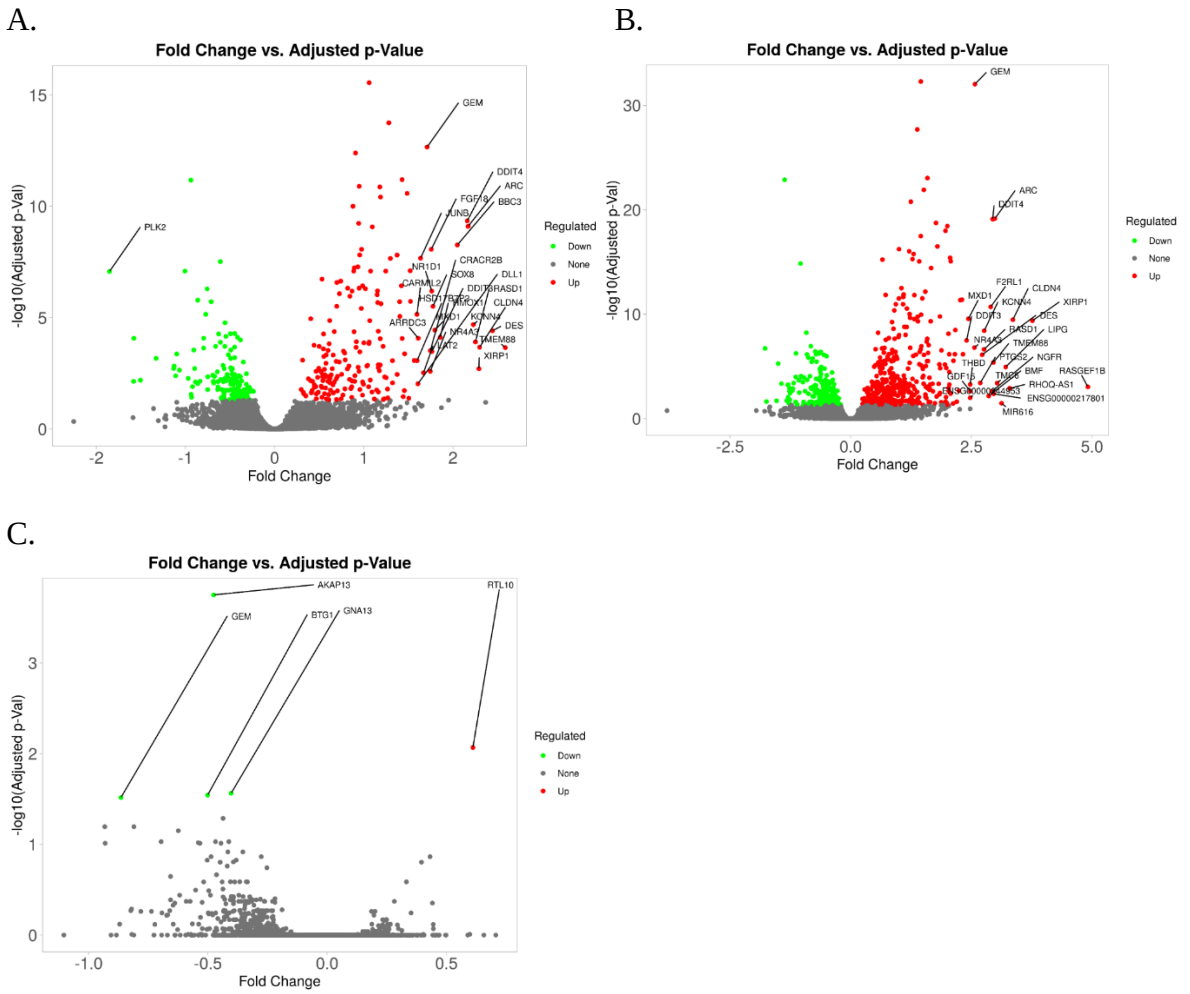

Figure 3.60: A volcano plot of the DEGs for the comparison E-C (**A**), V-C (**B**) and E-V (**C**). The top 25 genes according to log2fold values have been labelled.

The volcano plots in Figure 3.60 show the top 25 genes labelled according to the log2fold value. Due to the presence of only 2 upregulated genes having an adj.Pval of less than 0.05, these genes are labelled even though they have a log2fold of less than 1. Overall the PPE does not seem to have any outward effect on unstressed HDFs, with the majority of DEGs observed in the comparison E-C also being expressed in V-C as exemplified in the comparison E-V as seen in Figure 3.58. The upregulated and downregulated genes seem to be largely due to the effect of the PPEC in which the extract is dissolved.

3.8.2. Effect of heat stress on human dermal fibroblasts

The following section is related to the RNA-seq work carried out to elucidate the effects of heat stress on human dermal fibroblasts. Figure 3.61 gives a visual overview of the difference in gene expression between heat treated samples and the control. Upregulation of HSPA7 and HSPA6 can be clearly observed in heat-treated samples, illustrating the classic heat shock response. These top up and downregulated genes are also illustrated in the volcano plot in Figure 3.62. These two figures show the top genes according to log2fold values. Genes of note are then further investigated and discussed. Figure 3.63 shows the upregulation of various pro-inflammatory cytokines in the heat-stressed HDFs. This follows the classic heat-shock response with the cytokines serving as signals to immune system. The upregulation of various lncRNAs as seen in Table 3.7 are another indication of a classic heat-shock response. These genes are in integral component of this stress response and have been found to be on the front line by regulating the genes directly related to the heat stress response.

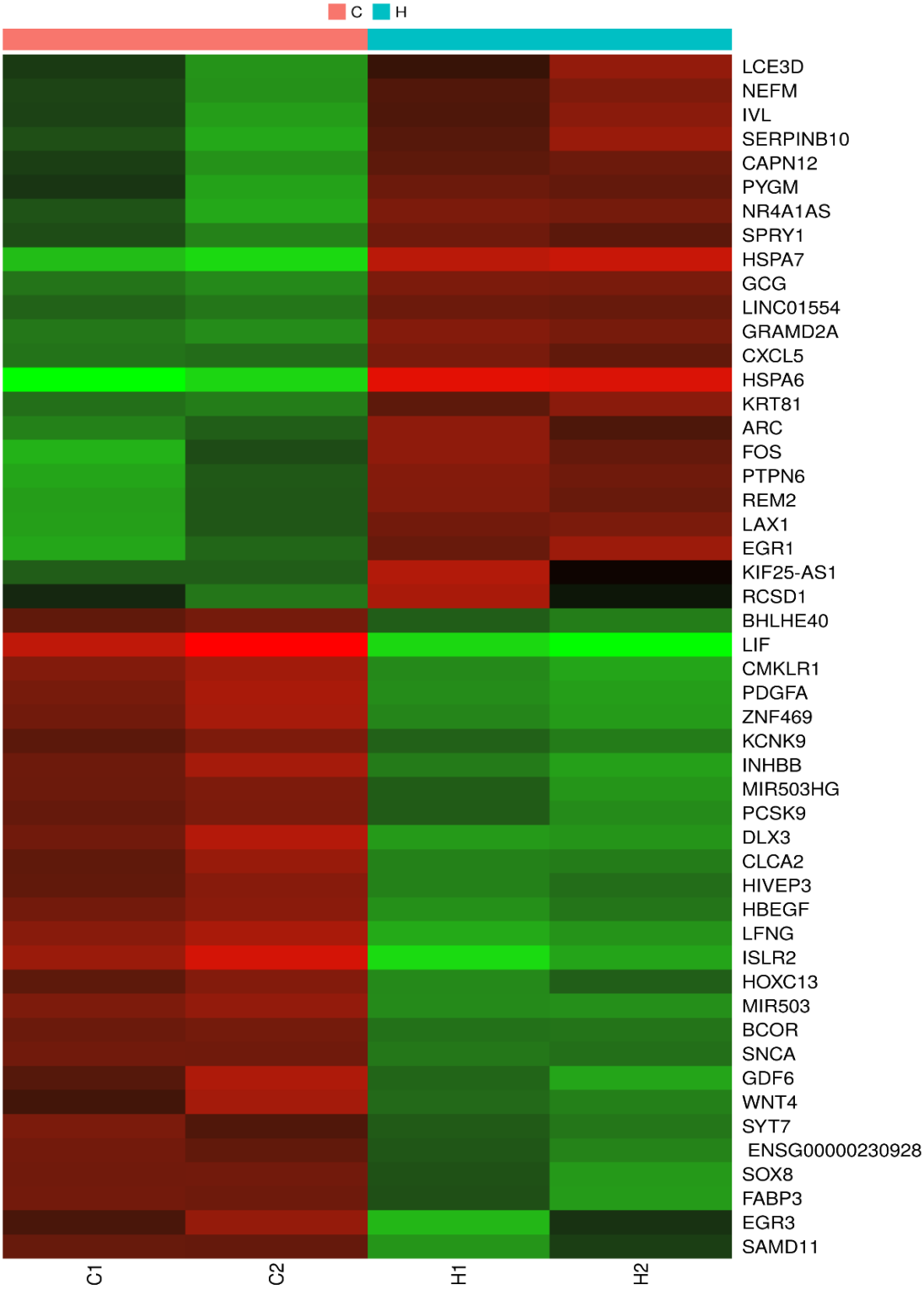

Figure 3.61: Heat map showing hierarchical clustering of top 50 gene showing gene expression patterns across the samples for control and samples subjected to heat stress. Green represents downregulated genes while red represents upregulated genes. The heatmap shows a clear distinction in the expression of genes amongst untreated cells and heat stressed cells.

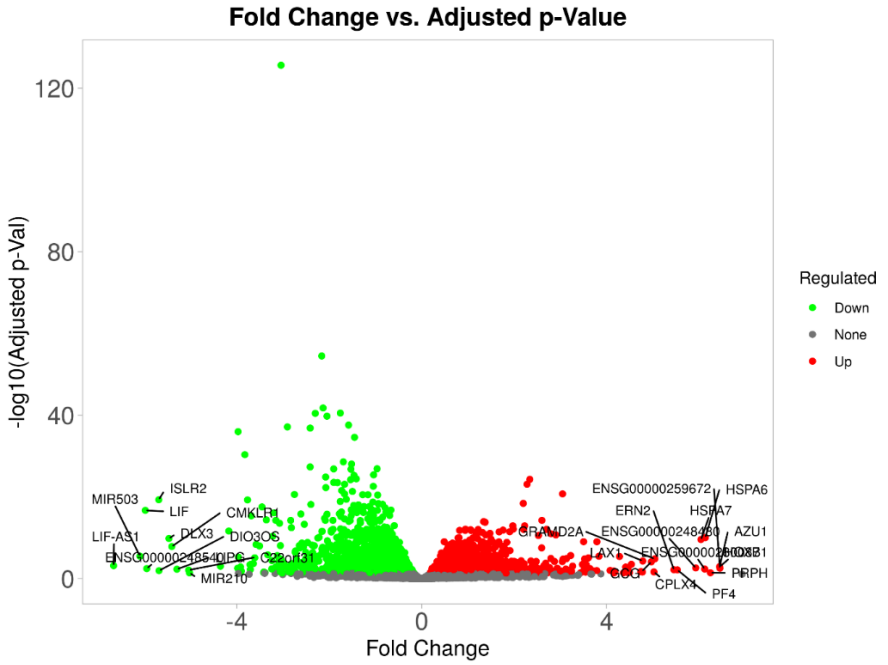

Figure 3.62: A volcano plot of the DEGs for the comparison H-C. The top 25 genes according to log2fold values have been labelled.

Table 3.4: Up and downregulated pathways of note in the comparison H-C. Enrichment analysis for the DEGs in the comparison H-C was conducted using the iDEP96 platform and top enriched pathways for GO biological process, GO cellular component and GO molecular function were analysed and identified (Ge et al., 2018).

Direction	Adj.Pval	nGenes	Pathways
Down regulated	5.4e-32	319	Biological adhesion
	7.5e-32	317	Cell adhesion
	2.5e-16	123	Extracellular matrix
Up regulated	1.6e-35	176	DNA repair

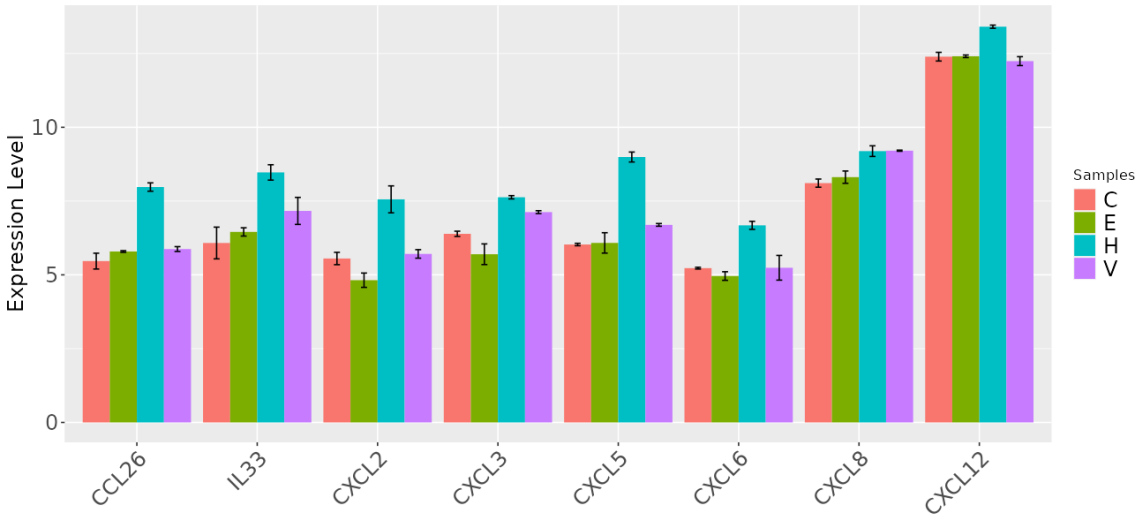

log2 Fold Change	Adj.Pval	Gene
2.599377694	4.21E-22	*CCL26*
2.370343868	0.007319792	*IL33*
2.141610524	1.07E-06	*CXCL2*
1.264214492	0.090093681	*CXCL3*
3.038860998	3.78E-17	*CXCL5*
1.546269627	0.002294048	*CXCL6*
1.085571924	0.312685279	*CXCL8*
0.996945183	1.01E-05	*CXCL12*

Figure 3.63: Gene bar graph showing the upregulation of various cytokines in HDFs exposed to heat stress. The relavant statsitcal data is representing the difference between H-C.

Table 3.5: Top 10 DEGs involved in the upregulated DNA repair pathway in the comparison H-C

log2 Fold Change	Adj.Pval	Gene	Function
1.910702	3.80E-11	*EME1*	Endonuclease crucial to DNA damage repair and maintaining of genomic stability
1.82379	5.23E-09	*NEIL3*	DNA glycosylase which initiates the first base excision repair step and is an important mediator in the cross-link repair
1.802246	7.91E-05	*HELB*	Helicase necessary for DNA unwinding in the DNA damage response repair process
1.740313	2.83E-02	*EYA2*	Protein which is an important promotor for efficient DNA repair
1.561423	4.94E-11	*BRCA2*	Involved in maintaining genomic stability through DNA double-strand repair homologous recombination pathway
1.461584	1.87E-03	*HMGB2*	Protein which can bend DNA and is part of the final steps of ligation in DNA double-strand break repair
1.441719	2.52E-06	*FANCB*	DNA repair protein which takes part in the repair of DNA lesions
1.438608	3.01E-10	*FANCD2*	Required during DNA double-strand break repair together with FANCB protein
1.411927	8.16E-07	*ESCO2*	Protein which is involved in double-strand break repair and the maintaining of genomic stability
1.382483	4.59E-14	*NABP1*	Single-stranded DNA binding protein crucial to the DNA damage response repair process

When the HDFs were exposed to heat stress, one of the top upregulated genes was *HSPA6* – a member of the HSP70 protein family. Expression of other members of this family as well as *DNAJA4* (a member of HSP40 family) can be seen in Table 3.6 and Figure 3.64.

Table 3.6: Genes coding for members of the HSP70 and HSP40 protein family. Expression of these genes when HDFs are exposed to heat shock.

log2Fold Change	Adj.Pval	Gene
6.145305	3.48E-93	*HSPA6*
6.04084	1.89E-24	*HSPA7*
2.281755	2.84E-62	*HSPA1B*
1.762805	1.57E-41	*HSPA1A*
1.679635	1.22E-12	*DNAJA4*

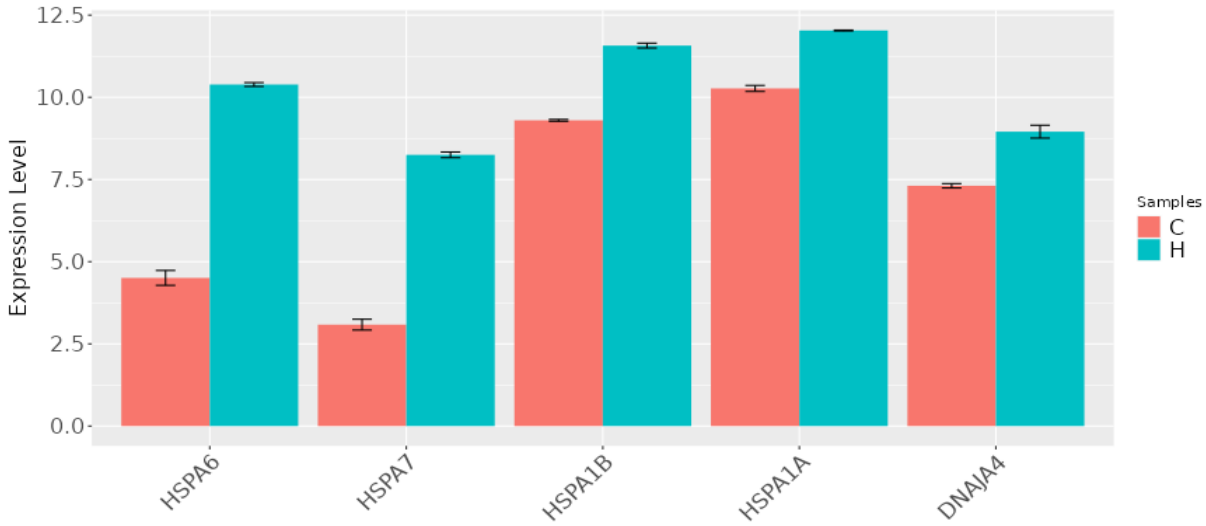

Figure 3.64: Expression of genes belonging to the HSP70 and HSP40 protein family in the control and HDFs exposed to heat shock. The increase in HSP expression indicated that the heat treatment was effective.

Table 3.7: Top 10 highest lncRNAs according to log2 fold change upregulated in the comparison H-C.

log2 Fold Change	Adj.Pval	Gene
6.938704	4.77E-02	*KIF25-AS1*
4.530429	6.86E-06	*NR4A1AS*
4.459732	1.33E-04	*LINC01554*
3.636454	8.62E-03	*LINC01168*
3.432146	2.45E-03	*LINC00691*
3.249439	2.95E-02	*A2M-AS1*
2.935074	1.87E-03	*LINC00707*
2.881777	1.70E-02	*LINC02551*
2.589883	1.95E-05	*SLC8A1-AS1*
2.497771	2.32E-02	*LINC01936*

3.8.3. Effect of PPE / PPEC on fibroblasts subjected to heat stress

The following section is related to the RNA-seq work carried out to elucidate the effects of heat stress on human dermal fibroblasts when subjected to PPE or PPEC treatments.

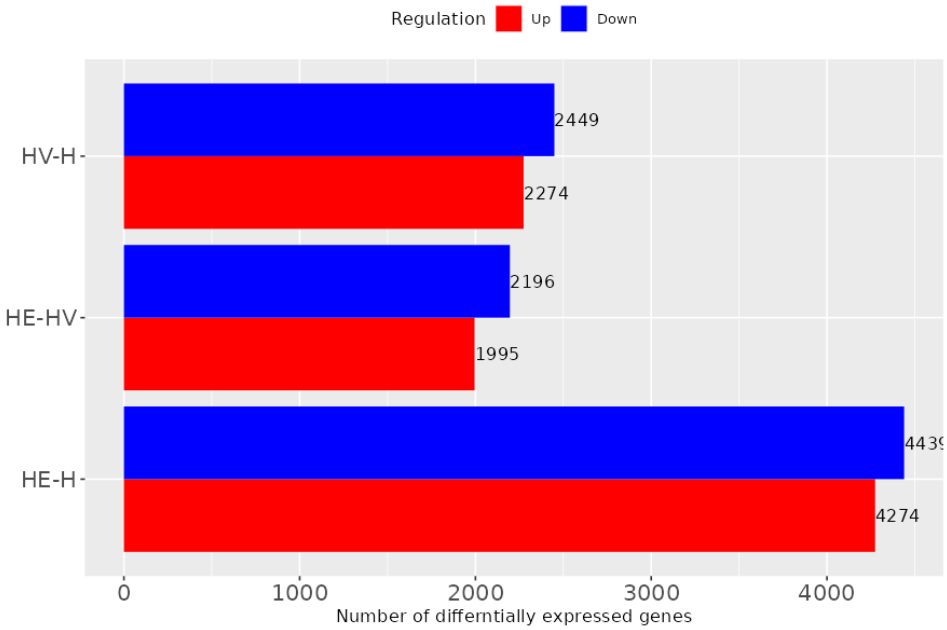

Figure 3.65: A bar graph showing the number of DEGs per comparison, using DESeq2 integrated in iDEP (Ge et al., 2018). A visual overview of the effect of treatment with PPE prior to heat shock can be seen.

The comparison HE-HV shows 2196 downregulated genes and 1995 upregulated genes. Although treatment with the vehicle has also induced increase expression of genes, it can be seen that PPE treatment had a more pronounced effect on the expression of genes than the vehicle under the same conditions.

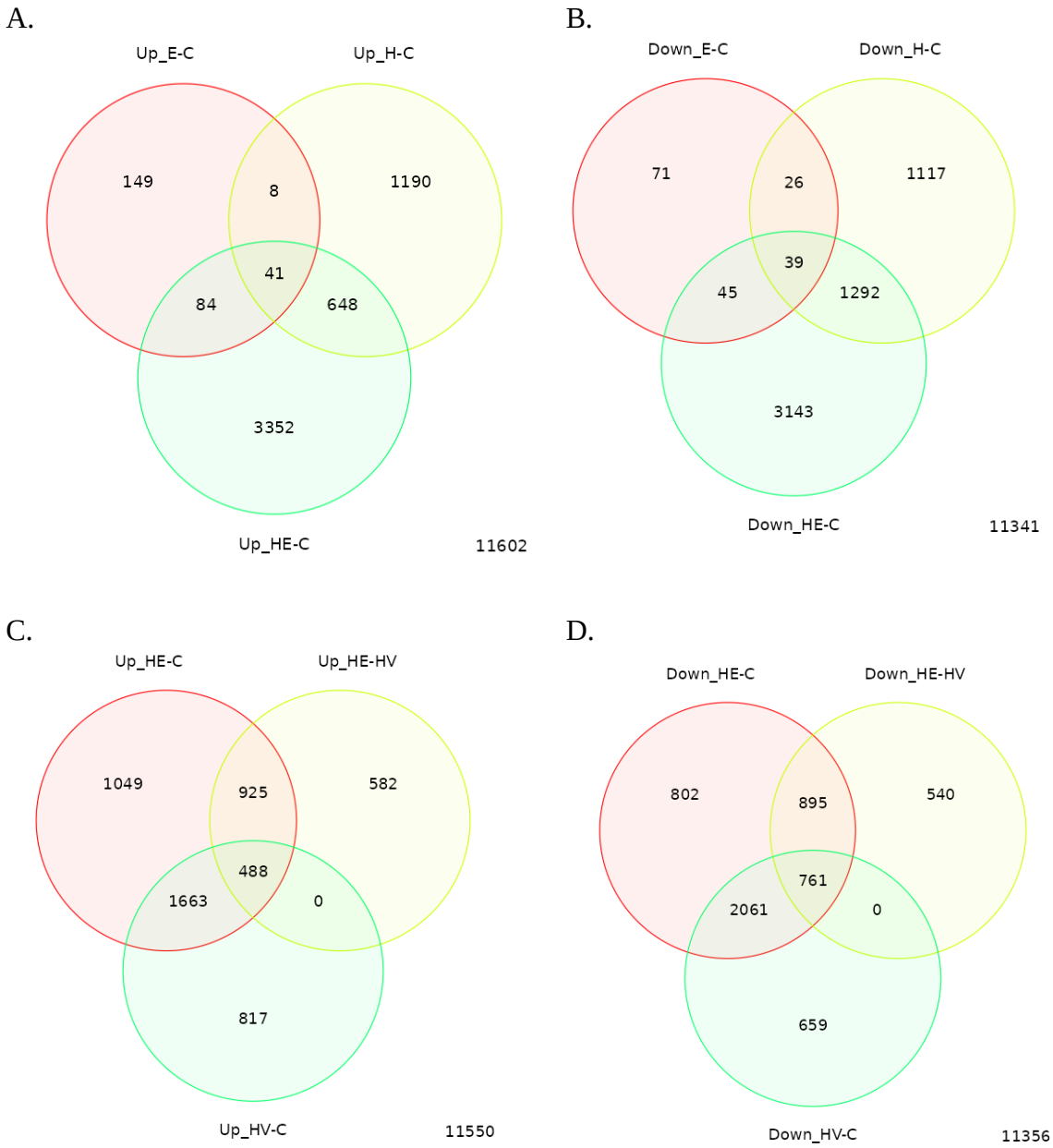

Figure 3.66: Venn diagram showing the upregulated (A.) and downregulated (B.) DEGs in common between the comparisons HE-C, E-C, H-C and the upregulated (C.) and downregulated (D.) DEGs in common between the comparisons HE-C, HV-C, HE-HV.

Figure 3.66 shows the DEGs for the comparisons HE-C, E-C, H-C and highlights the fact that treatment with PPE prior to heat stress induces the expression of genes which were otherwise not expressed in either treatment with extract alone or due to the effect of heat stress alone. The comparison HE-C shows that 3352 genes which were upregulated were not in common with the comparisons E-C or H-C. The comparison HE-C shows 3143 genes which were downregulated which were not in common with the comparisons E-C or H-C. This supports the notion that the PPE is exerting an effect on the expression of genes. In addition, there are DEGS that are common amongst the E, H and HE samples, with 648 upregulated and 1292 downregulated genes in common between the comparisons H-C and HE-C. These are most likely the genes expressed due to the effect of the heat stress. There are 1663 genes upregulated between the comparisons HE-C and HV-C. These genes are likely the genes which are upregulated due to the effect of the vehicle. However, 1049 genes are upregulated in the PPE and heat treated cells compared to the control. These are not in common with the HV samples. There are 2061 genes downregulated between the comparisons HE-C and HV-C. These genes are likely the genes which are downregulated due to the effect of the vehicle.

These DEGs make part of different pathways which are expressed in the comparison HE-H. Some significant pathways can be seen in Table 3.8. Figures 3.67 and 3.68 show the top differentially expressed genes in HDFs subjected to heat stress compared to those treated with PPE and then heat-stressed. The further upregulation of HSPA5, HSPA6 and HSPA7 in PPE treated samples is to be noted. Genes of notes are then further investigated and discussed. The comparison HE-HV in Figure 3.68 highlights the top expressed genes directly caused by the PPE and not due to the PG.

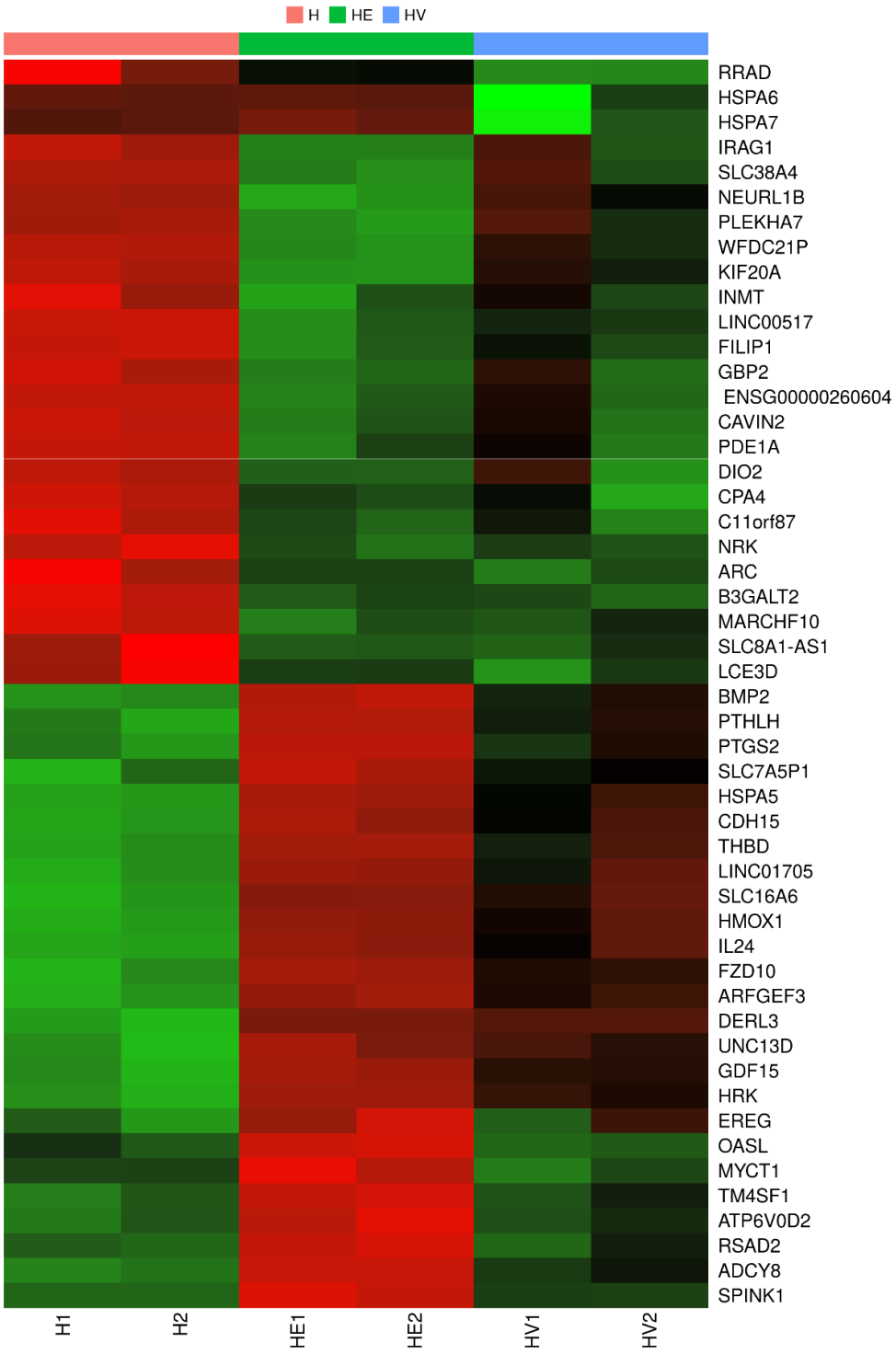

Figure 3.67: Heat map showing hierarchical clustering of top 50 gene showing gene expression patterns across H, HE and HV including both replicates for each sample. This shows the expression of genes between HDFs after heat shock and HDFs treated with PPE or vehicle prior to heat shock. Green represents downregulated genes while red represents upregulated genes. This shows that the extract has an effect on the expression of genes in heat stressed cells, which is not observed in the heat shock control and the PG heat shock cells

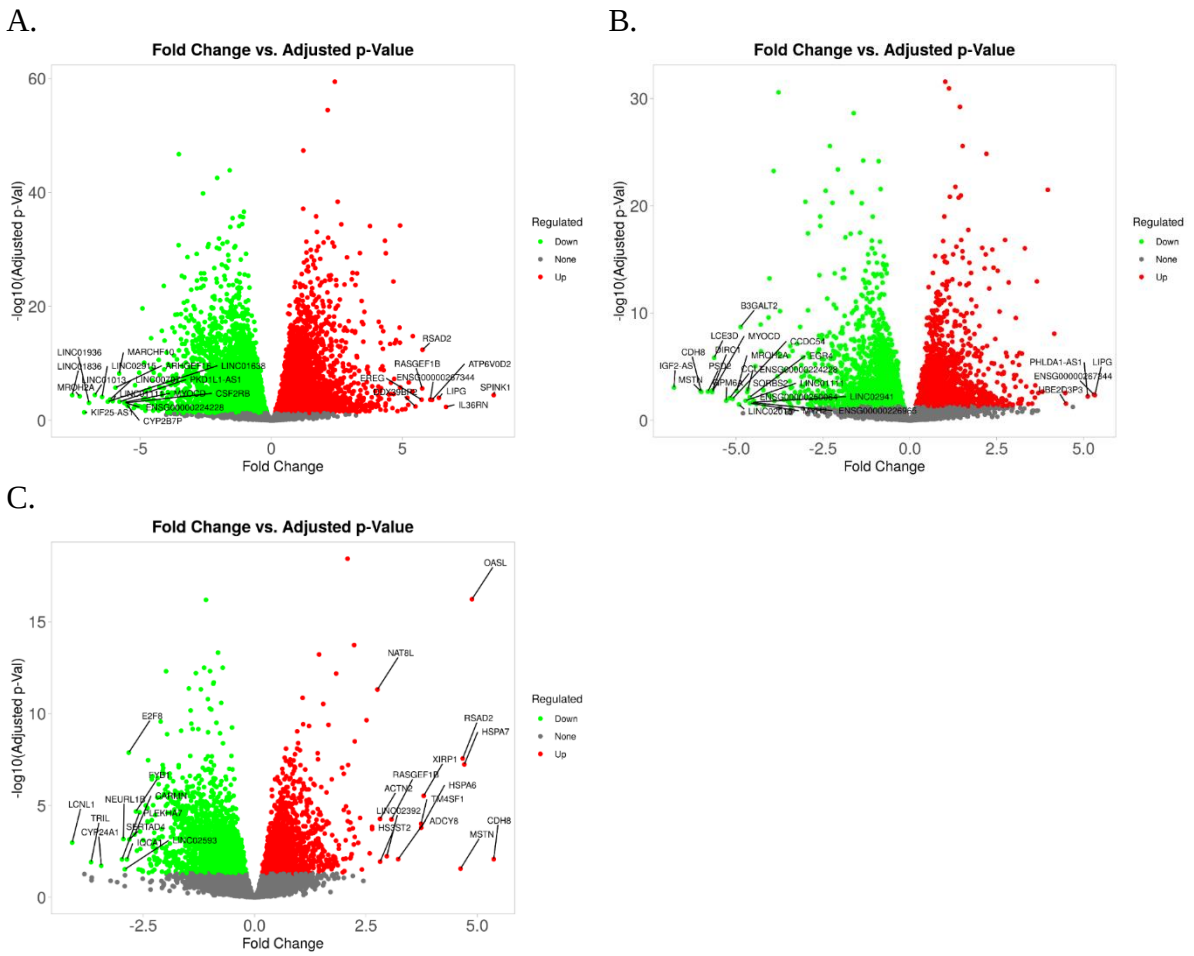

Figure 3.68: A volcano plot of the DEGs for the comparison HE-H (A.), HV-H (B.), HE-HV (C.). The top 25 genes according to log2fold values have been labelled.

Table 3.8 shows the top up and downregulated pathways in the comparison HE-H. this isolates the pathways which were affected directly due to the effect of the PPE when HDFs are subjected to heat stress. The downregulated pathways are mainly related to the cell cycle while the upregulated pathways are mainly related to the unfolded protein response. To further investigate the pathways of note, H, HE and HV are compared to the control to identify the changes when HDFs are heat stressed, and heat stressed in the presence of PG or PPE, allowing for comparisons between the conditions. Table 3.9 shows Downregulated pathways of note regarding morphogenesis, differentiation and development in the comparisons H-C, HE-C, HV-C.

Table 3.8: Up and downregulated pathways of note in the comparison HE-H. Enrichment analysis for the DEGs in the comparison H-C was carried out and top enriched pathways for GO biological process, GO cellular component and GO molecular function were analysed and identified (Ge et al., 2018).

Direction	Adj.Pval	nGenes	Pathways
Down regulated	3.8e-32	531	Cell cycle process
	3.5e-29	662	Cell cycle
	2.4e-28	441	Mitotic cell cycle
	2.4e-28	441	Mitotic cell cycle
Up regulated	4.2e-16	141	Response to endoplasmic reticulum stress
	3.0e-12	101	Response to topologically incorrect protein
	2.6e-11	91	Response to unfolded protein
	5.0e-10	83	Cellular response to topologically incorrect protein
	1.9e-09	74	Cellular response to unfolded protein
	1.2e-08	65	Endoplasmic reticulum unfolded protein response
	3.7e-08	47	Regulation of response to endoplasmic reticulum stress
	1.2e-14	343	Endoplasmic reticulum membrane
	6.0e-12	516	Endoplasmic reticulum

Table 3.9: Downregulated pathways of note regarding morphogenesis, differentiation and development in the comparisons H-C, HE-C, HV-C. Enrichment analysis for the DEGs in these comparisons was carried out and top pathways were analysed and identified (Ge et al., 2018).

Comparison	Adj.Pval	nGenes	Pathways
H-C	1.4e-23	527	Anatomical structure morphogenesis
	4.3e-23	487	Regulation of developmental process
	4.4e-21	286	Positive regulation of developmental process
	5.4e-20	692	Cell differentiation
	6.3e-19	699	Cellular developmental process
	3.4e-18	286	Regulation of multicellular organismal development
	3.5e-18	328	Regulation of cell differentiation
	3.8e-18	375	Tissue development
HE-C	1.6e-42	894	Anatomical structure morphogenesis
	3.1e-26	768	Regulation of developmental process
HV-C	8.8e-31	702	Anatomical structure morphogenesis
	1.5e-25	631	Regulation of developmental process
	1.7e-21	524	Cell development
	2.2e-21	919	Cellular developmental process
	3.7e-21	901	Cell differentiation
	1.1e-20	260	Positive regulation of cell differentiation
	1.1e-20	355	Positive regulation of developmental process
	1.6e-20	423	Regulation of cell differentiation

A.

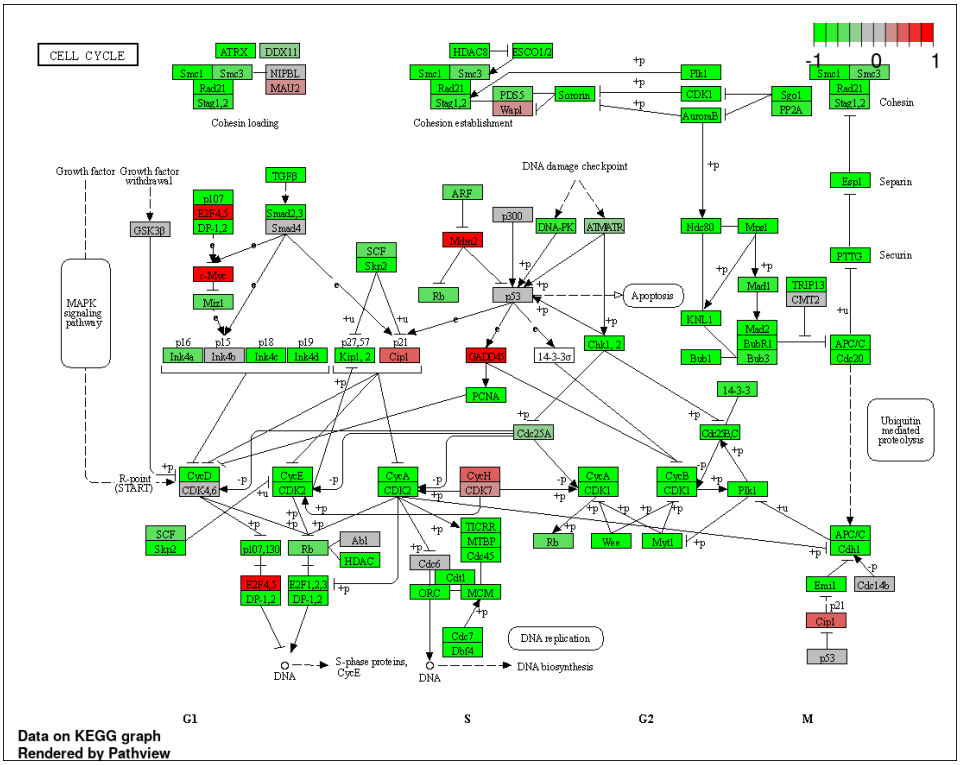

B.

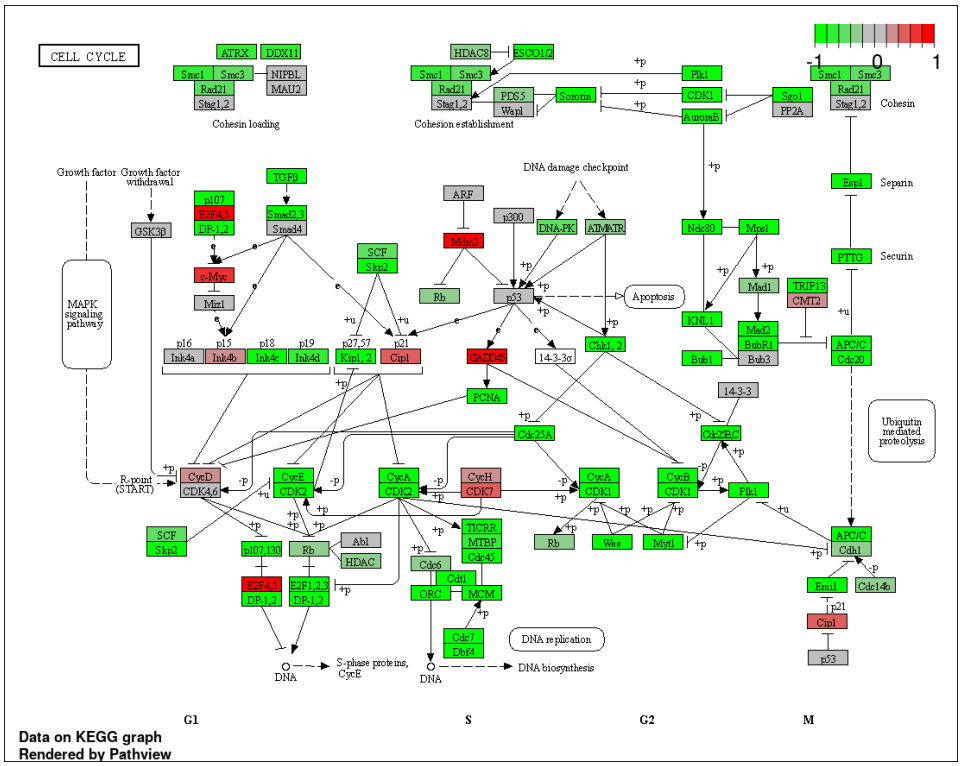

Figure 3.69: KEGG cycle representing the downregulation of the cell cycle pathway in HE-H (A.) and in HE-HV (B.) (Kanehisa et al., 2020b; Luo & Brouwer, 2013b). The comparison HE-HV highlights the genes being up or down regulated due to the effect of the PPE and not the vehicle.

The downregulation of the cell cycle as seen in figure 3.69 is a response to stress. It is to be noted that the P53 protein is neither up nor downregulated even though the cell cycle is itself downregulated. The expression of genes in the comparison HE-HV, confirms that the downregulation of the cell cycle is due to the effect of the PPE and not due to the PPEC. The upregulation of the P53 inhibitor MDM2 is to be noted.

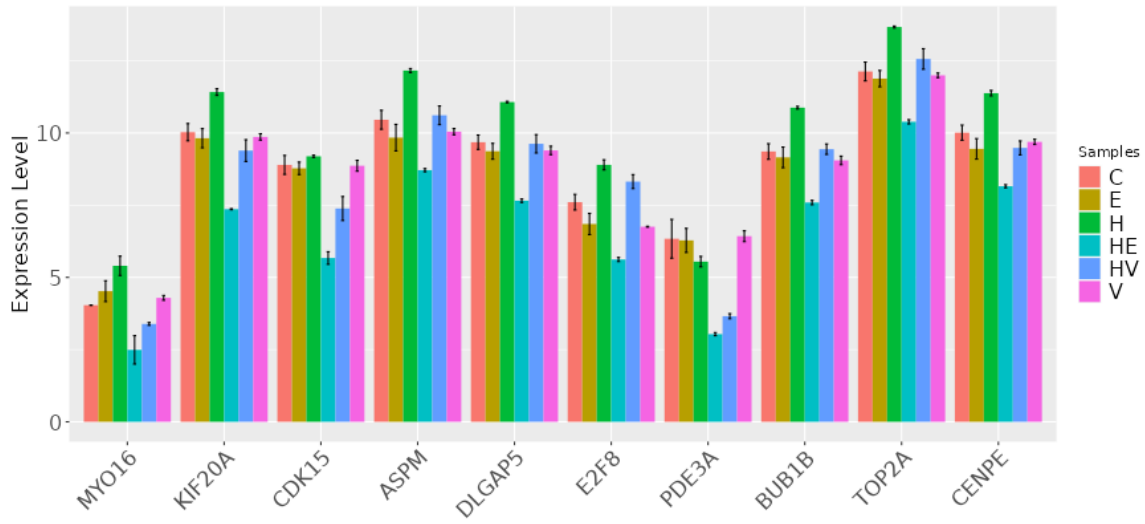

Figure 3.70: Gene plot showing top 10 downregulated genes according to log2fold involved in the cell cycle pathway for HE-H.

Of the over 500 genes which are downregulated in relation to this pathway, the top 10 genes according to log2fold change can be seen in Figure 3.70. Although expression of these genes can be observed in H, HE and HV, it is clearly observed that the highest degree of downregulation of these genes is in HE. The fold change and adjusted p value for each of the genes in Figure 3.70 in the comparison HE-H are presented in Table 3.10.

Although these genes are also differentially expressed in the comparison HV-H it can be seen by Figure 3.70 and Table 3.11 that the expression level in HE is less than in HV, highlighting the effect of the PPE on these genes. Table 3.11 shows the fold change and adj. pval for each of these genes in the comparison HE-HV. This highlights the fact that even though PG has an effect on these genes, it is further downregulated by the PPE. The genes *MYO16* and *PDE3A* are seen to have a fold change of more than 1 however the adjusted p value is higher than 0.05 allowing for the possibility of a false result.

Table 3.10: Top 10 DEGs involved in the downregulation of cell cycle pathway in the comparison HE-H.

log2 Fold Change	Adj.Pval	Gene	Function
-4.182509359	1.85E-04	*MYO16*	Regulates cell cycle progression
-4.09618308	7.37E-22	*KIF20A*	Induces cell cycle arrest when downregulated
-3.620759816	3.95E-10	*CDK15*	Regulates transcription in G1/S cell cycle stage transition
-3.464002854	1.07E-15	*ASPM*	Regulates mitotic spindle
-3.442418065	9.84E-18	*DLGAP5*	Cell cycle regulator
-3.39556855	2.04E-13	*E2F8*	Regulates progression of cell cycle by regulating expression of genes required
-3.37290757	4.30E-05	*PDE3A*	Regulates messengers which play roles in cell cycle
-3.312274029	7.94E-17	*BUB1B*	Required for progression of mitosis
-3.286469567	1.25E-13	*TOP2A*	Codes for enzymes which are involved in DNA topology
-3.245710839	2.08E-17	*CENPE*	Codes for a protein which accumulates during G2 phase of the cell cycle

Table 3.11: Top 10 DEGs involved in the downregulation of cell cycle pathway in the comparison HE-HV. The downregulation of *MYO16* in the comparison HE-HV has an adjusted p value of more than 0.05 and so is not statistically significant.

log2 Fold Change	Adj.Pval	Gene
-1.56431	0.261294	*MYO16*
-2.10597	3.00E-16	*KIF20A*
-1.85474	1.26E-07	*CDK15*
-1.94366	5.14E-19	*ASPM*
-2.02379	6.00E-19	*DLGAP5*
-2.81388	1.17E-22	*E2F8*
-1.05293	0.341181	*PDE3A*
-1.87502	7.36E-25	*BUB1B*
-2.22014	3.55E-24	*TOP2A*
-1.36123	2.41E-11	*CENPE*

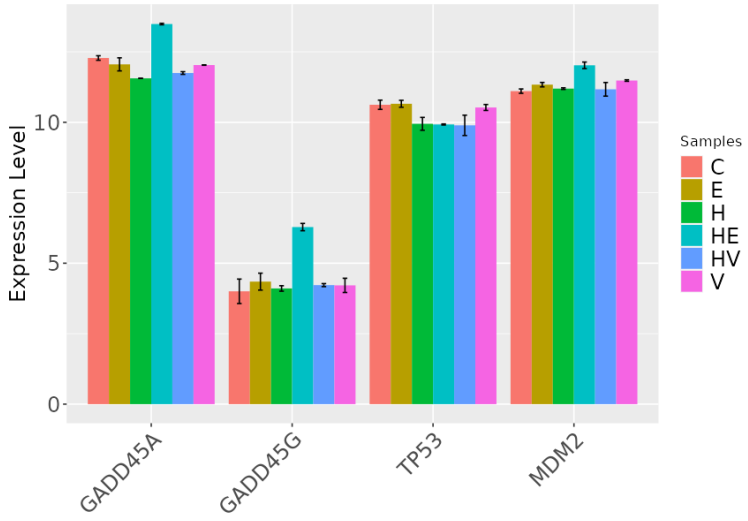

Figure 3.71: Gene plot showing the expression of the genes *GADD45A*, *GADD45B*, *TP53* and *MDM2*. Significant upregulation of the genes *GADD45A*, *GADD45B* and *MDM2* in HE is to be noted. TP53 is seen to have a lower expression in HE, HV and H, with no change between its expression in HE compared to H.

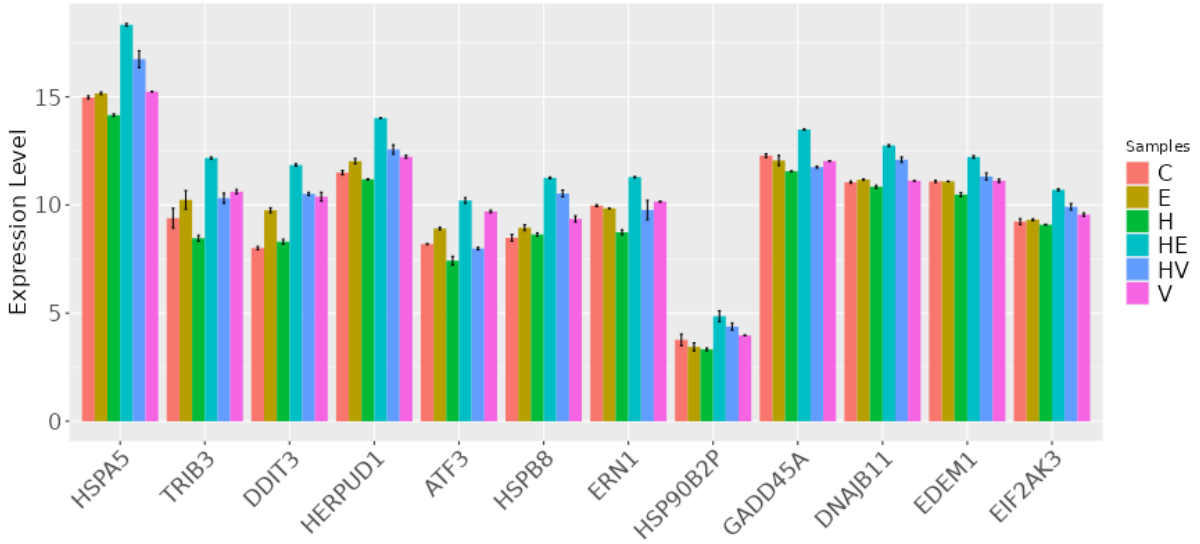

Figure 3.72: Significant DEGs associated with ER stress response/UPR. Genes associated with the unfolded protein response can be seen to be significantly upregulated in HE compared to heat shock alone. These genes are also seen to be the most highly expressed when the HDFs are exposed to the extract before being exposed to heat shock (HE).

Table 3.12: DEGs in the comparison HE-H which are classically associated with ER induced stress response/UPR

log2 Fold Change	Adj.Pval	Symbol	Role
4.177458	1.05E-10	*HSPA5*	Heat shock protein which plays a key role in protein folding and quality control
3.71595	5.96E-07	*TRIB3*	Cell-death regulator
3.55804	3.95E-16	*DDIT3*	Cell-death regulator
2.83251	2.54E-11	*HERPUD1*	Component of ER quality control
2.80286	9.81E-25	*ATF3*	Activating transcription factor involved in cellular stress response
2.62398	5.79E-19	*HSPB8*	Heat Shock protein which plays a key role in protein folding and quality control
2.55627	3.22E-11	*ERN1*	Signalling factor
2.045534	1.89E-03	*HSP90B2P*	Heat shock protein involved in protein folding
1.95417	8.07E-20	*PPP1R15A*	Facilitates recovery of cells from stress
1.92637	4.53E-08	*GADD45A*	Growth arrest and DNA-damage inducible gene.
1.900977	4.28E-14	*DNAJB11*	Heat shock protein chaperone require for folding and assembly of proteins
1.73639	2.57E-16	*EDEM1*	ER-associated degradation factor
1.617905	1.56E-14	*EIF2AK3*	Key activator of stress response

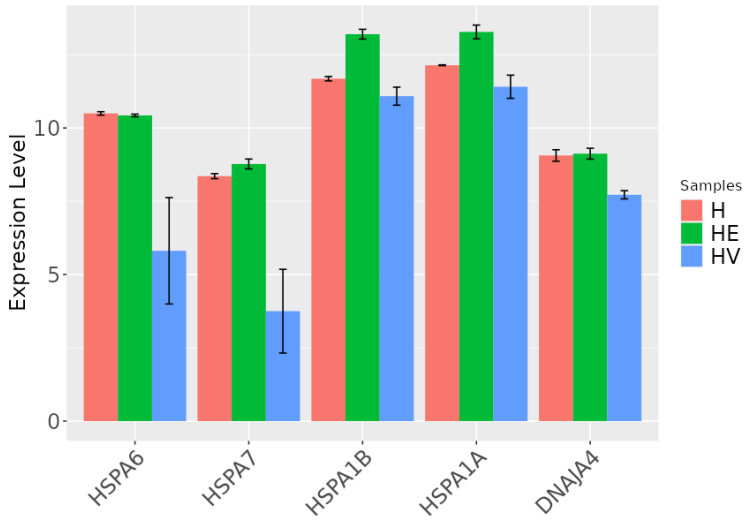

Figure 3.73: Gene plot of heat shock response-related genes which were already identified as DEGs in the comparison H-C. This figure shows that the genes expressed as a result of heat stress alone are consistently expressed when the HDFs are treated with PPE and then subjected to heat stress. *HSPA1B* and *HSPA1A* are seen to be upregulated in HE-H with a log2fold of 1.54 and 1.17 respectively.

A.

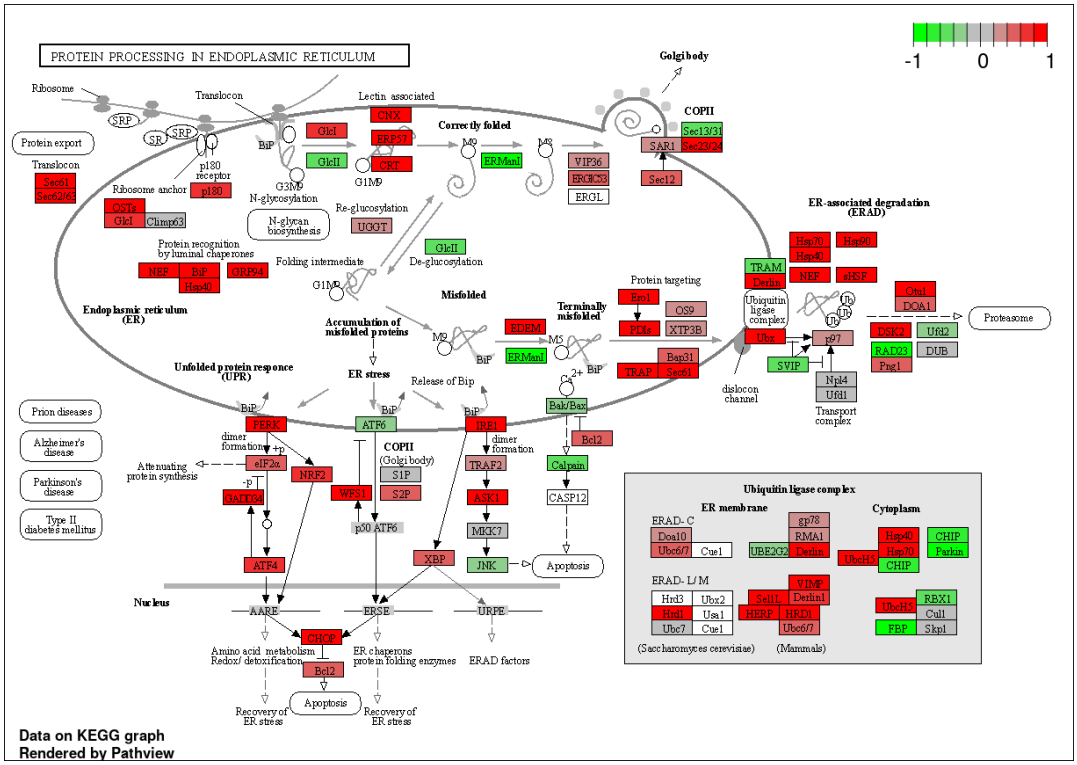

B.

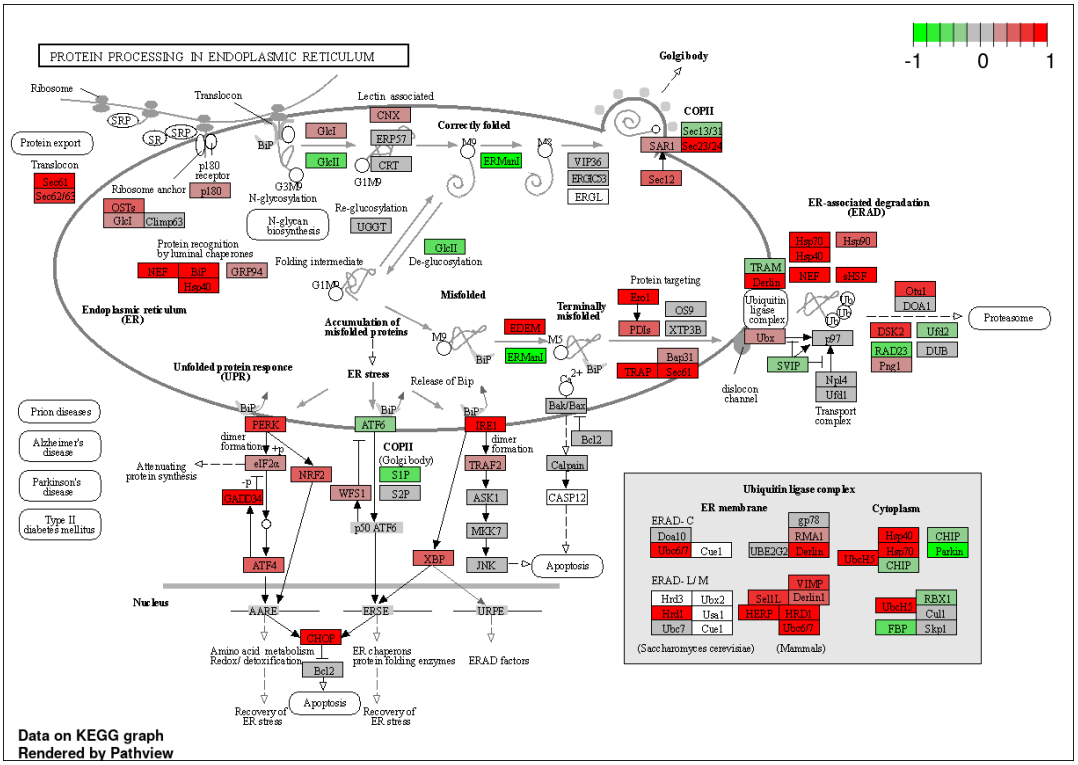

Figure 3.74: KEGG cycle representing the overall upregulation of the protein processing in the endoplasmic reticulum in HE-H (A.) and HE-HV (B.) The comparison HE-HV excludes the effect of the vehicle by showing the DEGs in HE compared to those already expressed in HV (Kanehisa et al., 2020b; Luo & Brouwer, 2013b).

The response to unfolded and improperly folded proteins is exemplified by the KEGG cycle as seen in Figure 3.74, showing the pathways related to the role of the endoplasmic reticulum in protein folding. Of note is the upregulation of the HSP40 and HSP70 protein related genes. This upregulation can also be observed in the comparison HE-HV showing that the expression is due to the effect of the PPE and not of the PPEC it is dissolved in.

Table 3.13: Upregulated pathways of note in the comparison HE-HV (Ge, S. X. et al., 2018b). These pathways prove that the response to unfolded proteins is due to the effect of the PPE.

Direction	Adj.Pval	nGenes	Pathways
Up regulated	5.3e-13	74	Response to topologically incorrect protein
	3.9e-12	67	Response to unfolded protein
	6.0e-12	63	Cellular response to topologically incorrect protein
	1.6e-11	57	Cellular response to unfolded protein
	8.7e-11	89	Response to endoplasmic reticulum stress

Table 3.14: Upregulated genes of note which corroborate the observation of improved wound resolution in cells pre-treated with PPE and subjected to heat shock.

log2 Fold Change	Adj.Pval	Symbol	Function
5.724631	1.54E-03	*EREG*	Epidermal growth factor activated during wound healing
4.698494	5.99E-07	*TM4SF1*	Helps to organise membrane and cytoskeleton interactions and facilitates migration of fibroblasts
5.121931	1.44E-02	*MYO1G*	Myosin motor protein which helps with cell shape and forming of structures during cell migration

3.8.4. Effect of oxidative stress on human dermal fibroblasts

The following section is related to the RNA-seq work carried out to elucidate the effects of oxidative stress on human dermal fibroblasts.

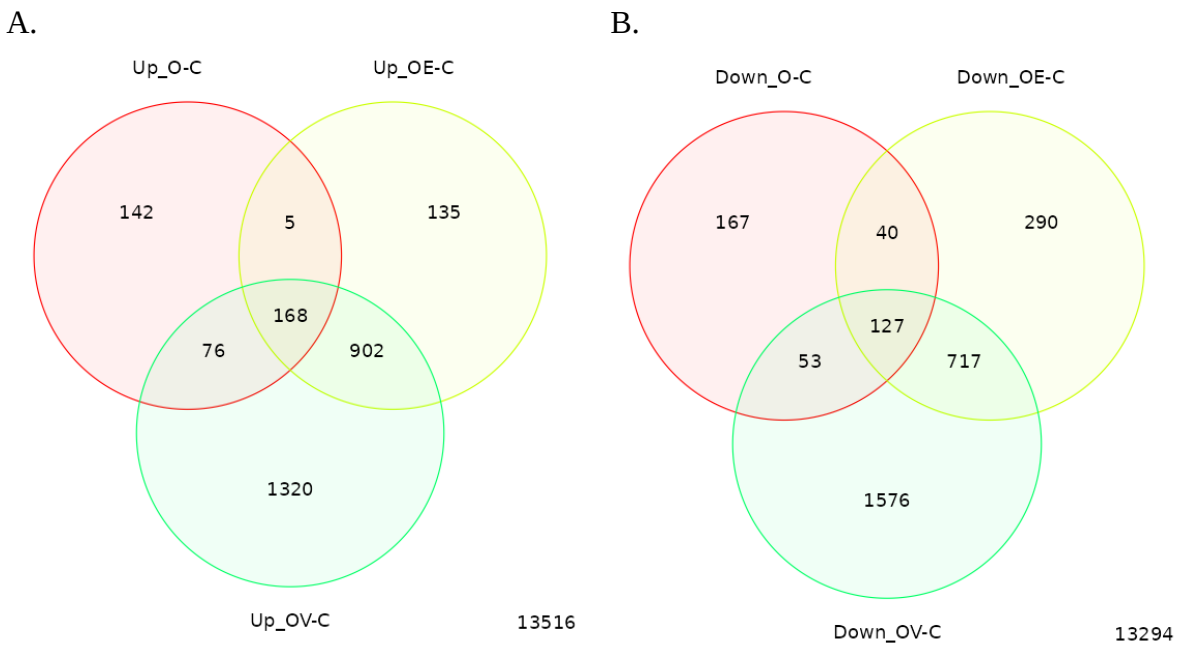

Figure 3.75: Venn diagram showing the upregulated (A.) and downregulated (B.) DEGs in common between the comparisons O-C, OE-C, OV-C.

There are 168 commonly upregulated and 127 commonly downregulated genes between the three comparisons. These genes are likely to be the genes upregulated in response to oxidative stress.

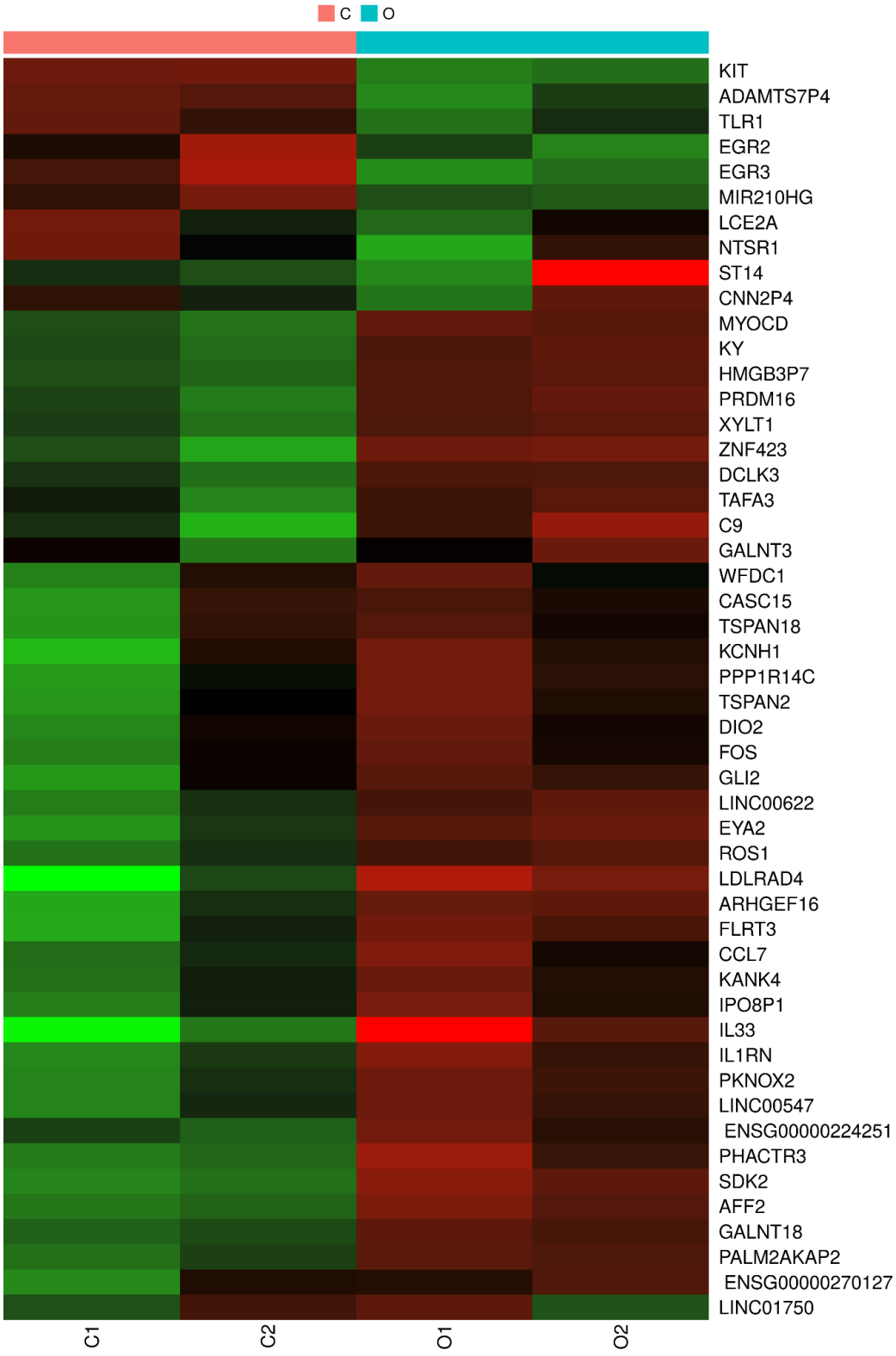

Figure 3.76: Heat map showing hierarchical clustering of top 50 gene showing gene expression patterns across the samples for control, extract and vehicle. Green represents downregulated genes while red represents upregulated genes.

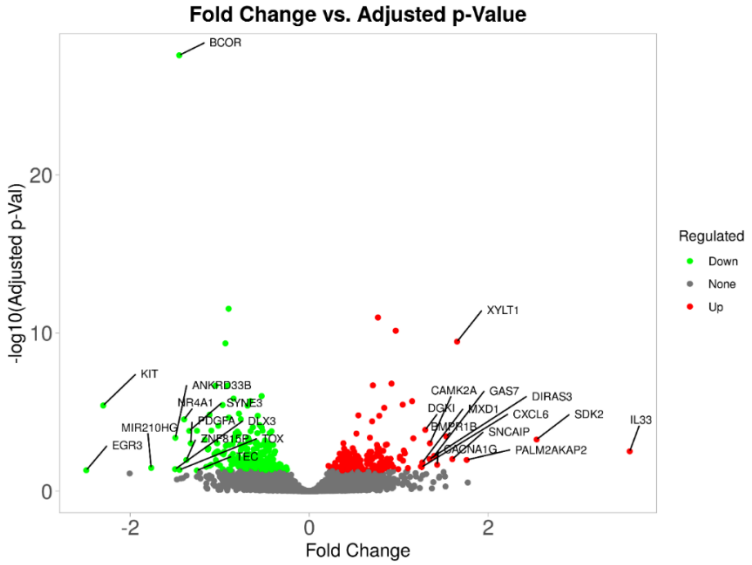

Figure 3.77: A volcano plot of the DEGs for the comparison O-C. The top 25 genes according to log2fold values have been labelled.

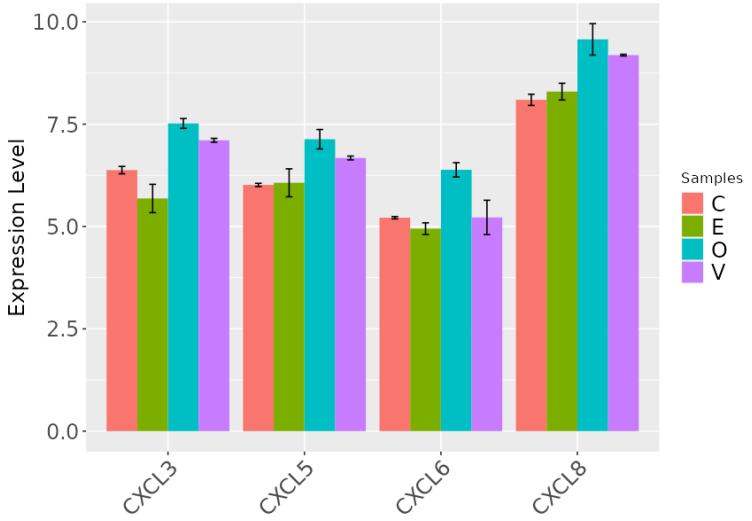

Figure 3.78: Gene bar graph showing increased expression of cytokines in HDFs exposed to oxidative stress compared to C, V and E.

Table 3.15: Log2fold and adjusted p values for upregulated cytokines in the comparison O-C

log2 Fold Change	**Adj.Pval**	**Gene**
1.177733	3.14E-03	*CXCL3*
1.181798	1.34E-02	*CXCL5*
1.26314	4.38E-02	*CXCL6*
1.532648	7.86E-08	*CXCL8*

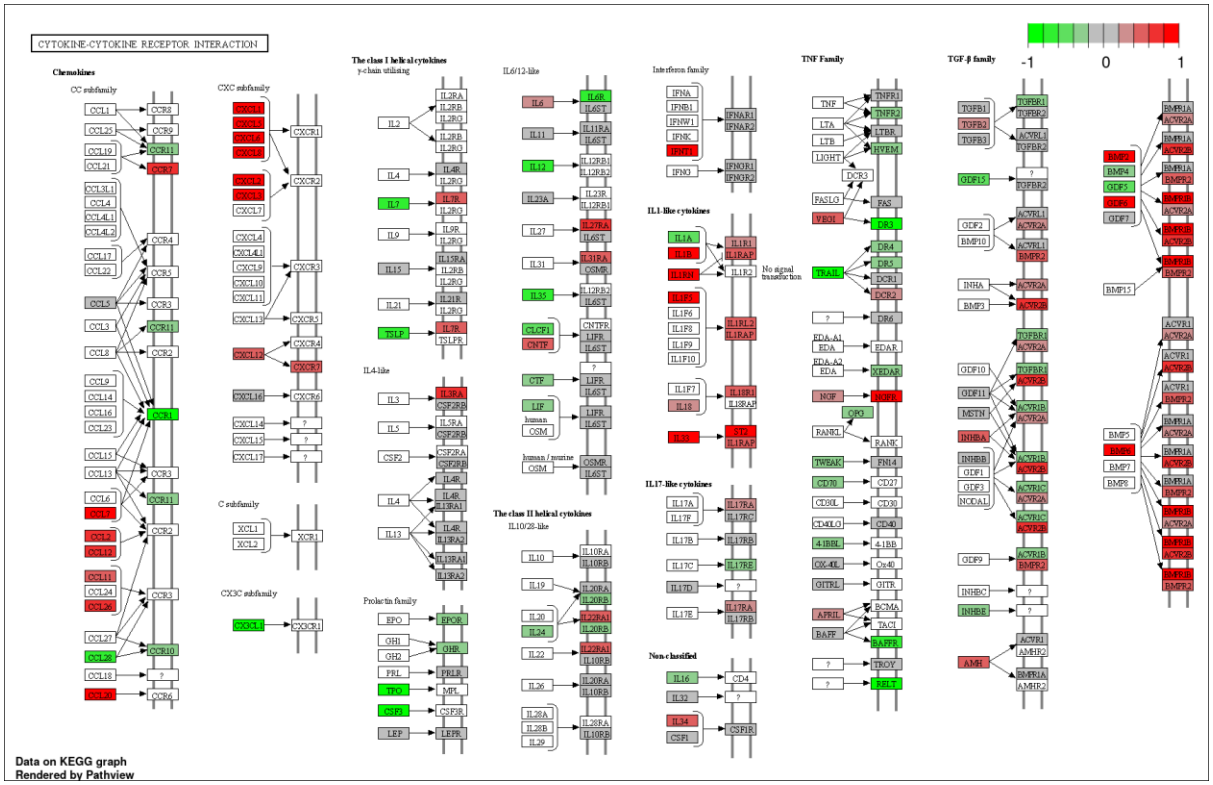

Figure 3.79: KEGG diagram representing the cytokine-cytokine receptor interaction in O-C. An upregulation in chemokines can be observed (Kanehisa et al., 2020b; Luo & Brouwer, 2013b).

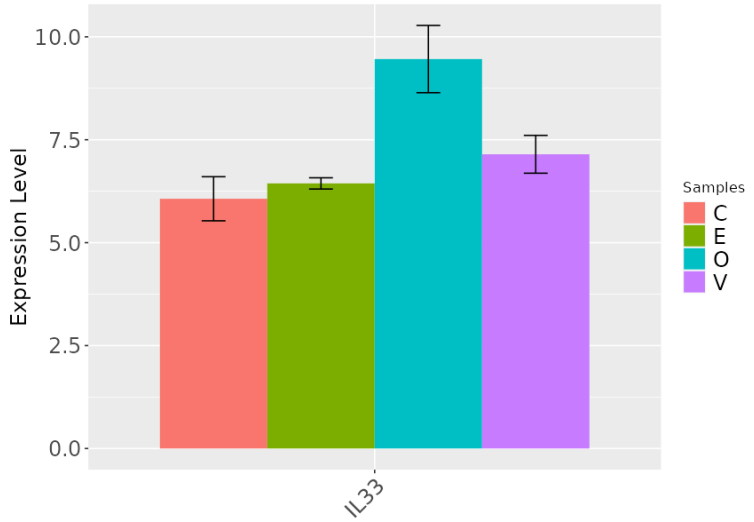

Figure 3.80: Gene bar graph showing the increased expression of *IL33* in HDFs exposed to oxidative stress. The log2fold for *IL33* in the comparison O-C was 3.59 and the adjusted p value, 3.87E-03.

The upregulation in cytokine expression can be observed in figures 3.78 – 3.80 as well as table 3.15. Cytokines are part of the body's first response to oxidative stress and are involved in the induction of the inflammatory response. The observed upregulation in cytokine expression is indicative of the HDFs response to oxidative stress.

Table 3.16: Downregulated pathways of note in the comparison O-C. Enrichment analysis for the DEGs in the comparison O-C was carried out and top enriched pathways for GO biological process, GO cellular component and GO molecular function were analysed and identified (Ge et al., 2018). The main downregulated pathways are all related to a decrease in cell differentiation.

Direction	Adj.Pval	nGenes	Pathways
Down regulated	6.4e-04	17	Anatomical structure morphogenesis
	6.4e-04	16	Regulation of developmental process
	9.7e-04	6	T cell differentiation
	4.1e-03	7	Leukocyte differentiation
	4.1e-03	6	Lymphocyte differentiation
	6.7e-03	5	Fat cell differentiation
	6.7e-03	11	Regulation of cell differentiation
	6.7e-03	6	Mononuclear cell differentiation
	9.7e-03	4	Regulation of lymphocyte differentiation

3.8.5. Effect of PPE / PPEC on fibroblasts exposed to oxidative stress

The following section is related to the RNA-seq work carried out to elucidate the effects of oxidative stress on human dermal fibroblasts in the presence of PPE or PPEC.

A differential comparison of the expressed genes in the cells that were treated with both extract and menadione (OE) with menadione stressed cells (O) demonstrates that a number of genes are up and down regulated (Figure 3.81). The effect of the vehicle stress (OV) during oxidative on gene expression however, was more pronounced. In despite of this observation, a number of genes are differentially expressed in OE when compared to OV. This indicates that the extract is stimulating a cellular response that is independent of the vehicle under these conditions.

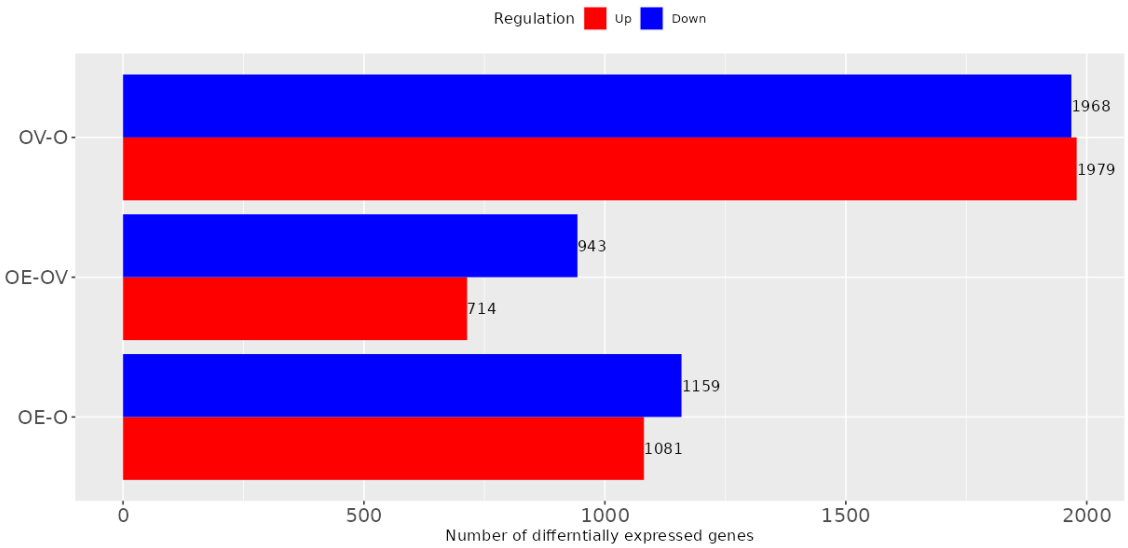

Figure 3.81: DEGs of OE, OV and O comparisons. , This data was analysed by iDESeq2 integrated in iDEP (Ge et al., 2018). A visual overview of the effect of treatment with PPE and oxidative stress can be seen. Although treatment with the vehicle has also induced increased expression of genes it can be seen that PPE treatment induced expression of genes over and above those expressed by treatment with vehicle (OE-OV).

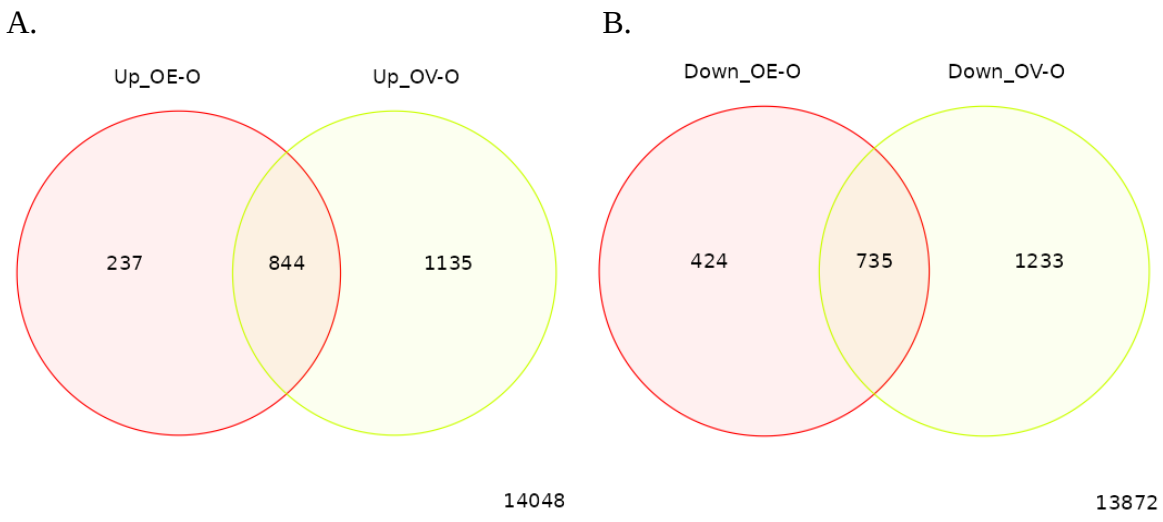

Figure 3.82: Venn diagram showing the upregulated (A.) and downregulated (B.) DEGs in common between the comparisons OE-O and OV-O

The two comparisons share 844 upregulated and 735 downregulated genes, highlighting the effect of the vehicle when HDFs are treated with PPE. OE-O has 237 upregulated and 424 downregulated genes which are not shared with OV-O. These genes are likely the genes upregulated due to the effect of the PPE

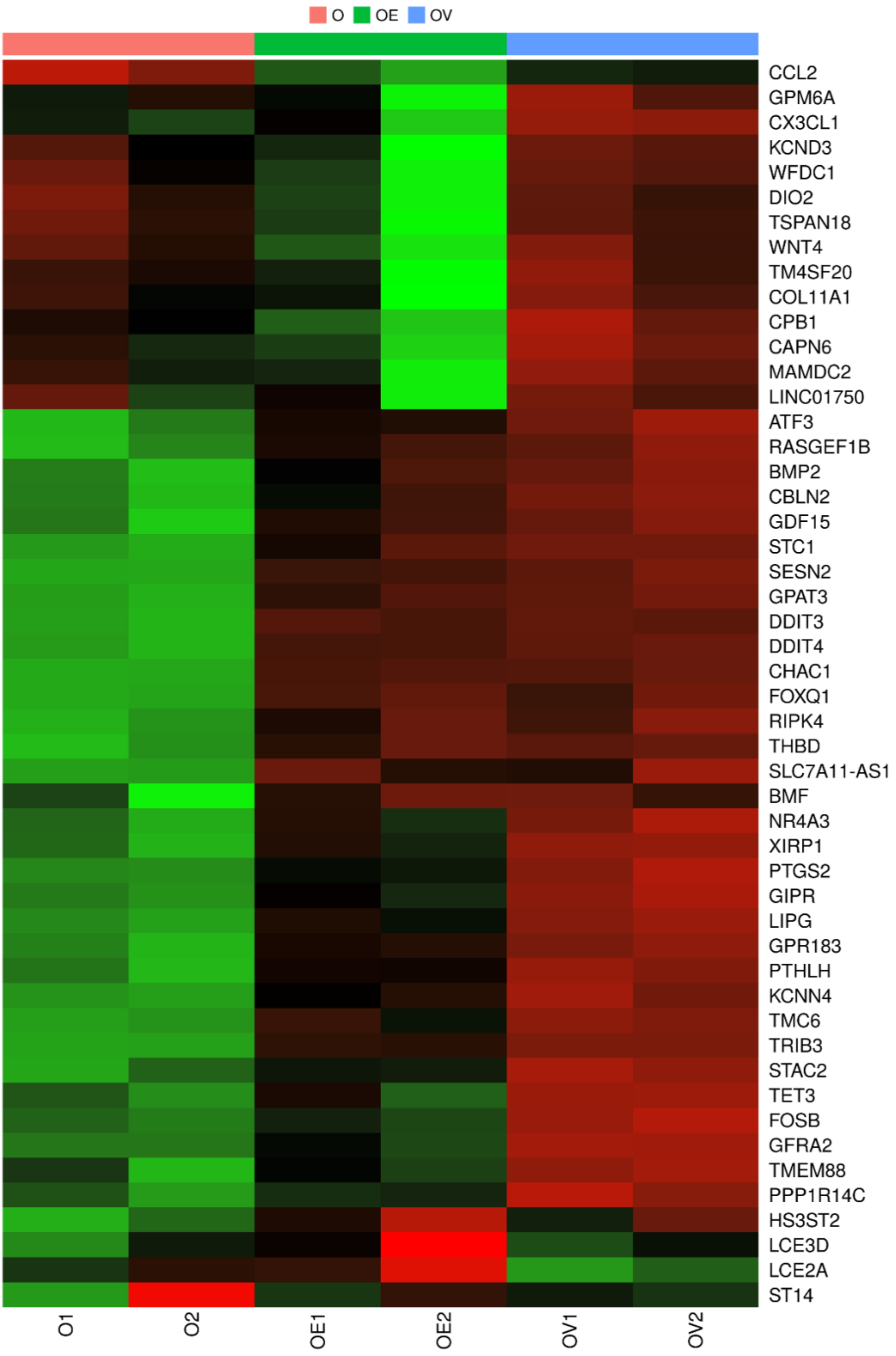

Figure 3.83: Heat map showing hierarchical clustering of top 50 gene showing gene expression patterns across O, OE and OV including both replicates for each sample. This shows the expression of genes between HDFs after heat shock and HDFs treated with PPE or vehicle prior to heat shock. Green represents downregulated genes while red represents upregulated genes.

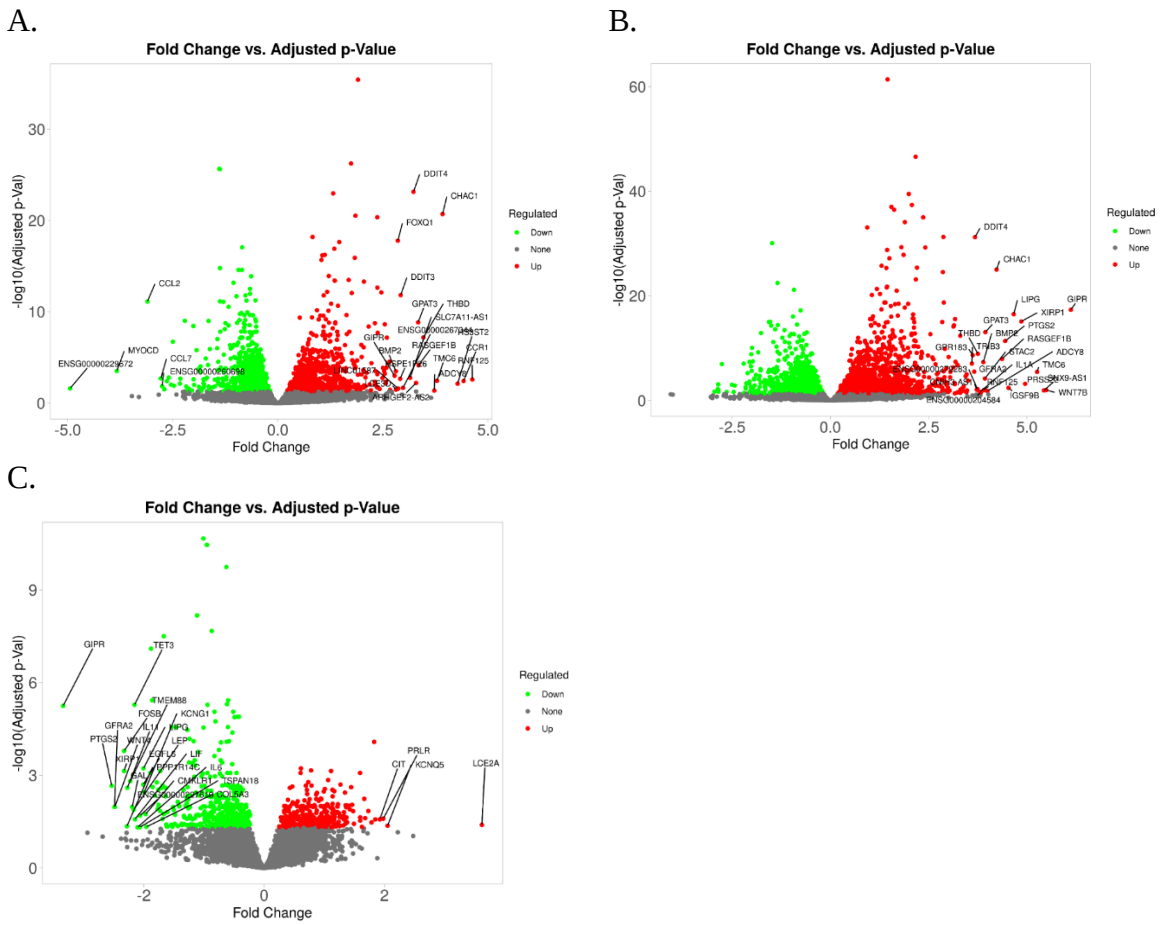

Figure 3.84: A volcano plot of the DEGs for the comparison OE-O (A.), OV-O (B.) and OE-OV (C.). The top 25 genes according to log2fold values have been labelled.

Table 3.17: Up and downregulated pathways of note in the comparison OE-OV.

Direction	Adj.Pval	nGenes	Pathways
Down regulated	1.3e-36	371	Cell differentiation
	1.3e-36	376	Cellular developmental process
	1.4e-36	290	Anatomical structure morphogenesis
	5.0e-32	264	Regulation of developmental process
	2.4e-30	216	Tissue development
	6.2e-28	169	Regulation of multicellular organismal development
Up regulated	1.5e-27	140	Mitotic cell cycle
	2.2e-27	157	Cell cycle process
	1.4e-26	127	Mitotic cell cycle process
	8.7e-26	184	Cell cycle
	1.8e-22	93	Cell division
	2.5e-16	59	Mitotic nuclear division

Enrichment analysis for the DEGs in the comparison OE-OV was carried out and top enriched pathways for GO biological process, GO cellular component and GO molecular function were analysed and identified (Ge et al., 2018). The comparison OE-OV was investigated to try and identify the pathways which are due solely to the effect of the PPE rather than the effect of the vehicle.

Table 3.18: DEG of note in the comparison OE-OV related to the decrease in morphogenesis and differentiation

log2 Fold Change	Adj.Pval	Symbol
-2.86854	9.39E-05	*GJA5*

Table 3.19: Enriched downregulated pathways of note in the comparison OE-O with regards to RNA and ribosome metabolism

adj.Pval	nGenes	Pathways
3.8e-19	167	RNA processing
3.4e-12	93	MRNA processing
4.7e-11	129	MRNA metabolic process
6.2e-10	68	Ribosome biogenesis
4.2e-08	56	RRNA metabolic process

Enrichment analysis for the DEGs in the comparison OE-O was carried out and top enriched pathways for GO biological process, GO cellular component and GO molecular function were analysed and identified (Ge et al., 2018). The comparison OE-O was investigated to identify the different response when the HDFs were treated with PPE and then subjected to oxidative stress, highlighting the effect of the PPE in response.

Table 3.20: Different pathways related to DNA repair in the comparison OE-OV.

GAGE analysis: OE vs OV	Statistic	Genes	Adj.Pval
Double-strand break repair	5.8778	245	1.4e-06
Recombinational repair	5.4149	129	1.8e-05
Double-strand break repair via homologous recombination	5.3425	127	2.4e-05

Table 3.21: Genes of note involved in DNA double stranded repair in the comparison OE-OV

log2 Fold Change	Adj.Pval	Symbol
1.290323	2.67E-03	*ESCO2*
1.24758	1.85E-03	*POLQ*
1.150281	1.69E-03	*GINS2*
1.004837	3.53E-03	*RAD51AP1*

Table 3.22: Top 10 DEGs involved in the upregulation of the cell cycle pathway in the comparison OE-OV

log2 Fold Change	Adj.Pval	Gene	Function
1.922502	3.42E-02	*CIT*	Protein kinase functioning in cell division
1.84698	3.20E-05	*PKIA*	Plays a regulatory role in the activity of protein kinase A – an enzyme involve in cell cycle regulation
1.830559	7.67E-06	*PRIM1*	DNA primase which plays a role in DNA synthesis
1.426971	1.29E-04	*SPC25*	Involved in spindle checkpoint activity
1.378379	2.63E-02	*E2F2*	Transcription factor which is crucial to the cell cycle control
1.376719	5.03E-03	*TDRKH*	Protein coding gene involved in the processes of nucleic acid binding and RNA binding
1.367148	2.04E-05	*DLGAP5*	Cell cycle regulator
1.3548	4.55E-05	*PBK*	Protein kinase involved in mitosis
1.345665	9.54E-05	*NUF2*	Key component required for chromosome segregation and spindle checkpoint
1.327254	7.38E-04	*NEK2*	Kinase involved in mitotic regulation

Table 3.23: Upregulated pathways of note in the comparison OV-O.

Direction	Adj.Pval	nGenes	Pathways
Up regulated	1.5e-14	458	Response to organic substance
	1.4e-13	384	Cellular response to organic substance
	2.8e-13	440	Cellular response to chemical stimulus
Down regulated	1.9e-33	325	Cell cycle process

Enrichment analysis for the DEGs in the comparison OV-O was carried out and top enriched pathways for GO biological process, GO cellular component and GO molecular function were analysed and identified (Ge et al., 2018). The comparison OV-O was investigated to identify whether pathways in relation to response to organic substance and stimulus was due to the effect of the PPE or of the PG (vehicle).

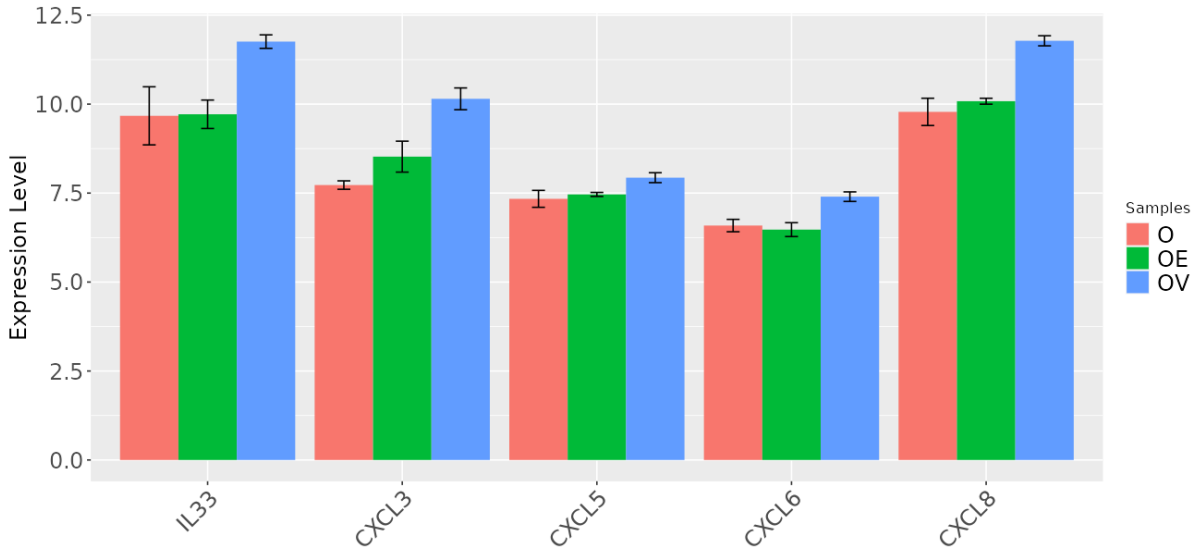

Figure 3.85: Gene bar graph showing expression of cytokines which were previously noted to be upregulated in O-C. Cytokine expression in OE is very similar to O, but highest expression is observed in OV.

Table 3.24: Log2fold and adjusted pvalues for cytokines which were upregulated in O-C and OV-O but are downregulated in OE-OV

log2 Fold Change	Adj.Pval	Gene
-1.59734	3.47E-06	*CXCL3*
-1.70448	3.24E-12	*CXCL8*
-1.99992	1.97E-02	*IL33*

Although cytokine expression in OE is very similar to O as seen in Figure 3.85, 3 cytokines where found to be downregulated when investigating the comparison OE-OV (table 3.24). Changes in the inflammatory response in PPE treated HDFs subjected to oxidative stress can be observed in Figures 3.86– 3.88. Downregulation of the *IL6* gene and overall downregulation in the JAK-STAT pathway and the genes involved is to be noted, showing the role of the PPE on the immune response. This effect is further corroborated by the increased expression of *SOCS1*. The KEGG pathway for the comparison OE-O as seen in figure 3.86A shows the effect of the PPE as well as the PPEC it is dissolved in while the comparison OE-OV (Figure 3.86B) highlights the sole effect of the PPE. The PPE is seen to be the cause of the downregulation of *IL6* as well as of the SOCS proteins, indicating the PPE's effect on the inflammatory response.

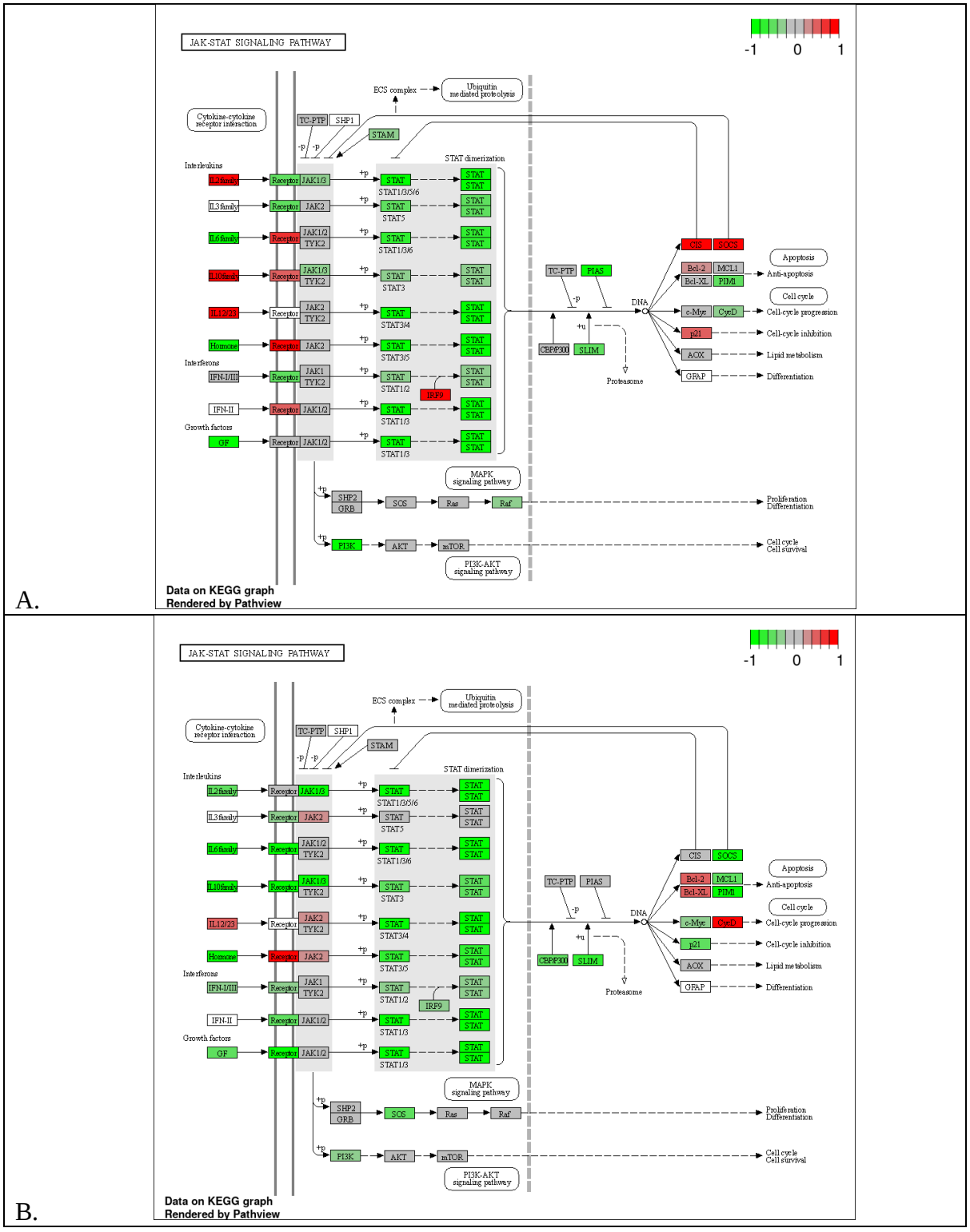

Figure 3.86: KEGG cycle representing the JAK-STAT signalling pathway for the comparison OE-O (A.) and OE-OV (B.) (Kanehisa et al., 2020b; Luo & Brouwer, 2013b). The comparison OE-OV highlights the effect of the PPE, removing the effect of the vehicle

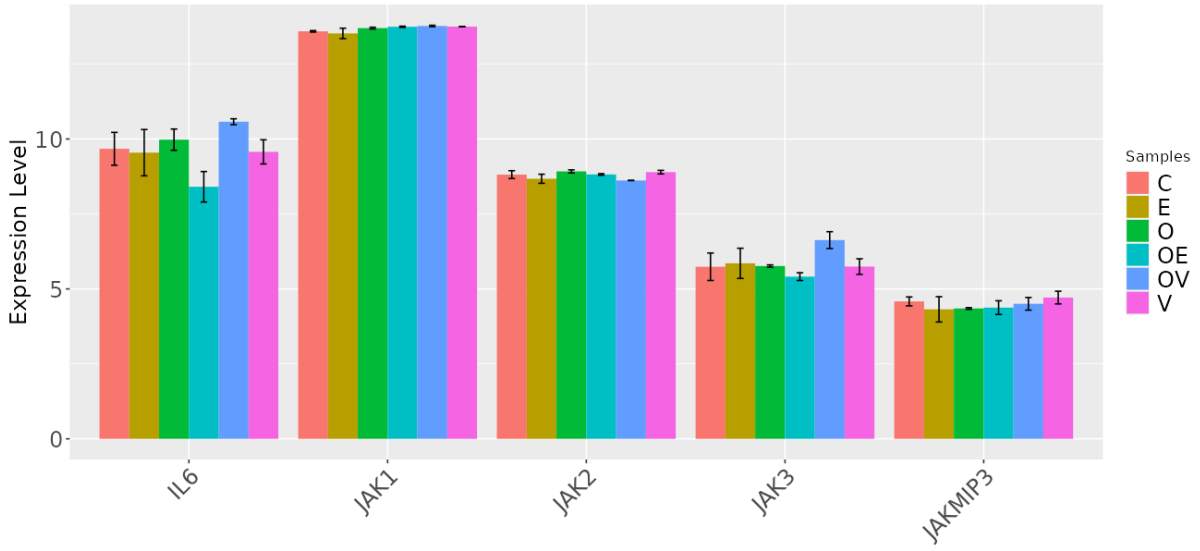

Figure 3.87: Gene bar graph showing the expression of IL6 which is downregulated when OE is compared to OV and expression of different JAK genes involved in the JAK-STAT pathway. The *IL6* gene is related to the JAK-STAT pathway, with the pathway being known as the IL6 pathway. The *JAK3* gene is shown to have an increased expression in OV compared to the other conditions. The OE-OV comparison showed a downregulation of the *JAK3* gene with a log2fold of -1.32 and an adjusted p value of 2.38E-02.

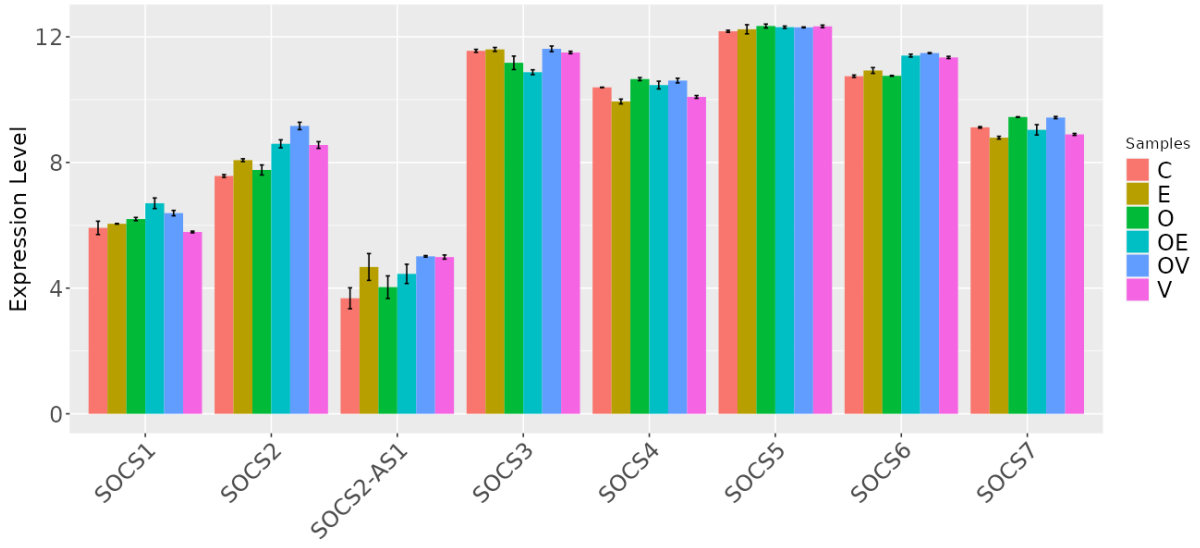

Figure 3.88: Gene bar graph showing the expression of different *SOCS* genes involved in the JAK-STAT pathway. Genes showed an increased expression in OE compared to O, however the greatest expression was noted in OV. *SOCS1* is seen to have a larger expression in OE compared to OV.

Table 3.25: DEGs in the comparison OE-OV which are related to skin barrier and possible links to psoriasis.

log2 Fold Change	Adj.Pval	Symbol
3.614337	1.32E-02	*LCE2A*
2.470824	3.28E-02	*LCE3D*

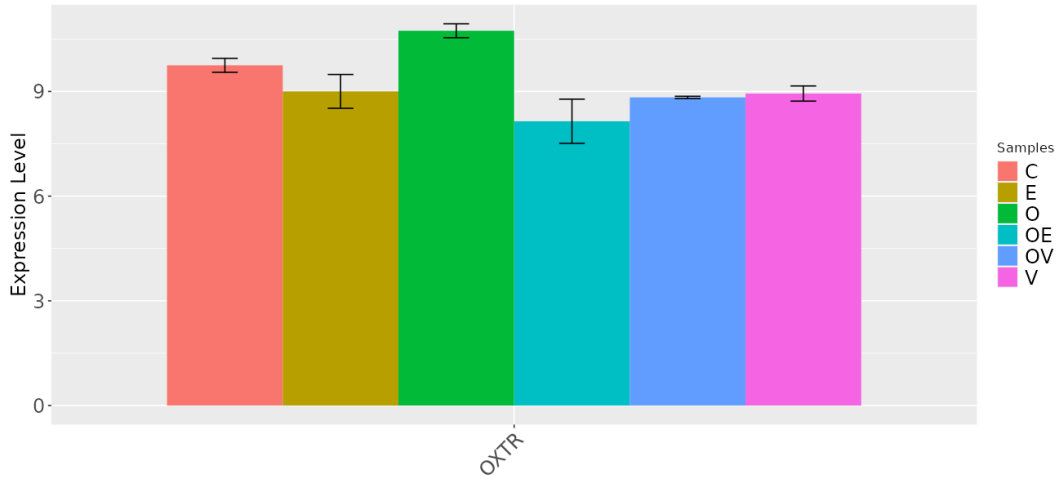

Figure 3.89: : Gene bar graph showing expression of *OXTR*. A downregulation of the gene in OE can be seen when compared to O with the comparison OE-O showing a log2fold of -2.494 and an adj.pval of 2.42E-06.

Table 3.26: Upregulation of the gene *SESN2* in the comparisons OE-O and OE-OV. Significant upregulation of the gene in both comparisons proves that its expression is due to the effect of the PPE.

Comparison	log2 Fold Change	Adj.Pval
OE-O	2.367353	4.15E-17
OE-OV	2.378445714	1.85E-68

Chapter 4 Discussion

The aim of this study was to analyse the effectiveness of the prickly pear extract (PPE) as a mode of protection against the cellular damage induced by heat, oxidative stress and ultraviolet (UV) as these insults contribute to clinical sunburns, ageing and carcinogenesis amongst other possible pathologies. Global transcriptome analysis of changes in gene expression was employed to identify the cellular systems that are influenced by PPE and the carrier it is dissolved in. The information gathered by this study may contribute to the understanding of how the cell responds to the extract and to the development of an innovative approach to the protection against cellular damage caused by UV irradiation, heat, and oxidative stress through the utilization of PPE. This, thus may result in a possible defence against, including but is not limited to, sunburn, photoaging, pigmentation and carcinogenesis and other related pathologies. Cellular survival on contact with exogenous and endogenous stress stimuli hinges critically on the ability of said cells to mount an appropriate response. This cellular response is initially geared towards mounting a steadfast defense against / recovery from the insulting stress stimulus through the activation of survival pathways. However, if overwhelmed, the cellular responses pivot towards the programed cell death pathway signaling to remove critical damaged cells (Fulda et al., 2010). The focus of this study was on the protection the prickly pear extract provides to fibroblasts against the effects of exogenous insults on fibroblasts cell which were obtained directly from the tissue of origin and were used as a model of biological processes, without the potential effects of natural/synthetic genomic alterations required for creation of cell lines (Kaur & Dufour, 2012). Fibroblasts are the ubiquitous cellular unit of the most essential tissue which keeps the human body together – connective tissue. It is in this tissue that fibroblasts produce that extracellular matrix proteins, ground substances and adhesive proteins which comprise the extracellular matrix (ECM) that is essential for the structure of connective tissue. However, the roles played by fibroblast stretches beyond ECM production and encompasses ECM maintenance and reabsorption, cancer progression, inflammation, wound healing as well as various ancillary biological (physiological/pathological) roles in response to endocrine signals such cytokines and growth factors (Kendall & Feghali-Bostwick, 2014). Following the totality of viability analysis with respect to cytotoxicity and cytoprotectivity of the PPE and identification of ideal target dose for desired biological effect, RNA sequencing was conducted to elucidate the mechanisms behind the observed protective effect seen using viability assays in HDFs. The transcriptome

analysis offered by RNA sequencing confers the cells identity and provides insight into the regulation of all biological activities within the cell. The unparalleled high resolution provided by this transcriptional landscape provides the ability to unravel differential gene expressional quantitatively. (Kukurba & Montgomery, 2015; Stark et al., 2019).

4.1. General Consideration

The first step in this study involved the establishment and maintenance of a stable primary cell culture of HDF and the familiarization of growth profile of this primary culture as shown in Section 3.1. To this extent a stable primary cell cultures of HDF was created and utilized between passage 6 and 12 for the entirety of experimentation with attention to any potential morphological changes. This was done to ensure no issue with destabilization of cell culture due to possible aberration or senescence which could have an impact on the outcome of this study. Furthermore, as seen in the qPCR results (Section 3.1.2) the CD marker expression profile (CD90+ and CD105+) for the pHDF are all positive indicators of the pHDFs being correctly isolated into a homogenous primary culture (Alt et al., 2011; Jiang & Rinkevich, 2018). In addition to the pHDF it was considered necessary to repeat with biological replicates using Human Neonatal Dermal Fibroblasts (nHDFs) - ATCC PCS-201-010 (LCG Standards, Germany) to provide a greater degree of assurance of the findings of the results. In addition to ensure the viability results these were repeated using two different assays namely the Cell-Titre glo assay (Section 3.2) and Presto blue assay (Section 3.3). The chemical composition of the PPE normalised from the PPEC was carried out and the results can be seen in Section 3.6. This work was carried out to quantify different potentially bioactive components and their effect, these were not present in massive amounts however the profile could be potentially interesting for future identification of active agent within the PPE and groundwork has been performed to that effect.

Viability, in a cellular biology context, can be defined as the ability of a cell to retain the ability to both grow and divide (Pegg, 1989; Stoddart, 2011). The cell viability assay was used to study the effect of PPE when in contact with HDF *in vitro* (Section 3.2.1 & Section 3.3.1). This was done to observe the effect of the PPE on the viability of HDF for up to 72 h and deduce the optimal exposure duration time in the subsequent experiments. For the successful outcome of this project the PPE must be non-cytotoxic at the concentrations utilized. The viability

protocol follows a logic path that is required for the assessment of plant extracts irrespective of the targeted outcome of experimentation. The utilization of one form or another of viability assay as seen in numerous studies involving natural products is an important step in the understanding the effect of the plant extracts on the cell population being studied (Lee et al., 2003; Lombardi et al., 2017; Nemudzivhadi & Masoko, 2014). To that respect, PPE at the concentration of 0.002, 0.004, 0.01, 0.02, 0.04 and 0.08 % caused no visible deleterious effect on cellular viability over a 72-h period, and thus, these concentrations were utilized for subsequent experimentation. The PPEC was also found to have no effect on the HDF viability at the aforementioned concentrations. The important fact of note is when taking into account that the PPE values have been equalised to the PPEC is that on comparing the PPEC to the PPE it highly indicative of the toxic nature of the carrier beyond the 0.08 % concentrations. Further viability studies were carried and these are discussed in subsequent sections related to heat stress (Section 3.2.2 and Section 3.3.2), Oxidative stress (Section 3.2.3) and UV radiation (Sections 3.2.5 – 3.2.7 and Sections 3.3.5 - 3.3.6). However, a summary of the major consequential findings related to the protective effect of the PPE against cellular stressor can be found Section 3.4 and was used to aggregate all findings and identify the peak protective concentration against the cellular stressors utilised in this study. This was seen to be that of PPE 0.04 % and this was as such used for all subsequent experiments.

As seen in Section 3.7 and 3.8 the coded RNA samples were seen to be of exceptional purity and quality fulfilling the requirements for processing. The first step in the analysis of the RNASeq data was to identify the changes in gene expression that were caused by the presence of the propylene glycol (PG) which was vehicle (PPEC) rather than the PPE itself. Through transcriptome analysis, as seen in Section 3.8, the PPE (E) does not seem to have any effect on the unstressed HDFs. Any effect observed in the comparison E-C appears to be predominantly due to the propylene glycol in which the PPE is dissolved. The effect of the PPEC (V) is vital to understanding the key effects of the PPE. In the cells that were not subjected to any form of stress, the differential expression between the PPE (E) and the negative control (C), is similar to that between PPEC (V) and negative control (C) (Section 3.8). Propylene glycol PPEC has proven to have certain effects. One effect is that PG acts as a penetration enhancer, allowing for a more efficient delivery of the bioactive molecule through skin. Also known as sorption promoters or accelerants, it causes a decrease in the barrier resistance of the skin which is reversible. Used as a solvent for many drugs, propylene glycol causes a change in the solubility of the compound in contact with it, possibly causing changes

in the skin lipid layer, making penetration of hydrophilic compounds easier (Allaw et al., 2020; Carrer et al., 2020). PG has been proven to specifically increase the permeability of the skin to plant extracts (Zhang, Q. et al., 2011). Identified also as an antioxidant, PG has been found to suppress the production of oxidative stress by causing a reduction of oxidative tension and inhibition of ROS production (Kao et al., 2021; Nishigori et al., 1995; Volkov et al., 2021). These properties may contribute to the observed protective effect of PPEC on the HDFs when exposed to oxidative stress (Section 3.2.3).

These observations however, do not necessarily infer that the PPE is ineffective. In fact, when the PPE-treated HDFs were also subjected to either heat stress or oxidative stress many DEGs were observed. This implies that the PPE plays an active role in a stressed cellular environment while all the while showing no phenotypic observed effect when the cell is unstressed. Two questions that arise are ‘does PPE attenuate stress?’ and ‘is this due to the effect of the vehicle?’ Comparative analysis of the RNA sequencing data of the treated primary fibroblasts, both heat-treated HE-HV and oxidative stress-treated OE-OV, indicates that the PPE has actually had its own effect irrespective of the vehicle, with DEGs being up or downregulated with relation to the vehicle alone.

4.2. Effect of heat stress on human dermal fibroblasts

Cells grow optimally in a relatively narrow range of temperature, tolerating only moderate deviation from the optimal. However, such deviations may have structural or functional consequences on the cells, as well as the activation of the eukaryotic heat shock response. This results in an alteration in gene expression and the synthesis of plethora of cytoprotective proteins known as heat shock proteins (Verghese et al., 2012). Heat stress protocol C which consisted of a thermal dose of 44° C for a duration 1 h was utilized to bring about a stress response in HDF cells (Hitraya et al., 1995; Pedersen & Gregersen, 2010). Through the utilisation of viability assays this stress response in HDFs (Section 3.2.2 and Section 3.3.2) was noted as a significant reduction in viability in negative control

The effect a thermal insult may have on a cell and its viability is dependent on the thermal dose (temperature + time) as well as the cell type (Roti Roti, 2008). On average heat stress becomes evident in eukaryotic cells when the temperature is 3 - 8°C above normal (Welch & Suhan, 1985). This small temperature increase can cause extensive protein denaturation and may result in a massive imbalance in proteostasis, precipitating many of the phenotypic effects and counter effects (enhanced synthesis of HSPs) of heat shock, as well the production of ROS which has its own deleterious effects upon the cell (Lepock, 1997; Lepock, 2005; Richter et al., 2010; Roti Roti, 2008). Heat Stress (44 °C 1 h) was utilized in a manner where a stress response was observed in HDF. This stress effect on HDF was noted as a significant reduction in viability (Section 3.2.2 and Section 3.3.2) when compared to the corresponding negative control. This cytotoxic response was transient in nature and decreased as a result of temporal distance from insulting stimuli until was no longer apparent after 72 h (24 h > 47 h > 72 h).

Stress conditions such as heat stress can be a major cause of protein destabilization and misfolding, which can in turn trigger signaling pathways leading to repression or activation of important cellular functions (Alderson et al., 2016). Stress proteins which are produced in response to improperly folded or denatured proteins are key to the protection from further denaturation as well as to the proper folding of these proteins. The aggregation of proteins and overall imbalance in protein homeostasis acts as the main explanation of the morphological and phenotypic impacts of heat stress. – in this case proving that a classic heat stress response has been activated in the current study, this is done by analyzing the response to the noxious buildup of unfolded proteins by the nHDFs. A point of note is that this implies that cells can

not directly detect heat stress, but rather detect the unfolded or improperly folded proteins caused by this stress (Richter et al., 2010).

The HSP 70 family of proteins is one of the more known stress proteins which are key components in the stress response and anti-stress mechanisms (Brocchieri et al., 2008; Tavaria et al., 1996). The HSP 70 protein family contains multiple genes which have been upregulated in H-C as seen in Table 3.6 and Figure 3.64. These genes show a response to the protein damage caused by heat stress and are known to be induced by heat shock, with the HSP70 proteins known to be particularly important in protecting proteins in times of cell stress and a sign of a heat stress response (Lu et al., 2023; Nagayach et al., 2017; Ran et al., 2007). The expression of these genes indicates that the HDFs are reacting in a predicted manner to the heat shock they were subjected to and a successful heat- stress model has been established. This is highlighted by the difference in expression levels of these genes between the control and the nHDFs subjected to heat shock.

Also of note is the upregulation of the gene *DNAJA4* (log2fold of 1.68) which is a member of the HSP40 heat shock protein family. It acts as a co-chaperone to the HSP70 proteins mentioned previously and aids in cellular protection after stress induced damage (Sun et al., 2018). Heat shock proteins have also been found to influence the inflammatory response by inducing the release of cytokines (Cantet et al., 2021). This can be observed in the comparison H-C in the upregulation of the cytokine-coding genes as seen in Figure 3.63. By upregulating various pro-inflammatory cytokines, HSPs act as a signal to danger to the immune system at the damage site (Tsan & Gao, 2004).

In the absence of substantial DNA damage due to heat shock, it has also been theorized that heat can cause a domino effect of changes in chromatin which upregulate DNA damage responses (Oei et al., 2015). This is in line with the observations from this study, with DNA repair being one of the significant upregulated pathways. The top genes involved in this pathway and their function can be seen in Table 3.5. Other indications of the effect of the thermal stress on the nHDFs include the downregulation of the biological adhesion and cell adhesion pathways as well as the extracellular matrix pathway. Hyperthermia has been known to decrease levels of integrins (receptors in animal cells involved in binding to the intracellular matrix (Takada et al., 2007), causing the adhesion of the HDFs to be weakened.

The heat shock response tends to upregulate many stress-induced genes. The most obvious indicator of a functioning heat shock response however is the upregulation of genes coding for

HSPs (Toivola et al., 2010). This makes it clear that the heat shock response in this study was in line with the classic response expected.

When looking at the top DEGs for the comparison H-C, the upregulation of various long non-coding RNAs (lncRNAs) can be noted (Table 3.7). LncRNAs are characterised by having over 200 nucleotides in length, lack protein-coding potential and are produced by around 75% of the genome (Sun et al., 2018). LncRNAs have been found to have an important role in the heat shock response by interacting with transcription factors and proteins involved in the stress response, with the presence of lncRNAs being identified when various animal cells were subjected to heat stress. Research indicates that the lncRNAs can act as first responders to heat stress and are functionally fundamental for the regulation of heat stress related genes in a post-transcriptional manner (Audas & Lee, 2016; Dou et al., 2021; Place & Noonan, 2014). Although research into which specific lncRNAs are expressed in response to heat shock as well as specific lncRNA functions is still in its infant stages, the mere presence of the upregulated lncRNAs in the comparison H-C are potentially indicative of standard heat stress response.

4.3. Effect of PPE / PPEC on human dermal fibroblasts subjected to heat stress

A pronounced protective effect was observed to various extents with PPE concentrations (0.002, 0.004, 0.01, 0.02, 0.04 and 0.08 %) at both 24 h and 48 h post heat stress (44 °C 1hr) using Cell-Titre Glo (Section 3.2) and Preston Blue (Section 3.3) assays. A summary of the result can be seen in Section 3.4 and clearly indicate that the protective effect conferred by the PPE is evident up until PPE (0.08 %) and reaches its peak at PPE (0.04%). This is indicative that the PPE confers thermal protection to the HDF. This form of thermal protection has been noted in previous studies and provides a clue to a possible mode of action of the PPE (Belhadj Slimen et al., 2014). Furthermore, other extracts originating from the prickly pear have been seen to affect HSP production in invertebrates such as brine shrimp *Artemia franciscana* (Baruah et al., 2012). Since HSPs have an important role in the cellular heat stress response, this is indicative that components of PPE influence the regulation of HSP production.

Primary fibroblasts were pre-treated with PPE and incubated at 44˚C for one hour. Under these conditions, the main observations obtained from differential gene analysis (DEG2) of the RNA sequencing data reveal that the level of expression of a greater number of genes is

altered when the HE (heat-treated extract) sample is compared to the H (heat-treated sample) and also when compared to the HV (heat-treated vehicle) sample (Figure 3.65). The differential expression between HE and H shows an upregulation of 1679 genes and a downregulation of 2096 genes. On the other hand, analysis the differential expression of HV and H showed an upregulation of only 660 genes and a downregulation of 768 genes. In fact, a comparison of the altered gene expression amongst HE and HV resulted in an upregulation of 276 genes and a downregulation of 625 genes. This suggests that the under these conditions of induced thermal stress, the PPE is exerting an effect due to its own properties, in addition to the putative contribution by the vehicle.

Enrichment analysis of the RNA sequencing data for the comparison HE-H showed a downregulation in morphogenesis, differentiation and development, a downregulation of the cell cycle process, an increase in cellular quiescence and an upregulation in cellular response to protein folding (Table 3.8, Table 3.9). These findings help shed light on the possible mechanisms and processes which are being induced because of the PPE and therefore which are imparting cellular protection.

Although all samples subjected to heat-treatment (H, HE and HV) showed a decrease in the expression of genes associated with morphogenesis, differentiation and development, this effect was more pronounced in the H samples. Exposure to heat stress has been shown to increase the reactive oxygen species (ROS) in a cell, which cause DNA and protein damage, leading to improperly folded proteins. The capacity for differentiation is also seen to be decreased when cells are exposed to heat shock as well as a decrease in cell division and cell morphology (Belhadj Slimen et al., 2014; Cooke et al., 2003; Shimoni et al., 2020). Mitochondrial function and structure were shown to be directly impaired during periods of heat stress and on a larger scale, heat stress has been shown to cause harm in organism growth and cause increased health problems and a weaker immunity (Lu et al., 2023). The less pronounced decrease in these processes observed in HE is indicative of the PPE's protective effect on cells exposed to heat shock. There were an increased number of genes involved in the anatomical structure morphogenesis pathway in HE-C compared to H-C, consistent with the downregulation of the cell cycle also observed in HE. Although further analysis is required with regards to cell cycle analysis. The reduced expression of pathways related to differentiation and development in HE may be indicative of the PPE's protective effect, with the cells pre-treated with PPE having a less of an effect due to the heat shock, retaining their normal functions exhibited during homeostasis.

Another significant observation was a downregulation in processes related to the cell cycle, mitotic and DNA replication in the PPE heat-treated fibroblasts (HE samples) when compared to the PPE only-treated fibroblasts (E), the only heat-treated fibroblasts (H) and also when compared to the cells which were heat-treated in the presence of the vehicle alone (HV). When compared to the control, the heat-treated samples H and HV resulted in an increase in cell division processes while HE showed no significant change and a down regulation when compared to H or HV. This gives the impression that the PPE is moderating the effect heat shock has on cells. Under these conditions, downregulation of cell division processes may be considered a manner by which the cells may direct their energy and time towards the cell's response to stress and damage repair and away from cell division (Barnum & O'Connell, 2014). Being an energetically demanding process, cell division is only possible if cells have the sufficient energy resources to support it, with growing evidence supporting the theory that metabolism regulates cell cycle progression (Kalucka et al., 2015). Mammalian cells have been known to use glucose as their main source of fuel during proliferation and production of ATP. A decrease in glucose supply to mouse embryonic fibroblasts resulted in a significant effect on cell cycle arrest as a response. This is an adaptation seen in mammalian cells as a response to cellular stress, to ensure the maintenance of viability and integrity until the stress is over (Jones et al., 2005). Considered an adaptive response by cells, downregulation of cell cycle in response to heat stress can also trigger a state known as acquired thermotolerance. This can act as a protection against the effects of heat shock and cell death (Kühl & Rensing, 2000). Cell cycle arrest is consistent with the larger strategy adopted by cells to prevent DNA damage to ensure that the cells may survive and recover without having compromised genomic integrity. If cells experience heat stress-induced cellular damage, it is often more beneficial to undergo processes of repair rather than focusing energy on the cell cycle (Johnson & Cook, 2023). This allows the cells the opportunity to assess the extent of the damage and then initiate repair or apoptosis depending on the extent of the damage as well as prevent damaged DNA from being replicated (Shimoni et al., 2020). These observations are significant because they support the theory that the PPE helps the cells to adjust to heat stress by diverting energy and focusing on damage control and repair. This diversion of energy can also allow the cells valuable time to not only focus on the repair but to restore cellular homeostasis before resuming normal cell function, decreasing the chances of damaged cells affecting the future of the cell line.

A rise in cellular quiescence was concurrent with the above observations, with the downregulation of the mitotic cell cycle pathway being a hallmark for cellular quiescence

Cellular stress and DNA damage are frequently linked to cellular quiescence, causing a reversible stop to cell division. The cellular response to DNA damage is highly dependent on the length and amount of stimulus, and a reversible arrest in the cell cycle. An arrest, particularly at the G2 phase, is known to be triggered as a response to temporary or lower levels of DNA damage (Lukin et al., 2015). Treatment with PPE may have enhanced the tolerance of the nHDFs to heat stress by increasing quiescence which acts as a defence mechanism stopping compromised cells from proliferating and perpetuating the damage. Unlike senescence, quiescence is characterized by the ability of cells to re-enter the cell cycle after arrest. Under these conditions, this cell cycle arrest acts as a preventative measure and helps to preserve the general health and integrity of the cellular structure through its halting of cell replication and division (Marescal & Cheeseman, 2020). Analysis of the results of the viability assays conducted on the nHDFs, demonstrated that even though there was an initial slowing down of growth at 24 h and 48 h, the state of the HDFs was similar to that of the negative control after 72 h. This may be suggestive of quiescence and not senescence however further work is required to confirm this observation. The P53 tumour suppresser protein is induced in response to cell stress and DNA damage in human fibroblasts and is key in inducing either quiescence through temporary cell cycle arrest or senescence in cases of high and irreversible DNA damage (Itahana et al., 2002). The *TP53* gene codes for the P53 protein, which is crucial for the growth of cells. The presence of different stressors is known to activate *TP53*, causing it to activate various critical cellular pathways required to maintain cell function and homeostasis. In normal conditions, P53 regulates the cell cycle in response to DNA damage, however when the P53 is mutated it loses its tumour suppression functions , the cell cycle remains unregulated leading to the replication of damaged DNA and unrestrained cell proliferation (Hu et al., 2021; Marei et al., 2021).

The *TP53* in the cell cycle pathway was neither up nor downregulated in the comparison of HE-H (Figure 3.69). This is suggestive that no DNA damage was detected while the cell cycle is notably downregulated and is a avenue that deserved futher study. This brings to question whether the PPE influenced the cell cycle itself and bypassed P53 signalling. Of note to this hypothesis is the upregulation of the genes *GADD45G* (log2fold 2.48) and *GADD45A* (log2fold1.93) (Figure 3.71), P53 target genes which have been observed to be key to causing cell cycle arrest during early mitosis in human fibroblasts (Lukin et al., 2015). An increased expression of *GADD45* is significant as it does not induce the typical morphological changes usually characterised by P53 expression (Wang et al., 1996; Wang et al., 1999). It is important

to note that although both *GADD45A* and *B* genes are expressed in the comparison HV-H, they are significantly upregulated when comparing HE-HV showing the effect of the PPE on their expression. *MDM2* codes for the main P53 inhibitor, binding to and inactivating P53 by targeting it for proteosome degradation under normal conditions. P53 activity is greatly affected by its negative regulator, with overexpression of MDM2 not usually observed in cases of P53 mutation (Hu et al., 2021). Under normal conditions, the expression of P53 activates *MDM2* which in turn represses the activation of the protein, creating a negative feedback loop which regulates the P53 expression levels (Mendoza et al., 2014). When comparing the different expression levels, *MDM2* can be seen to be expressed more in HE while the expression of *TP53* remains the same in H, HE and HV (Figure 3.71). This opens the interesting possibility that the MDM2 upregulation possibily lead to MDM2 protein formation and is inhibiting the P53 while the downregulation of the cell cycle process still proceeds however protein expression levels need to be analysed for this to be confirmatory For P53 activation in times of stress, the mechanism of MDM2 effect needs to be interrupted (Chène, 2003; Haronikova et al., 2021; Hu et al., 2012; Moll & Petrenko, 2003). This observation in HE indicates that the presence of the PPE is protecting the nHDFs from the heat stress, maintaining normal function where possible.

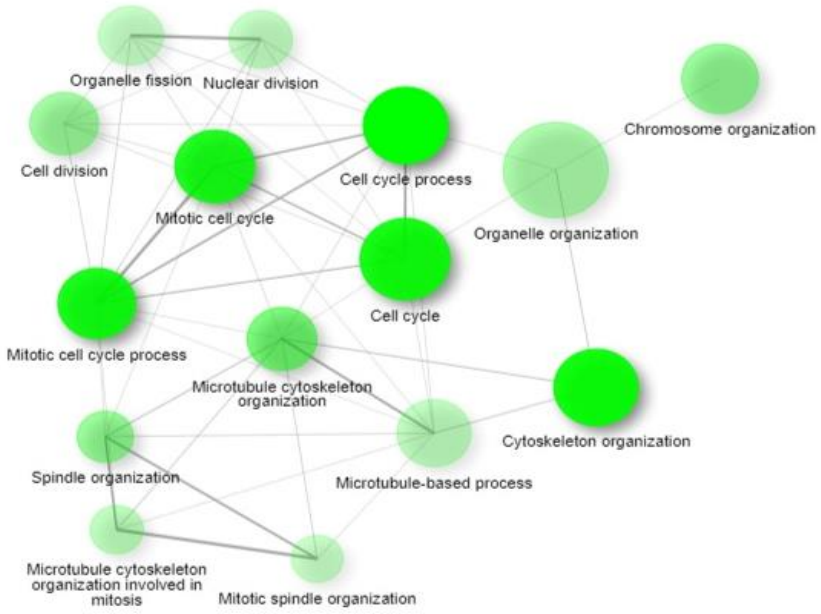

Figure 4.1: Enrichment analysis for the DEGs GO biological process for the comparison HE-H using iDEP (Ge et al., 2018). Network pathway diagram shows the linkage between top downregulated pathways.

The relationship between the cell cycle pathway and other pathways can be seen in the network pathway diagram seen in Figure 4.1. As discussed previously, the downregulation of the cell cycle causes a cascade effect which also decreases cell division, causing quiescence (Marescal & Cheeseman, 2020).

Together with the downregulation of the cell cycle, a marked increase in upregulated pathways related to response to unfolded/incorrectly folded proteins and protein folding in the endoplasmic reticulum was observed. Although this response is seen in the comparison HV-H, it is further upregulated by the PPE as seen in the comparison HE-HV. It may be hypothesised that the nHDFs exposed to PPE prior to heat shock experience a downregulation in cell cycle process to conserve energy and an upregulation of pathways that protect cells against stress instead.

A disruption in protein homeostasis results in a cellular response. There are two main cellular systems know to combat these effects: the heat shock system (HS) and the unfolded protein response (UPR). The latter describes the pathways related to the role of the endoplasmic reticulum in protein folding in response to cellular stresses such as heat shock (Acosta-Alvear et al., 2018). When exposed to heat stress, cells tend to follow a very similar UPR response, with activation of the genes *DNAJB9* and *HSPA5*, both of which are upregulated in HE-H with a log2fold of 3.47 and 4.18 respectively (Figure 3.72, Table 3.12) (Heldens et al., 2011). Heat stress has been found to cause endoplasmic reticulum stress (ER stress) by triggering an accumulation of proteins in the ER which are improperly folded. The UPR is the pathway which is then triggered as a way for the cell to respond to ER stress (Doerrler & Lehrman, 1999; Liu, Yu & Chang, 2008; Sharma et al., 2021). A key element in the UPR is the heat shock protein coded for by the gene *HSPA5* and is the main chaperone in the ER. *HSPA5* was seen to have a log2fold of 4.18 in HE-H showing its upregulation as a response to heat stress triggering the ER stress response (Nowakowska et al., 2020). The endoplasmic reticulum is the site where most transmembrane proteins are synthesized and these ER pathways are crucial to cell physiology. ER stress, the common term for protein-folding imbalances is a common link in the activation of the UPR. This UPR is key pro-survival mechanism that leads to a reduction in quantity of unfolded proteins and results in improved cell survival (Hetz, 2012; Liu, Man & Dudley, 2018). Mitigation of ER stress is an important cellular response to avoid the triggering of apoptosis and ensuring the possibility of cell recovery from damage (Walter & Ron, 2011). An upregulation in pathways related to protein synthetic machinery was noted, further indicating the protein response by the nHDFs. Protein synthesis occurs in the ribosomes

through the function of mRNA transcription , with ribosome and RNA activity both seen to be upregulated pathways (Hoerter & Ellis, 2023; Vanzi et al., 2003). Being an energy-demanding process, ribosome biogenesis is usually decreased when cells are under conditions of stress (Albert et al., 2019). Classically, the decrease in ribosome biogenesis is regulated by the P53 tumour suppressor, leading to a decrease in cell cycle and is usually induced in response to DNA damage (Gentilella et al., 2017; Jiao et al., 2023). When treated with the PPE, cells undergoing heat stress were observed to have an increase in ribosome biogenesis and a decrease in cell cycle, without the upregulation of P53. This perhaps indicates that DNA damage was not detected, and the PPE is expressing the various pathways to impart its protective effect on the nHDFs.

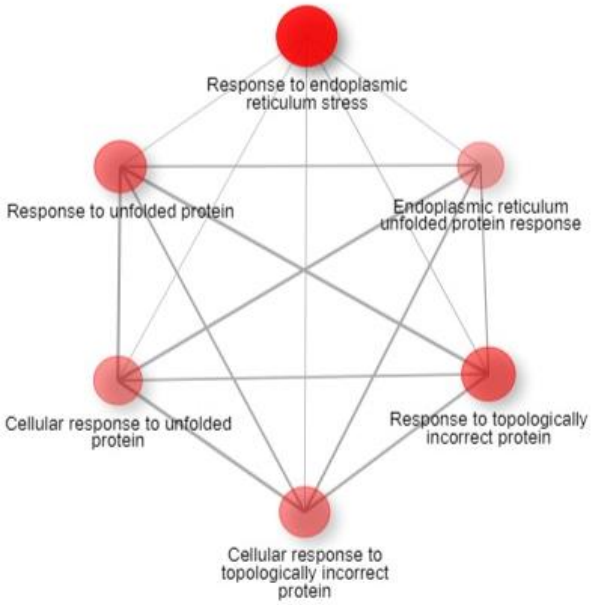

Figure 4.4: Enrichment analysis for the DEGs GO biological process for the comparison HE-H. Network pathway diagram shows the linkage between top upregulated pathways. Protein folding and endoplasmic reticulum pathways are all linked with at least 30% of genes being shared between linked pathways.

Table 3.12 and Figure 3.72 show DEGs in the comparison HE-H which show a significant upregulation and are classically known and associated with a functional UPR (Dombroski et al., 2010; Rouillard et al., 2016). When compared to heat shock alone, these genes show that the PPE has propelled the nHDFs into a higher state of stress-response and management by upregulating pathways related to UPR. A significant observation is that the highest level of

expression of these genes is in HE, showing that even though the vehicle has had an upward effect on these pathways, the PPE keeps amplifying this stress response**.**

Cellular response to unfolded and improperly folded proteins was also significant when the nHDFs were exposed to heat shock without pre-treatment with PPE. This is not to say that the PPE has had no effect, but rather that the PPE has enhanced and further upregulated the stress-response pathways already being followed and on top of that has also activated further mechanisms of stress-response. This can be seen when comparing the DEGs in the comparison H-C which were identified as key to heat stress response, to their expression in HE-H. All genes previously identified in H-C are seen to be also expressed in HE-H, with two genes – *HSPA1A* and *HSPA1B* – being further upregulated in HE-H. This indicates the enhanced effect of the PPE on the heat stress response of the nHDFs. The KEGG cycle diagram (Figure 3.74) for 'protein processing in the endoplasmic reticulum' for the comparison HE-HV highlights that although the vehicle (PG) is having an effect on the UPR, the PPE is having its own effect as well as further upregulating genes expressed in HV-H.

Overall, it can be observed that the PPE seems to not only impart protection from heat stress but also offer stress response mechanisms to counteract any possible damage. Even though certain effects have been also observed when the nHDFs were exposed to heat stress as well as when the nHDFs were treated with the vehicle alone prior to heat stress, the PPE seems to enhance and improve on said effects to provide further protection.

The scratch assay results (Section 3.5) for PPE concentrations (0.002 %, 0.004 %, 0.04 % and 0.08 %) following heat stress protocol C exposure do not show inter-scratch variation and thus commenced with comparable denuded areas. The pre-treatment with PPE was shown to have a significant effect on proliferation/migration of HDF when compared to the corresponding negative control lacking PPE pre-treatment. This pronounced protective effect indicated by a deceased percentage of the denuded area was observed most notably with PPE concentrations at 0.04 % at 12 h (by 3 %), 0.004 % (by 4 %) and 0.04 % (by 6 %) at 24 h, 0.004 % (by 3 %) and 0.04 % (by 5 %) at 36 h and 0.002 % (by 4 %) at 48 h when compared to the corresponding negative control. The PPE concentration (0.08 %) was seen to have an overall negative effect on HDF migration and proliferation as denuded area appeared to remain at the same percentage from 24 – 48 h. However, although the scratch assay has shown that the PPE at various concentrations to be protective against heat stress 44°C in HDF, it does not shed further light

on the mechanisms of action, however the results are supportive of the viability assay outcome except for PPE (0.08%).

Wound resolution using a scratch assay was observed to be prolonged on exposure to heat shock, however comparatively hastened in cells which were pre-treated with PPE. This points towards the cells being somehow protected from the effect of the heat stress, allowing them to follow the usual procedure of wound healing.

Fibroblasts can produce an epidermal growth factor receptor ligand known as epiregulin (EREG), coded for by the gene *EREG* which was seen to be significantly upregulated in HE-H (Table 3.14). This growth factor plays a role in wound healing migration when expressed in fibroblasts. In fact, *EREG* is found to be one of the genes which is most altered during wound healing and activation of normal or even quiescent fibroblasts. A study on the presence of EREG on wound gap closure showed a significant acceleration in wound healing, indicating the important role of *EREG* on wound healing (Iwata et al., 2021; Neufert et al., 2013; Wang et al., 2019).

Another gene which corroborates the observed faster wound closure is *TM4SF1* which was found to be upregulated. Coding for a membrane protein, *TM4SF1* helps to organise membrane and cytoskeleton interactions and facilitates migration of fibroblasts. The use of wound healing assay to investigate the relationship of the gene found that its downregulation was seen to impair wound closure (Xu, Mingyuan et al., 2020; Zukauskas et al., 2011).

Cell migration is one of the hallmark signs of the complex process that is wound repair and healing, with myosin being a key factor in this process. The class 1 myosin motor protein *MYO1G* was found to be upregulated in the comparison HE-H. Class 1 myosins bind to actin filaments and the plasma membrane, allowing for their effect on the motility of the cell. The MYO1G protein was found to have a role in regulating the force exerted on the membrane by actin filaments which help with cell shape and forming of structures during cell migration. Without the protein, cells have reduced capacity to make the membrane structures required during migration (Cruz-Zárate et al., 2021; Lopez-Ojeda et al., 2023).

The presence of these upregulated genes (Table 3.14) all point towards a better scenario for wound healing in the HDFs pretreated with PPE compared to those only treated with heat shock, indicating the effect of the PPE on prevention of cellular damage and a return to normal cell function.

4.4. Effect of oxidative stress on human dermal fibroblasts

Oxidative stress is a state in which the net production and retention of reactive oxygen species (ROS) within cells outweighs the intrinsic ability of a biological system to nullify and remove these reactive species (Pizzino et al., 2017). This was achieved *in vitro* through the utilization of menadione, an important tool in the study of oxidative stress that is utilized as a model for studies of oxidative damage due to the mechanism to which a cytotoxic effect is instigated, through the generation of large quantities of ROS through the transfer of electrons from the electron transport chain directly to oxygen which can overwhelm the standard biological defenses and lead to cellular injury and death (Castro et al., 2008; Chung et al., 1999; Goffart et al., 2021). Menadione (25 µM, 12.5 µM and 6.25 µM) was utilized in a manner where a stress response was observed in HDF. This stress effect on HDF was noted as a significant reduction in viability (Section 3.2.3 & Section 3.2.4) when compared to the corresponding negative control. This cytotoxic response was only intensified by increased duration of exposure (4 h > 2 h) as well as menadione concentration (25 µM >12.5 µM > 6.25 µM). This pattern of cytotoxic response is normal and is supported by various studies (Laux & Nel, 2001; Loor et al., 2010; Morrison et al., 1985). In this case the lowest level of menadione (6.25 µM) to induce a loss of HDF viability was selected in order to study the effect of mild oxidative stress and the effect PPE has at reducing this at a cellular level.

HDFs are part of the framework of the largest organ in the body and the first line of defense for the human immune system– the skin. Reactive oxygen species (ROS) are oxygen-containing molecules known to be chemically reactive and are naturally formed as byproducts of oxygen metabolism. At high levels, often due to external stresses on cells, ROS levels can overwhelm the natural levels of antioxidants in the cells, resulting in oxidation stress. The increased levels of ROS can cause DNA and protein damage leading to an increase in apoptosis. In times of oxidative stress, cells are known to protect themselves by inducing anti-oxidant protection (Liu et al., 2015; Matés, 2000; Scandalios, 2002). An increase in ROS and decrease in ROS removal leading to the lack of regulation of cellular senescence have long been linked to cellular aging. Thus, investigating the anti-oxidative role of cells has been an active field of research in molecular biology. Nevertheless, the exact effect and role of oxidative stress on age still remains a topic of controversy, due to the fact that it alone cannot explain the aging process in full (Gladyshev, 2014; Harman, 1956; Iakovou & Kourti, 2022).

The study of cell response to oxidative stress can be highly varied with different results, making comparing of studies on the effects of oxidative stress on cellular response difficult to compare. Cell viability can be one way to further assess cellular sensitivity to oxidative stress in the hopes of understanding the particular response occurring (Shatrova et al., 2016). The two primary HDF cell lines used in this study were treated with menadione concentrations of 25μM, 12.5μM and 6.25μM and exposed for two and four hours. The results from the viability assay showed a decrease in viability with increased menadione concentration and longer exposure time. Given the extent of the effect on cell viability, the conditions chosen for RNA extraction and analysis were a concentration of 6.25μM and exposure time of two hours**,** the lowest concentration and time. The purpose of this was to keep cell death to the minimum in hopes of understanding the underlying oxidative response however the concentration and exposure time might have been too low to analyze this and might indicate why the oxidative response was not overwhelmingly obvious in O-C. It seems to be that the oxidative stress had minimal effect on the nHDFs at this concentration and time of exposure.

Research has shown a link between oxidative stress and the production of chemokines, with neutrophil-activating chemokines being involved in the inflammation response to oxidative stress. ROS may be detected by the body as danger signals, activating innate immunity. Cytokines have been found to be part of the body's first response (Sozzani et al., 2005). The upregulation of cytokines in the nHDFs exposed to oxidative stress indicated this same possible response (Figure 3.78, Figure 3.79, Table 3.15).

The expression of *IL33* was found to be upregulated in response to oxidative stress (Aizawa et al., 2018) in the comparison of O-C (Figure 3.80). Research into the link between oxidative stress and expression of *IL33* is still ongoing to further document the expression of *IL33* in these scenarios. *IL33* induces an inflammatory response which can lead to harmful effects of cells. NRF2, a transcription factor has been found to regulate this response. The lack of upregulation of NRF2 activating gene (*NFE2L2*) in the comparison O-C indicates that the *IL33* upregulated in response to ROS is not being controlled, which may be the cause of cellular damage (Uchida et al., 2017). *IL33* belongs to a cytokine family which is usually upregulated following conditions which induce inflammation. It acts as an 'alarmin' which is produced once cell necrosis occurs and acts to alert the immune system to damage to tissue and stress. Over-activation of the *IL33* however, can lead to several chronic inflammatory diseases such as asthma due to allergic over inflammation, mostly due to *IL33* inducing the Th2 immune response (Miller, 2011).

The main downregulatory effect seen in O-C involves cellular differentiation, with anatomical structure morphogenesis being the most affected pathway (Table 3.16). A decrease in cell specialization following stress can be crucial for the regulatory processes which need to take place. Prioritization of cell processes needs to take place in order to decrease the overall harm done on the cells, with an increase of ROS production being proven to affect differentiation (Lee et al., 2018). Cell differentiation can lead to an increase to ROS levels, with its downregulation possibly a mechanism to decrease the introduction of further ROS during periods of oxidative stress (Hansberg et al., 2008).

4.5. Effect of PPE/PPEC on human dermal fibroblasts exposed to oxidative stress

A pronounced protective effect was observed to various extents with PPE concentrations (0.002, 0.004, 0.01, 0.02, 0.04 and 0.08 %) at both 2 h and 4 h post menadione exposure picked using Cell-Titre Glo (Section 3.2.3 and Section 3.2.4). A summary of the result can be seen in Section 3.4 and clearly indicate that the protective effect conferred by the PPE up until PPE (0.08 %) and reaches its peak at around PPE 0.04 %. The use of exogenous compounds for the prevention of cellular oxidative stress is not a new concept and numerous compounds have been identified for the alleviation of such stress. Lactate has been seen to improve the medial survival of neuronal cells being exposed to H_2O_2 by 26 % (Tauffenberger et al., 2019). Sulforaphane extracted from broccoli effectively reduces the mean effect dose of menadione significantly on keratinocytes (Gao et al., 2001), *Alpinia officinarum, Glycyrrhiza uralensis* and *Cinnamomun cassia* plant extracts were seen to increase survival of Chinese hamster lung fibroblast (V79-4) cells by 48 %, 42 % and 40 % respectively when exposed to 100 ug/ml H_20_2 (Lee et al., 2003). The results obtained using PPE to negate the oxidative stress are comparable to the above or greater making the values obtained noteworthy and merit further investigation. However, although the viability assay has shown that the PPE (0.002, 0.004, 0.01, 0.02, 0.04 and 0.08 %) provides protection against menadione-induced oxidative stress in nHDF to varying degrees, it did not provide concrete evidence on the exact mechanism of action and thus this remains elusive. However, the very fact that oxidative stress has been negated to such extent may indicate a possible mode of action, namely the upregulation of HSPs or/and the intrinsic antioxidant ability of the PPE or a combination of means that result in the overall observed cytoprotective effect. This hypothesis can be supported by the fact that prickly pear juice has been seen to possess antioxidant abilities (Madrigal-Santillán et al., 2013) and as previously mentioned HSP70 upregulation has been in using different prickly pear extracts (Baruah et al., 2012). The implementation of the scratch assay results for oxidative stress (data not shown) were not able to provide usable data. The reason behind this is that at the prolonged durations required for scratch assay testing (48 h) were not compatible with the cytotoxic effect of menadione at the tested concentrations of 25 µM, 12.5 µM and 6.25 µM. This meant that scratch closure was impossible as cell front migration/proliferation did not occur.

Primary fibroblasts were pre-treated with PPE for one hour prior to being treated with a menadione concentration of 6.25μM for two hours. Under these conditions, the main observations obtained from differential gene analysis (DEG2) of the RNA sequencing data reveal that the level of expression of a greater number of genes is altered when looking at the OE (oxidative exposed HDFs treated with extract) sample compared to O (oxidative exposed HDFs). Comparisons with OV (oxidative exposed HDFs treated with vehicle) also show a greater level of differential expression. The differential expression between OE and O shows an upregulation of 1081 genes and a down regulation of 1159 genes. On the other hand, analysis of the differential expression of OV and O showed an upregulation of 1979 genes and a downregulation of 1968 genes. Despite this greater upregulation by OV, a comparison of the altered gene expression amongst OE and OV resulted in an upregulation of 714 genes and a downregulation of 943 genes (Figure 3.81). This suggests that under these conditions of induced oxidative stress, the PPE is exerting an effect due to its own properties, in addition to the putative contribution by the vehicle.

Just like in the comparison O-C, the most significant downregulated pathways are related to anatomical structure morphogenesis and cell differentiation. Although the downregulated pathways are similar in cellular role, the number of genes involved in these pathways is much greater in OE-OV (Table 3.17), showing a substantially increased response. One such gene is *GJA5* (Table 3.18), a gene which codes for a gap junction protein CX40, also known as connexion 40. Being the main components of gap junctions, connexins are key to the movement of small molecules and ions between cells (Goodenough et al., 1996; Goodenough & Paul, 2009). Gap junctions play a crucial role during the process of morphogenesis and differentiation, with their structure being the perfect channel for the transfer of information during development, allowing for efficient communication between cells and tissues and allowing for different mechanisms to guide and regulate cell differentiation and proliferation (Levin, 2007). CX40 was found to be expressed during neuronal differentiation, cardiac chamber morphogenesis as well as during the differentiation of mature somatic cells (Paige et al., 2015; Talukdar et al., 2022). Fibroblasts are found to also express connexions, allowing for the facilitation of electrical signalling, which is key to the communication between myocytes and fibroblasts or myofibroblasts (McArthur et al., 2015). The downregulation of the morphogenesis and differentiation pathways may possibly be due to the effect of the PPE acting as a protective agent by shifting cell energy away from differentiation and towards pathways which are more needed in times of cell stress. Since cell differentiation was found

to have a link with increased ROS production, the PPE could be acting protectively by decreasing processes which could impact the amount of ROS in the cells (Oka et al., 2022). When studying the role of differentiated and undifferentiated cells in oxidative stress production, undifferentiated cells were seen to impart a better oxidative defence than differentiated cells as well as having a better repair system for DNA strand breaks. It was noted that when cells were in the process of differentiation, the antioxidant capacity of said cells was decreased early on during the process of differentiation (Saretzki et al., 2004; Sart et al., 2015). Therefore, downregulation of differentiation pathways by the PPE equips the cells with a better oxidative defence system.

Various downregulated enriched pathways were observed to be related to a downregulation in RNA and ribosome processing in the comparison OE-O as seen in Table 3.19. This is also reflected in the GAGE analysis for that comparison (Table 3.20). Generally Applicable Gene-set Enrichment (GAGE) is an established method for gene set and pathway analysis which focuses on sets of genes which are related, producing enriched pathways (Luo et al., 2009). Compared to DNA, RNA is usually present in larger quantities in cells, around 4.4 times the amount of DNA in mammals and has been found to be overall more susceptible to oxidative stress in comparison. Although the DNA repair pathway is usually activated in response to DNA damage, they are no such protective mechanisms against RNA damage (Li et al., 2006). Oxidatively damaged RNA has been linked to a reduction in protein synthesis and expression as well as stalling of ribosomes and ribosome functions as well as a decrease in translation (Kong & Lin, 2010). In contrast to the observed decrease in RNA and ribosome metabolism, is the upregulation in DNA repair pathways as seen in the comparison OE-OV. Unlike RNA, damaged DNA cannot be replaced and so, needs to be repaired to avoid further damage to the cells. This is considered one of the main cellular responses to oxidative damage, with cells activating the DNA damage response pathways to repair any double-strand breaks (Maynard et al., 2009). Persistent DNA damage can lead to genomic instability, errors in replication and transcription and ultimately lead to the development of cancer as well as possibly contribute to cellular aging, therefore highlighting the importance of repairing any damaged DNA (Bohr, 2002). The gene *RAD51AP1* (Table 3.21), which codes for the RAD51AP1 protein was seen to be upregulated in OE-OV and is one of the key proteins involved in DNA double-stranded break repair as well as being found to protect against genotoxicity. The PPE therefore seems to be giving the cells a better chance at survival post oxidative stress by not only decreasing the amount of DNA damage but also repairing any unavoidable, yet repairable damage

(Norbury & Hickson, 2001; Pires et al., 2017; Selemenakis et al., 2022). Also of note is the gene *ESCO2*- which codes for a key protein involved in chromosome separation as well as being key to proper DNA repair, *POLQ* – which codes for a DNA polymerase key to double-strand break repair and the gene *GINS2*, which forms part of a subunit helicase involved in the DNA replication fork (Chi et al., 2020; Mfarej & Skibbens, 2020; Wood & Doublié, 2016).

The main upregulated pathways in OE-OV involve the cell cycle. This was not observed in O-C and therefore appears to be due to the action of the PPE on the nHDFs. Most of the cell cycle effects seem to be due to the chemical nature of the vehicle, with the cell cycle pathway being a significantly downregulated pathway in the comparison OV-O (Table 3.23). It is interesting to note that the PPE seems to be opposing and moderating this downregulation. This may be due to an intrinsic ability of the PPE or due to the fact that the PPEC is diluted to give PPE. ROS are required for progression of stages in the cell cycle and have been identified as important factors in many cell functions (Havens et al., 2006; Heo et al., 2020). Since upregulation of cell cycle is observed in OE-OV, this may indicate that the increased levels of ROS due to oxidative stress have been managed and the cell is returning to its pre-stress levels of ROS, hence the return to a functioning cell cycle. The top upregulated genes in the cell cycle pathway and their function can be seen in Table 3.22.

When looking at the upregulated pathways for the comparison OE-O, a number of pathways related to cellular response to chemical stimulus are observed. However, these are also observed in the comparison OV-O, indicating that these upregulated pathways are due to the effect of the vehicle and not the PPE. This however does not mean that the effect of the extract in relation to these pathways is nullified, but rather that the extract is working in synergy with the vehicle to increase the nHDFs response to the oxidative stress. The vehicle's (PG) role in these pathways is likely due to the anti-oxidative effects of PG. GAGE analysis of the comparison OE-O showed no significant upregulated enriched pathways

Cytokine expression in OE seems to be very similar to that in O with regards to the genes *IL33*, *CXCL3*, *CXCL5*, *CXCL6* and *CXCL8* (Figure 3.85). However, there seems to be an increased expression of these cytokines in OV, possibly due to a concentration effect, with a higher concentration of PG in OV compared to OE. Although it seems that the vehicle might be further upregulating these cytokines, when looking at the comparison OE-OV three of these cytokines are being downregulated (Table 3.24). This indicates that overall, the PPE is having a downregulatory effect, despite the effect of the vehicle. Inflammatory cytokines can be the

trigger for various chronic diseases as well as have an effect on the inflammatory response (Miller, 2011; Taherkhani et al., 2020). Inflammation-related diseases contribute to more than half the deaths world-wide, highlighting the importance of regulating the inflammatory response and likelihood of forming chronic inflammation (Furman et al., 2019; Gabryelska et al., 2019). A downregulation of the *IL33* and other cytokines by the PPE could indicate a decreased need for said cytokines due to the better regulation of the ROS due to an increased response or could also be a protective effect imparted by the PPE to reduce unneeded inflammation. Supporting this theory is the fact that the IL33 protein is not usually observed in resting, unstressed nHDFs (Byrne et al., 2011).

Analysis of the JAK-STAT pathway shows that the PPE affects factors involved in immune system function and immune response. JAK-STAT is the main pathway which regulates the inflammatory response by a cell by sending signals to the nucleus and influencing cellular response. This pathway is also known as the IL-6 pathway, and in fact a downregulation of the *IL6* gene (log2fold -2.1) was observed in the comparison OE-OV (Figure 3.86). Evidence shows that *IL6* is a predictor of malignant cells and is linked to disorders caused by chronic inflammation. An activation of this pathway could lead to various inflammatory diseases and so the downregulation of this pathway by the PPE further corroborates the theory that the PPE is having a protective anti-inflammatory effect (Čokić et al., 2015; Hu et al., 2023; Xin et al., 2020)

One of the genes involved in the JAK-STAT pathway is the *JAK3* gene (Figure 3.87), with the highest expression of this gene being observed in OV. The comparison OE-OV shows a downregulation of the *JAK3* gene with a log2fold of -1.32. The *JAK3* gene holds an important role in immune system functioning and regulation and is known to directly influence the IL-2R pathway in fibroblasts (Fujii, 2007). This pathway has been found to be crucial to the maintenance of immune homeostasis and is known to directly increase the proliferation of T-cells, therefore activating an immune response (Gaffen & Liu, 2004; Peerlings et al., 2021). The observed downregulation of *JAK3* is consistent with the downregulation of pathways on cell differentiation as well as the decreased cytokine activity seen in OE-OV(Rane & Reddy, 1994; Rane et al., 2002). *JAK3* is key to the development of T-cells as part of its role in the immune response and has been found to have an inhibitory effect on the immune response

when expression is decreased. Downregulation of *JAK3* by the PPE is likely part of the PPE's function in prevention of excess inflammation (Kolenko et al., 1999; Wang et al., 2013).

The *SOCS* genes – *SOCS1, SOCS2, SOCS2 – AS1, SOCS3 SOCS4, SOCS5 SOCS6* and *SOCS7*- which code for SOCS (suppressors of cytokine signalling) proteins were also overall expressed more under OE conditions compared to O alone (Figure 3.88). All the *SOCS* genes with the exception of *SOCS1* were also overexpressed in OV. This further points towards the PPE exerting its own effects, together with the effect of the vehicle. SOCS proteins play a central role in the regulation of the immune response and have a role in the regulation of the JAK-STAT pathway and cytokine response. *SOCS1*, in particular, inhibits *JAK1* and *JAK2* and also causes a decrease in the levels of pro-inflammatory cytokines such as IL-6, IFN and various proteins involved in the JAK-STAT pathway (Alexander, 2002; Sobah et al., 2021). Expression of *SOCS1* was found to be a protective response to ROS levels, making the expression of *SOCS1* a cellular defence against oxidative stress. An increase in *SOCS3* activity participates in the promotion of allergic responses while *SOCS2* appears to modulate the immune system and regulate immune and oxidative stress functions (Kim et al., 2020; Monti-Rocha et al., 2019; Oh et al., 2009; Tamiya et al., 2011). The decrease in SOCS expression in OE is consistent with the downregulation of the JAK-STAT pathway and decreased cytokine activity, all pointing towards the ability of PPE to decrease the immune and inflammatory response (Seif et al., 2017). The increase in *SOCS1* expression in OE further points to the effect of the PPE in regulating oxidative stress and ROS levels. With an increase in inflammatory response being associated with multiple chronic illnesses as well as possible formation of tumours, the decrease in inflammatory and immune response to stress as seen through the expression of SOCS genes is an important protective effect imparted by the PPE as well as the effect of PG which has been proven to be an anti-oxidant (Lin & Karin, 2007; O'Shea & Murray, 2008).

When looking at the comparison OE-OV, the genes *LCE2A* and *LCE3D* were found to be upregulated (Table 3.25). Both genes are involved in the keratinisation and formation of the skin barrier, as well as *LCE3D* coding for proteins which are involved in the skin barrier repair as a response to inflammation or injury (Bergboer et al., 2011). Deletion of the *LCE3D* gene causes an incomplete response with regards to the repair of the skin barrier and can lead to chronic proinflammatory repercussions, such as psoriasis – an inflammatory skin disease (Julià et al., 2012). Overexpression of *LCE3* genes, including *LCE3D*, was proposed as possible

treatment to compensate for deletion of the *LCE3C* and *LCE3B* genes which could lead to psoriasis (Karrys et al., 2018).

A DEG of note in the comparison OE-O is the downregulation of *OXTR* (Figure 3.89). Coding for an oxytocin receptor, downregulation of the gene in fibroblasts was found to decrease the levels of oxidative stress in the cells as well as increase the levels of antioxidative enzymes (Deing et al., 2013a; McKay & Counts, 2020). The comparison OE-O did not result in any observed significant increase in anti-oxidant enzymes such as superoxide dismutases, catalse and glutathione peroxidases and reductase. A possible reason could be that the multiple effects of the PPE reduced the need for said enzymes and so they were not produced. Found also to modulate the inflammatory processes with the OXTR protein being produced as a result of an inflammation, the downregulation of the *OXTR* gene is in line with the decrease of the inflammatory response seen in OE. Although knockdown of the *OXTR* gene was found to be linked to an increased expression of *IL6*, *CCL5* and *CXCL10*, this was not observed in the comparisons OE-OV or OE-O (Deing et al., 2013b). The IL-6 cytokine however, was found to have an effect and increase the expression of *OXTR* during an inflammatory response, with the downregulation of the *IL6* gene in OE possibly being linked to the downregulation of *OXTR* (McKay & Counts, 2020; Szeto et al., 2017).

A further hint to the antioxidant capacity of the PPE is the upregulation of the gene *SESN2*. The gene is upregulated in both OE-O and OE-OV, yet not found to be significantly upregulated in the comparison O-C (Table 3.26). This proves that the presence of the PPE has caused the expression of this gene and that its expression is not due to the effect of the vehicle the extract is dissolved in but to the PPE itself. The gene codes for SESN2, a protein associated with the stress response and known to be activated in response to oxidative stress. The protein is known to function as an oxidoreductase and directly target ROS in its attempts to decrease the amount of oxidative stress on a cell and when induced, considered to act as a cellular defender, providing cytoprotection against harmful stimuli (Fan et al., 2020; Lu et al., 2023). Once expressed it works by both a directly influencing the activity of antioxidant enzymes as well as affecting multiply oxidative-stress related signalling pathways (Liu, Yunxia et al., 2021). The expression of this gene further proves the antioxidant as well as protective features of the PPE.

4.6. Effect of UV Radiation on HDFs in the presence/absence of PPE/PPEC

Excessive solar exposure is a well-accepted risk factor for the development and aggravation of several pathologies (Queirós & Freitas, 2019). UVA is minimally attenuated by stratospheric ozone and accounts for the majority of terrestrial UVR (95 %), where its intensity is independent of the time of the day or year (Gasparro, 2000; Park, H. Y. et al., 2009; Skotarczak et al., 2015). UVA has an indirect photosensitization effect on key subcellular biomolecules, mediated by chromophores/photosensitizer such as flavins, porphyrins, tetracyclines, and in most circumstances in the presence of molecular oxygen (DeRosa & Crutchley, 2002). These chromophores absorb a photon of radiation. This leads to their excitation to a higher energy state which causes them to interact with adjacent molecules that undergo energy- or electron transfer resulting in the generation of reactive species capable of inducing oxidation (Cadet et al., 2009; DeRosa & Crutchley, 2002; Wondrak et al., 2006)**.** Although not generally attributed to an overt cutaneous response (sunburn erythema), UVA is still considered as a major causative agent towards the induction of photoaging, immunosuppression and photocarcinogenesis through the generation of reactive oxygen species that have a destructive effect on the structure of proteins and nucleic acids (Gasparro, 2000; Seite et al., 2010). The most dangerous of all the UV radiation, UVC has the shortest wavelength thus the highest energy, however it is absorbed in a large part by the stratospheric ozone layer (Skotarczak et al., 2015). UVC is the most proficient at DNA damage coming in the form of pyrimidine dimers and 6-4 photoproducts in turn making it the most consequential with respect to carcinogenesis (Gentile et al., 2003). However, likely owing to the fact that UVC does not reach the earth's surface and as such this wavelength of UVR remains poorly studied with respect to bio-analysis of toxicity, although artificial sources do exist from welding lights. bactericidal lamps and photocuring devices (Masuma et al., 2013).

The HDFs were exposed to UV radiation in a manner adapted from work carried out by Crowley & Waterhouse, 2016, with UVC doses (10 $\mu J/m^2$ or 25 $\mu J/m^2$) following a similar range to that of work carried out by Latonen, Taya, & Laiho, 2001 and Gentile, Latonen, & Laiho, 2003 and with UVA doses (5 J/cm^2) following a similar range to that of work carried out by Zhang et al., 2020 and Scharffetter et al., 1991. This stress effect on HDF was noted as a significant reduction in viability when compared to the corresponding negative control. This cytotoxic response was only intensified by increased duration of exposure (12 h < 24 h) as well as UVR dose for UVC (10 $\mu J/m^2$ < 25 $\mu J/m^2$). This pattern of cytotoxic response is normal and is supported by various studies include those used to select the UVR doses. While no protective

effect was observed in protecting fibroblasts against the deleterious effects of UVC doses (10 $\mu J/m^2$ or 25 $\mu J/m^2$), using the presto blue assay (Section 3.3.4 – 3.3.6) this was not the case using the Cell-Titre Glo assay (Section 3.2.5 – Section 3.2.7) were a protective effect was observed that decreased with time (12hr > 24 h). Furthermore, a pronounced protective effect was observed to various extents with PPE concentrations (0.002, 0.004, 0.01, 0.02, 0.04 and 0.08 %) at both 12 h & 24 hr post UVA exposure. A summary of the result can be seen in Section 3.4 and clearly indicate the pattern of protective effect conferred by the PPEs.

Limited information is available with respect to the effect of *Opuntia ficus-indica* extracts against UV related damage, however some studies have indicated a potential alleviating effect. Although *Opuntia ficus-indica* extract was not seen to possess any significant sun protective factor (SPF) properties, extract pre-treatment prior to UVA exposure on human keratinocytes appeared to provide a clear protective effect against UV-induced cellular stress processes, including ROS production, GSH depletion and lipid peroxidation as well as a reduction of apoptosis as indicated by the lack of caspase-3 or caspase-7 cleavage (Petruk et al., 2017). Furthermore, opuntiol (6-hydroxy¬methyl-4-meth-oxy-2H-pyran-2-one, C7H8O4). extracted from *Opuntia ficus-indica* was seen to prevent UVA-induced cytotoxicity in NIH-3T3 (Mouse embryo fibroblasts) cells preventing DNA single stand breaks and the loss of mitochondrial transmembrane potential as well as the prevention of UVA mediated ROS generation, lipid peroxidation as well as the loss of enzymatic antioxidant activity (superoxide dismutase [SOD], catalase, and glutathione peroxidase (Ponniresan et al., 2020). *Opuntia humifusa* was seen to protect skin from UVB-induced skin degeneration in HaCaT cells and SKH-1 hairless mice (Park et al., 2017).

4.7. Conclusions

Varying concentration of PPE were seen to provide a cytoprotective effect against the various stressor under study the level of protection in most cases was provided by PPE 0.04 %. Mechanistically the protective effect against heat stress was seen when comparing pathways related to morphogenesis, differentiation and development. There was a larger decrease in these pathways when the HDFs were not exposed to PPE, highlighting that heat stress had a more prominent harmful effect. The downregulation in cell cycle is also indicative of the PPE's protective effect by redirecting energy towards processes of stress response and damage repair. The shift towards cellular quiescence is protective defense mechanism by the PPE to stop any damaged cells from replication during periods of cell stress and damage. The *TP53* gene was neither up nor downregulated in HE while the P53 target genes *GADD45G* and *GADD45A* and P53 inhibitor *MDM2* were upregulated, suggesting that the cell cycle is being downregulated bypassing P53. The protective effect of the PPE is also characterised by the upregulation in pathways related to the cellular response to unfolded and incorrectly folded proteins and protein synthesis, characterised by the upregulation of the *DNAJB9, HSPA5, HSPA1A, HSPA1B* genes. The PPE's effect on wound closure can be characterised by the upregulation of the genes *EREG, TM4SF1* and *MYO1G.* Mechanistically the protective effect against oxidative stress was seen as an increased in expression of genes in various up and downregulated pathways. The downregulated pathways of note are related to anatomical structure morphogenesis and cell differentiation and RNA and ribosome processing, characterised by expression of the gene *GJA5*. The upregulated pathway of note is the upregulation of the DNA repair pathways, cell cycle, characterised by the upregulation of the genes *RAD51AP1, ESCO2, POLQ* and *GINS2*. The upregulation of *SESN2* is further proof of the antioxidant effects of the PPE. The anti-inflammatory properties of the PPE can be seen by the downregulation of inflammatory cytokines *CXCL3, CXCL8, IL33, SOCS* cytokine signaling genes, keratinisation related genes *LCE2A* and *LCE3D,* oxytocin receptor gene *OXTR* as well as the overall downregulation of the JAK-STAT pathway and the genes *IL6, JAK3.*

4.8. Limitations

While this study has provided valuable insights into utilisation of natural products, specifically *Opuntia ficus-indica* extracts carried in a propylene glycol vehicle as a measure for the protection against cellular stressors, it is important to acknowledge certain inherent limitations. Firstly, due to the means of prickly pear extract preparations the effectiveness may vary depending on cultivar, cultivation conditions and extraction process, a variation that could impact the consistency of results. Genetic variation within a population may influence how the extract performs and although two distinct biological replicates (HDF and nHDF) with 9 technical replicates each were utilised with positive findings this does not necessarily translate to the broader populous. This was an *in vitro* study, which although provided valuable mechanistic insights, the findings may not fully replicate the complex interaction that occur within a biological organism and thus translating findings from cellular studies to clinical applications, such as skin cancer prevention or anti-aging treatments, may face challenges in terms of formulation, dosage, and regulatory approval. Access to specific equipment, reagents, and technologies was also in the background as a limiting factor affecting the overall scope and depth experimentation, requiring focusing of limited resourses on targeted techniques rather than spreading funding too thinly. Lastly, although best efforts were made to ensure accurate UVA and UVC doses using the Stratalinker® UV Crosslinker 2400 this apparatus has not been serviced and calibrated on changing of light bulbs as recommended by manufacturer due to age of apparatus and ‘end of life’ with respect to instrument support. Furthermore, research projects have time limitations and conducting comprehensive studies on plant extracts may not be feasible within the scope of a single thesis. It is imperative for future research to consider these limitations and build upon this foundation to further enhance our understanding of this field of research.

4.9. Future Work

Future research serves as a compass, guiding the trajectory of scientific inquiry beyond the scope of this current study. It lays the foundation for prospective investigations aimed at enhancing our understanding of plant-extract triggered cellular mechanisms in safeguarding against cellular stressors both endogenous and exogenous. As we peer into the horizon of future research endeavours, several promising directions emerge, each poised to deepen our comprehension and broaden the applicability of plant extract interventions in dermatological health. These avenues span a spectrum of scientific approaches, from fundamental mechanistic studies to translational applications, with the ultimate aim of contributing to the development of innovative skincare solutions and therapeutic strategies. Through the pursuit of these future research avenues, we aim to not only advance the frontiers of knowledge in plant-based dermatoprotection but also contribute meaningfully to the development of evidence-based interventions that promote skin health and resilience in the face of environmental challenges. Possible avenues may include the repetition of experimentation on different cell cultures such as keratinocytes and melanocytes to observe and understand more comprehensively the effects of the PPE on the cellular population of the dermis. The study of the effect of PPE over chronic period of time or following multiple dosing. The study of PPE that has been produced from a different extraction run carried out by Nutribiotech Services Limited, Malta for any drift in biological efficacy. The multiplexing of PPE and possible synergetic antagonistic effect. The utilisation of different carriers to propylene glycol for the crude prickly pear extract and comparison of biological effects. The identification of the active agent/s within the PPE possibly aided by; thin-layer chromatography, high-performance liquid chromatography, nuclear magnetic resonance and mass spectrometry as well the investigation through bioassays of each fraction for expected biological effect. The confirmation of findings of RNA sequencing through the utilisation of qRTPCR and other molecular techniques such as western blotting. The creation of custom UV exposure system and elucidation effects of PPE on HDFs through RNA sequencing. The study of the potential protective effect of PPE induced by different environmental stressors not included in this study. Lastly the advancement further into preclinical research with respect to the assessment of safety, efficacy and mechanisms of action in animal models as a pretext to clinical trials. Through the pursuit of these future research avenues, the aim is not only to advance the frontiers of knowledge in plant-based dermatoprotection but also contribute meaningfully to the development of evidence-based interventions that promote skin health and resilience in the face of environmental challenges.

References

Acosta-Alvear, D., Karagöz, G. E., Fröhlich, F., Li, H., Walther, T. C., & Walter, P. (2018). The unfolded protein response and endoplasmic reticulum protein targeting machineries converge on the stress sensor IRE1. *eLife, 7*, 10.7554/eLife.43036. 10.7554/eLife.43036

Agar, N., & Young, A. R. (2005). Melanogenesis: a photoprotective response to DNA damage? *Mutation Research, 571*(1-2), 121-132. S0027-5107(04)00490-7 [pii]

Aizawa, H., Koarai, A., Shishikura, Y., Yanagisawa, S., Yamaya, M., Sugiura, H., Numakura, T., Yamada, M., Ichikawa, T., Fujino, N., Noda, M., Okada, Y., & Ichinose, M. (2018). Oxidative stress enhances the expression of IL-33 in human airway epithelial cells. *Respiratory Research, 19*(1), 52. 10.1186/s12931-018-0752-9

Alagar Boopathy, L. R., Jacob-Tomas, S., Alecki, C., & Vera, M. (2022). Mechanisms tailoring the expression of heat shock proteins to proteostasis challenges. *The Journal of Biological Chemistry, 298*(5), 101796. 10.1016/j.jbc.2022.101796

Albert, B., Kos-Braun, I. C., Henras, A. K., Dez, C., Rueda, M. P., Zhang, X., Gadal, O., Kos, M., & Shore, D. (2019). A ribosome assembly stress response regulates transcription to maintain proteome homeostasis. *eLife, 8*, e45002. 10.7554/eLife.45002

Alderson, T. R., Kim, J. H., & Markley, J. L. (2016). Dynamical Structures of Hsp70 and Hsp70-Hsp40 Complexes. *Structure, 24*(7), 1014-1030. 10.1016/j.str.2016.05.011

Alexander, W. S. (2002). Suppressors of cytokine signalling (SOCS) in the immune system. *Nature Reviews.Immunology, 2*(6), 410-416. 10.1038/nri818

Alfred F. Hess, Lester J. Unger. (1921). THE CURE OF INFANTILE RICKETS BY SUNLIGHT: PRELIMINARY NOTE. *Journal of the American Medical Association, 77*(1), 39. 10.1001/jama.1921.02630270037013

Alimi, H., Hfaeidh, N., Bouoni, Z., Sakly, M., & Ben Rhouma, K. (2012). Protective effect of Opuntia ficus indica f. inermis prickly pear juice upon ethanol-induced damages in rat erythrocytes. *Alcohol, 46*(3), 235-243. https://doi.org/10.1016/j.alcohol.2011.09.024

Allaw, M., Pleguezuelos-Villa, M., Manca, M. L., Caddeo, C., Aroffu, M., Nacher, A., Diez-Sales, O., Saur\'\i Amparo Ruiz, Ferrer, E. E., Fadda, A. M., & Manconi, M. (2020). Innovative strategies to treat skin wounds with mangiferin: fabrication of transfersomes modified with glycols and mucin. *Nanomedicine, 15*(17), 1671-1685. 10.2217/nnm-2020-0116

Alt, E., Yan, Y., Gehmert, S., Song, Y. H., Altman, A., Gehmert, S., Vykoukal, D., & Bai, X. (2011). Fibroblasts share mesenchymal phenotypes with stem cells, but lack their differentiation and colony-forming potential. *Biology of the Cell, 103*(4), 197-208. 10.1042/BC20100117 [doi]

Antunes-Ricardo, M., Moreno-García, B. E., Gutiérrez-Uribe, J. A., Aráiz-Hernández, D., Alvarez, M. M., & Serna-Saldivar, S. O. (2014). Induction of apoptosis in colon cancer cells treated with isorhamnetin glycosides from Opuntia ficus-indica pads. *Plant Foods for Human Nutrition (Dordrecht, Netherlands), 69*(4), 331-336. 10.1007/s11130-014-0438-5 [doi]

Apak, R., Özyürek, M., Güçlü, K., & Çapanoğlu, E. (2016). Antioxidant Activity/Capacity Measurement. 1. Classification, Physicochemical Principles, Mechanisms, and Electron

Transfer (ET)-Based Assays. *Journal of Agricultural and Food Chemistry, 64*(5), 997-1027. 10.1021/acs.jafc.5b04739

Ashburner, M., Ball, C. A., Blake, J. A., Botstein, D., Butler, H., Cherry, J. M., Davis, A. P., Dolinski, K., Dwight, S. S., Eppig, J. T., Harris, M. A., Hill, D. P., Issel-Tarver, L., Kasarskis, A., Lewis, S., Matese, J. C., Richardson, J. E., Ringwald, M., Rubin, G. M., & Sherlock, G. (2000). Gene ontology: tool for the unification of biology. The Gene Ontology Consortium. *Nature Genetics, 25*(1), 25-29. 10.1038/75556

Aslantürk, Ö. (2018). In Vitro Cytotoxicity and Cell Viability Assays: Principles, Advantages, and Disadvantages. ()10.5772/intechopen.71923

Atkin, A. S., Moin, A. S. M., Nandakumar, M., Al-Qaissi, A., Sathyapalan, T., Atkin, S. L., & Butler, A. E. (2021). Impact of severe hypoglycemia on the heat shock and related protein response. *Scientific Reports, 11*(1), 17057-8. 10.1038/s41598-021-96642-8

Attard, K., Oztop, M. H., & Lia, F. (2022). The Effect of Hydrolysis on the Antioxidant Activity of Olive Mill Waste. *Applied Sciences, 12*(23)10.3390/app122312187

Audas, T. E., & Lee, S. (2016). Stressing out over long noncoding RNA. *Biochimica Et Biophysica Acta, 1859*(1), 184-191. 10.1016/j.bbagrm.2015.06.010

Autier, P., & Gandini, S. (2007). Vitamin D Supplementation and Total Mortality: A Meta-analysis of Randomized Controlled Trials. *Archives of Internal Medicine, 167*(16), 1730-1737. 10.1001/archinte.167.16.1730

Awad, A. B., & Fink, C. S. (2000). Phytosterols as Anticancer Dietary Components: Evidence and Mechanism of Action. *The Journal of Nutrition, 130*(9), 2127-2130. 10.1093/jn/130.9.2127

Babior, B. M., Kipnes, R. S., & Curnutte, J. T. (1973). Biological defense mechanisms. The production by leukocytes of superoxide, a potential bactericidal agent. *The Journal of Clinical Investigation, 52*(3), 741-744. 10.1172/JCI107236 [doi]

Bae, Y. S., Oh, H., Rhee, S. G., & Yoo, Y. D. (2011). Regulation of reactive oxygen species generation in cell signaling. *Molecules and Cells, 32*(6), 491-509. 10.1007/s10059-011-0276-3

Bardaa, S., Turki, M., Ben Khedir, S., Mzid, M., Rebai, T., Ayadi, F., & Sahnoun, Z. (2020). The Effect of Prickly Pear, Pumpkin, and Linseed Oils on Biological Mediators of Acute Inflammation and Oxidative Stress Markers. *BioMed Research International, 2020*, 5643465. 10.1155/2020/5643465 [doi]

Barnham, K. J., Masters, C. L., & Bush, A. I. (2004). Neurodegenerative diseases and oxidative stress. *Nature Reviews.Drug Discovery, 3*(3), 205-214. nrd1330 [pii]

Barnum, K. J., & O'Connell, M. J. (2014). Cell cycle regulation by checkpoints. *Methods in Molecular Biology (Clifton, N.J.), 1170*, 29-40. 10.1007/978-1-4939-0888-2_2

Baruah, K., Norouzitallab, P., Roberts, R. J., Sorgeloos, P., & Bossier, P. (2012a). A novel heat-shock protein inducer triggers heat shock protein 70 production and protects Artemia franciscana nauplii against abiotic stressors. *Aquaculture, 334-337*, 152-158. 10.1016/j.aquaculture.2011.12.015

Baruah, K., Norouzitallab, P., Roberts, R. J., Sorgeloos, P., & Bossier, P. (2012b). A novel heat-shock protein inducer triggers heat shock protein 70 production and protects Artemia franciscana nauplii against abiotic stressors. *Aquaculture, 334-337*, 152-158. https://doi.org/10.1016/j.aquaculture.2011.12.015

Beere, H. M. (2004). "The stress of dying": the role of heat shock proteins in the regulation of apoptosis. *Journal of Cell Science, 117*(Pt 13), 2641-2651. 10.1242/jcs.01284 [doi]

Belhadj Slimen, I., Najar, T., & Abderrabba, M. (2017). Chemical and Antioxidant Properties of Betalains. *Journal of Agricultural and Food Chemistry, 65*(4), 675-689. 10.1021/acs.jafc.6b04208 [doi]

Belhadj Slimen, I., Chabaane, H., Chniter, M., Mabrouk, M., Ghram, A., Miled, K., Behi, I., Abderrabba, M., & Najar, T. (2019). Thermoprotective properties of Opuntia ficus-indica f. inermis cladodes and mesocarps on sheep lymphocytes. *Journal of Thermal Biology, 81*, 73-81. https://doi.org/10.1016/j.jtherbio.2019.02.018

Belhadj Slimen, I., Najar, T., Ghram, A., Dabbebi, H., Ben Mrad, M., & Abdrabbah, M. (2014). Reactive oxygen species, heat stress and oxidative-induced mitochondrial damage. A review. *Null, 30*(7), 513-523. 10.3109/02656736.2014.971446

Benjamin, I. J., & McMillan, D. R. (1998). Stress (heat shock) proteins: molecular chaperones in cardiovascular biology and disease. *Circulation Research, 83*(2), 117-132.

Benjamini, Y., & Hochberg, Y. (1995). Controlling the False Discovery Rate: A Practical and Powerful Approach to Multiple Testing. *Journal of the Royal Statistical Society.Series B (Methodological), 57*(1), 289-300. http://www.jstor.org/stable/2346101

Bensadón, S., Hervert-Hernández, D., Sáyago-Ayerdi, S. G., & Goñi, I. (2010). By-products of Opuntia ficus-indica as a source of antioxidant dietary fiber. *Plant Foods for Human Nutrition (Dordrecht, Netherlands), 65*(3), 210-216. 10.1007/s11130-010-0176-2 [doi]

Benzie, I. F. F., & Strain, J. J. (1996). The Ferric Reducing Ability of Plasma (FRAP) as a Measure of "Antioxidant Power": The FRAP Assay. *Analytical Biochemistry, 239*(1), 70-76. 10.1006/abio.1996.0292

Bergboer, J. G. M., Tjabringa, G. S., Kamsteeg, M., van Vlijmen-Willems, Ivonne M J J, Rodijk-Olthuis, D., Jansen, P. A. M., Thuret, J., Narita, M., Ishida-Yamamoto, A., Zeeuwen, Patrick L J M, & Schalkwijk, J. (2011). Psoriasis risk genes of the late cornified envelope-3 group are distinctly expressed compared with genes of other LCE groups. *The American Journal of Pathology, 178*(4), 1470-1477. 10.1016/j.ajpath.2010.12.017

Besta, C. (2014, *Primary Fibroblast Culture From Human Skin Biopsy.* . https://www.google.com.mt/url?sa=t&rct=j&q=&esrc=s&source=web&cd=6&cad=rja&uact=8&ved=0ahUKEwiEj4-m4YHMAhUDIg8KHS_0B38QFgg5MAU&url=http%3A%2F%2Fwww.eurobiobank.org%2Fcommon_docs%2FPrimary_fibroblast_culture_from_human_skin_biopsy.doc&usg=AFQjCNEVYRVA7f1W7hVNasZIl2Ibw6eX8A&sig2=8xggqlIWU89u2OY7s0ayNw&bvm=bv.119028448,d.bGg

Beyer, D. M., Faurschou, A., Haedersdal, M., & Wulf, H. C. (2010). Clothing reduces the sun protection factor of sunscreens. *The British Journal of Dermatology, 162*(2), 415-419. 10.1111/j.1365-2133.2009.09478.x [doi]

Bhattacharyya, A., Chattopadhyay, R., Mitra, S., & Crowe, S. E. (2014). Oxidative stress: an essential factor in the pathogenesis of gastrointestinal mucosal diseases. *Physiological Reviews, 94*(2), 329-354. 10.1152/physrev.00040.2012

Bikle, D. (2000). Vitamin D: Production, Metabolism, and Mechanisms of Action. In K. R. Feingold, B. Anawalt, A. Boyce, G. Chrousos, K. Dungan, A. Grossman, J. M. Hershman,

G. Kaltsas, C. Koch, P. Kopp, M. Korbonits, R. McLachlan, J. E. Morley, M. New, L. Perreault, J. Purnell, R. Rebar, F. Singer, D. L. Trence, . . . D. P. Wilson (Eds.), *Endotext* (). MDText.com, Inc. NBK278935 [bookaccession]

Birben, E., Sahiner, U. M., Sackesen, C., Erzurum, S., & Kalayci, O. (2012). Oxidative stress and antioxidant defense. *The World Allergy Organization Journal, 5*(1), 9-19. 10.1097/WOX.0b013e3182439613

Bohr, V. A. (2002). Repair of oxidative DNA damage in nuclear and mitochondrial DNA, and some changes with aging in mammalian cells. *Free Radical Biology & Medicine, 32*(9), 804-812. 10.1016/s0891-5849(02)00787-6

Bouchama, A., Aziz, M. A., Mahri, S. A., Gabere, M. N., Dlamy, M. A., Mohammad, S., Abbad, M. A., & Hussein, M. (2017). A Model of Exposure to Extreme Environmental Heat Uncovers the Human Transcriptome to Heat Stress. *Scientific Reports, 7*(1), 9429. 10.1038/s41598-017-09819-5

Boya, P. (2012). Lysosomal function and dysfunction: mechanism and disease. *Antioxidants & Redox Signaling, 17*(5), 766-774. 10.1089/ars.2011.4405 [doi]

Brenner, M., & Hearing, V. J. (2008). The Protective Role of Melanin Against UV Damage in Human Skin. *Photochemistry and Photobiology, 84*(3), 539-549. 10.1111/j.1751-1097.2007.00226.x

Brocchieri, L., Conway de Macario, E., & Macario, A. J. L. (2008). hsp70 genes in the human genome: Conservation and differentiation patterns predict a wide array of overlapping and specialized functions. *BMC Evolutionary Biology, 8*(1), 19. 10.1186/1471-2148-8-19

Butera, D., Tesoriere, L., Di Gaudio, F., Bongiorno, A., Allegra, M., Pintaudi, A. M., Kohen, R., & Livrea, M. A. (2002). Antioxidant activities of sicilian prickly pear (Opuntia ficus indica) fruit extracts and reducing properties of its betalains: betanin and indicaxanthin. *Journal of Agricultural and Food Chemistry, 50*(23), 6895-6901. jf025696p [pii]

Byrne, S. N., Beaugie, C., O'Sullivan, C., Leighton, S., & Halliday, G. M. (2011). The immune-modulating cytokine and endogenous Alarmin interleukin-33 is upregulated in skin exposed to inflammatory UVB radiation. *The American Journal of Pathology, 179*(1), 211-222. 10.1016/j.ajpath.2011.03.010

Cadet, J., Douki, T., Ravanat, J. L., & Di Mascio, P. (2009). Sensitized formation of oxidatively generated damage to cellular DNA by UVA radiation. *Photochemical & Photobiological Sciences : Official Journal of the European Photochemistry Association and the European Society for Photobiology, 8*(7), 903-911. 10.1039/b905343n [doi]

Camaré, C., Pucelle, M., Nègre-Salvayre, A., & Salvayre, R. (2017). Angiogenesis in the atherosclerotic plaque. *Redox Biology, 12*, 18-34. 10.1016/j.redox.2017.01.007

Cantet, J. M., Yu, Z., & Ríus, A. G. (2021). Heat Stress-Mediated Activation of Immune-Inflammatory Pathways. *Antibiotics (Basel, Switzerland), 10*(11), 1285. doi: 10.3390/antibiotics10111285. 10.3390/antibiotics10111285

Carrer, V., Alonso, C., Pont, M., Zanuy, M., Córdoba, M., Espinosa, S., Barba, C., Oliver, M. A., Martí, M., & Coderch, L. (2020). Effect of propylene glycol on the skin penetration of drugs. *Archives of Dermatological Research, 312*(5), 337-352. 10.1007/s00403-019-02017-5

Castillo, S. L., Heredia, N., Contreras, J. F., & García, S. (2011). Extracts of edible and medicinal plants in inhibition of growth, adherence, and cytotoxin production of Campylobacter jejuni and Campylobacter coli. *Journal of Food Science, 76*(6), 421. 10.1111/j.1750-3841.2011.02229.x [doi]

Castro, F. A. V., Mariani, D., Panek, A. D., Eleutherio, E. C. A., & Pereira, M. D. (2008). Cytotoxicity mechanism of two naphthoquinones (menadione and plumbagin) in Saccharomyces cerevisiae. *PloS One, 3*(12), e3999. 10.1371/journal.pone.0003999

Chanock, S. J., el Benna, J., Smith, R. M., & Babior, B. M. (1994). The respiratory burst oxidase. *The Journal of Biological Chemistry, 269*(40), 24519-24522. S0021-9258(17)31418-7 [pii]

Chau, L. (2015). Heme oxygenase-1: emerging target of cancer therapy. *Journal of Biomedical Science, 22*(1), 22. 10.1186/s12929-015-0128-0

Chen, J., Liu, Y., Zhao, Z., & Qiu, J. (2021). Oxidative stress in the skin: Impact and related protection. *International Journal of Cosmetic Science, 43*(5), 495-509. 10.1111/ics.12728

Chène, P. (2003). Inhibiting the p53–MDM2 interaction: an important target for cancer therapy. *Nature Reviews Cancer, 3*(2), 102-109. 10.1038/nrc991

Chi, F., Wang, Z., Li, Y., & Chang, N. (2020). Knockdown of GINS2 inhibits proliferation and promotes apoptosis through the p53/GADD45A pathway in non-small-cell lung cancer. *Bioscience Reports, 40*(4), BSR20193949. doi: 10.1042/BSR20193949. 10.1042/BSR20193949

Chong, W. C., Shastri, M. D., & Eri, R. (2017). Endoplasmic Reticulum Stress and Oxidative Stress: A Vicious Nexus Implicated in Bowel Disease Pathophysiology. *International Journal of Molecular Sciences, 18*(4), 771. 10.3390/ijms18040771

Chung, S., Chung, S., Lee, J., Kim, S., Park, K., & Chung, J. (1999). The biological significance of non-enzymatic reaction of menadione with plasma thiols: enhancement of menadione-induced cytotoxicity to platelets by the presence of blood plasma. *FEBS Letters*, *449*(2), 235-240. https://doi.org/10.1016/S0014-5793(99)00452-4

Church, D. F., & Pryor, W. A. (1985). Free-radical chemistry of cigarette smoke and its toxicological implications. *Environmental Health Perspectives, 64*, 111-126. 10.1289/ehp.8564111 [doi]

Čokić, V. P., Mitrović-Ajtić, O., Beleslin-Čokić, B. B., Marković, D., Buač, M., Diklić, M., Kraguljac-Kurtović, N., Damjanović, S., Milenković, P., Gotić, M., & Raj, P. K. (2015). Proinflammatory Cytokine IL-6 and JAK-STAT Signaling Pathway in Myeloproliferative Neoplasms. *Mediators of Inflammation, 2015*, 453020. 10.1155/2015/453020

Conklin, K. A. (2004). Chemotherapy-associated oxidative stress: impact on chemotherapeutic effectiveness. *Integrative Cancer Therapies, 3*(4), 294-300. 3/4/294 [pii]

Cooke, M. S., Evans, M. D., Dizdaroglu, M., & Lunec, J. (2003). Oxidative DNA damage: mechanisms, mutation, and disease. *FASEB Journal : Official Publication of the Federation of American Societies for Experimental Biology*, *17*(10), 1195-1214. 10.1096/fj.02-0752rev

Corchete, L. A., Rojas, E. A., Alonso-López, D., De Las Rivas, J., Gutiérrez, N. C., & Burguillo, F. J. (2020). Systematic comparison and assessment of RNA-seq procedures

for gene expression quantitative analysis. *Scientific Reports*, *10*(1), 19737. 10.1038/s41598-020-76881-x

Cory, H., Passarelli, S., Szeto, J., Tamez, M., & Mattei, J. (2018). The Role of Polyphenols in Human Health and Food Systems: A Mini-Review. *Frontiers in Nutrition, 5*, 87. 10.3389/fnut.2018.00087

Crowley, L. C., & Waterhouse, N. J. (2016). Triggering Death of Adherent Cells with Ultraviolet Radiation. *Cold Spring Harbor Protocols*, *2016*(7), 10.1101/pdb.prot087148. 10.1101/pdb.prot087148 [doi]

Cruz-Zárate, D., López-Ortega, O., Girón-Pérez, D. A., Gonzalez-Suarez, A., García-Cordero, J. L., Schnoor, M., & Santos-Argumedo, L. (2021). Myo1g is required for efficient adhesion and migration of activated B lymphocytes to inguinal lymph nodes. *Scientific Reports, 11*(1), 7197. 10.1038/s41598-021-85477-y

Davies, K. J. (2000). Oxidative stress, antioxidant defenses, and damage removal, repair, and replacement systems. *IUBMB Life, 50*(4-5), 279-289. 10.1080/713803728 [doi]

De Cock, R., Knibbe, C. A. J., Kulo, A., de Hoon, J., Verbesselt, R., Danhof, M., & Allegaert, K. (2013). Developmental pharmacokinetics of propylene glycol in preterm and term neonates. *British Journal of Clinical Pharmacology, 75*(1), 162-171. 10.1111/j.1365-2125.2012.04312.x

Debacq-Chainiaux, F., Leduc, C., Verbeke, A., & Toussaint, O. (2012). UV, stress and aging. *Dermato-Endocrinology, 4*(3), 236-240. 10.4161/derm.23652

Deing, V., Roggenkamp, D., Kühnl, J., Gruschka, A., Stäb, F., Wenck, H., Bürkle, A., & Neufang, G. (2013a). Oxytocin modulates proliferation and stress responses of human skin

cells: implications for atopic dermatitis. *Experimental Dermatology, 22*(6), 399-405. 10.1111/exd.12155

Deing, V., Roggenkamp, D., Kühnl, J., Gruschka, A., Stäb, F., Wenck, H., Bürkle, A., & Neufang, G. (2013b). Oxytocin modulates proliferation and stress responses of human skin cells: implications for atopic dermatitis. *Experimental Dermatology, 22*(6), 399-405. 10.1111/exd.12155

Del Socorro Santos Díaz, Barba de la Rosa, A. P., Héliès-Toussaint, C., Guéraud, F., & Nègre-Salvayre, A. (2017). Opuntia spp.: Characterization and Benefits in Chronic Diseases. *Oxidative Medicine and Cellular Longevity, 2017*, 8634249. 10.1155/2017/8634249 [doi]

DeRosa, M. C., & Crutchley, R. J. (2002). Photosensitized singlet oxygen and its applications. *Coordination Chemistry Reviews, 233–234*, 351-371. https://doi.org/10.1016/S0010-8545(02)00034-6

Di Meo, S., Reed, T. T., Venditti, P., & Victor, V. M. (2016). Role of ROS and RNS Sources in Physiological and Pathological Conditions. *Oxidative Medicine and Cellular Longevity, 2016*, 1245049. 10.1155/2016/1245049

Díaz-Villanueva, J. F., Díaz-Molina, R., & García-González, V. (2015). Protein Folding and Mechanisms of Proteostasis. *International Journal of Molecular Sciences, 16*(8), 17193-17230. 10.3390/ijms160817193

Dick, M. K., Miao, J. H., & Limaiem, F. (2023). Histology, Fibroblast. *StatPearls* (). StatPearls Publishing LLC.

Diffey, B. L. (2001). Sun protection with clothing. *The British Journal of Dermatology, 144*(3), 449-450. bjd4122 [pii]

Dobson, C. M., Šali, A., & Karplus, M. (1998). Protein Folding: A Perspective from Theory and Experiment. *Angewandte Chemie International Edition, 37*(7), 868-893. 10.1002/(SICI)1521-3773(19980420)37:73.0.CO;2-H

Doerrler, W. T., & Lehrman, M. A. (1999). Regulation of the dolichol pathway in human fibroblasts by the endoplasmic reticulum unfolded protein response. *Proceedings of the National Academy of Sciences of the United States of America, 96*(23), 13050-13055. 10.1073/pnas.96.23.13050

Dombroski, B. A., Nayak, R. R., Ewens, K. G., Ankener, W., Cheung, V. G., & Spielman, R. S. (2010). Gene expression and genetic variation in response to endoplasmic reticulum stress in human cells. *American Journal of Human Genetics, 86*(5), 719-729. 10.1016/j.ajhg.2010.03.017

D'Orazio, J., Jarrett, S., Amaro-Ortiz, A., & Scott, T. (2013). UV radiation and the skin. *International Journal of Molecular Sciences, 14*(6), 12222-12248. 10.3390/ijms140612222 [doi]

Dou, J., Schenkel, F., Hu, L., Khan, A., Khan, M. Z., Yu, Y., Wang, Y., & Wang, Y. (2021). Genome-wide identification and functional prediction of long non-coding RNAs in Sprague-Dawley rats during heat stress. *BMC Genomics, 22*(1), 122-8. 10.1186/s12864-021-07421-8

Eide, M. J., & Weinstock, M. A. (2006). Public health challenges in sun protection. *Dermatologic Clinics, 24*(1), 119-124. S0733-8635(05)00106-3 [pii]

Ellis, J. (1987). Proteins as molecular chaperones. *Nature, 328*(6129), 378-379. 10.1038/328378a0 [doi]

El-Mostafa, K., El Kharrassi, Y., Badreddine, A., Andreoletti, P., Vamecq, J., El Kebbaj, M. S., Latruffe, N., Lizard, G., Nasser, B., & Cherkaoui-Malki, M. (2014). Nopal cactus (Opuntia ficus-indica) as a source of bioactive compounds for nutrition, health and disease. *Molecules (Basel, Switzerland)*, *19*(9), 14879-14901. 10.3390/molecules190914879 [doi]

Fan, Y., Xing, Y., Xiong, L., & Wang, J. (2020). Sestrin2 overexpression alleviates hydrogen peroxide-induced apoptosis and oxidative stress in retinal ganglion cells by enhancing Nrf2 activation via Keap1 downregulation. *Chemico-Biological Interactions*, *324*, 109086. 10.1016/j.cbi.2020.109086

Fang, I., & Trewyn, B. G. (2012). In Düzgüneş N. (Ed.), *Chapter three - Application of Mesoporous Silica Nanoparticles in Intracellular Delivery of Molecules and Proteins*. Academic Press. https://doi.org/10.1016/B978-0-12-391860-4.00003-3

Feder, M. E., & Hofmann, G. E. (1999). Heat-shock proteins, molecular chaperones, and the stress response: evolutionary and ecological physiology. *Annual Review of Physiology*, *61*, 243-282. 10.1146/annurev.physiol.61.1.243 [doi]

Feugang, Konarski, P., Zou, D., Stintzing, F. C., & Zou, C. (2006). Nutritional and medicinal use of Cactus pear (Opuntia spp.) cladodes and fruits. *Frontiers in Bioscience : A Journal and Virtual Library*, *11*, 2574-2589. 1992 [pii]

Feugang, Ye, F., Zhang, D. Y., Yu, Y., Zhong, M., Zhang, S., & Zou, C. (2010). Cactus Pear Extracts Induce Reactive Oxygen Species Production and Apoptosis in Ovarian Cancer Cells. *Null*, *62*(5), 692-699. 10.1080/01635581003605508

Fowles, J. R., Banton, M. I., & Pottenger, L. H. (2013). A toxicological review of the propylene glycols. *Critical Reviews in Toxicology, 43*(4), 363-390. 10.3109/10408444.2013.792328

Freshney, R. (2010). *Culture of Animal Cells: A Manual of Basic Technique and Specialized Applications, Sixth Edition*10.1002/9780470649367

Frydman, J. (2001). Folding of newly translated proteins in vivo: the role of molecular chaperones. *Annual Review of Biochemistry, 70*, 603-647. 70/1/603 [pii]

Fuentes, M. (2010, ().). *Hemocytometer protocol.* . http://www.hemocytometer.org/2013/04/04/hemocytometer-protocol/

Fujii, H. (2007). Cell type-specific roles of Jak3 in IL-2-induced proliferative signal transduction. *Biochemical and Biophysical Research Communications, 354*(3), 825-829. 10.1016/j.bbrc.2007.01.067

Furman, D., Campisi, J., Verdin, E., Carrera-Bastos, P., Targ, S., Franceschi, C., Ferrucci, L., Gilroy, D. W., Fasano, A., Miller, G. W., Miller, A. H., Mantovani, A., Weyand, C. M., Barzilai, N., Goronzy, J. J., Rando, T. A., Effros, R. B., Lucia, A., Kleinstreuer, N., & Slavich, G. M. (2019). Chronic inflammation in the etiology of disease across the life span. *Nature Medicine, 25*(12), 1822-1832. 10.1038/s41591-019-0675-0

Gabryelska, A., Kuna, P., Antczak, A., Białasiewicz, P., & Panek, M. (2019). IL-33 Mediated Inflammation in Chronic Respiratory Diseases-Understanding the Role of the Member of IL-1 Superfamily. *Frontiers in Immunology, 10*, 692. 10.3389/fimmu.2019.00692

Gaffen, S. L., & Liu, K. D. (2004). Overview of interleukin-2 function, production and clinical applications. *Cytokine, 28*(3), 109-123. 10.1016/j.cyto.2004.06.010

Galati, E. M., Monforte, M. T., Tripodo, M. M., d'Aquino, A., & Mondello, M. R. (2001). Antiulcer activity of Opuntia ficus indica (L.) Mill. (Cactaceae): ultrastructural study. *Journal of Ethnopharmacology*, *76*(1), 1-9. https://doi.org/10.1016/S0378-8741(01)00196-9

Ganceviciene, R., Liakou, A. I., Theodoridis, A., Makrantonaki, E., & Zouboulis, C. C. (2012). Skin anti-aging strategies. *Dermato-Endocrinology*, *4*(3), 308-319. 10.4161/derm.22804

Ganesan, K., & Xu, B. (2017). A Critical Review on Polyphenols and Health Benefits of Black Soybeans. *Nutrients*, *9*(5), 455. 10.3390/nu9050455

Gao, X., Dinkova-Kostova, A. T., & Talalay, P. (2001). Powerful and prolonged protection of human retinal pigment epithelial cells, keratinocytes, and mouse leukemia cells against oxidative damage: the indirect antioxidant effects of sulforaphane. *Proceedings of the National Academy of Sciences of the United States of America*, *98*(26), 15221-15226. 98/26/15221 [pii]

Gasparro, F. P. (2000). Sunscreens, skin photobiology, and skin cancer: the need for UVA protection and evaluation of efficacy. *Environmental Health Perspectives*, *108*(Suppl 1), 71-78.

Ge. (2021). iDEP Web Application for RNA-Seq Data Analysis. (pp. 417-443)10.1007/978-1-0716-1307-8_22

Ge, S. X., Son, E. W., & Yao, R. (2018). iDEP: an integrated web application for differential expression and pathway analysis of RNA-Seq data. *BMC Bioinformatics*, *19*(1), 534. 10.1186/s12859-018-2486-6

Ge, Son, E. W., & Yao, R. (2018). iDEP: an integrated web application for differential expression and pathway analysis of RNA-Seq data. *BMC Bioinformatics, 19*(1), 534. 10.1186/s12859-018-2486-6

Geback, T., Schulz, M. M., Koumoutsakos, P., & Detmar, M. (2009). TScratch: a novel and simple software tool for automated analysis of monolayer wound healing assays. *BioTechniques, 46*(4), 265-274. 10.2144/000113083 [doi]

Gentile, M., Latonen, L., & Laiho, M. (2003). Cell cycle arrest and apoptosis provoked by UV radiation-induced DNA damage are transcriptionally highly divergent responses. *Nucleic Acids Research, 31*(16), 4779-4790. gkg675 [pii]

Gentilella, A., Morón-Duran, F. D., Fuentes, P., Zweig-Rocha, G., Riaño-Canalias, F., Pelletier, J., Ruiz, M., Turón, G., Castaño, J., Tauler, A., Bueno, C., Menéndez, P., Kozma, S. C., & Thomas, G. (2017). Autogenous Control of 5′TOP mRNA Stability by 40S Ribosomes. *Molecular Cell, 67*(1), 55-70.e4. 10.1016/j.molcel.2017.06.005

Gething, M. J., & Sambrook, J. (1992). Protein folding in the cell. *Nature, 355*(6355), 33-45. 10.1038/355033a0 [doi]

Ghosh, S., Sarkar, P., Basak, P., Mahalanobish, S., & Sil, P. C. (2018). Role of Heat Shock Proteins in Oxidative Stress and Stress Tolerance. In A. A. A. Asea, & P. Kaur (Eds.), *Heat Shock Proteins and Stress* (pp. 109-126). Springer International Publishing. 10.1007/978-3-319-90725-3_6

Giacco, F., & Brownlee, M. (2010). Oxidative stress and diabetic complications. *Circulation Research, 107*(9), 1058-1070. 10.1161/CIRCRESAHA.110.223545

Giacomoni, P. U., Teta, L., & Najdek, L. (2010). Sunscreens: the impervious path from theory to practice. *Photochemical & Photobiological Sciences : Official Journal of the European Photochemistry Association and the European Society for Photobiology, 9*(4), 524-529. 10.1039/b9pp00150f [doi]

Gies, P. (2007). Photoprotection by clothing. *Photodermatology, Photoimmunology & Photomedicine, 23*(6), 264-274. PPP309 [pii]

Gilaberte, Y., Prieto-Torres, L., Pastushenko, I., & Juarranz, Á. (2016). Chapter 1 - Anatomy and Function of the Skin. In M. R. Hamblin, P. Avci & T. W. Prow (Eds.), *Nanoscience in Dermatology* (pp. 1-14). Academic Press. 10.1016/B978-0-12-802926-8.00001-X

Gilchrest, B. A., & Eller, M. S. (1999). DNA photodamage stimulates melanogenesis and other photoprotective responses. *The Journal of Investigative Dermatology.Symposium Proceedings / the Society for Investigative Dermatology, Inc.[and] European Society for Dermatological Research, 4*(1), 35-40. S1087-0024(15)30231-8 [pii]

Gladyshev, V. N. (2014). The free radical theory of aging is dead. Long live the damage theory! *Antioxidants & Redox Signaling, 20*(4), 727-731. 10.1089/ars.2013.5228

Goffart, S., Tikkanen, P., Michell, C., Wilson, T., & Pohjoismäki, Jaakko L O L O. (2021). The Type and Source of Reactive Oxygen Species Influences the Outcome of Oxidative Stress in Cultured Cells. *Cells, 10*(5), 1075. doi: 10.3390/cells10051075. 10.3390/cells10051075

Gomes, R. N., Manuel, F., & Nascimento, D. S. (2021). The bright side of fibroblasts: molecular signature and regenerative cues in major organs. *Npj Regenerative Medicine, 6*(1), 43. 10.1038/s41536-021-00153-z

Gong, Y., Kakihara, Y., Krogan, N., Greenblatt, J., Emili, A., Zhang, Z., & Houry, W. A. (2009). An atlas of chaperoneâ€“protein interactions in Saccharomyces cerevisiae: implications to protein folding pathways in the cell. *Molecular Systems Biology*, *5*, 275. 10.1038/msb.2009.26

Goodenough, Goliger, J. A., & Paul, D. L. (1996). Connexins, connexons, and intercellular communication. *Annual Review of Biochemistry*, *65*, 475-502. 10.1146/annurev.bi.65.070196.002355

Goodenough, & Paul, D. L. (2009). Gap junctions. *Cold Spring Harbor Perspectives in Biology*, *1*(1), a002576. 10.1101/cshperspect.a002576

Gouws, C. A., Georgousopoulou, E. N., Mellor, D. D., McKune, A., & Naumovski, N. (2019). Effects of the Consumption of Prickly Pear Cacti (Opuntia spp.) and its Products on Blood Glucose Levels and Insulin: A Systematic Review. *Medicina (Kaunas, Lithuania)*, *55*(5), 138. 10.3390/medicina55050138

Griessmeier, J. M., Stadelmann, A., Motschmann, U., Belisheva, N. K., Lammer, H., & Biernat, H. K. (2005). Cosmic ray impact on extrasolar earth-like planets in close-in habitable zones. *Astrobiology*, *5*(5), 587-603. 10.1089/ast.2005.5.587 [doi]

Grigoryev, Y. (2014, ().). *Cell Counting with a Hemocytometer: Easy as 1, 2, 3.* . http://bitesizebio.com/13687/cell-counting-with-a-hemocytometer-easy-as-1-2-3/

Han, A., Chien, A. L., & Kang, S. (2014). Photoaging. *Dermatologic Clinics*, *32*(3), 291-299. 10.1016/j.det.2014.03.015

Hansberg, W., Aguirre, J., Rís-Momberg, M., Rangel, P., Peraza, L., Montes de Oca, Y., & Cano-Domínguez, N. (2008). Chapter 15 Cell differentiation as a response to oxidative

stress. *British Mycological Society Symposia Series, 27,* 235-257. 10.1016/S0275-0287(08)80057-4

Harman, D. (1956). Aging: A Theory Based on Free Radical and Radiation Chemistry. *Journal of Gerontology, 11*(3), 298-300. 10.1093/geronj/11.3.298

Haronikova, L., Bonczek, O., Zatloukalova, P., Kokas-Zavadil, F., Kucerikova, M., Coates, P. J., Fahraeus, R., & Vojtesek, B. (2021). Resistance mechanisms to inhibitors of p53-MDM2 interactions in cancer therapy: can we overcome them? *Cellular & Molecular Biology Letters, 26*(1), 53. 10.1186/s11658-021-00293-6

Hartl, F. U., Bracher, A., & Hayer-Hartl, M. (2011). Molecular chaperones in protein folding and proteostasis. *Nature, 475*(7356), 324-332. 10.1038/nature10317 [doi]

Hassanpour, S. H., & Dehghani, M. (2017). Review of cancer from perspective of molecular. *Journal of Cancer Research and Practice, 4*(4), 127-129. 10.1016/j.jcrpr.2017.07.001

Havens, C. G., Ho, A., Yoshioka, N., & Dowdy, S. F. (2006). Regulation of late G1/S phase transition and APC Cdh1 by reactive oxygen species. *Molecular and Cellular Biology, 26*(12), 4701-4711. 10.1128/MCB.00303-06

HAYFLICK, L., & MOORHEAD, P. S. (1961). The serial cultivation of human diploid cell strains. *Experimental Cell Research, 25,* 585-621. 10.1016/0014-4827(61)90192-6

Heckman, C. J., Chandler, R., Kloss, J. D., Benson, A., Rooney, D., Munshi, T., Darlow, S. D., Perlis, C., Manne, S. L., & Oslin, D. W. (2013). Minimal Erythema Dose (MED) Testing. *Journal of Visualized Experiments : JoVE,* (75), 50175. 10.3791/50175

Heldens, L., Hensen, S. M. M., Onnekink, C., van Genesen, S. T., Dirks, R. P., & Lubsen, N. H. (2011). An atypical unfolded protein response in heat shocked cells. *PloS One, 6*(8), e23512. 10.1371/journal.pone.0023512

Henderson, E., Kempf, M., Yip, C., Davenport, L., Jones, E., Kong, S., Pearson, E., Kearns, A., & Cuttle, L. (2022). The lethal heat dose for 50% primary human fibroblast cell death is 48 °C. *Archives of Dermatological Research, 314*(8), 809-814. 10.1007/s00403-021-02217-y

Heo, S., Kim, S., & Kang, D. (2020). The Role of Hydrogen Peroxide and Peroxiredoxins throughout the Cell Cycle. *Antioxidants (Basel, Switzerland), 9*(4), 280. doi: 10.3390/antiox9040280. 10.3390/antiox9040280

Hetz, C. (2012). The unfolded protein response: controlling cell fate decisions under ER stress and beyond. *Nature Reviews Molecular Cell Biology, 13*(2), 89-102. 10.1038/nrm3270

Hibler, B., & Wang, S.,Q. (2016). *Education, Motivation, and Compliance*10.1007/978-3-319-29382-0_27

Hitraya, E. G., Varga, J., & Jimenez, S. A. (1995). Heat shock of human synovial and dermal fibroblasts induces delayed up-regulation of collagenase-gene expression. *The Biochemical Journal, 308 (Pt 3)*, 743-747. 10.1042/bj3080743

Ho, C. Y., & Dreesen, O. (2021). Faces of cellular senescence in skin aging. *Mechanisms of Ageing and Development, 198*, 111525. 10.1016/j.mad.2021.111525

Hoeijmakers, J. H. J. (2001). Genome maintenance mechanisms for preventing cancer. *Nature, 411*(6835), 366-374. 10.1038/35077232

Hoerter, J. E., & Ellis, S. R. (2023). Biochemistry, Protein Synthesis. *StatPearls* (). StatPearls Publishing LLC.

Hoffmann, K., Laperre, J., Avermaete, A., Altmeyer, P., & Gambichler, T. (2001). Defined UV protection by apparel textiles. *Archives of Dermatology, 137*(8), 1089-1094. re10006 [pii]

Höhn, A., Weber, D., Jung, T., Ott, C., Hugo, M., Kochlik, B., Kehm, R., König, J., Grune, T., & Castro, J. P. (2017). Happily (n)ever after: Aging in the context of oxidative stress, proteostasis loss and cellular senescence. *Redox Biology, 11*, 482-501. 10.1016/j.redox.2016.12.001

Holick. (2001). In Giacomoni P. U. (Ed.), *Chapter 2 - A perspective on the beneficial effects of moderate exposure to sunlight: bone health, cancer prevention, mental health and well being*. Elsevier. https://doi.org/10.1016/S1568-461X(01)80037-5 "

Vitamin D: A millenium perspective: Vitamin D: A millenium perspective: Vitamin D: A millenium perspective: 2nd (2003). 10.1002/jcb.10338 https://onlinelibrary.wiley.com/doi/abs/10.1002/jcb.10338

Holick. (2011). Health benefits of vitamin D and sunlight: a D-bate. *Nature Reviews Endocrinology, 7*(2), 73-75. 10.1038/nrendo.2010.234

Holick, M. F., MacLaughlin, J. A., & Doppelt, S. H. (1981). Regulation of cutaneous previtamin D3 photosynthesis in man: skin pigment is not an essential regulator. *Science, 211*(4482), 590-593. 10.1126/science.6256855

Holick, M. F. (2006). High Prevalence of Vitamin D Inadequacy and Implications for Health. *Mayo Clinic Proceedings, 81*(3), 353-373. 10.4065/81.3.353

Hu, Bian, Q., Rong, D., Wang, L., Song, J., Huang, H., Zeng, J., Mei, J., & Wang, P. (2023). JAK/STAT pathway: Extracellular signals, diseases, immunity, and therapeutic regimens. *Frontiers in Bioengineering and Biotechnology, 11*10.3389/fbioe.2023.1110765

Hu, Cao, J., Topatana, W., Juengpanich, S., Li, S., Zhang, B., Shen, J., Cai, L., Cai, X., & Chen, M. (2021). Targeting mutant p53 for cancer therapy: direct and indirect strategies. *Journal of Hematology & Oncology*, *14*(1), 157. 10.1186/s13045-021-01169-0

Hu, Feng, Z., & Levine, A. J. (2012). The Regulation of Multiple p53 Stress Responses is Mediated through MDM2. *Genes & Cancer*, *3*(3-4), 199-208. 10.1177/1947601912454734

Huang, A. H., & Chien, A. L. (2020). Photoaging: a Review of Current Literature. *Current Dermatology Reports*, *9*(1), 22-29. 10.1007/s13671-020-00288-0

Iacopetta, D., Ceramella, J., Catalano, A., Saturnino, C., Pellegrino, M., Mariconda, A., Longo, P., Sinicropi, M. S., & Aquaro, S. (2022). COVID-19 at a Glance: An Up-to-Date Overview on Variants, Drug Design and Therapies. *Viruses*, *14*(3), 573. doi: 10.3390/v14030573. 10.3390/v14030573

Iakovou, E., & Kourti, M. (2022). A Comprehensive Overview of the Complex Role of Oxidative Stress in Aging, The Contributing Environmental Stressors and Emerging Antioxidant Therapeutic Interventions. *Frontiers in Aging Neuroscience, 14*10.3389/fnagi.2022.827900

Ichihashi, M., Ando, H., Yoshida, M., Niki, Y., & Matsui, M. (2009). Photoaging of the skin. *Anti-Aging Medicine, 6*(6), 46-59. 10.3793/jaam.6.46

Itahana, K., Dimri, G. P., Hara, E., Itahana, Y., Zou, Y., Desprez, P., & Campisi, J. (2002). A role for p53 in maintaining and establishing the quiescence growth arrest in human cells. *The Journal of Biological Chemistry, 277*(20), 18206-18214. 10.1074/jbc.M201028200

Iwata, H., Haga, N., & Ujiie, H. (2021). Possible role of epiregulin from dermal fibroblasts in the keratinocyte hyperproliferation of psoriasis. *The Journal of Dermatology, 48*(9), 1433-1438. 10.1111/1346-8138.16003

Jakóbisiak, M., Lasek, W., & Gołąb, J. (2003). Natural mechanisms protecting against cancer. *Immunology Letters, 90*(2), 103-122. 10.1016/j.imlet.2003.08.005

Jaswal, S., Mehta, H. C., Sood, A. K., & Kaur, J. (2003). Antioxidant status in rheumatoid arthritis and role of antioxidant therapy. *Clinica Chimica Acta; International Journal of Clinical Chemistry, 338*(1-2), 123-129. S0009898103003772 [pii]

Javid, B., MacAry, P. A., & Lehner, P. J. (2007). Structure and function: heat shock proteins and adaptive immunity. *Journal of Immunology (Baltimore, Md.: 1950), 179*(4), 2035-2040. 179/4/2035 [pii]

Jeanmougin, M., Bouloc, A., & Schmutz, J. L. (2014). A new sunscreen application technique to protect more efficiently from ultraviolet radiation. *Photodermatology, Photoimmunology & Photomedicine, 30*(6), 323-331. 10.1111/phpp.12138 [doi]

Jiang, D., & Rinkevich, Y. (2018). Defining Skin Fibroblastic Cell Types Beyond CD90. *Frontiers in Cell and Developmental Biology, 6*, 133. 10.3389/fcell.2018.00133

Jiao, L., Liu, Y., Yu, X., Pan, X., Zhang, Y., Tu, J., Song, Y., & Li, Y. (2023). Ribosome biogenesis in disease: new players and therapeutic targets. *Signal Transduction and Targeted Therapy, 8*(1), 15. 10.1038/s41392-022-01285-4

Johnson, M. S., & Cook, J. G. (2023). Cell cycle exits and U-turns: Quiescence as multiple reversible forms of arrest. *Faculty Reviews, 12*, 5-5. eCollection 2023. 10.12703/r/12-5

Jonak, C., Klosner, G., & Trautinger, F. (2006). Heat shock proteins in the skin. *International Journal of Cosmetic Science, 28*(4), 233-241. 10.1111/j.1467-2494.2006.00327.x [doi]

Jonak, C., Klosner, G., & Trautinger, F. (2009). Significance of heat shock proteins in the skin upon UV exposure. *Frontiers in Bioscience (Landmark Edition), 14*(12), 4758-4768. 10.2741/3565

Jones, R. G., Plas, D. R., Kubek, S., Buzzai, M., Mu, J., Xu, Y., Birnbaum, M. J., & Thompson, C. B. (2005). AMP-activated protein kinase induces a p53-dependent metabolic checkpoint. *Molecular Cell, 18*(3), 283-293. 10.1016/j.molcel.2005.03.027

Julià, A., Tortosa, R., Hernanz, J. M., Cañete, J. D., Fonseca, E., Ferrándiz, C., Unamuno, P., Puig, L., Fernández-Sueiro, J. L., Sanmartí, R., Rodríguez, J., Gratacós, J., Dauden, E., Sánchez-Carazo, J. L., López-Estebaranz, J. L., Moreno-Ramírez, D., Queiró, R., Montilla, C., Torre-Alonso, J. C., . . . Marsal, S. (2012). Risk variants for psoriasis vulgaris in a large case–control collection and association with clinical subphenotypes. *Human Molecular Genetics, 21*(20), 4549-4557. 10.1093/hmg/dds295

Kalucka, J., Missiaen, R., Georgiadou, M., Schoors, S., Lange, C., De Bock, K., Dewerchin, M., & Carmeliet, P. (2015). Metabolic control of the cell cycle. *Cell Cycle (Georgetown, Tex.), 14*(21), 3379-3388. 10.1080/15384101.2015.1090068

Kanehisa, M., Furumichi, M., Sato, Y., Ishiguro-Watanabe, M., & Tanabe, M. (2020a). KEGG: integrating viruses and cellular organisms. *Nucleic Acids Research, 49*(D1), D545-D551. 10.1093/nar/gkaa970

Kanehisa, M., Furumichi, M., Sato, Y., Ishiguro-Watanabe, M., & Tanabe, M. (2020b). KEGG: integrating viruses and cellular organisms. *Nucleic Acids Research, 49*(D1), D545-D551. 10.1093/nar/gkaa970

Kao, T., Wang, M., Chen, Y., Chung, Y., & Hwang, P. (2021). Propylene Glycol Improves Stability of the Anti-Inflammatory Compounds in Scutellaria baicalensis Extract. *Processes, 9*(5)10.3390/pr9050894

Karrys, A., Rady, I., Chamcheu, R. N., Sabir, M. S., Mallick, S., Chamcheu, J. C., Jurutka, P. W., Haussler, M. R., & Whitfield, G. K. (2018). Bioactive Dietary VDR Ligands Regulate Genes Encoding Biomarkers of Skin Repair That Are Associated with Risk for Psoriasis. *Nutrients, 10*(2), 174. doi: 10.3390/nu10020174. 10.3390/nu10020174

Katschinski, D. M., Boos, K., Schindler, S. G., & Fandrey, J. (2000). Pivotal role of reactive oxygen species as intracellular mediators of hyperthermia-induced apoptosis. *The Journal of Biological Chemistry, 275*(28), 21094-21098. S0021-9258(19)79729-4 [pii]

Kaur, & Dufour, J. M. (2012). Cell lines: Valuable tools or useless artifacts. *Spermatogenesis, 2*(1), 1-5. SPMG19885 [pii]

Kaur, Kaur, A., & Sharma, R. (2012). Pharmacological actions of Opuntia ficus indica: A Review. *Journal of Applied Pharmaceutical Science, 2*, 15-18. 10.7324/JAPS.2012.2703

Kendall, R. T., & Feghali-Bostwick, C. A. (2014). Fibroblasts in fibrosis: novel roles and mediators. *Frontiers in Pharmacology, 5*, 123. 10.3389/fphar.2014.00123 [doi]

Khalil, S., Luciano, J., Chen, W., & Liu, A. Y. (2006). Dynamic regulation and involvement of the heat shock transcriptional response in arsenic carcinogenesis. *Journal of Cellular Physiology, 207*(2), 562-569. 10.1002/jcp.20599 [doi]

Kim, G., Jeong, H., Yoon, H., Yoo, H., Lee, J. Y., Park, S. H., & Lee, C. (2020). Anti-inflammatory mechanisms of suppressors of cytokine signaling target ROS via NRF-2/thioredoxin induction and inflammasome activation in macrophages. *BMB Reports, 53*(12), 640-645. 10.5483/BMBRep.2020.53.12.161

Kim, S. H., Jeon, B. J., Kim, D. H., Kim, T. I., Lee, H. K., Han, D. S., Lee, J. H., Kim, T. B., Kim, J. W., & Sung, S. H. (2012). Prickly pear cactus (Opuntia ficus indica var. saboten) protects against stress-induced acute gastric lesions in rats. *Journal of Medicinal Food, 15*(11), 968-973. 10.1089/jmf.2012.2282 [doi]

Koch, C. M., Chiu, S. F., Akbarpour, M., Bharat, A., Ridge, K. M., Bartom, E. T., & Winter, D. R. (2018). A Beginner's Guide to Analysis of RNA Sequencing Data. *American Journal of Respiratory Cell and Molecular Biology, 59*(2), 145-157. 10.1165/rcmb.2017-0430TR

Kolarsick, P. A. J., Kolarsick, M. A., & Goodwin, C. (2011). Anatomy and Physiology of the Skin. *Journal of the Dermatology Nurses' Association, 3*(4) https://journals.lww.com/jdnaonline/fulltext/2011/07000/anatomy_and_physiology_of_the_skin.3.aspx

Kolate, A., Baradia, D., Patil, S., Vhora, I., Kore, G., & Misra, A. (2014). PEG — A versatile conjugating ligand for drugs and drug delivery systems. *Journal of Controlled Release, 192*, 67-81. 10.1016/j.jconrel.2014.06.046

Kolenko, V., Rayman, P., Roy, B., Cathcart, M. K., O'Shea, J., Tubbs, R., Rybicki, L., Bukowski, R., & Finke, J. (1999). Downregulation of JAK3 protein levels in T lymphocytes by prostaglandin E2 and other cyclic adenosine monophosphate-elevating agents: impact on interleukin-2 receptor signaling pathway. *Blood, 93*(7), 2308-2318.

Komura, M., Sato, T., Yoshikawa, H., Nitta, N. A., Suzuki, Y., Koike, K., Kodama, Y., Seyama, K., & Takahashi, K. (2022). Propylene glycol, a component of electronic cigarette liquid, damages epithelial cells in human small airways. *Respiratory Research, 23*(1), 216. 10.1186/s12931-022-02142-2

Kong, Q., & Lin, C. G. (2010). Oxidative damage to RNA: mechanisms, consequences, and diseases. *Cellular and Molecular Life Sciences : CMLS, 67*(11), 1817-1829. 10.1007/s00018-010-0277-y

Kowaltowski, A. J., de Souza-Pinto, N. C., Castilho, R. F., & Vercesi, A. E. (2009). Mitochondria and reactive oxygen species. *Free Radical Biology & Medicine, 47*(4), 333-343. 10.1016/j.freeradbiomed.2009.05.004 [doi]

Kruk, J., Aboul-Enein, H. Y., Kładna, A., & Bowser, J. E. (2019). Oxidative stress in biological systems and its relation with pathophysiological functions: the effect of physical activity on cellular redox homeostasis. *Free Radical Research, 53*(5), 497-521. 10.1080/10715762.2019.1612059 [doi]

Kühl, N. M., & Rensing, L. (2000). Heat shock effects on cell cycle progression. *Cellular and Molecular Life Sciences : CMLS, 57*(3), 450-463. 10.1007/PL00000707

Kukurba, K. R., & Montgomery, S. B. (2015). RNA Sequencing and Analysis. *Cold Spring Harbor Protocols, 2015*(11), 951-969. 10.1101/pdb.top084970

Latchman, D. S. (2001). Heat shock proteins and cardiac protection. *Cardiovascular Research, 51*(4), 637-646. S0008636301003546 [pii]

Latha, M. S., Martis, J., Shobha, V., Sham Shinde, R., Bangera, S., Krishnankutty, B., Bellary, S., Varughese, S., Rao, P., & Naveen Kumar, B. R. (2013). Sunscreening agents: a review. *The Journal of Clinical and Aesthetic Dermatology, 6*(1), 16-26.

Latonen, L., Taya, Y., & Laiho, M. (2001). UV-radiation induces dose-dependent regulation of p53 response and modulates p53-HDM2 interaction in human fibroblasts. *Oncogene, 20*(46), 6784-6793. 10.1038/sj.onc.1204883

Laux, I., & Nel, A. (2001). Evidence That Oxidative Stress-Induced Apoptosis by Menadione Involves Fas-Dependent and Fas-Independent Pathways. *Clinical Immunology, 101*(3), 335-344. https://doi.org/10.1006/clim.2001.5129

Lecour, S., & Lamont, K. T. (2011). Natural polyphenols and cardioprotection. *Mini Reviews in Medicinal Chemistry, 11*(14), 1191-1199. BSP/MRMC/E-Pub/263 [pii]

Lee, J. C., Kim, H. R., Kim, J., & Jang, Y. S. (2002). Antioxidant property of an ethanol extract of the stem of Opuntia ficus-indica var. saboten. *Journal of Agricultural and Food Chemistry, 50*(22), 6490-6496. jf020388c [pii]

Lee, J., Cho, Y. S., Jung, H., & Choi, I. (2018). Pharmacological Regulation of Oxidative Stress in Stem Cells. *Oxidative Medicine and Cellular Longevity, 2018*, 4081890. 10.1155/2018/4081890

Lee, S. E., Hwang, H. J., Ha, J., Jeong, H., & Kim, J. H. (2003). Screening of medicinal plant extracts for antioxidant activity. *Life Sciences, 73*(2), 167-179. https://doi.org/10.1016/S0024-3205(03)00259-5

Lepock. (1997). Protein Denaturation During Heat Shock. *Advances in Molecular and Cell Biology, 19*, 223-259. https://doi.org/10.1016/S1569-2558(08)60079-X

Lepock. (2005). How do cells respond to their thermal environment? *International Journal of Hyperthermia : The Official Journal of European Society for Hyperthermic Oncology, North American Hyperthermia Group, 21*(8), 681-687. U259R1711458226Q [pii]

Lepock, J. R. (2004). Role of nuclear protein denaturation and aggregation in thermal radiosensitization. *International Journal of Hyperthermia : The Official Journal of European Society for Hyperthermic Oncology, North American Hyperthermia Group, 20*(2), 115-130. 8TFKU2VPV99RG1A5 [pii]

Levin, M. (2007). Gap junctional communication in morphogenesis. *Progress in Biophysics and Molecular Biology, 94*(1-2), 186-206. 10.1016/j.pbiomolbio.2007.03.005

Li, Z., Wu, J., & Deleo, C. J. (2006). RNA damage and surveillance under oxidative stress. *IUBMB Life, 58*(10), 581-588. 10.1080/15216540600946456

Liang, C. C., Park, A. Y., & Guan, J. L. (2007). In vitro scratch assay: a convenient and inexpensive method for analysis of cell migration in vitro. *Nature Protocols, 2*(2), 329-333. nprot.2007.30 [pii]

Liguori, I., Russo, G., Curcio, F., Bulli, G., Aran, L., Della-Morte, D., Gargiulo, G., Testa, G., Cacciatore, F., Bonaduce, D., & Abete, P. (2018). Oxidative stress, aging, and diseases. *Clinical Interventions in Aging, 13*, 757-772. 10.2147/CIA.S158513

Lin, W., & Karin, M. (2007). A cytokine-mediated link between innate immunity, inflammation, and cancer. *The Journal of Clinical Investigation, 117*(5), 1175-1183. 10.1172/JCI31537

Lindquist, S., & Craig, E. A. (1988). The heat-shock proteins. *Annual Review of Genetics, 22*, 631-677. 10.1146/annurev.ge.22.120188.003215 [doi]

Linos, E., Swetter, S. M., Cockburn, M. G., Colditz, G. A., & Clarke, C. A. (2009). Increasing burden of melanoma in the United States. *The Journal of Investigative Dermatology, 129*(7), 1666-1674. 10.1038/jid.2008.423 [doi]

Liu, M., & Dudley, S. C. J. (2018). The role of the unfolded protein response in arrhythmias. *Channels (Austin, Tex.), 12*(1), 335-345. 10.1080/19336950.2018.1516985

Liu, Y., & Chang, A. (2008). Heat shock response relieves ER stress. *The EMBO Journal, 27*(7), 1049-1059. 10.1038/emboj.2008.42

Liu, Y., Li, M., Du, X., Huang, Z., & Quan, N. (2021). Sestrin 2, a potential star of antioxidant stress in cardiovascular diseases. *Free Radical Biology and Medicine, 163*, 56-68. 10.1016/j.freeradbiomed.2020.11.015

Liu, Liu, F., Wang, Y., Tsai, H., & Yu, H. (2015). Aloin Protects Skin Fibroblasts from Heat Stress-Induced Oxidative Stress Damage by Regulating the Oxidative Defense System. *PloS One, 10*(12), e0143528. 10.1371/journal.pone.0143528

Lombardi, V. R. M., Carrera, I., & Cacabelos, R. (2017). In Vitro Screening for Cytotoxic Activity of Herbal Extracts. *Evidence-Based Complementary and Alternative Medicine, 2017*, 2675631. 10.1155/2017/2675631

Loor, G., Kondapalli, J., Schriewer, J. M., Chandel, N. S., Vanden Hoek, T. L., & Schumacker, P. T. (2010). Menadione triggers cell death through ROS-dependent mechanisms involving PARP activation without requiring apoptosis. *Free Radical Biology & Medicine, 49*(12), 1925-1936. 10.1016/j.freeradbiomed.2010.09.021 [doi]

Lopez-Ojeda, W., Pandey, A., Alhajj, M., & Oakley, A. M. (2023). Anatomy, Skin (Integument). *StatPearls* (). StatPearls Publishing LLC.

Lu, T., Lim, K., Molostvov, G., Yang, Y., Yiao, S., Zehnder, D., & Hsiao, L. (2012). Induction of intracellular heat-shock protein 72 prevents the development of vascular smooth muscle cell calcification. *Cardiovascular Research, 96*(3), 524-532. 10.1093/cvr/cvs278

Lu, Jiang, Y., Xu, W., & Bao, X. (2023). Sestrin2: multifaceted functions, molecular basis, and its implications in liver diseases. *Cell Death & Disease, 14*(2), 160. 10.1038/s41419-023-05669-4

Lukin, D. J., Carvajal, L. A., Liu, W., Resnick-Silverman, L., & Manfredi, J. J. (2015). p53 Promotes cell survival due to the reversibility of its cell-cycle checkpoints. *Molecular Cancer Research : MCR, 13*(1), 16-28. 10.1158/1541-7786.MCR-14-0177

Luo, W., & Brouwer, C. (2013a). Pathview: an R/Bioconductor package for pathway-based data integration and visualization. *Bioinformatics, 29*(14), 1830-1831. 10.1093/bioinformatics/btt285

Luo, W., & Brouwer, C. (2013b). Pathview: an R/Bioconductor package for pathway-based data integration and visualization. *Bioinformatics, 29*(14), 1830-1831. 10.1093/bioinformatics/btt285

Luo, W., Friedman, M. S., Shedden, K., Hankenson, K. D., & Woolf, P. J. (2009). GAGE: generally applicable gene set enrichment for pathway analysis. *BMC Bioinformatics, 10*(1), 161. 10.1186/1471-2105-10-161

Madrigal-Santillán, E., García-Melo, F., Morales-González, J. A., Vázquez-Alvarado, P., Muñoz-Juárez, S., Zuñiga-Pérez, C., Sumaya-Martínez, M. T., Madrigal-Bujaidar, E., & Hernández-Ceruelos, A. (2013). Antioxidant and anticlastogenic capacity of prickly pear juice. *Nutrients, 5*(10), 4145-4158. 10.3390/nu5104145 [doi]

Marei, H. E., Althani, A., Afifi, N., Hasan, A., Caceci, T., Pozzoli, G., Morrione, A., Giordano, A., & Cenciarelli, C. (2021). p53 signaling in cancer progression and therapy. *Cancer Cell International, 21*(1), 703. 10.1186/s12935-021-02396-8

Marescal, O., & Cheeseman, I. M. (2020). Cellular Mechanisms and Regulation of Quiescence. *Developmental Cell, 55*(3), 259-271. 10.1016/j.devcel.2020.09.029

Marrot, L., & Meunier, J. (2008). Skin DNA photodamage and its biological consequences. *Journal of the American Academy of Dermatology, 58*(5), S139-S148. 10.1016/j.jaad.2007.12.007

Martin, A. E., & Murphy, F. H. (2000). Glycols, Propylene Glycols. *Kirk-Othmer Encyclopedia of Chemical Technology* ()10.1002/0471238961.1618151613011820.a01

Martinod, S. R., Bernard, B., Serrar, M., & Gutierrez, G. (2007). (2007). Release of Heat-Shock Protein Hsp72 After Exercise and Supplementation With an Opuntia ficus indica Extract TEX-OE. Paper presented at the *Proceedings of the American Association of Equine Practitioners, , 53* 72-76.

Masuma, R., Kashima, S., Kurasaki, M., & Okuno, T. (2013). Effects of UV wavelength on cell damages caused by UV irradiation in PC12 cells. *Journal of Photochemistry and Photobiology B: Biology, 125,* 202-208. 10.1016/j.jphotobiol.2013.06.003

Matés, >. M. (2000). Effects of antioxidant enzymes in the molecular control of reactive oxygen species toxicology. *Toxicology, 153*(1), 83-104. 10.1016/S0300-483X(00)00306-1

Matias, A., Nunes, S. L., Poejo, J., Mecha, E., Serra, A. T., Madeira, P. J., Bronze, M. R., & Duarte, C. M. (2014). Antioxidant and anti-inflammatory activity of a flavonoid-rich

concentrate recovered from Opuntia ficus-indica juice. *Food & Function, 5*(12), 3269-3280. 10.1039/c4fo00071d [doi]

Matsuoka, L. Y., Ide, L., Wortsman, J., MacLaughlin, J. A., & Holick, M. F. (1987). Sunscreens suppress cutaneous vitamin D3 synthesis. *The Journal of Clinical Endocrinology and Metabolism, 64*(6), 1165. https://www.ncbi.nlm.nih.gov/pubmed/3033008

Matsuoka, L. Y., Wortsman, J., Dannenberg, M. J., Hollis, B. W., Lu, Z., & Holick, M. F. (1992). Clothing prevents ultraviolet-B radiation-dependent photosynthesis of vitamin D3. *The Journal of Clinical Endocrinology and Metabolism, 75*(4), 1099-1103. 10.1210/jc.75.4.1099

Maynard, S., Schurman, S. H., Harboe, C., de Souza-Pinto, N. C., & Bohr, V. A. (2009). Base excision repair of oxidative DNA damage and association with cancer and aging. *Carcinogenesis, 30*(1), 2-10. 10.1093/carcin/bgn250

McArthur, L., Chilton, L., Smith, G. L., & Nicklin, S. A. (2015). Electrical consequences of cardiac myocyte: fibroblast coupling. *Biochemical Society Transactions, 43*(3), 513-518. 10.1042/BST20150035

McGowan, M. A., Scheman, A., & Jacob, S. E. (2018). Propylene Glycol in Contact Dermatitis: A Systematic Review. *Dermatitis : Contact, Atopic, Occupational, Drug, 29*(1), 6-12. 10.1097/DER.0000000000000307

McKay, E. C., & Counts, S. E. (2020). Oxytocin Receptor Signaling in Vascular Function and Stroke. *Frontiers in Neuroscience, 14*, 574499. 10.3389/fnins.2020.574499

McMartin, K. (2014). Propylene Glycol. In P. Wexler (Ed.), *Encyclopedia of Toxicology (Third Edition)* (pp. 1113-1116). Academic Press. 10.1016/B978-0-12-386454-3.01029-0

Meechan, P., & Wilson, C. (2006). Use of Ultraviolet Lights in Biological Safety Cabinets: A Contrarian View. *Applied Biosafety, 11*(4), 222.

Melamed, M. L., Michos, E. D., Post, W., & Astor, B. (2008). 25-Hydroxyvitamin D Levels and the Risk of Mortality in the General Population. *Archives of Internal Medicine, 168*(15), 1629-1637. 10.1001/archinte.168.15.1629

Mendoza, M., Mandani, G., & Momand, J. (2014). The MDM2 gene family. *Biomolecular Concepts, 5*(1), 9-19. 10.1515/bmc-2013-0027

Merwald, H., Kokesch, C., Klosner, G., Matsui, M., & Trautinger, F. (2006). Induction of the 72-kilodalton heat shock protein and protection from ultraviolet Bâ€“induced cell death in human keratinocytes by repetitive exposure to heat shock or 15-deoxy-Î”12,14-prostaglandin J2. *Cell Stress & Chaperones, 11*(1), 81-88. 10.1379/CSC-89R.1

Mfarej, M. G., & Skibbens, R. V. (2020). An ever-changing landscape in Roberts syndrome biology: Implications for macromolecular damage. *PLoS Genetics, 16*(12), e1009219. 10.1371/journal.pgen.1009219

Mifsud, S. (2010, October). *Opuntia ficus-indica.* MaltaWildPlants.com. Retrieved 2021-Jan-24, from http://www.maltawildplants.com/CACT/Opuntia_ficus-indica.php

Miller, A. M. (2011). Role of IL-33 in inflammation and disease. *Journal of Inflammation (London, England), 8*(1), 22-22. 10.1186/1476-9255-8-22

Mirończuk-Chodakowska, I., Witkowska, A. M., & Zujko, M. E. (2018). Endogenous non-enzymatic antioxidants in the human body. *Advances in Medical Sciences, 63*(1), 68-78. 10.1016/j.advms.2017.05.005

Moll, U. M., & Petrenko, O. (2003). The MDM2-p53 Interaction. *Molecular Cancer Research, 1*(14), 1001-1008.

Monti-Rocha, R., Cramer, A., Gaio Leite, P., Antunes, M. M., Pereira, R. V. S., Barroso, A., Queiroz-Junior, C. M., David, B. A., Teixeira, M. M., Menezes, G. B., & Machado, F. S. (2019). SOCS2 Is Critical for the Balancing of Immune Response and Oxidate Stress Protecting Against Acetaminophen-Induced Acute Liver Injury. *Frontiers in Immunology, 9*, 3134. 10.3389/fimmu.2018.03134

Morrison, H., DI Monte, D., Nordenskjöld, M., & Jernström, B. (1985). Induction of cell damage by menadione and benzo(a)-pyrene-3,6-quinone in cultures of adult rat hepatocytes and human fibroblasts. *Toxicology Letters, 28*(1), 37-47. https://doi.org/10.1016/0378-4274(85)90007-4

Morshed, K. M., Jain, S. K., & McMartin, K. E. (1998). Propylene glycol-mediated cell injury in a primary culture of human proximal tubule cells. *Toxicological Sciences : An Official Journal of the Society of Toxicology, 46*(2), 410-417. 10.1006/toxs.1998.2521

Murphy, G.,M., & Ralph, N. (2016). *Photoprotection, Photoimmunology and Autoimmune Diseases*10.1007/978-3-319-29382-0_5

Mylonas, A., & O'Loghlen, A. (2022). Cellular Senescence and Ageing: Mechanisms and Interventions. *Frontiers in Aging, 3* https://www.frontiersin.org/articles/10.3389/fragi.2022.866718

Nagayach, R., Gupta, U. D., & Prakash, A. (2017). Expression profiling of hsp70 gene during different seasons in goats (Capra hircus) under sub-tropical humid climatic conditions. *Small Ruminant Research, 147*, 41-47. 10.1016/j.smallrumres.2016.11.016

Narayanan, D. L., Saladi, R. N., & Fox, J. L. (2010). Ultraviolet radiation and skin cancer. *International Journal of Dermatology, 49*(9), 978-986. 10.1111/j.1365-4632.2010.04474.x [doi]

Naselli, F., Tesoriere, L., Caradonna, F., Bellavia, D., Attanzio, A., Gentile, C., & Livrea, M. A. (2014). Anti-proliferative and pro-apoptotic activity of whole extract and isolated indicaxanthin from Opuntia ficus-indica associated with re-activation of the onco-suppressor p16(INK4a) gene in human colorectal carcinoma (Caco-2) cells. *Biochemical and Biophysical Research Communications, 450*(1), 652-658. S0006-291X(14)01103-6 [pii]

Nemudzivhadi, V., & Masoko, P. (2014). In Vitro Assessment of Cytotoxicity, Antioxidant, and Anti-Inflammatory Activities of Ricinus communis (Euphorbiaceae) Leaf Extracts. *Evidence-Based Complementary and Alternative Medicine : eCAM, 2014*, 625961. 10.1155/2014/625961

Neufert, C., Becker, C., Türeci, Ö, Waldner, M. J., Backert, I., Floh, K., Atreya, I., Leppkes, M., Jefremow, A., Vieth, M., Schneider-Stock, R., Klinger, P., Greten, F. R., Threadgill, D. W., Sahin, U., & Neurath, M. F. (2013). Tumor fibroblast-derived epiregulin promotes growth of colitis-associated neoplasms through ERK. *The Journal of Clinical Investigation, 123*(4), 1428-1443. 10.1172/JCI63748

Nishigori, H., Lee, J. W., & Iwatsuru, M. (1995). Glucocorticoid-induced cataract of the developing chick embryo-prevention by propylene glycol. *Ophthalmic Research, 27*(6), 350-355. 10.1159/000267747

Nitta, M., Okamura, H., Aizawa, S., & Yamaizumi, M. (1997). Heat shock induces transient p53-dependent cell cycle arrest at G1/S. *Oncogene, 15*(5), 561-568. 10.1038/sj.onc.1201210 [doi]

Norbury, C. J., & Hickson, I. D. (2001). Cellular responses to DNA damage. *Annual Review of Pharmacology and Toxicology, 41*, 367-401. 10.1146/annurev.pharmtox.41.1.367

Nowakowska, M., Gualtieri, F., von Rüden, E., Hansmann, F., Baumgärtner, W., Tipold, A., & Potschka, H. (2020). Profiling the Expression of Endoplasmic Reticulum Stress Associated Heat Shock Proteins in Animal Epilepsy Models. *Neuroscience, 429*, 156-172. 10.1016/j.neuroscience.2019.12.015

Oei, A. L., Vriend, L. E. M., Crezee, J., Franken, N. A. P., & Krawczyk, P. M. (2015). Effects of hyperthermia on DNA repair pathways: one treatment to inhibit them all. *Radiation Oncology, 10*(1), 165. 10.1186/s13014-015-0462-0

Ogburn, R. M., & Edwards, E. J. (2010). Chapter 4 - The Ecological Water-Use Strategies of Succulent Plants. *Advances in Botanical Research, 55*, 179-225. https://doi.org/10.1016/B978-0-12-380868-4.00004-1

Oh, J., Hur, M., & Lee, C. (2009). SOCS1 protects protein tyrosine phosphatases by thioredoxin upregulation and attenuates Jaks to suppress ROS-mediated apoptosis. *Oncogene, 28*(35), 3145-3156. 10.1038/onc.2009.169

Oka, S., Tsuzuki, T., Hidaka, M., Ohno, M., Nakatsu, Y., & Sekiguchi, M. (2022). Endogenous ROS production in early differentiation state suppresses endoderm differentiation via transient FOXC1 expression. *Cell Death Discovery, 8*(1), 150. 10.1038/s41420-022-00961-2

Olokoba, A. B., Obateru, O. A., & Olokoba, L. B. (2012). Type 2 diabetes mellitus: a review of current trends. *Oman Medical Journal, 27*(4), 269-273. 10.5001/omj.2012.68

Ongena, K., Das, C., Smith, J. L., Gil, S., & Johnston, G. (2010). Determining cell number during cell culture using the Scepter cell counter. *Journal of Visualized Experiments : JoVE, (45):2204. doi*(45), 10.3791/2204. 2204 [pii]

Orioli, D., & Dellambra, E. (2018). Epigenetic Regulation of Skin Cells in Natural Aging and Premature Aging Diseases. *Cells, 7*(12)10.3390/cells7120268

O'Shea, J. J., & Murray, P. J. (2008). Cytokine signaling modules in inflammatory responses. *Immunity, 28*(4), 477-487. 10.1016/j.immuni.2008.03.002

Ostlund, R. E.,Jr. (2004). Phytosterols and cholesterol metabolism. *Current Opinion in Lipidology, 15*(1), 37-41. 00041433-200402000-00008 [pii]

Osuna-Martínez, L., Reyes Esparza, J., & Rodríguez-Fragoso, L. (2014). Cactus (Opuntia ficus-indica): A review on its antioxidants properties and potential pharmacological use in chronic diseases. *Natural Products Chemistry & Research, 2*, 153-160. 10.4172/2329-6836.1000153

Ottolenghi, S., Sabbatini, G., Brizzolari, A., Samaja, M., & Chiumello, D. (2020). Hyperoxia and oxidative stress in anesthesia and critical care medicine. *Minerva Anestesiologica, 86*(1), 64-75. 10.23736/S0375-9393.19.13906-5 [doi]

Paige, S. L., Plonowska, K., Xu, A., & Wu, S. M. (2015). Molecular regulation of cardiomyocyte differentiation. *Circulation Research, 116*(2), 341-353. 10.1161/CIRCRESAHA.116.302752

Palmeri, R., Parafati, L., Restuccia, C., & Fallico, B. (2018). Application of prickly pear fruit extract to improve domestic shelf life, quality and microbial safety of sliced beef. *Food and Chemical Toxicology, 118*, 355-360. https://doi.org/10.1016/j.fct.2018.05.044

Pandey, K. B., & Rizvi, S. I. (2009). Plant polyphenols as dietary antioxidants in human health and disease. *Oxidative Medicine and Cellular Longevity, 2*(5), 270-278. 10.4161/oxim.2.5.9498

Park, E. H., Kahng, J. H., & Paek, E. A. (1998). Studies on the pharmacological action of cactus: identification of its anti-inflammatory effect. *Archives of Pharmacal Research, 21*(1), 30-34. 10.1007/BF03216749 [doi]

Park, H. Y., Kosmadaki, M., Yaar, M., & Gilchrest, B. A. (2009). Cellular mechanisms regulating human melanogenesis. *Cellular and Molecular Life Sciences : CMLS*, *66*(9), 1493-1506. 10.1007/s00018-009-8703-8 [doi]

Park, Choi, H., Hong, Y. H., Jung, E. Y., & Suh, H. J. (2017). Cactus cladodes (Opuntia humifusa) extract minimizes the effects of UV irradiation on keratinocytes and hairless mice. *Pharmaceutical Biology*, *55*(1), 1032-1040. 10.1080/13880209.2017.1286357

Parsell, D. A., & Lindquist, S. (1993). The function of heat-shock proteins in stress tolerance: degradation and reactivation of damaged proteins. *Annual Review of Genetics, 27*, 437-496. 10.1146/annurev.ge.27.120193.002253 [doi]

Pedersen, C. B., & Gregersen, N. (2010). Stress response profiles in human fibroblasts exposed to heat shock or oxidative stress. *Methods in Molecular Biology (Clifton, N.J.), 648*, 161-173. 10.1007/978-1-60761-756-3_10 [doi]

Peerlings, D., Mimpen, M., & Damoiseaux, J. (2021). The IL-2 - IL-2 receptor pathway: Key to understanding multiple sclerosis. *Journal of Translational Autoimmunity, 4*, 100123. 10.1016/j.jtauto.2021.100123

Pegg, D. E. (1989). *Viability assays for preserved cells, tissues, and organs*https://doi.org/10.1016/0011-2240(89)90016-3 "

Persson, H. L., Kurz, T., Eaton, J. W., & Brunk, U. T. (2005). Radiation-induced cell death: importance of lysosomal destabilization. *The Biochemical Journal, 389*(Pt 3), 877-884. BJ20050271 [pii]

Petruk, G., Di Lorenzo, F., Imbimbo, P., Silipo, A., Bonina, A., Rizza, L., Piccoli, R., Monti, D. M., & Lanzetta, R. (2017). Protective effect of Opuntia ficus-indica L. cladodes against UVA-induced oxidative stress in normal human keratinocytes. *Bioorganic & Medicinal Chemistry Letters, 27*(24), 5485-5489. S0960-894X(17)31037-5 [pii]

Pham-Huy, L., He, H., & Pham-Huy, C. (2008). Free radicals, antioxidants in disease and health. *International Journal of Biomedical Science : IJBS, 4*(2), 89-96. https://pubmed.ncbi.nlm.nih.gov/23675073 https://www.ncbi.nlm.nih.gov/pmc/articles/PMC3614697/

Phaniendra, A., Jestadi, D. B., & Periyasamy, L. (2015). Free radicals: properties, sources, targets, and their implication in various diseases. *Indian Journal of Clinical Biochemistry : IJCB, 30*(1), 11-26. 10.1007/s12291-014-0446-0

Phelan, K., & May, K. M. (2016). Basic Techniques in Mammalian Cell Tissue Culture. *Current Protocols in Toxicology*, *70*(1), A.3B.1-A.3B.22. https://doi.org/10.1002/cptx.13

Piano, A., Valbonesi, P., & Fabbri, E. (2004). Expression of cytoprotective proteins, heat shock protein 70 and metallothioneins, in tissues of Ostrea edulis exposed to heat and heavy metals. *Cell Stress & Chaperones*, *9*(2), 134-142.

Pires, E., Sung, P., & Wiese, C. (2017). Role of RAD51AP1 in homologous recombination DNA repair and carcinogenesis. *DNA Repair*, *59*, 76-81. 10.1016/j.dnarep.2017.09.008

Pizzino, G., Irrera, N., Cucinotta, M., Pallio, G., Mannino, F., Arcoraci, V., Squadrito, F., Altavilla, D., & Bitto, A. (2017). Oxidative Stress: Harms and Benefits for Human Health. *Oxidative Medicine and Cellular Longevity*, *2017*, 8416763. 10.1155/2017/8416763

Place, R. F., & Noonan, E. J. (2014). Non-coding RNAs turn up the heat: an emerging layer of novel regulators in the mammalian heat shock response. *Cell Stress & Chaperones*, *19*(2), 159-172. 10.1007/s12192-013-0456-5

Plikus, M. V., Wang, X., Sinha, S., Forte, E., Thompson, S. M., Herzog, E. L., Driskell, R. R., Rosenthal, N., Biernaskie, J., & Horsley, V. (2021). Fibroblasts: Origins, definitions, and functions in health and disease. *Cell*, *184*(15), 3852-3872. 10.1016/j.cell.2021.06.024

Polefka, T. G., Meyer, T. A., Agin, P. P., & Bianchini, R. J. (2012). Effects of solar radiation on the skin. *Journal of Cosmetic Dermatology*, *11*(2), 134-143. 10.1111/j.1473-2165.2012.00614.x [doi]

Ponniresan, V., Balupillai, A., Kanimozhi, G., Khan, H., Alhomida, A., & Prasad, N. (2020). Opuntiol Prevents Photoaging of Mouse Skin via Blocking Inflammatory Responses and

Collagen Degradation. *Oxidative Medicine and Cellular Longevity*, *2020*, 1-12. 10.1155/2020/5275178

Powers, E. T., Morimoto, R. I., Dillin, A., Kelly, J. W., & Balch, W. E. (2009). Biological and chemical approaches to diseases of proteostasis deficiency. *Annual Review of Biochemistry*, *78*, 959-991. 10.1146/annurev.biochem.052308.114844 [doi]

Queirós, C. S., & Freitas, J. P. (2019). Sun Exposure: Beyond the Risks. *Dermatology Practical & Conceptual*, *9*(4), 249-252. 10.5826/dpc.0904a01

Radons, J. (2016). The human HSP70 family of chaperones: where do we stand? *Cell Stress & Chaperones*, *21*(3), 379-404. 10.1007/s12192-016-0676-6

Rahman, M. M., Islam, M. B., Biswas, M., & Khurshid Alam, A. H. M. (2015). In vitro antioxidant and free radical scavenging activity of different parts of Tabebuia pallida growing in Bangladesh. *BMC Research Notes*, *8*(1), 621. 10.1186/s13104-015-1618-6

Rajurkar, N. S., & Hande, S. M. (2011a). Estimation of phytochemical content and antioxidant activity of some selected traditional Indian medicinal plants. *Indian Journal of Pharmaceutical Sciences*, *73*(2), 146-151. 10.4103/0250-474x.91574

Rajurkar, N. S., & Hande, S. M. (2011b). Estimation of phytochemical content and antioxidant activity of some selected traditional Indian medicinal plants. *Indian Journal of Pharmaceutical Sciences*, *73*(2), 146-151. 10.4103/0250-474x.91574

Ramadan, M. F., & Mörsel, J. (2003). Recovered lipids from prickly pear [Opuntia ficus-indica (L.) Mill] peel: a good source of polyunsaturated fatty acids, natural antioxidant vitamins and sterols. *Food Chemistry*, *83*(3), 447-456. https://doi.org/10.1016/S0308-8146(03)00128-6

Ran, R., Lu, A., Xu, H., Tang, Y., & Sharp, F. R. (2007). Heat-Shock Protein Regulation of Protein Folding, Protein Degradation, Protein Function, and Apoptosis. In A. Lajtha, & P. H. Chan (Eds.), *Handbook of Neurochemistry and Molecular Neurobiology: Acute Ischemic Injury and Repair in the Nervous System* (pp. 89-107). Springer US. 10.1007/978-0-387-30383-3_6

Rane, Mangan, J. K., Amanullah, A., Wong, B. C., Vora, R. K., Liebermann, D. A., Hoffman, B., Graña, X., & Reddy, E. P. (2002). Activation of the Jak3 pathway is associated with granulocytic differentiation of myeloid precursor cells. *Blood, 100*(8), 2753-2762. 10.1182/blood.V100.8.2753

Rane, & Reddy, E. P. (1994). JAK3: a novel JAK kinase associated with terminal differentiation of hematopoietic cells. *Oncogene, 9*(8), 2415-2423.

Ray, P. D., Huang, B., & Tsuji, Y. (2012). Reactive oxygen species (ROS) homeostasis and redox regulation in cellular signaling. *Cellular Signalling, 24*(5), 981-990. 10.1016/j.cellsig.2012.01.008

Reimand, J. ü, Isserlin, R., Voisin, V., Kucera, M., Tannus-Lopes, C., Rostamianfar, A., Wadi, L., Meyer, M., Wong, J., Xu, C., Merico, D., & Bader, G. D. (2019). Pathway enrichment analysis and visualization of omics data using g:Profiler, GSEA, Cytoscape and EnrichmentMap. *Nature Protocols, 14*(2), 482-517. 10.1038/s41596-018-0103-9

Richter, K., Haslbeck, M., & Buchner, J. (2010). The Heat Shock Response: Life on the Verge of Death. *Molecular Cell, 40*(2), 253-266. https://doi.org/10.1016/j.molcel.2010.10.006

Riss, T. (2014, ().). *Is Your MTT Assay Really the Best Choice?*. . http://www.promega.com/~/pdf/resources/pubhub/is-your-mtt-assay-really-the-best-choice/

Ritossa, F. (1962). A new puffing pattern induced by temperature shock and DNP in drosophila. *Experientia, 18*(12), 571-573. 10.1007/BF02172188

Rivas-Arancibia, S., Guevara-Guzmán, R., López-Vidal, Y., Rodríguez-Martínez, E., Zanardo-Gomes, M., Angoa-Pérez, M., & Raisman-Vozari, R. (2010). Oxidative stress caused by ozone exposure induces loss of brain repair in the hippocampus of adult rats. *Toxicological Sciences : An Official Journal of the Society of Toxicology, 113*(1), 187-197. 10.1093/toxsci/kfp252 [doi]

Roberts, R. J., Agius, C., Saliba, C., Bossier, P., & Sung, Y. Y. (2010). Heat shock proteins (chaperones) in fish and shellfish and their potential role in relation to fish health: a review. *Journal of Fish Diseases, 33*(10), 789-801. 10.1111/j.1365-2761.2010.01183.x [doi]

Rodriguez-Amaya, D. B. (2019). Betalains. In L. Melton, F. Shahidi & P. Varelis (Eds.), *Encyclopedia of Food Chemistry* (pp. 35-39). Academic Press. https://doi.org/10.1016/B978-0-08-100596-5.21607-7

Roti Roti, J. L. (2008). Cellular responses to hyperthermia (40–46°C): Cell killing and molecular events. *Null, 24*(1), 3-15. 10.1080/02656730701769841

Rouillard, A. D., Gundersen, G. W., Fernandez, N. F., Wang, Z., Monteiro, C. D., McDermott, M. G., & Ma'ayan, A. (2016). The harmonizome: a collection of processed datasets gathered to serve and mine knowledge about genes and proteins. *Database, 2016*, baw100. 10.1093/database/baw100

Saenz, C. (2000). Processing technologies: an alternative for cactus pear (Opuntia spp.) fruits and cladodes. *Journal of Arid Environments*, *46*(3), 209-225. https://doi.org/10.1006/jare.2000.0676

Salminen, A. (2023). The plasticity of fibroblasts: A forgotten player in the aging process. *Ageing Research Reviews*, *89*, 101995. 10.1016/j.arr.2023.101995

Sánchez, E., García, S., & Heredia, N. (2010). Extracts of Edible and Medicinal Plants Damage Membranes of *Vibrio cholerae*. *Applied and Environmental Microbiology*, *76*(20), 6888-6894. 10.1128/AEM.03052-09

Saretzki, G., Armstrong, L., Leake, A., Lako, M., & von Zglinicki, T. (2004). Stress Defense in Murine Embryonic Stem Cells Is Superior to That of Various Differentiated Murine Cells. *Stem Cells*, *22*(6), 962-971. 10.1634/stemcells.22-6-962

Sarkar, S., Singh, M. D., Yadav, R., Arunkumar, K. P., & Pittman, G. W. (2011). Heat shock proteins: Molecules with assorted functions. *Frontiers in Biology*, *6*(4), 312. 10.1007/s11515-011-1080-3

Sart, S., Song, L., & Li, Y. (2015). Controlling Redox Status for Stem Cell Survival, Expansion, and Differentiation. *Oxidative Medicine and Cellular Longevity*, *2015*, 105135. 10.1155/2015/105135

Scandalios, J. G. (2002). Oxidative stress responses - what have genome-scale studies taught us? *Genome Biology*, *3*(7), reviews1019.1. 10.1186/gb-2002-3-7-reviews1019

Scharffetter, K., Wlaschek, M., Hogg, A., Bolsen, K., Schothorst, A., Goerz, G., Krieg, T., & Plewig, G. (1991). UVA irradiation induces collagenase in human dermal fibroblasts in

vitro and in vivo. *Archives of Dermatological Research, 283*(8), 506-511. 10.1007/BF00371923

Schrader, M., & Fahimi, H. D. (2006). Peroxisomes and oxidative stress. *Biochimica Et Biophysica Acta, 1763*(12), 1755-1766. S0167-4889(06)00282-5 [pii]

Schwarz, D. S., & Blower, M. D. (2016). The endoplasmic reticulum: structure, function and response to cellular signaling. *Cellular and Molecular Life Sciences : CMLS, 73*(1), 79-94. 10.1007/s00018-015-2052-6

Seif, F., Khoshmirsafa, M., Aazami, H., Mohsenzadegan, M., Sedighi, G., & Bahar, M. (2017). The role of JAK-STAT signaling pathway and its regulators in the fate of T helper cells. *Cell Communication and Signaling, 15*(1), 23. 10.1186/s12964-017-0177-y

Seite, S., Fourtanier, A., Moyal, D., & Young, A. R. (2010). Photodamage to human skin by suberythemal exposure to solar ultraviolet radiation can be attenuated by sunscreens: a review. *The British Journal of Dermatology, 163*(5), 903-914. 10.1111/j.1365-2133.2010.10018.x [doi]

Selemenakis, P., Sharma, N., Uhrig, M. E., Katz, J., Kwon, Y., Sung, P., & Wiese, C. (2022). RAD51AP1 and RAD54L Can Underpin Two Distinct RAD51-Dependent Routes of DNA Damage Repair via Homologous Recombination. *Frontiers in Cell and Developmental Biology, 10*, 866601. 10.3389/fcell.2022.866601

Seluanov, A., Vaidya, A., & Gorbunova, V. (2010). Establishing primary adult fibroblast cultures from rodents. *Journal of Visualized Experiments : JoVE, (44):2033. doi*(44), 10.3791/2033. 10.3791/2033

Seo, J. Y., & Chung, J. H. (2006). Thermal aging: A new concept of skin aging. *Journal of Dermatological Science Supplement, 2*(1), S13-S22. 10.1016/j.descs.2006.08.002

Sharifi-Rad, M., Anil Kumar, N. V., Zucca, P., Varoni, E. M., Dini, L., Panzarini, E., Rajkovic, J., Tsouh Fokou, P. V., Azzini, E., Peluso, I., Prakash Mishra, A., Nigam, M., El Rayess, Y., Beyrouthy, M. E., Polito, L., Iriti, M., Martins, N., Martorell, M., Docea, A. O., . . . Sharifi-Rad, J. (2020). Lifestyle, Oxidative Stress, and Antioxidants: Back and Forth in the Pathophysiology of Chronic Diseases. *Frontiers in Physiology, 11* https://www.frontiersin.org/article/10.3389/fphys.2020.00694

Sharma, S., Chaudhary, P., Sandhir, R., Bharadwaj, A., Gupta, R. K., Khatri, R., Bajaj, A. C., Baburaj, T. P., Kumar, S., Pal, M. S., Reddy, P. K., & Kumar, B. (2021). Heat-induced endoplasmic reticulum stress in soleus and gastrocnemius muscles and differential response to UPR pathway in rats. *Cell Stress & Chaperones, 26*(2), 323-339. https://www.jstor.org/stable/48724342

Shatrova, A. N., Lyublinskaya, O. G., Borodkina, A. V., & Burova, E. B. (2016). Oxidative stress response of human fibroblasts and endometrial mesenchymal stem cells. *Cell and Tissue Biology, 10*(1), 18-28. 10.1134/S1990519X16010090

Shi, H., & Bressan, R. (2006). RNA Extraction. In J. Salinas, & J. J. Sanchez-Serrano (Eds.), *Arabidopsis Protocols* (pp. 345-348). Humana Press. 10.1385/1-59745-003-0:345

Shimoni, C., Goldstein, M., Ribarski-Chorev, I., Schauten, I., Nir, D., Strauss, C., & Schlesinger, S. (2020). Heat Shock Alters Mesenchymal Stem Cell Identity and Induces Premature Senescence. *Frontiers in Cell and Developmental Biology, 8,* 565970. 10.3389/fcell.2020.565970

Skotarczak, K., Osmola-Mankowska, A., Lodyga, M., Polanska, A., Mazur, M., & Adamski, Z. (2015). Photoprotection: facts and controversies. *European Review for Medical and Pharmacological Sciences, 19*(1), 98-112. 8343 [pii]

Slimen, I. B., Najar, T., Ghram, A., Dabbebi, H., Ben Mrad, M., & Abdrabbah, M. (2014). Reactive oxygen species, heat stress and oxidative-induced mitochondrial damage. A review. *International Journal of Hyperthermia : The Official Journal of European Society for Hyperthermic Oncology, North American Hyperthermia Group, 30*(7), 513-523. 10.3109/02656736.2014.971446 [doi]

Slinkard, K., & Singleton, V. L. (1977). Total phenol analysis automation and comparison with manual methods. *American Journal of Enology and Viticulture, 28*(1), 49-55. https://eurekamag.com/research/006/815/006815587.php

Sobah, M. L., Liongue, C., & Ward, A. C. (2021). SOCS Proteins in Immunity, Inflammatory Diseases, and Immune-Related Cancer. *Frontiers in Medicine, 8*, 727987. 10.3389/fmed.2021.727987

Soetan, K., Olaiya, C., & Oyewole, O. (2009). The importance of mineral elements for humans, domestic animals and plants: A review. *Afr J Food Sci, 4*

Soheilifar, M. H., Masoudi-Khoram, N., Shirkavand, A., & Ghorbanifar, S. (2022). Non-coding RNAs in photoaging-related mechanisms: a new paradigm in skin health. *Biogerontology, 23*(3), 289-306. 10.1007/s10522-022-09966-x

Song, H., Kim, Y., Seok, S., Gil, H., Yang, J., Lee, E., & Hong, S. (2012). Cellular toxicity of surfactants used as herbicide additives. *Journal of Korean Medical Science, 27*(1), 3-9. 10.3346/jkms.2012.27.1.3

Sonna, L. A., Fujita, J., Gaffin, S. L., & Lilly, C. M. (2002). Invited review: Effects of heat and cold stress on mammalian gene expression. *Journal of Applied Physiology (Bethesda, Md.: 1985), 92*(4), 1725-1742. 10.1152/japplphysiol.01143.2001

Sozzani, S., Bosisio, D., Mantovani, A., & Ghezzi, P. (2005). Linking stress, oxidation and the chemokine system. *European Journal of Immunology, 35*(11), 3095-3098. 10.1002/eji.200535489

Sreekanth, D., Arunasree, M. K., Roy, K. R., Chandramohan Reddy, T., Reddy, G. V., & Reddanna, P. (2007). Betanin a betacyanin pigment purified from fruits of Opuntia ficus-indica induces apoptosis in human chronic myeloid leukemia Cell line-K562. *Phytomedicine : International Journal of Phytotherapy and Phytopharmacology, 14*(11), 739-746. S0944-7113(07)00051-7 [pii]

Stark, R., Grzelak, M., & Hadfield, J. (2019). RNA sequencing: the teenage years. *Nature Reviews Genetics, 20*(11), 631-656. 10.1038/s41576-019-0150-2

Stelzer, G., Rosen, N., Plaschkes, I., Zimmerman, S., Twik, M., Fishilevich, S., Stein, T. I., Nudel, R., Lieder, I., Mazor, Y., Kaplan, S., Dahary, D., Warshawsky, D., Guan-Golan, Y., Kohn, A., Rappaport, N., Safran, M., & Lancet, D. (2016). The GeneCards Suite: From Gene Data Mining to Disease Genome Sequence Analyses. *Current Protocols in Bioinformatics, 54*(1), 1.30.1-1.30.33. 10.1002/cpbi.5

Stetter, K. O. (2006). Hyperthermophiles in the history of life. *Philosophical Transactions of the Royal Society of London.Series B, Biological Sciences, 361*(1474), 1837-1843. 10.1098/rstb.2006.1907

Stintzing, F. C., & Carle, R. (2007). Betalains – emerging prospects for food scientists. *Trends in Food Science & Technology*, *18*(10), 514-525. https://doi.org/10.1016/j.tifs.2007.04.012

Stoddart, M. J. (2011). Cell viability assays: introduction. *Methods in Molecular Biology (Clifton, N.J.), 740*, 1-6. 10.1007/978-1-61779-108-6_1 [doi]

Strack, D., Vogt, T., & Schliemann, W. (2003). Recent advances in betalain research. *Phytochemistry, 62*(3), 247-269. S0031942202005642 [pii]

Suh, Y. A., Arnold, R. S., Lassegue, B., Shi, J., Xu, X., Sorescu, D., Chung, A. B., Griendling, K. K., & Lambeth, J. D. (1999). Cell transformation by the superoxide-generating oxidase Mox1. *Nature, 401*(6748), 79-82. 10.1038/43459 [doi]

Sun, Y., Ren, Y., Zhang, Y., Han, Y., Yang, Y., Gao, Y., Zhu, L., Qi, R., Chen, H., & Gao, X. (2018). DNAJA4 deficiency enhances NF-kappa B-related growth arrest induced by hyperthermia in human keratinocytes. *Journal of Dermatological Science, 91*(3), 256-267. 10.1016/j.jdermsci.2018.05.006

Sung, Y. Y., Roberts, R. J., & Bossier, P. (2012). Enhancement of Hsp70 synthesis protects common carp, Cyprinus carpio L., against lethal ammonia toxicity. *Journal of Fish Diseases, 35*(8), 563-568. 10.1111/j.1365-2761.2012.01397.x [doi]

Szeto, A., Sun-Suslow, N., Mendez, A. J., Hernandez, R. I., Wagner, K. V., & McCabe, P. M. (2017). Regulation of the macrophage oxytocin receptor in response to inflammation. *American Journal of Physiology.Endocrinology and Metabolism, 312*(3), E183-E189. 10.1152/ajpendo.00346.2016

Taherkhani, S., Suzuki, K., & Castell, L. (2020). A Short Overview of Changes in Inflammatory Cytokines and Oxidative Stress in Response to Physical Activity and Antioxidant Supplementation. *Antioxidants (Basel, Switzerland), 9*(9), 886. doi: 10.3390/antiox9090886. 10.3390/antiox9090886

Takada, Y., Ye, X., & Simon, S. (2007). The integrins. *Genome Biology, 8*(5), 215. 10.1186/gb-2007-8-5-215

Talukdar, S., Emdad, L., Das, S. K., & Fisher, P. B. (2022). GAP junctions: multifaceted regulators of neuronal differentiation. *Tissue Barriers, 10*(1), 1982349. 10.1080/21688370.2021.1982349

Tamiya, T., Kashiwagi, I., Takahashi, R., Yasukawa, H., & Yoshimura, A. (2011). Suppressors of cytokine signaling (SOCS) proteins and JAK/STAT pathways: regulation of T-cell inflammation by SOCS1 and SOCS3. *Arteriosclerosis, Thrombosis, and Vascular Biology, 31*(5), 980-985. 10.1161/ATVBAHA.110.207464

Tan, B. L., Norhaizan, M. E., & Liew, W. (2018). Nutrients and Oxidative Stress: Friend or Foe? *Oxidative Medicine and Cellular Longevity, 2018*, 9719584. 10.1155/2018/9719584

Tauffenberger, A., Fiumelli, H., Almustafa, S., & Magistretti, P. J. (2019). Lactate and pyruvate promote oxidative stress resistance through hormetic ROS signaling. *Cell Death & Disease, 10*(9), 653. 10.1038/s41419-019-1877-6

Tavaria, M., Gabriele, T., Kola, I., & Anderson, R. L. (1996). A hitchhiker's guide to the human Hsp70 family. *Cell Stress & Chaperones, 1*(1), 23-28. 10.1379/1466-1268(1996)001

Tobin, D. J. (2017). Introduction to skin aging. *Journal of Tissue Viability, 26*(1), 37-46. 10.1016/j.jtv.2016.03.002

Toivola, D. M., Strnad, P., Habtezion, A., & Omary, M. B. (2010). Intermediate filaments take the heat as stress proteins. *Trends in Cell Biology, 20*(2), 79-91. 10.1016/j.tcb.2009.11.004

Tomasek, J. J., Gabbiani, G., Hinz, B., Chaponnier, C., & Brown, R. A. (2002). Myofibroblasts and mechano-regulation of connective tissue remodelling. *Nature Reviews Molecular Cell Biology, 3*(5), 349-363. 10.1038/nrm809

Traber, M. G., & Atkinson, J. (2007). Vitamin E, antioxidant and nothing more. *Free Radical Biology & Medicine, 43*(1), 4-15. S0891-5849(07)00219-5 [pii]

Tsan, M., & Gao, B. (2004). Cytokine function of heat shock proteins. *American Journal of Physiology.Cell Physiology, 286*(4), 739. 10.1152/ajpcell.00364.2003

Uchida, M., Anderson, E. L., Squillace, D. L., Patil, N., Maniak, P. J., Iijima, K., Kita, H., & O'Grady, S. M. (2017). Oxidative stress serves as a key checkpoint for IL-33 release by airway epithelium. *Allergy, 72*(10), 1521-1531. 10.1111/all.13158

VanderWaal, R. P., Griffith, C. L., Wright, W. D., Borrelli, M. J., & Roti, J. L. (2001). Delaying S-phase progression rescues cells from heat-induced S-phase hypertoxicity. *Journal of Cellular Physiology, 187*(2), 236-243. 10.1002/jcp.1073 [pii]

Vanzi, F., Vladimirov, S., Knudsen, C. R., Goldman, Y. E., & Cooperman, B. S. (2003). Protein synthesis by single ribosomes. *RNA (New York, N.Y.), 9*(10), 1174-1179. 10.1261/rna.5800303

Velichko, A. K., Markova, E. N., Petrova, N. V., Razin, S. V., & Kantidze, O. L. (2013). Mechanisms of heat shock response in mammals. *Cellular and Molecular Life Sciences, 70*(22), 4229-4241. 10.1007/s00018-013-1348-7

Velichko, A. K., Petrova, N. V., Razin, S. V., & Kantidze, O. L. (2015). Mechanism of heat stress-induced cellular senescence elucidates the exclusive vulnerability of early S-phase cells to mild genotoxic stress. *Nucleic Acids Research, 43*(13), 6309-6320. 10.1093/nar/gkv573

Verghese, J., Abrams, J., Wang, Y., & Morano, K. A. (2012). Biology of the heat shock response and protein chaperones: budding yeast (Saccharomyces cerevisiae) as a model system. *Microbiology and Molecular Biology Reviews : MMBR, 76*(2), 115-158. 10.1128/MMBR.05018-11 [doi]

Vinson, J. A. (2006). Oxidative stress in cataracts. *Pathophysiology : The Official Journal of the International Society for Pathophysiology, 13*(3), 151-162. S0928-4680(06)00052-6 [pii]

Volkov, V. A., Voronkov, M. V., Misin, V. M., Fedorova, E. S., Rodin, I. A., & Stavrianidi, A. N. (2021). Aqueous Propylene Glycol Extracts from Medicinal Plants: Chemical Composition, Antioxidant Activity, Standardization, and Extraction Kinetics. *Inorganic Materials, 57*(14), 1404-1412. 10.1134/S0020168521140120

Walter, P., & Ron, D. (2011). The unfolded protein response: from stress pathway to homeostatic regulation. *Science (New York, N.Y.), 334*(6059), 1081-1086. 10.1126/science.1209038

Wang, Brown, J., Gao, S., Liang, S., Jotwani, R., Zhou, H., Suttles, J., Scott, D. A., & Lamont, R. J. (2013). The Role of JAK-3 in Regulating TLR-Mediated Inflammatory Cytokine Production in Innate Immune Cells. *The Journal of Immunology, 191*(3), 1164-1174. 10.4049/jimmunol.1203084

Wang, Jing, Y., Ding, L., Zhang, X., Song, Y., Chen, S., Zhao, X., Huang, X., Pu, Y., Wang, Z., Ni, Y., & Hu, Q. (2019). Epiregulin reprograms cancer-associated fibroblasts and facilitates oral squamous cell carcinoma invasion via JAK2-STAT3 pathway. *Journal of Experimental & Clinical Cancer Research, 38*(1), 274. 10.1186/s13046-019-1277-x

Wang, Vermeulen, W., Coursen, J. D., Gibson, M., Lupold, S. E., Forrester, K., Xu, G., Elmore, L., Yeh, H., Hoeijmakers, J. H., & Harris, C. C. (1996). The XPB and XPD DNA helicases are components of the p53-mediated apoptosis pathway. *Genes & Development, 10*(10), 1219-1232. 10.1101/gad.10.10.1219

Wang, Zhan, Q., Coursen, J. D., Khan, M. A., Kontny, H. U., Yu, L., Hollander, M. C., O'Connor, P. M., Fornace, A. J. J., & Harris, C. C. (1999). GADD45 induction of a G2/M cell cycle checkpoint. *Proceedings of the National Academy of Sciences of the United States of America, 96*(7), 3706-3711. 10.1073/pnas.96.7.3706

Warraich, U., Hussain, F., & Kayani, H. U. R. (2020). Aging - Oxidative stress, antioxidants and computational modeling. *Heliyon, 6*(5), e04107. 10.1016/j.heliyon.2020.e04107

Waterhouse, A. (2003). Current Protocols in Food Analytics Chemistry. ()10.1002/0471142913.faa0101s06

Webb, A. R., Kline, L., & Holick, M. F. (1988). Influence of season and latitude on the cutaneous synthesis of vitamin D3: exposure to winter sunlight in Boston and Edmonton will not promote vitamin D3 synthesis in human skin. *The Journal of Clinical Endocrinology and Metabolism, 67*(2), 373. https://www.ncbi.nlm.nih.gov/pubmed/2839537

Welch, W. J., & Suhan, J. P. (1985). Morphological study of the mammalian stress response: characterization of changes in cytoplasmic organelles, cytoskeleton, and nucleoli, and appearance of intranuclear actin filaments in rat fibroblasts after heat-shock treatment. *The Journal of Cell Biology, 101*(4), 1198-1211. 10.1083/jcb.101.4.1198

Wiese, J., McPherson, S., Odden, M. C., & Shlipak, M. G. (2004). Effect of Opuntia ficus indica on symptoms of the alcohol hangover. *Archives of Internal Medicine, 164*(12), 1334-1340. 164/12/1334 [pii]

Wijeweera, J. B., Thomas, C. M., Gandolfi, A. J., & Brendel, K. (1995). Sodium arsenite and heat shock induce stress proteins in precision-cut rat liver slices. *Toxicology, 104*(1-3), 35-45.

Willcox, J. K., Ash, S. L., & Catignani, G. L. (2004). Antioxidants and prevention of chronic disease. *Critical Reviews in Food Science and Nutrition, 44*(4), 275-295. 10.1080/10408690490468489 [doi]

Woisky, R. G., & Salatino, A. (1998). Analysis of propolis: some parameters and procedures for chemical quality control. *Journal of Apicultural Research, 37*(2), 99-105. 10.1080/00218839.1998.11100961

Wondrak, G. T., Jacobson, M. K., & Jacobson, E. L. (2006). Endogenous UVA-photosensitizers: mediators of skin photodamage and novel targets for skin photoprotection. *Photochemical & Photobiological Sciences : Official Journal of the European Photochemistry Association and the European Society for Photobiology, 5*(2), 215-237. 10.1039/b504573h [doi]

Wong, Q. Y. A., & Chew, F. T. (2021). Defining skin aging and its risk factors: a systematic review and meta-analysis. *Scientific Reports, 11*(1), 22075-z. 10.1038/s41598-021-01573-z

Wood, R. D., & Doublié, S. (2016). DNA polymerase θ (POLQ), double-strand break repair, and cancer. *DNA Repair, 44*, 22-32. 10.1016/j.dnarep.2016.05.003

Xin, P., Xu, X., Deng, C., Liu, S., Wang, Y., Zhou, X., Ma, H., Wei, D., & Sun, S. (2020). The role of JAK/STAT signaling pathway and its inhibitors in diseases. *International Immunopharmacology, 80*, 106210. 10.1016/j.intimp.2020.106210

Xu, M., McCanna, D. J., & Sivak, J. G. (2015). Use of the viability reagent PrestoBlue in comparison with alamarBlue and MTT to assess the viability of human corneal epithelial cells. *Journal of Pharmacological and Toxicological Methods, 71*, 1-7. S1056-8719(14)00280-9 [pii]

Xu, M., Sun, J., Yu, Y., Pang, Q., Lin, X., Barakat, M., Lei, R., & Xu, J. (2020). TM4SF1 involves in miR-1-3p/miR-214-5p-mediated inhibition of the migration and proliferation in keloid by regulating AKT/ERK signaling. *Life Sciences, 254*, 117746. 10.1016/j.lfs.2020.117746

Young. (2000). More about: Sunscreen use and duration of sun exposure: a double-blind, randomized trial. *Journal of the National Cancer Institute, 92*(18), 1532-1533. 10.1093/jnci/92.18.1532 [doi]

Young, A. R., Claveau, J., & Rossi, A. B. (2017). Ultraviolet radiation and the skin: Photobiology and sunscreen photoprotection. *Journal of the American Academy of Dermatology, 76*(3), S100-S109. 10.1016/j.jaad.2016.09.038

Young, Agashe, V. R., Siegers, K., & Hartl, F. U. (2004). Pathways of chaperone-mediated protein folding in the cytosol. *Nature Reviews.Molecular Cell Biology, 5*(10), 781-791. 10.1038/nrm1492 [doi]

Zhang, M., Zhang, T., Tang, Y., Ren, G., Zhang, Y., & Ren, X. (2020). Concentrated growth factor inhibits UVA-induced photoaging in human dermal fibroblasts via the MAPK/AP-1 pathway. *Bioscience Reports, 40*(7), BSR20193566. doi: 10.1042/BSR20193566. 10.1042/BSR20193566

Zhang, Q., Li, P., & Roberts, M. S. (2011). Maximum transepidermal flux for similar size phenolic compounds is enhanced by solvent uptake into the skin. *Journal of Controlled Release, 154*(1), 50-57. 10.1016/j.jconrel.2011.04.018

Ziegler, A., Jonason, A. S., Leffell, D. J., Simon, J. A., Sharma, H. W., Kimmelman, J., Remington, L., Jacks, T., & Brash, D. E. (1994). Sunburn and p53 in the onset of skin cancer. *Nature, 372*(6508), 773-776. 10.1038/372773a0 [doi]

Zukauskas, A., Merley, A., Li, D., Ang, L., Sciuto, T. E., Salman, S., Dvorak, A. M., Dvorak, H. F., & Jaminet, S. S. (2011). TM4SF1: a tetraspanin-like protein necessary for nanopodia formation and endothelial cell migration. *Angiogenesis, 14*(3), 345-354. 10.1007/s10456-011-9218-0

Zwinkels, J. (2015). *Light, Electromagnetic Spectrum*10.1007/978-3-642-27851-8_204-1

Appendix

This shows some basic information on each RNA sample. RNA quality number (RQN) ranges from 1 – 10 according to the quality of the RNA samples. An RQN of 1 indicates RNA which is highly degraded while an RQN of 10 shows the highest possible quality of RNA.

Sample Name	Sample Type	Volume (µl)	Quantity (ng)	RNA Concentration (ng/µl)	Absorption 260/280 nm	RQN
C1	Total RNA	16	872	54.5	2.07	10
C2	Total RNA	16	866	54.1	2.08	7.2
E1	Total RNA	16	626	39.1	2.09	10
E2	Total RNA	16	853	53.3	2.08	10
V1	Total RNA	16	813	50.8	2.09	10
V2	Total RNA	16	778	48.6	2.08	10
H1	Total RNA	16	462	28.9	2.04	10
H2	Total RNA	16	462	28.9	1.94	10
HE1	Total RNA	16	413	25.8	2.02	10
HE2	Total RNA	16	566	35.4	1.99	10
HV1	Total RNA	16	376	23.5	2.01	9.8
HV2	Total RNA	16	582	36.4	2.05	10
O1	Total RNA	16	717	44.8	2.06	10
O2	Total RNA	16	1128	70.5	2.05	10
OE1	Total RNA	16	930	58.1	2.05	10
OE2	Total RNA	16	766	47.9	2.05	10
OV1	Total RNA	16	1334	84.4	2.03	10
OV2	Total RNA	16	885	5.3	2.07	10

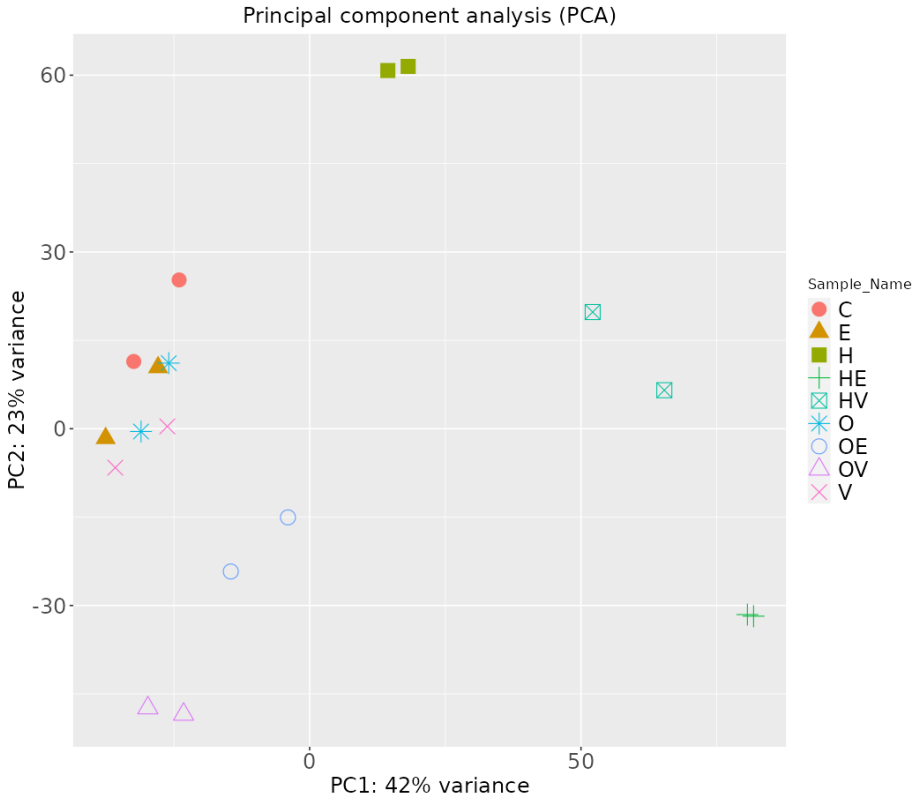

Principle component analysis (PCA) showing each sample. The top two principle components are visualised with PC1 accounting for 45% of the variance and PC2, 19%. Clustering of samples shows similarity.

Principal component analysis is a method used to reduce dimensionality while mapping RNA-seq samples on a scatter plot. The variability in the expression profiles should show replicates plotted close to each other while samples which show variance from each other should be plotted further away from each other. This is reflected above, with replicates for each condition observed to be plotted clustered together. Intraspecific variation between replicate clusters is low while interspecific variation between clusters is evident, in particular between stressed (HE, HV, OE, OV and H) and unstressed clusters (C, V and E) with the expetion of O which was in a similar loci as unstressed culsters. The principal components are axis which show the directional changes in gene expression variation (Ge, 2021).

Scatter plots were generated using iDEP (Ge, S. X., Son, & Yao, 2018b) to visualise and compare gene expression between the two technical replicates for each condition (Figure 3.55). Clustering around a diagonal line indicated similarity in the expression of genes between the two conditions and is expected to be observed in scatter plots between two replicates, indicating the similarity and correlation of the two (Koch et al., 2018).

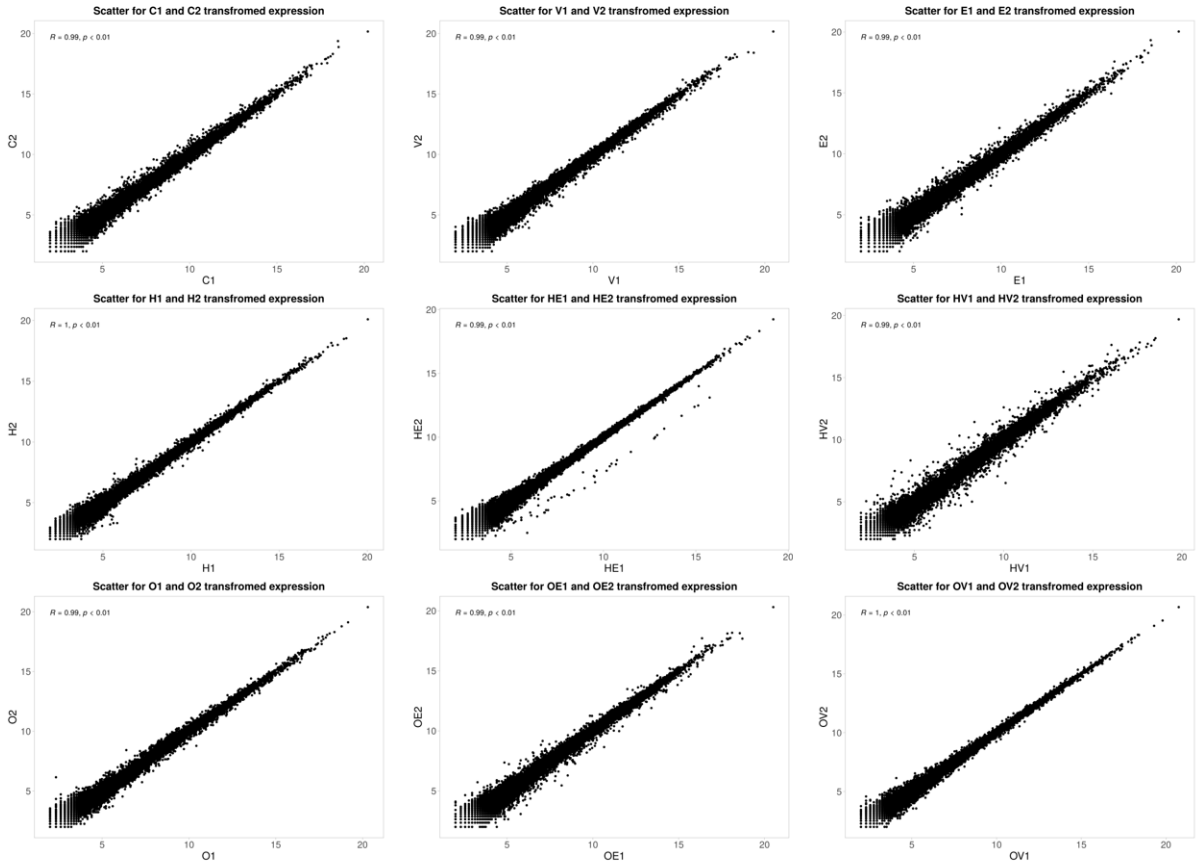

Scatter plots showing gene expression changes between technical duplicate samples. Clustering around the diagonal line indicates similarity in expression between replicates.